SMHYLES

SAFE, SUSTAINABLE AND MODULAR HYBRID SYSTEMS
FOR LONG-DURATION ENERGY STORAGE AND GRID SERVICES

SMHYLES #101138029

D2.3: Report on techno-economic sizing analysis

Activity: T2.3 “Techno-economic analysis for HESS sizing”

April 2025 (M16)

DELIVERABLE NAME

D2.3 Report on techno-economic sizing analysis

WORK PACKAGE

WP2: “LCA and techno-economics of HESSs exploiting digital tools”

PROJECT GRANT N.

Grant ID: 101138029

DISSEMINATION LEVEL:

Public (PU)

MAIN AUTHORS:

Lead benificiary: Fondazione Bruno Kessler (FBK)

Marcin Buchajczyk (FBK)

Saman Korjani (FBK)

Amir Naebi Toutounchi (FBK)

Flor Garcia Velasco (RINA-C)

Siddharth Marthak (RINA-C)

Ahlem Ben Abdallah (COME-ENG)

DATE OF SUBMISSION:

23 May 2025

CONTENT

ABBREVIATION AND ACRONYM LIST

Abbreviation / Acronym	Full Form
BESS	Battery Energy Storage System
CAPEX	Capital Expenditure
CO_{2e}	Carbon Dioxide Emissions
@DG	Diesel Generator
DGCF	Diesel Generator Capacity Factor
DOD	Depth of Discharge
EAC	Equivalent Annual Cost
EFC	Equivalent Full Cycles
ESS	Energy Storage System
FLH	Full Load Hours
FR	Fast Reserve
GA	Genetic Algorithm
GWP	Global Warming Potential
HESS	Hybrid Energy Storage System
HOMER	Hybrid Optimization of Multiple Energy Resources
IRR	Internal Rate of Return
KPI	Key Performance Indicator
LCOS	Levelized Cost of Storage
MB	Mercato di Bilanciamento (Balancing Market)
MGP	Mercato del Giorno Prima (Day-Ahead Market)
MILP	Mixed-Integer Linear Programming
MI	Mercato Infragiornaliero (Intraday Market)
NPV	Net Present Value
OPEX	Operational Expenditure

Abbreviation / Acronym	Full Form
PI	Profitability Index
PV	Photovoltaic
REF	Reference signal (in control equations)
RES	Renewable Energy Sources
RFB	Redox Flow Battery
RTE	Round-Trip Efficiency
SAFB	Smoothing and Fluctuation Benefit
SC	Supercapacitor
SOC	State of Charge
SPP	Simple Payback Period
SSR	Self-Sufficiency Rate
UC	Use Case
VRFB	Vandium Redox Flow Battery
WACC	Weighted Average Cost of Capital
ZEBRA	Zero Emission Battery Research Activities (a type of $NaNiCl_2$ battery)

1. INTRODUCTION

1.1. CONTEXT OF THE DELIVERABLE

Deliverable D2.3 provides a detailed techno-economic analysis and sizing methodology for Hybrid Energy Storage Systems (HESSs) under varying use cases, business cases, and regional conditions. This deliverable is prepared within the framework of Task 2.3 of the project, which builds upon the insights gained from:

Task 2.1 – *D2.1 HESS business cases assessment*: identification of relevant storage applications, market mechanisms and revenue streams, profitable use cases and business cases for HESSs.

Task 2.2 – *D2.2 Digital twins for HESSs design*: development of simulation and optimization tools to evaluate the performance and profitability of hybrid storage solutions.

By combining these foundational tasks, D2.3 focuses on optimal sizing guidelines for HESS implementations. The study includes an examination of how different technologies such as salt-based battery, RFB and SC can be combined and optimized to meet various operational, economic, and regulatory requirements. Particular attention is given to three European countries, Portugal, Germany, and Italy and one African context, recognizing the diverse market structures, electricity pricing schemes, and considering the system limits that influence HESS feasibility.

1.2. SCOPE AND OBJECTIVES

The primary scope of this deliverable is to present the optimal sizing of the proposed Hybrid Energy Storage System (HESS) solutions: Redox Flow Battery (RFB) + Supercapacitor (SC) and Salt-based battery + Supercapacitor (SC), for the selected use cases. This includes:

- Demonstrating how the results from Task 2.2's optimization framework can be applied to sizing scenarios in particular for Portugal and Germany case studies.
- Identifying the most advantageous balance between system capacity, Capital Expenditure (CAPEX) and Operational Expenditure (OPEX), and revenue potential in each geographical setting.
- Providing actionable recommendations on HESS design and deployment that will feed into subsequent tasks, including practical demonstration activities.

Within the scope of SMHYLES, this deliverable address both the technical and economic aspects of HESS integration. Through this work, the deliverable targets the following objectives:

- Definition and Application of Methodologies: outline of the approach to evaluate storage requirements, from sizing (power and energy capacities) to assessing cost-benefit outcomes under various operational strategies.
- Analysis of Geographical Variations: demonstration of how differences in market rules, and grid conditions drive HESS feasibility and potential revenue streams.
- Recommendation of Optimal Sizing Approaches: proposition of strategies for configuring HESS to provide multi-purpose services (e.g., peak shaving, frequency regulation, renewable integration) while maintaining financial viability.
- Identification of Opportunities for Further Development: highlights of areas for refining modeling techniques, scaling real-world demonstrations, and adaptation of regulations to better accommodate HESS deployments.

By fulfilling these objectives, the project aims to establish robust guidelines for designing and implementing HESS solutions that are both technically sound and economically viable. These guidelines will incorporate a techno-economic sizing methodology for HESS, which varies by use-case, as summarized below.

Within the four addressed cases, we deploy distinct yet complementary optimization tools tailored to each use case’s objectives and the resolution of available data. For the Portuguese case, the Graciosa Island microgrid is analyzed, while for the German case, the Technology Center for Energy (TZE) at the University of Landshut is simulated. In both cases, FBK applies a data-driven, two-tier, multi-objective genetic algorithm (GA) framework, based on the HESS optimization approach introduced in D2.2 [1]and briefly described in Appendix 1, which outlines its application for system sizing.

Since the objectives and data contexts of the Italian and African cases differ from those of the Portuguese and German studies, alternative optimization methodologies are selected to better suit each case’s specific requirements. In the Italian case, FBK models a stand-alone utility-scale PV plant with HESS using a Mixed-Integer Linear Programming (MILP) formulation, aiming to maximize project profitability by stacking revenues from the day-ahead, intra-day, balancing, and Fast-Reserve markets, while accounting for battery ageing, SC power limits, and Italian market constraints.

Finally, the African case is analyzed by COMETE/ RINA using HOMER (Hybrid Optimization of Multiple Energy Resources), a software tool specialized in the techno-economic modeling and optimization of hybrid energy systems. HOMER employs an exhaustive, scenario-based simulation approach, automatically evaluating hundreds or even thousands of potential system configurations by combining various production, storage, and energy conversion technologies.

2. INPUT AND BACKGROUND

2.1. USE CASES AND BUSINESS CASES

Task 2.1 laid the groundwork for analyzing and selecting the most relevant use cases (UCs) and business cases (BCs) for HESSs. These use cases reflect a range of operational conditions, market opportunities, and regulatory environments. By identifying the unique drivers and constraints of each scenario, Task 2.1 established a foundation for subsequent techno-economic evaluations for this deliverable. Using D2.1 as a starting point, four case studies were selected for analysis in Task 2.3. Key highlights of these case studies are summarized below:

Portugal – Graciosa Island, Graciólica demonstration site (Demo #1)

Graciosa Island, part of the Azores archipelago, operates as a microgrid with limited interconnection to mainland Portugal. The Graciólica facility currently supplies over 60% of the island's energy from renewable sources, significantly reducing diesel consumption. Despite the existing wind and solar infrastructure and a battery storage system, challenges remain in minimizing renewable curtailment and increasing clean energy penetration. A properly sized HESS could enhance grid regulation, stabilize fluctuations from intermittent renewables, and further reduce reliance on diesel, leading to lower fuel costs and emissions.

Objective: Minimize curtailment of existing wind and solar power plants and reduce reliance on diesel generators to enhance sustainability and lower operational costs.

Germany – Passau, Technology Center for Energy (TZE – Landshut University)

Germany's energy market, characterized by a high share of renewable energy and dynamic pricing structures, is facing new challenges in managing fluctuations in supply and demand. With the increasing reliance on renewable sources, the market experiences significant variations in electricity prices between off-peak and peak periods, highlighting the need for efficient energy storage and management solutions. Additionally, as electrification progresses and demand-side loads such as EV charging stations continue to grow, there is an increasing focus on enhancing energy flexibility and optimizing grid performance.

By implementing HESSs, the study addresses capitalization on price differentials through energy arbitrage, charging during periods of low demand (e.g., weekends) and discharging during high-demand periods (e.g., weekdays). Advanced storage solutions will also support grid stability by providing services such as momentary reserve, improving system efficiency, and facilitating the integration of additional renewable capacity. These measures contribute to maximizing financial returns while supporting the transition to a more flexible, sustainable, and resilient energy system.

Objective: Optimize HESS dispatch to leverage energy arbitrage, charging during periods of low demand (and low electricity prices) and discharging during periods of high demand (and higher prices).

Italy – Utility-scale HESS with PV local production

Italy's energy landscape is characterized by a growing interest in integrating renewables with energy storage to enhance self-consumption, optimize grid operations, and participate in diverse market mechanisms. With multiple layers in its energy market, such as intraday, day-ahead, balancing, and capacity markets, there are significant opportunities for energy storage systems to play a crucial role in improving the flexibility and efficiency of the grid. As more utility-scale PV systems are deployed, there is an increasing focus on managing surplus generation, reducing curtailment, and providing ancillary services to stabilize the grid.

By implementing HESSs, this case study unlocks additional revenue streams by acting as a flexible resource that supports both the energy market and grid operations. HESSs can store excess solar generation during times of low demand and dispatch it during periods of high demand, participating in balancing or frequency regulation services as needed for further revenue. This approach not only maximizes the economic value of renewable energy investments but also contributes to the broader goal of achieving a more sustainable, reliable, and resilient energy system.

Objective: Integrate a standalone utility-scale PV system with HESS to participate in market mechanisms such as day-ahead, intra-day, balancing, and fast reserve.

Tunisia – Medium-Voltage Industrial Facility with PV production capacity

In Tunisia, a medium-voltage, grid-connected industrial facility serves as the demonstration site for evaluating the applicability of HESS under African regulatory and economic conditions. The site features a rooftop PV system designed to maximize on-site energy consumption. However, current grid regulations impose restrictions on exporting excess PV generation, with limited compensation for the energy fed back into the grid. These constraints significantly reduce the economic incentive for exporting solar energy, thereby increasing the appeal of local energy storage and self-consumption strategies. To address this challenge, the study proposes a HESS configuration that integrates a RFB for long-duration energy storage and a SC for fast-response, high-power demands. The techno-economic assessment was conducted using the HOMER Pro simulation platform, enabling a comprehensive evaluation of thousands of system configurations to identify optimal performance and financial viability.

Objective: Optimize HESS design to reduce grid dependency, mitigate peak loads, and assess the economic viability of storage in Tunisia's regulatory context.

2.2. SMHYLES Optimizer for HESS Sizing (Portugal & Germany)

Task 2.2 focused on designing and validating a flexible, data-driven techno-economic optimization framework for detailed assessments of HESSs in diverse operational contexts. This framework accommodates multiple storage technologies, such as Redox Flow Batteries, salt-based batteries, and supercapacitors, and evaluates how these components can be optimally combined to meet various energy management objectives (e.g., self-consumption, arbitrage, load shifting, etc). The tool's multi-period optimization capabilities allow subtle comparisons of battery-only vs. hybrid solutions across different timescales and market conditions. Validation against real data further strengthens its robustness, making it a solid foundation for Task 2.3, which will address optimal HESS sizing under specific use cases and regional contexts outlined in this deliverable. Figure 2.1 provides a general overview of the approach of using multi-period optimization for battery and HESS arrangements as reported in D2.2 [1].

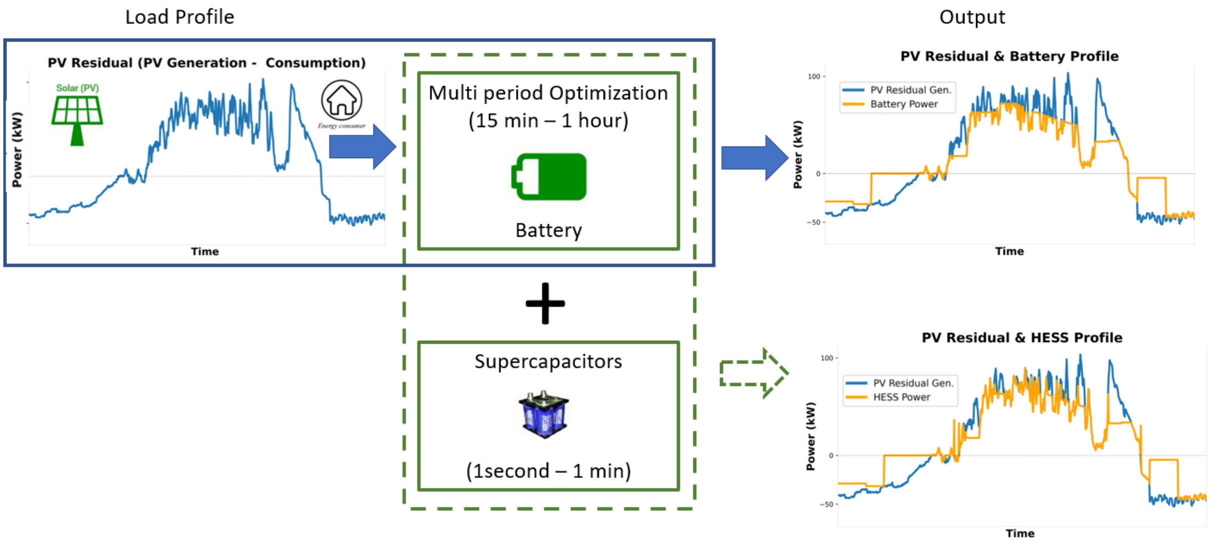

Figure 2.1 Overview of Using Multi-Period Optimization for Battery and HESS combinations as reported in D2.2

2.2.1. HESS Components and Interaction Models

Redox Flow Batteries (RFBs)

RFBs are well-suited for energy-intensive applications, providing substantial energy capacity that allows them to store and release energy over extended periods, such as from midday solar surplus to evening demand. This makes them an attractive solution for bulk energy shifting and renewable integration in microgrids or utility-scale deployments. The electrolyte tanks in RFBs can be sized separately from the power stack, offering flexible design for varying power and energy requirements. Additionally, RFBs often exhibit lower capacity fade compared to conventional batteries, making them cost-effective over long lifetimes. During the charging process, RFBs may de-rate their power output to avoid exceeding certain voltage thresholds, particularly as the electrolyte's state of charge (SOC) approaches upper limits. This de-rating can reduce the effective charging rate, causing underutilization of available surplus renewable energy if high production spikes occur[2][3].

Role of SC: Supercapacitors can mitigate these limitations by quickly absorbing short-duration power spikes that exceed the RFB's safe charging rate, thus minimizing curtailment and ensuring the RFB remains within its optimal operational envelope.

Salt-Based Batteries ($NaNiCl_2$)

Similar to RFBs, salt-based ($NaNiCl_2$) batteries exhibit power de-rating under certain conditions, such as thermal management requirements and current/voltage limits. Their operating temperature must be maintained within a specific range, which can introduce further constraints and power limitations. Despite the need for careful thermal management, salt-based batteries offer high energy density and cycle stability, providing high cycle life and steady performance for daily deep discharge applications. Commonly used in industrial microgrids or remote locations where robust energy supply is essential, these batteries require operation at elevated temperatures (e.g., around 270–350 C) [4]. If the temperature falls below or rises above these setpoints, self-heating or de-rating measures are triggered. Self-heating consumes stored energy or external power to maintain the necessary temperature, thereby reducing net usable capacity. Overheating leads to power de-rating to prevent permanent damage or excessive wear. Additionally, salt-based cells follow constant current–constant voltage charging profiles, so the battery cannot charge or discharge beyond certain rates without risking cell damage. Approaching the minimum or maximum SOC can limit the battery's power output, causing suboptimal charging/discharging schedules if the battery alone must handle rapid load or generation changes[5].

Role of SC: By complementing salt-based batteries with a supercapacitor, fast fluctuations are offloaded to the SC, letting the main battery maintain a stable charging rate within safe thermal and electrical thresholds.

Supercapacitors (SCs)

SCs feature high power density and rapid charge/discharge capabilities, making them ideal for capturing brief power spikes and smoothing power output in real time. They cannot store large amounts of energy cost-effectively over long durations, but they excel at short-term buffering to compensate for the slower response of batteries. SCs excel at managing short-term power events, such as surges in load or sudden dips in generation, thanks to very high charge/discharge rates[6]. Because SCs do not rely on chemical phase changes like batteries, they are highly resistant to cycle wear, making them ideal for repetitive fast-charge scenarios. Although SCs deliver high bursts of power, their usable energy capacity is relatively small, making them unsuitable for long-duration shifting (e.g., storing power overnight) [7].

Buffering Role: By absorbing momentary spikes or dips that last seconds to minutes, SCs protect main battery technologies, such as RFB or salt-based batteries, from rapid cycles that cause increased degradation. The potential de-rating power limitations of these batteries can be also compensated by SCs.

2.3. SYNERGISTIC HESS OPERATION

By combining a battery, such as RFB or salt-based, with a supercapacitor, the HESS leverages the complementary strengths of each technology. The advantages of HESS operation can be categorized as follows:

Power Management and Efficiency:

- Power Smoothing: SCs handle high-frequency components of the load or generation profile, allowing the battery to focus on bulk energy management[8].
- Operational Efficiency: This synergy improves overall system efficiency by reducing energy curtailment, smoothing out battery power usage, and minimizing wear on the main battery[9].

Reliability and Lifespan:

- Increases Reliability: SCs manage sudden, short-lived power demands, freeing the battery from high-frequency cycling and enhancing overall system reliability[10].
- Extends System Lifespan: By reducing stress on the main battery, SC integration helps preserve long-term capacity and efficiency[11].

Economic and Market Benefits:

- Market Applications: The combined system can provide ancillary services (e.g., frequency regulation), capture energy arbitrage opportunities, and enhance self-consumption of renewables[12].
- Maximizes Economic Potential: HESS can pursue time-shifting, peak shaving, and frequency regulation strategies, ultimately enhancing return on investment[10].

2.4. MULTI-PERIOD OPTIMIZATION AND SOFTWARE PLATFORM

Multi-Objective Approach

A central innovation in Task 2.2 is the use of data-driven, multi-period, multi-objective optimization by deploying a genetic algorithm (GA) for revenue maximization, considering system operational limits. This tool, previously utilized in several BESS optimization problems[13][14][15], has been updated for multi-timeframe usage and HESS within Task 2.2, as reported in D2.2 [1]. Figure 2.2 shows the optimization procedure flow. The framework can evaluate scenarios at various time resolutions, hourly, minute-based, or even second-based, striking a practical balance between computational feasibility and operational fidelity. This approach accounts for key factors such as battery aging, temperature constraints, and power de-rating, ensuring that the optimized strategies remain viable in real-world conditions.

Dual-Timeframe Optimal Management

The HESS optimization process is designed to address optimal usage of the HESSS within two distinct timeframes, this dual-timescale approach offers a practical management strategy for conducting long-term techno-economic analyses, considering:

High Temporal timeframe (Seconds to Minutes): Supercapacitor capture rapid fluctuations in generation and load, mitigating short-lived power spikes or dips that the main battery might not handle efficiently. Beside it can be used to compensate the limits of the batteries.

Low temporal timeframe (15-Minute to Hourly Intervals): RFB or salt-based battery are used to store and release large quantities of energy. They are particularly effective for shifting surplus solar generation from midday to meet evening demand. Additionally, these batteries can be utilized to capitalize on time-dependent price differentials by storing energy when prices are low and releasing it when prices are high.

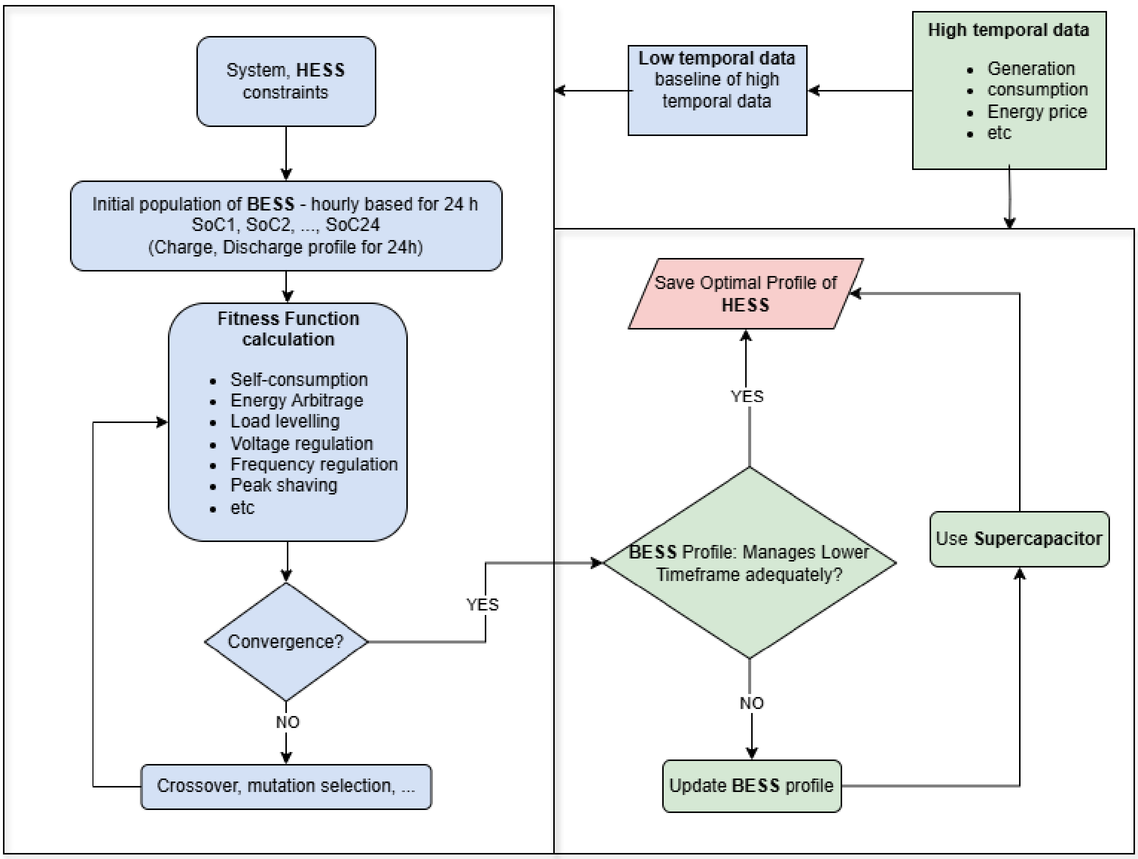

Figure 2.2 Workflow of Multi-Objective-Multi-Period optimization for HESS as reported in D2.2

Showcased Functionalities

The tool developed within Task 2.2 incorporates critical technical and system limits, including battery power de-rating, thermal boundaries, and SOC restrictions. It provides feasible, safe, and robust solutions under real operational conditions. This tool demonstrates how different operational strategies for HESS can be evaluated and optimized, and It has already been showcased for self-consumption maximization and energy arbitrage:

Self-Consumption Enhancement

The HESS can maximize the fraction of on-site renewable energy used by minimizing PV curtailment and unmet load. Batteries and SCs work together to match supply and demand, reducing grid imports and improving overall system efficiency[16].

Energy Arbitrage

The framework exploits price differentials in wholesale or retail electricity markets. During low-price (or high-renewable) periods, the HESS charges; then it discharges when prices are higher or when the system needs support, thereby increasing revenue or offsetting expensive grid purchases[17].

3. CASE STUDY - PORTUGAL

3.1. INTRODUCTION

Graciosa Island, part of the Azores archipelago in Portugal, has been at the forefront of integrating renewable energy sources (RES) into a remote, islanded power system. Until recently, its electricity supply depended primarily on diesel generators, leading to high fuel costs, logistical challenges, and significant greenhouse gas (GHG) emissions. In an effort to reduce diesel consumption and enhance energy autonomy, the island introduced a hybrid wind-solar-battery system that currently supplies over 60% of its energy demand from renewable resources. This integrated solution already saves approximately two million liters of diesel each year while ensuring stable electricity provision to local consumers.

Despite the tangible success of existing infrastructure, Graciosa Island still faces nontrivial levels of renewable curtailment, around 6 GWh of otherwise usable clean electricity per year. The limitations stem chiefly from the operational needs of diesel generators, which must run at or above minimum thresholds to maintain grid stability. As the penetration of variable renewable energy continues to rise, more sophisticated energy storage strategies become critical to balancing real-time supply and demand, buffering large power swings, and further minimizing diesel usage.

3.2. PURPOSE OF THE CASE STUDY

The Gracíolica Island case study illustrates how a HESS, specifically combining a salt-based battery ($NaNiCl_2$) with a supercapacitor, can address the challenges posed by variable renewable generation in a remote microgrid. The salt-based battery provides bulk energy storage and longer-duration shifting, while the supercapacitor offers rapid-response buffering to manage fast transient events and offset power de-rating constraints in the battery. By examining system sizing, operational profiles, and techno-economic results in this unique island context, the case study aims to:

- Quantify reductions in diesel consumption from higher renewable energy utilization.
- Evaluate how SC can mitigate rapid load changes (providing services) and battery power de-rating.
- Demonstrate the technical feasibility and economic viability of incorporating HESS in remote microgrids.
- Provide insights and guidelines that may be replicated in similarly constrained island or isolated power systems elsewhere.

Remote and islanded microgrids often grapple with the dual challenges of high diesel reliance and the underutilization of RES[18]. This tension arises when diesel generators are required to run at minimum load to maintain system stability, forcing renewable power to be curtailed when generation exceeds local demand. In response, HESS have emerged as an effective strategy to mitigate curtailment and minimize diesel consumption. By storing surplus renewable energy during peak generation periods, HESS can supply clean energy later, reducing both fuel costs and emissions. The Graciosa Island microgrid, exemplifies these challenges and opportunities. Similarly, research focusing on Graciosa Island's hybrid energy system highlighted the need to reduce diesel generation and excess renewable electricity curtailment through the integration of HESS[19].

Such combined battery-supercapacitor systems deliver multiple operational and economic benefits. On the operational side, supercapacitors relieve batteries from high-frequency cycling, thereby prolonging battery lifetime, improving overall system robustness, and delivering smoother, more reliable energy dispatch. On the economic side, an optimally sized HESS that captures energy otherwise curtailed leads to significant cost savings by offsetting diesel production and deferring expensive generator operating hours. Various techno-economic analyses underscore that a well-designed HESS, especially one tailored to local load profiles, climatic conditions, and renewable resource variability, can markedly lower total lifecycle costs while ensuring secure and stable electricity supply.

Accordingly, the forthcoming techno-economic assessment will concentrate on identifying the optimal sizing of both the salt-based battery and supercapacitor, with a strong focus on four key objectives: **reducing diesel consumption**, **increasing RES utilization with HESS**, **enhancing frequency regulation**, and **ensuring optimal sizing and techno-economic feasibility**. This includes evaluating the required power and energy capacities, frequency response capabilities, and temperature-related performance constraints. By capturing these interrelated parameters, the analysis will illuminate how best to reduce diesel usage and maximize RES utilization in Graciosa's unique setting, ultimately reinforcing the island's status as a leading example of high-renewable, low-carbon microgrid operation.

Reducing Diesel Consumption and Increasing RES Utilization with HESS

Integrating HESS into microgrids has been shown to effectively reduce reliance on diesel generators and increase the penetration of RES. By storing excess energy generated from RES, HESS can mitigate renewable energy curtailment and ensure a stable power supply during periods of low renewable generation. For instance, a study on optimizing hybrid renewable-diesel power plants introduced an innovative energy management system that incorporates battery energy storage systems, leading to enhanced economic benefits and reduced diesel consumption[20]. The integration of high levels of RES is often constrained by the necessity to maintain diesel generators at a minimum operational load and to curtail excess renewable generation to prevent system instability[21][20].

The high energy capacity of batteries is beneficial for absorbing excess generation over extended periods. However, their slower charge/discharge dynamics and specific operating requirements necessitate augmentation with supercapacitors to manage rapid power fluctuations. Consequently, studies have proposed HESS configurations that combine batteries with supercapacitors to effectively smooth the output of wind and PV power. This approach also provides a buffer, allowing diesel generators to operate less frequently or at more optimal load levels[21].

Frequency Regulation through HESS

HESS, particularly those combining batteries and supercapacitors, have demonstrated significant advantages in providing frequency regulation services. Supercapacitors, known for their rapid charge and discharge capabilities, are well-suited for handling short-term power fluctuations, thereby complementing batteries that manage longer-term energy storage. A study presented an effective hybrid supercapacitor-battery energy storage system for active power management in a wind-diesel system, emphasizing its role in frequency regulation and power quality improvement[22]. Furthermore, an economic analysis of a Li-ion battery-supercapacitor HESS highlighted its benefits in multitype frequency response services. The study developed an operational mode tailored to various frequency response requirements, demonstrating the HESS's capability to deliver distinct services efficiently[10].

Optimal Sizing and Techno-Economic Considerations

Optimal sizing of HESS, particularly those integrating batteries and supercapacitors, is crucial for maximizing technical performance and economic viability. Proper sizing ensures that each component operates within optimal parameters, significantly extending system lifespan, enhancing operational efficiency, and reducing overall costs. One of the main challenges in sizing HESS involves determining the appropriate capacity and power ratio between batteries and supercapacitors. Correctly sizing a supercapacitor in combination with battery storage can drastically reduce battery degradation caused by high-frequency cycling, thus extending battery life and minimizing replacement costs[23].

Moreover, advanced optimization algorithms and modeling techniques are essential for accurately determining HESS dimensions. It has been demonstrated that a well-sized HESS can significantly reduce operational costs by effectively capturing excess renewable energy, which would otherwise be curtailed, thereby reducing reliance on costly diesel generation[24]. Additionally, temperature management and environmental conditions significantly impact techno-economic considerations. Salt-based batteries, for instance, exhibit performance derating at extreme temperatures, limiting their effective utilization[25]. In this regard, supercapacitor can be used to compensate for these limitations, especially under temperature-induced power derating conditions.

3.3. SITE AND DATA DESCRIPTION

Currently, the site integrates a 4.5 MW wind farm, a 1 MW solar photovoltaic farm, and a lithium titanate oxide (LTO) battery system of 2.6 MWh/4 MW, allowing the island to achieve over 60% clean energy penetration and saving around 2 million liters of diesel annually. Nonetheless, to address a remaining annual curtailment of approximately 6 GWh and further boost the renewable fraction, a new salt-based HESS, comprising a 250 kW/750 kWh salt battery and a 250 kW supercapacitor, will be added. While the salt battery provides the bulk energy capacity for longer-duration storage, the supercapacitor's capability for rapid charge and discharge makes it essential for primary control, particularly frequency regulation. It also compensates for moments when the salt battery experiences power derating due to operating temperature constraints.

Figure 3.1. below shows a sample of the power profiles from the generation assets owned by Graciolica. In this example, curtailment of solar and wind power generation is observed in several instances (between hours 1-5, 11-14 and 22-24), given by the discrepancy between maximum possible generation and actual power generated. This illustrates the possible advantage of adding a salt-based battery, as the additional battery storage system could recharge using otherwise curtailed renewable power and discharge in times of high diesel power generation to reduce diesel consumption.

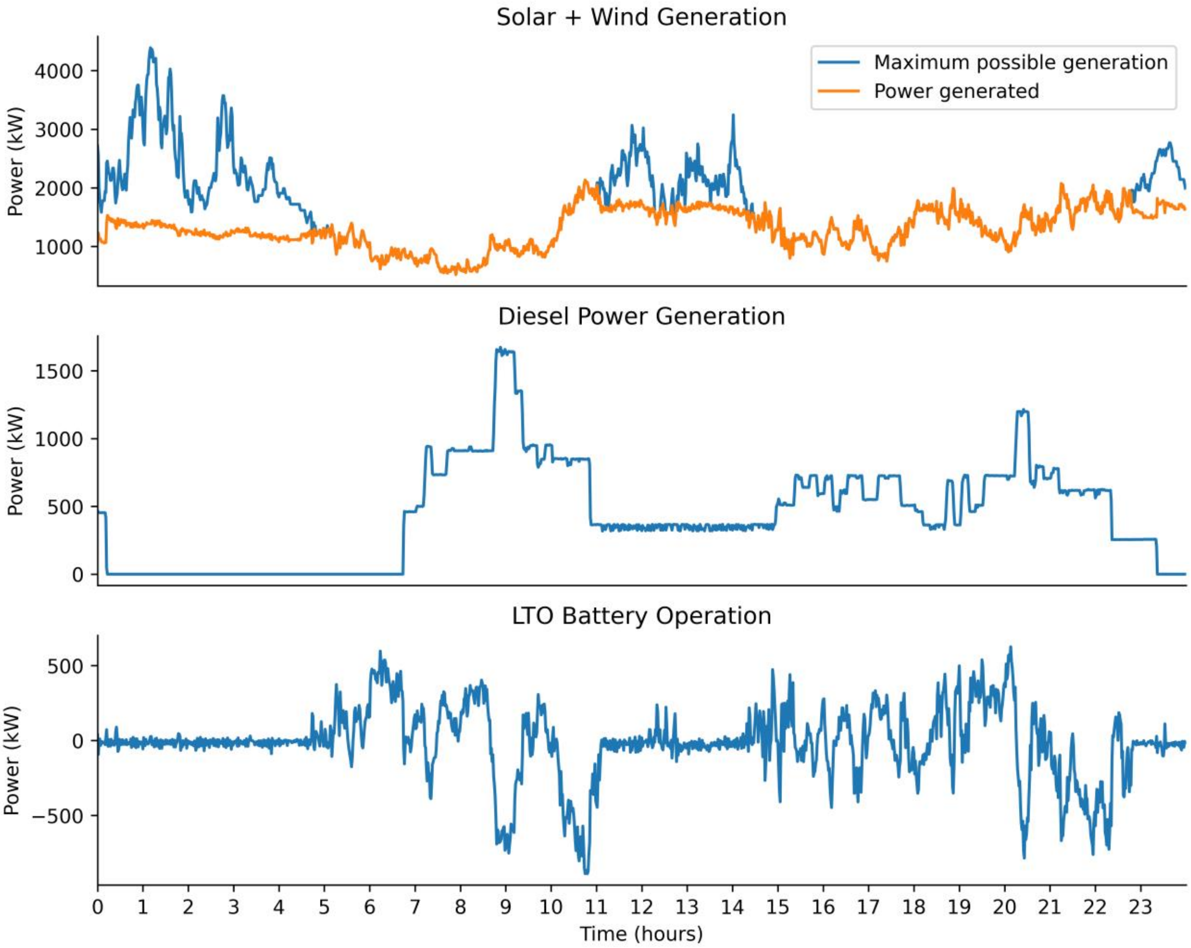

Figure 3.1. Sample of power profiles for the generation assets in Graciolica over a 24 hour period during 31 January 2024, at 1 minute temporal resolution.

3.4. METHODOLOGY

This section explains how we determine the optimal HESS size and operating strategy for the Gracíolica demo site. The procedure re-uses the multi-period optimization tool, workflow and component models already documented in D2.2[1], while Appendix 1 gathers the additional sizing details. Adapted to the site-specific objectives and constraints of this remote microgrid, the approach follows the main steps summarized below and visualized in Figure 3.2.

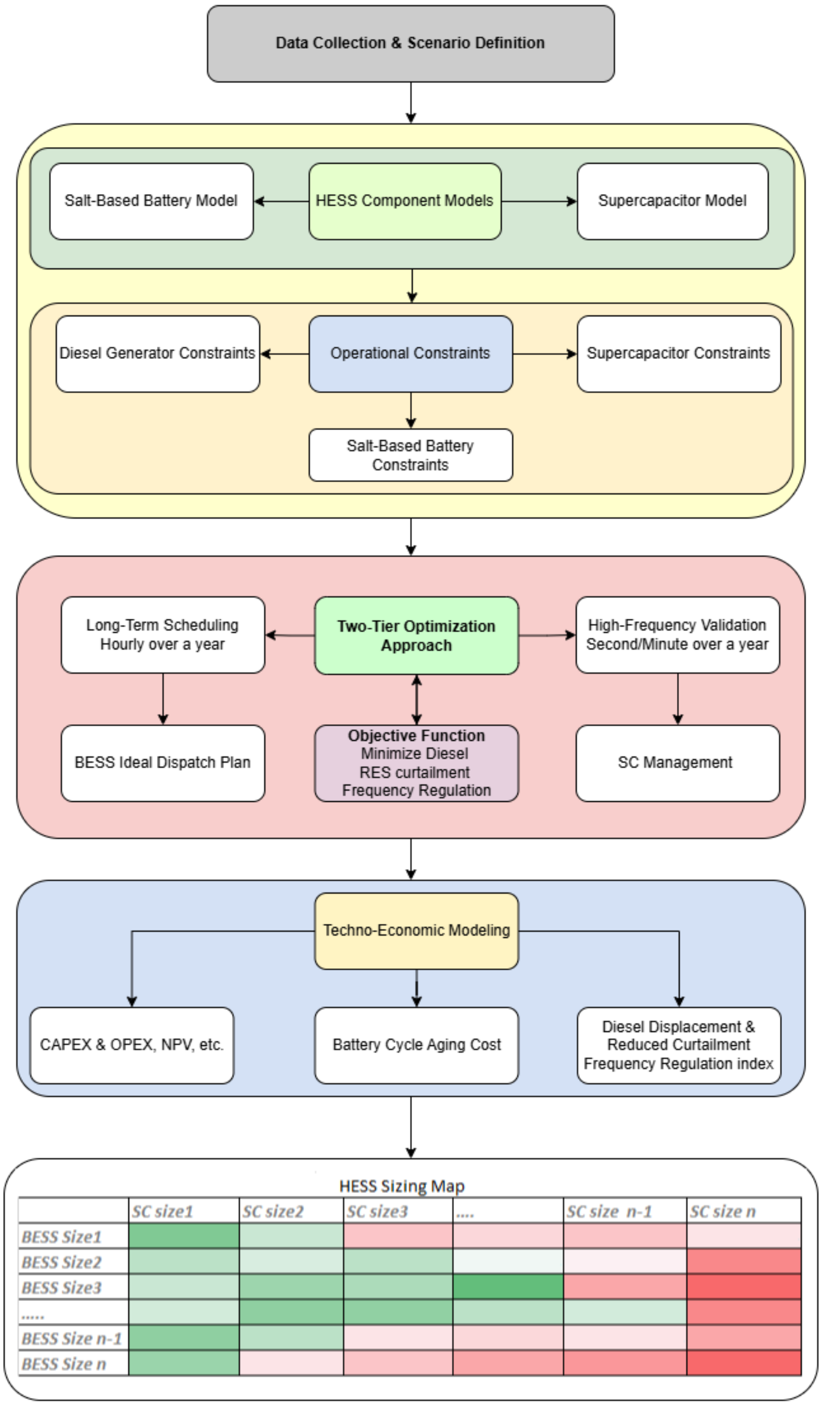

Figure 3.2 Workflow of optimal HESS size and operating strategy for Gracíolica demo site

3.4.1. Data Collection and Scenario Definition

Actual data on consumption, renewable production, renewable curtailment, and DPP generation, along with the existing battery profile was utilized as input for the optimization process. Historical data, provided on a minute-by-minute basis, served as the baseline for hourly-based battery optimization (averaged to hourly intervals). Minute-by-minute data was also employed to precisely identify the salt-based battery's operational limits. Additionally, the supercapacitor was integrated and optimized using minute-based data to enhance the system's response capabilities. This integration compensates for the battery's limitations that become apparent at higher data frequencies. Furthermore, the supercapacitor is used for showcasing proper frequency regulation with second-by-second data over a day, ensuring efficient frequency regulation through power smoothing and thereby improving power quality.

To evaluate the performance, flexibility, and techno-economic value of the HESS, a set of representative operational scenarios is defined. These scenarios are designed to reflect typical system behavior as well as stress conditions under which storage assets provide critical value. The first scenario describes the role of HESS in reducing reliance on conventional diesel generation and enhancing the utilization of renewable energy. This focuses on strategic charging and discharging of the HESS to maximize renewable self-consumption and minimize fuel-based generation. Another scenario extends the first by using SC to address short-term power fluctuations and support frequency regulation. This case evaluates the system's ability to respond to high-resolution variability, using minute and sub-minute data to assess the contribution of rapid energy balancing. Additionally, a high-renewable month scenario is explored, involving a period with sustained excess generation from solar and wind resources. This scenario is particularly useful for analyzing renewable curtailment risks, battery charging opportunities, and strategies to increase self-sufficiency under abundant renewable availability.

3.4.2. HESS components models

For this demo case, the HESS included a Sodium Nickel Chloride battery, often referred to a ZEBRA battery and henceforth referred to as the salt-based battery as well as a supercapacitor. This section will provide a brief description of these technologies; however, please refer to deliverable document D2.2[1] for a detailed explanation on the technical constraints of the salt-based battery and supercapacitor, and for a summary of the equations used to model these components.

The salt-based battery utilizes a molten salt electrolyte and must be maintained within a specific temperature range to operate. A summary of the technological parameters and constraints for a single battery module are provided in Table 3-1 below.

Table 3-1 Technological parameters and constraints for the salt-based battery

Parameter	Value
Model	250UP40 FZSonick
Battery type	Sodium Nickle Chloride or ZEBRA
Total Capacity	9.6 kWh/ 40Ah
Maximum Charge Current	9 - 10 A
Maximum Discharging Current	60 A
Maximum Discharging Power	12 kW
Max Charging Power	2.5 kW
Charging Scheme	CC - CV CC at ~9 A until terminal voltage of 274 V is reached CV at 274 V until 80% SOC and then 267 until 100% SOC
Operational Temperature	265 - 350 C
Heating Modes	When temperature goes below minimum temperature setpoint, the battery will reheat using an external power source (if available) or self-discharge (if it is charged > SOC_min)
Heating Power	External power heating - 340 W Self-discharge heating - 230 W
Cooling	No active cooling. When max temperature setpoint is reached, battery will cease operation and cool passively
Thermal Dissipation	110 W
Degradation	0.0044% per cycle (Assuming a 20% degradation after 4500 cycles)

The parameters for a single supercapacitor submodule are summarized in Table 3-2.

Table 3-2 Supercapacitor submodule parameters

Parameter	Value
Capacitance	150 - 200 F
Maximum open circuit voltage	27 V
Minimum open circuit voltage	12 V
Total energy storage capacity	50 – 60 kJ
Peak power	20 kWp
Internal Resistance	8 - 15 m Ω
Capacitance degradation rate	2 x 10-5 % / Cycle
Resistance degradation rate	1 x 10-4% / Cycle

In the techno-economic analysis, 5 salt-based battery sizes and 5 supercapacitor sizes were assessed, corresponding to a total of 25 HESS sizes that were simulated. Each HESS corresponded to a combination of 1 battery size and 1 supercapacitor. A ‘battery-only’ assessment was carried out for each battery size, hence a total of 30 simulations were carried out. The different sizes are summarized in Table 3-3. Size 1 corresponds to the battery and supercapacitor module arrangements that were proposed in the SMHYLES Initial Design proposal [26]. For the salt-based battery, this corresponds to a system of the 250UP40 FZSonick modules arranged in 3 series (s) and 32 parallel (p) scheme. For the supercapacitor, this corresponds to a 30 series, 2 parallel arrangements of the sub-modules. For each size step, we add another system in of 3 s, 32p in series to the battery arrangement, and 30s, 2p in series to the supercapacitor arrangement. Note that each SC size is presented in terms of their peak available power (kWp).

Table 3-3 Salt-based battery and supercapacitor sizes assessed in the techno-economic assessment.

Size	Battery		Supercapacitor	
	Energy and Power	**No. in Series & Parallel**	**Peak Power**	**No. in Series & Parallel**
Size 1	240 kW / 920 kWh	3 s, 32 p	1200 kWp	30 s, 2 p
Size 2	480 kW/ 1840 kWh	6 s, 32 P	2400 kWp	60 s, 2 p
Size 3	720 kW/ 2760 kWh	9 s, 32 p	3600 kWp	90 s, 2 p
Size 4	960 kW / 3680 kWh	12 s, 32 p	4800 kWp	120 s, 2 p
Size 5	1200 kW / 4600 kWh	15 s, 32 p	6000 kWp	150 s, 2 p

3.4.3. Operational constraints

Diesel Generator

The following section defines the constraints for diesel generator, which is based on its minimum runtime and minimum power output. This is an important consideration, as it affects the possible interaction with HESS. The constraints are described by equations (1) to (5), and the relevant variables are defined below.

- $P_{\text{diesel}}(t)$: Power output of the diesel generator at time t.
- $P_{\text{HESS}}(t)$: Power output of the hybrid energy storage system (HESS) at time t.
- $\delta(t) \in 0,1$: Binary variable indicating whether the diesel generator is ON ($\delta(t) = 1$) or OFF ($\delta(t) = 0$).
- Δt: Simulation time step (in minutes).
- $T_{\text{min}} = 180$: Minimum required runtime for the diesel generator (in minutes).
- M: A constant variable indicating max diesel generator capacity.

Minimum Runtime Constraint

Once the diesel generator is turned on, it must remain on for at least 3 hours (180 minutes). Equations (1) defines this, where t_{on} be the time the diesel generator is turned on.

$$\sum_{i=0}^{N} \delta(t_{on} + i\Delta t) \cdot \Delta t \geq T_{min}, \quad \text{where } N = \left\lfloor \frac{T_{\text{min}}}{\Delta t} \right\rfloor \tag{1}$$

Minimum Operating Power Constraint

The diesel generator cannot operate below 200 kW. Thus, when it is ON, its output must be either 0 kW (completely off) or at least 200 kW. This is defined by equations (2) and (3)

$$P_{diesel}(t) \geq 200 \cdot \delta(t) - M \cdot \big(1 - \delta(t)\big) \quad (2)$$

$$P_{diesel}(t) \leq M \cdot \delta(t) \quad (3)$$

Interaction with HESS

The HESS cannot reduce diesel generator output to within the range of $0 < P_{\text{diesel}}(t) < 200$ kW. Therefore, the residual diesel power after offsetting by HESS must satisfy equations (4) and (5) below.

$$P_{diesel}(t) = \max\big(0, P_{load}(t) - P_{HESS}(t)\big) \quad (4)$$

$$P_{diesel}(t) = 0 \quad \text{or} \quad P_{diesel}(t) \geq 200 \quad (5)$$

Based on these conditions, the partial offsetting of diesel load by HESS into the invalid operating band is avoided. For example, if the generator operates at 250 kW, the HESS must offset up to 50 kW, the entire 250 kW or not offset the load at all.

Salt-Based Battery

The technological parameters have been discussed in sub-section 3.4.2 and are also detailed in deliverable D2.2 [1]. Table 3-4 below summarizes the site specific operational constraints for a single FZSonick 250UP40 module. These operational constraints are equal to or more restricting than the default technological constraints summarized in Table 3-1.

As explained in document D2.2[1] and summarized in Table 3-4, one of the heating modes for the battery is via self-discharge. In practice, the battery can self-discharge beyond its minimum SOC limit to 0% when carrying out this heating process; however, in our model we have imposed the lower SOC limit of 12 % for both energy discharging and self-discharging modes, where the battery can self-discharge only until the lower SOC limit of 12% is reached. In a real-world scenario, it would be possible to extract additional heating energy by allowing the battery to self-discharge below 12%, to 0%. However, doing so would mean that, after heating, the battery would not be operational until it was recharged back above 12% SOC. In contrast, by enforcing the 12% SOC floor in our model, we forgo that last portion of energy that could be used for heating, but ensure that the battery is always immediately usable after reheating. This trade-off improves model simplicity and avoids modeling complications associated with deep depletion and recovery.

Table 3-4 Site specifc operational cosntraints for a single 250UP40 FZSonick module

Parameter	Value
Total Energy capacity	9.6 kWh
Rated Energy capacity	7.5 kWh
SOC Limits	12-90%
Maximum Discharging Power	2.8 kW
Max Charging Power	2.5 kW
Maximum Discharge Current	11.9 A
Maximum Charging current	8.9 A

Supercapacitor

No additional site-specific operational constraints were defined for the supercapacitor. Refer to the default technological parameters summarized in Table 3-.

3.4.4. Objective Function

Two cases are assessed for the HESS arrangements in the Graciolica case study, as summarized below:

- Case 1: The primary focus is to reduce the diesel consumption, by discharging the salt-based to substitute power output provided by the diesel generator. A secondary focus is to maximize renewable energy generation by using surplus RES that would otherwise be curtailed, to recharge the salt-based battery.
- Case 2: As per Case 1, with an additional third focus of using the supercapacitor to smooth out power fluctuations in output load profile, thereby supporting frequency regulation.

The objective functions for Case 1 and Case 2 are as per equation (6) and (7), respectively:

$$\min\left[\sum_{t=1}^{T} c_1 \cdot P_{\text{Residual Diesel}}(t) + c_2 \cdot P_{RES,curtail}(t)\right] \tag{6}$$

$$\min\left[\sum_{t=1}^{T} c_1 \cdot P_{\text{Residual diesel}}(t) + c_2 \cdot P_{RES,curtail}(t) + c_3 \cdot \sigma_{P_{\text{SC-on}}}\right] \tag{7}$$

Where:

$$P_{\text{residual diesel}}(t) = P_{\text{diesel}}(t) + P_{battery,disch}(t) \tag{8}$$

$$P_{RES,curtail}(t) = P_{\text{RES,avail}}(t) - P_{\text{RES,used}}(t) - P_{battery,ch}(t) \quad (9)$$

- $P_{\text{diesel}}(t)$ is the original diesel generator output at time t [kW]
- $P_{battery,\ disch}(t)$ is the discharge power of the salt-based battery at time t [kW]
- $P_{battery,\ ch}(t)$ is the charge power of the salt-based battery at time t [kW]
- $P_{\text{RES,avail}}(t)$ is the available renewable energy at time t [kW]
- $P_{\text{RES,used}}(t)$ is the original renewable energy used at time t [kW]
- c_1, c_2, c_3 are the weighting coefficients for each cost or performance term
- T is the total number of time steps in the optimization horizon
- $\sigma_{P_{\text{SC-on}}}$ is the standard deviation of power fluctuations with SC active
- $\sigma_{P_{\text{SC-off}}}$: Standard deviation of power fluctuations without SC

To evaluate the performance of frequency regulation provided by the supercapacitor, the Power Smoothing Index, also known as the Smoothing and Fluctuation Benefit (SAFB), is used, as defined in Equation (10). This metric quantifies the ability of the supercapacitor to reduce high-frequency power fluctuations that impact grid stability. A higher SAFB value indicates greater smoothing effectiveness, and thus, better frequency regulation performance.

$$\text{SAFB} = 1 - \frac{\sigma_{P_{\text{SC-on}}}}{\sigma_{P_{\text{SC-off}}}} \quad (10)$$

The standard deviations used in equation (10) is based on the standard deviation of the difference between a reference profile and the generation profile before smoothing (to calculate $\sigma_{P_{\text{SC -off}}}$) or between a reference profile and the generation profile after smoothing (to calculate $\sigma_{P_{\text{SC -on}}}$). This is summarized by equations (11) and (12) below.

$$\sigma_{P_{\text{SC -off}}} = std[P_{ref} - P_{gen}] \quad (11)$$

$$\sigma_{P_{\text{SC -on}}} = std[P_{ref} - (P_{gen} + P_{SC})] \quad (12)$$

Where:

- $P_{\text{ref}}(t)$ is a frequency regulation reference signal, representing the desired smoothed power profile at time t
- $P_{\text{gen}}(t)$ is the raw power output from generation sources (e.g., diesel, PV) at time t
- $P_{\text{SC}}(t)$ is the supercapacitor power injection/absorption at time t

The reference signal $P_{\text{ref}}(t)$ is typically constructed as a low-pass filtered version of the raw generation power to emphasize low-frequency components, and is given by equation (13).

$$P_{ref}(t) = \alpha \cdot P_{gen}(t) + (1 - \alpha) \cdot P_{gen}(t) \quad (13)$$

In this formulation, the supercapacitor is tasked with regulating the high-frequency mismatch between P_{gen} and P_{ref} , thereby supporting grid frequency stability. The reduction in the standard deviation from $\sigma_{P_{\text{SC-off}}}$ to $\sigma_{P_{\text{SC-on}}}$ directly reflects the system's frequency regulation effectiveness**.** $\alpha \in (0,1)$ is a filtering parameter that determines the responsiveness of the reference signal $P_{\text{ref}}(t)$. Lower values of α result in a smoother signal with slower dynamics, while higher values track $P_{\text{gen}}(t)$ more closely.

3.4.5. HESS Performance and Techno-Economic Modeling

In our HESS performance assessment, performance was based on the total annual diesel consumption that has been reduced. This given by value $E_{diesel,reduced}$ in kWh. To proceed with techno-economic modeling, annual revenue for each HESS arrangement was determined which was based on the cost savings due to avoided diesel use and CO_2 emissions. The annual CO_2 emissions in tonnes is given by equation (14**)** and the annual revenue or cash inflow is given by equation (15), with all related parameters summarized in Table 3-5.

$$m_{CO2e,reduced} = \frac{\gamma_{CO2e} \cdot \beta_{diesel} \cdot E_{diesel,reduced}}{1000} \tag{14}$$

$$CF_{in} = C_{diesel} \cdot \beta_{diesel} \cdot E_{diesel,reduced} + C_{CO2e} \cdot m_{CO2e,reduced} \tag{15}$$

Net present value (NPV) was the primary KPI used for the techno-economic assessment for each HESS arrangement, and this quantifies the financial viability of a project. This considers the present value of the initial project investment and all future cash inflows and outlfows over a specified period. This is calculated as per equation (16) below.

$$NPV = \sum_{Y=1}^{N} \frac{CF_{in} - CF_{Out}}{(1 + WACC)^{Y}} - CAPEX_{HESS} \tag{16}$$

Where:

- CF_{in} is the annual revenue generated by the HESS, and this corresponds to the cost savings due from avoided diesel use and avoided CO_2 emissions.
- CF_{out} is the annual operating expenditures for the HESS, as per equation (17).
- N is the project period and corresponds to the expected lifetime of the HESS where it still generates revenue (see Table 3-5.).
- Y is the assessment interval, and corresponds to 1 year.
- $WACC$ is the weighted average cost of capital (see Table 3-5.).
- $CAPEX_{HESS}$ is the capital expenditure and corresponds to the inital investment cost for implementing the HESS arrangement, as per (18) .

$$CF_{out} = OPEX_{battery} + OPEX_{SC} \tag{17}$$

$$CAPEX_{HESS} = S_{Battery} \cdot CAPEX_{battery} + S_{SC} \cdot CAPEX_{SC} + CAPEX_{SC,install} \tag{18}$$

Where:

- $OPEX_{battery}$ is the annual battery OPEX (see Table 3-5.).
- $OPEX_{SC}$ is the annual SC OPEX (see Table 3-5.).
- $S_{Battery}$ is the battery size in terms of energy storage capacity [kWh].
- S_{SC} is the SC size in terms of maximum power output [kW].
- $CAPEX_{battery}$ is the specific battery cost (see Table 3-5.). Note that battery installation cost is already accounted for in this specific cost
- $CAPEX_{SC}$ is the specific SC cost (see Table 3-5.)
- $CAPEX_{SC,install}$ is the SC installation cost (see Table 3-5.).

We assume that the cashflow remains constant for each assessed year as the battery and supercapacitor will have the same performance over the entire assessed period. This is not entirely accurate, as the battery and supercapacitor behavior is dependent on the renewable energy generation and diesel production, which are dependent on specific weather conditions and demand on the network. However, it is assumed that the production data used for assessed year of 2024 is representative of a typical year for Graciolica.

In our techno-economic analysis we also consider battery degradation and impact this will have on the battery performance and financial outcome. In deliverable D2.2[1] the degradation rate for the salt-based battery was stated as 0.0046% per cycle as per the study in [27], and using this we can determine a yearly degradation as per (19), and then use this to determine the degraded cash flow input as per (20) and the updated NPV as per (21).

$$D_{battery} = n_{cyc,bat}\delta_{battery} \tag{19}$$

$$CF_{in,degraded} = CF_{in}\left[1 - (Y - 1)D_{battery}\right] \tag{20}$$

$$NPV = \sum_{Y=1}^{N} \frac{CF_{in,degraded} - CF_{out}}{(1 + WACC)^{Y}} - CAPEX_{HESS} \tag{21}$$

Where:

- $n_{cyc,bat}$ is the annual battery cycles.
- $\delta_{battery}$ is the battery degradation rate.

- $D_{battery}$ is the annual battery degradation.

Table 3-5. Summary of parameters used for revenue and NPV calculations

Parameter	Description	Value	Reference
β_{diesel}	Specific diesel consumption by the generator	0.263 L / kWh	Graciolica
γ_{CO2e}	Specific CO_2 emissions for diesel	2.6 kg / L	-
C_{diesel}	Unit cost of diesel	€1.088 / L	Graciolica
C_{CO2e}	Unit cost per CO_2 emitted	€70 / tonne	2024 average
$CAPEX_{battery}$	Battery specific cost	€450 / kWh	Assumed
$CAPEX_{SC}$	SC specific cost	€32 /kW	Manufacturer Specified
$CAPEX_{SC,install}$	SC installation cost	€40,000	Manufacturer Specified
$OPEX_{battery}$	Battery annual OPEX	€2,000 / year	Assumed
$OPEX_{SC}$	SC annual OPEX	€2,000 / year	Manufacturer Specified
N	Project lifetime	10 – 20 years	-
$WACC$	Weighted average cost of capital	5.5 %	[28]
$\delta_{battery}$	Battery degradation rate	0.0046% / cycle	[27]

For the Case 2 analysis, where the SC is used to for battery assistance and ancillary service, we incorporated a hypothetical payment scheme to compensate for the contribution provided for power regulation. In reality, Graciolica cannot expect to receive revenue by utilizing the SC in this manner as Graciolica does not participate in an energy market and is only compensated for diesel and CO_2 emissions avoided. Additionally, the power regulation provided by the SC for the Case 2 scheme is applied to the power generated by Graciolica rather than to assist the external grid. In any case, applying a revenue scheme for this service was considered as a worthwhile exercise to evaluate the additional impact of that the supercapacitor could provide when used in this manner.

The renumeration for this power regulation service was set to 1 ₵ per kW minute of energy absorbed or injected by the SC. This is summarized in (22). This additional renumeration can be added to the NPV calculation with the NPV formula for Case 2 summarized in (23).

$$CF_{in,SC\ Reg} = C_{SC\ reg} \cdot \sum_{t=1\ minute}^{N} |P_{SC}| \tag{22}$$

$$NPV = \sum_{Y=1}^{N} \frac{CF_{in,degraded} + CF_{in,SC\ Reg} - CF_{Out}}{(1 + WACC)^{Y}} - CAPEX_{HESS} \tag{23}$$

Two other financial KPI’s were also considered, and these were payback time and internal rate of return (IRR). Payback time is the time in years for the HESS net revenues to recover the initial investment cost and this is calculated as per (24). IRR is the WACC required to make NPV = 0, and is represented in (25).

$$T_{payback} = \frac{CAPEX_{Hess}}{CF_{in,degraded} - CF_{Out}} \quad (24)$$

$$0 = \sum_{Y=1}^{N} \frac{CF_{in,degraded} - CF_{Out}}{(1 + IRR)^Y} - CAPEX_{HESS} \quad (25)$$

3.5. BATTERY AND HESS PERFORMANCE RESULTS

3.5.1. Battery Only Performance Results

Figure 3.1. shows an example of the original renewables and diesel power plant generation profiles, over a 48-hour period, starting from the 12 am on 3 January 2024. It also shows the augmented profiles when a 1200 kW/ 4800 kWh salt-based battery is simulated with the GA optimization tool. The salt-based battery is able to charge using renewable energy that was originally scheduled for curtailment, and discharge at a subsequent period to substitute some of the energy originally produced by the diesel power plant. Below is a summary of the generation system's behavior and the battery performance.

Time 0 - 5 hours:

- Power demand in Graciosa Island is met by a combination of diesel power generation and renewable energy.
- No curtailment of renewable energy, as the PV and windfarm are producing as much power as possible given by the current weather conditions.
- At this point, the salt-based battery is at its minimum SOC and therefore cannot discharge to offset some of the diesel generation. It cannot recharge as there is not curtailed renewable generation that it could use.
- The battery's temperature is at the minimum set point of 265°C, which decreases to 237 °C over this period. There is no external power available that can be used to heat the battery, and the battery does not have sufficient charge to self-heat.

Time 5 - 7 hours:

- The load demand on Graciosa Island can be met by renewable generation. In the original scenario, the renewable generation assets can produce up to 4000 kW, but only ~1500 kW is required; therefore 2500 kW are curtailed.
- With the salt-based battery, 170 kW of renewable energy that was originally curtailed, is now injected into the system and consumed by the salt-based battery, so that it can repeat itself to its minimum operating temperature of 265 °C.

Time 7 -13 hours:

- Over this period there is still ~1000 - 2000 kW of renewable power that is curtailed in the original scenario.

- The salt-based battery uses some of the curtailed renewable power to recharge to its maximum SOC of 90%.

Time 13 - 18 hours:

- There is still some renewable power curtailment over this period.
- Although the battery is at full SOC, it consumes some of the originally curtailed renewable power to heat itself and maintain temperature at its minimum operating setpoint.

Time 18 - 23 hours:

- There is no more curtailed renewable power, and the PV and wind generation assets are producing the maximum possible power based on the current weather conditions.
- In the original scenario, the diesel generator comes online to help meet some of the demand in the network.
- The salt-based battery discharges substitute the load originally met by the diesel generator. For the first hour, it can completely offset the diesel generation, and subsequently it only partially offsets the diesel generation. The battery discharges until it reaches its minimum SOC limit.
- The temperature of the battery has increased to 276 °C by the end of this period, due to the heating from the ohmic losses during discharge operation.

Time 23 - 38 hours:

- There is no curtailed renewable energy, and diesel generator is operating to meet the demand of the network.
- Battery cannot recharge as there is no curtailed renewable energy. Additionally, its temperature decreases to 194 °C as it does not have sufficient charge and there is no external power supply for heating.

Time 38 - 42 hours:

- There is a brief moment of curtailed renewables energy. The salt-based battery uses this for heating, however it does not occur for long enough for the battery to reach its minimum temperature, let alone for recharging.
- Following the brief curtailed energy, the battery cools down back to 194 °C

Time 42 - 48 hours:

- The renewable generation assets produce about 2000 KW in the original scenario and curtail a further 2000 kW. This gives the battery the opportunity to reheat and recharge.
- It takes ~ 3 hours for the battery to reheat itself to its minimum operating temperature, before it can start to recharge.

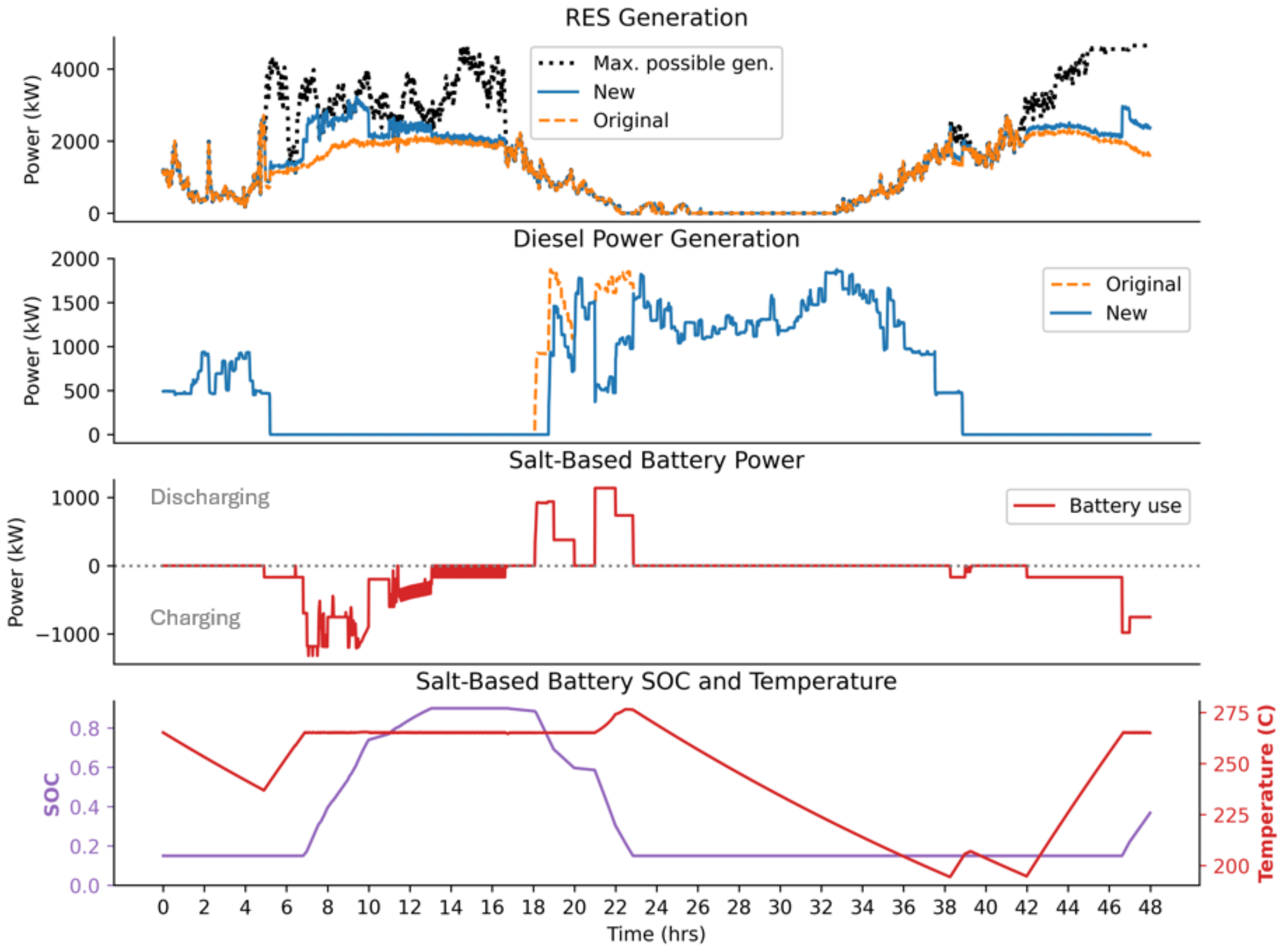

Figure 3.3 - Interaction of a 1200 kW/4600 kWh salt-based battery with Graciolica's generation assets over 48 hours (sample from 3 January 2024, 1-minute resolution).

Based on the example in Figure 3.3 and the detailed summary above, it is clear that the salt-based battery can reduce the renewable power curtailment and reduce diesel consumption. However, there is a notable drawback, where the battery will have to use available renewable power to first reheat itself, if it is below its minimum temperature, before it can use this power to recharge. Additionally, and not observed in this example, the battery will self-discharge to maintain its temperature at the minimum setpoint. During prolonged and intermittent periods of low renewable power curtailment, this will mean that the battery will remain on its minimum SOC and only use renewables to reheat, meaning that the battery will not provide any benefit during these times. To further illustrate this, Figure 3.4 shows yearlong results for the renewable and diesel generation profile and the 1200 kW / 4800 kWh battery performance. Additionally, Figure 3.5 shows the monthly RES energy used by each battery size, the monthly diesel reduction, and the energy profiles for surplus RES availability, original diesel usage by Graciolica. During the summer months (May – October), there is very low renewable power curtailment, and which is attributed to the low wind speeds and therefore low wind generation potential, compared to the rest of the year. This is typical for the Azores, where wind power generation is low over this period, with August being the lowest wind generation month [29]. This clearly impacts the performance of the salt-based battery, as it barely operates in these months, particularly during August and September. During these months, the periods of renewable energy curtailment occur briefly and too far apart, such that the battery can only partially reheat and then cool down before the next period of curtailed energy. Hence the salt-based battery cannot offset diesel generation for a significant portion of the year.

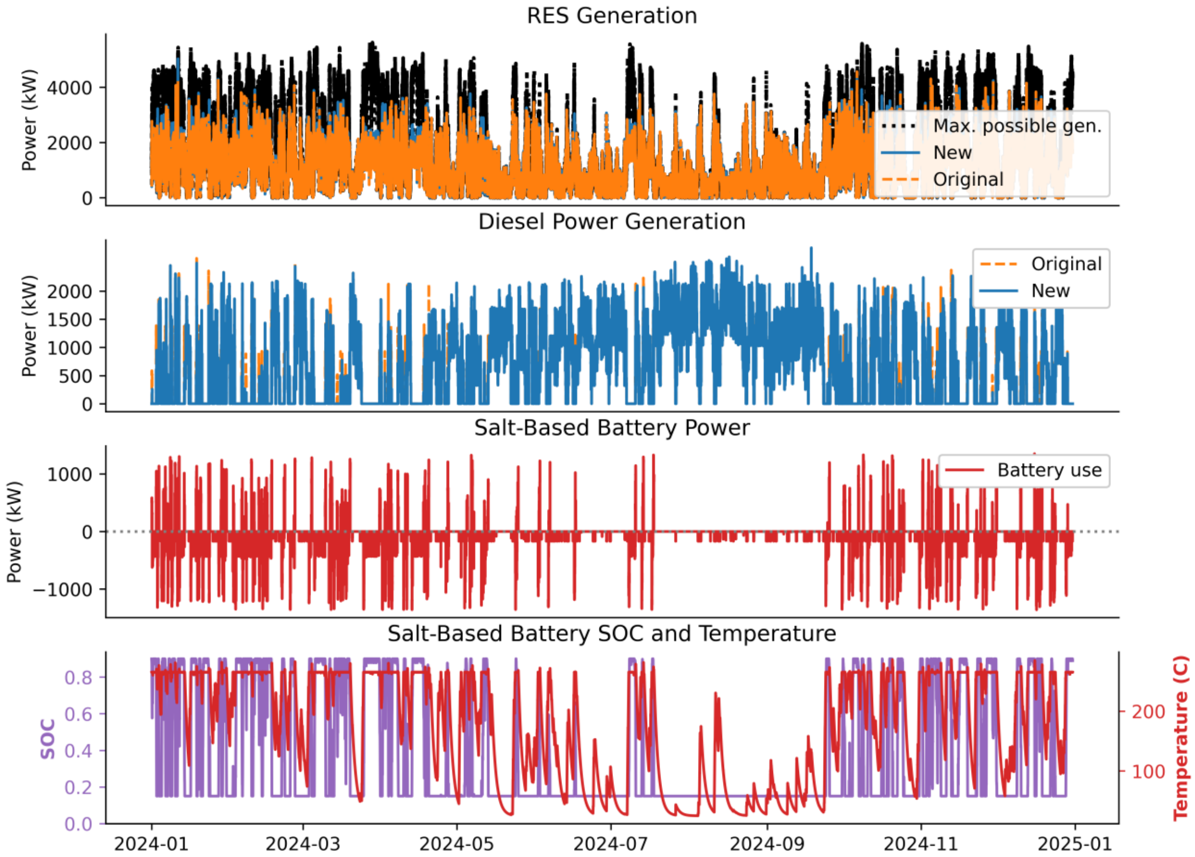

Figure 3.4 - Yearlong results for a 1200 kW / 4800 kWh salt-based battery, showing generation profiles, battery power, SOC, and temperature.

Figure 3.5 shows how the battery's ability to offset diesel usage is greatly affected by the available surplus RES to recharge the battery. This is reinforced by the clear trend between amount of RES available and the amount of diesel the batteries have reduced. We see that January is the best performing month, where all battery sizes reduce the most diesel, compared to their respective performance in the other months. This is followed by February and November and coincides with the months where there is high curtailed RES available for battery charging. As explained previously, we see the lowest diesel reduction during the summer months where surplus RES is at minimum availability.

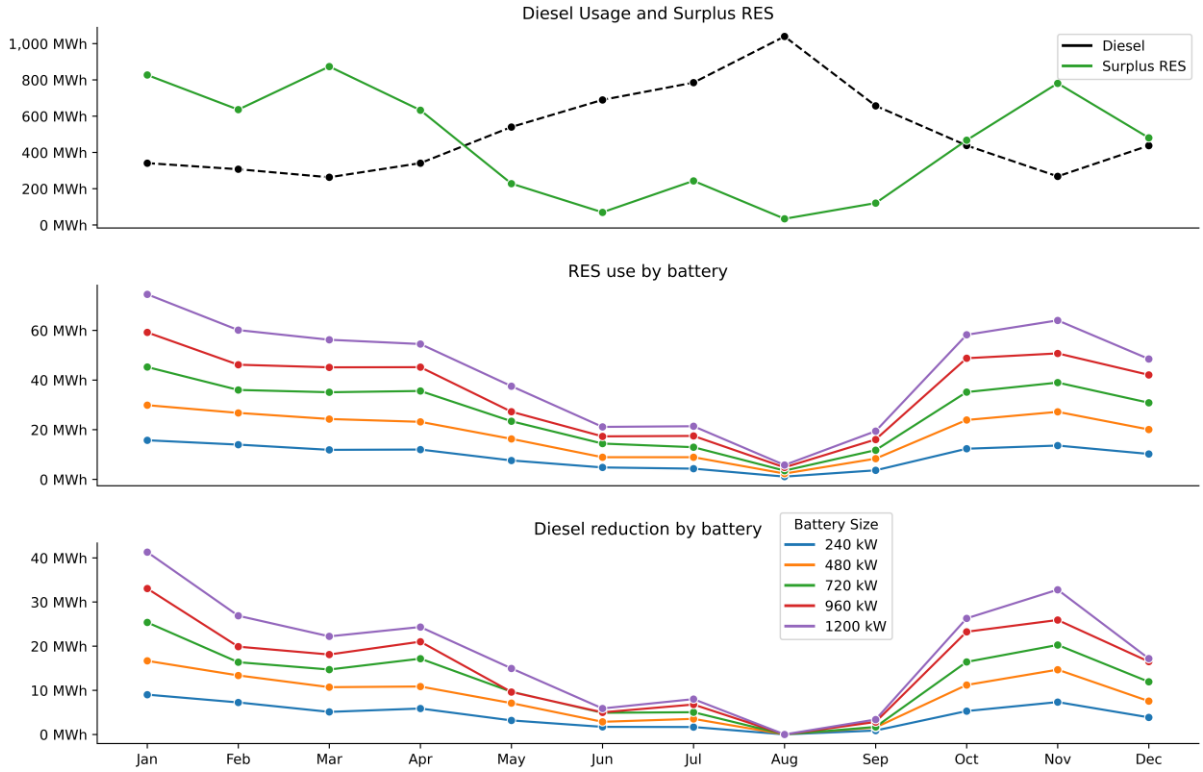

Figure 3.5 Monthly surplus RES and diesel use, and battery energy use

Table 3-6. shows the results for the battery-only simulation for each battery size, in terms of absolute and relative total diesel reduction over the year, where the original annual diesel energy produced 6,104,338 kWh and the total surplus RES is 5,391,654 kWh. The results also show the increase in renewable energy generation due to curtailment reduction and using the excess power to recharge the salt-based battery. We also show Table 3-7. , which shows the diesel reduction and renewable energy increase for the month of January 2024, which was the best performing month. For January, the total original diesel consumption is 340,723 kWh and the surplus RES is 826,839 kWh . The following observations are made:

- Increasing the battery size will increase the reduction of diesel and reduction of renewable energy curtailment. This would be expected as a larger battery size would have more energy storage capacity to both uptake renewable generation and offset diesel generation.
- For the 1 year-long results we see that the reduction in diesel consumption is ~ 0.8% to 3.7%. For the 1-month results, the relative reduction in diesel consumption is significantly higher at ~3% to 13.5 %. The discrepancy between the 1 month and 1-year results can be attributed to the surplus RES that is available to recharge the battery. For the yearlong results, surplus RES energy is equal to ~88% of the total original diesel consumption; however, for the 1-month results, surplus RES energy is equal to 242% of January's total diesel consumption. This comparison highlights how important surplus RES energy is to reduce meaningful amounts of diesel consumption.
- For the 1-year results, absolute renewable energy use increase is over 2 times greater than absolute diesel energy reduction for each battery size. Because the renewable energy increase corresponds to the charging energy supplied to the battery, and the diesel reduction corresponds to the energy discharged by the battery, it would be expected that the diesel

energy reduction would be about 10-15% less than renewable energy increase due to the internal losses of the battery and power converter. However, as we have hinted in Figure 3.3 and Figure 3.4, a large portion of curtailed renewable energy and energy stored in the battery must be used for heating the battery, hence why we see a significant difference between the increase of renewable energy and decrease of diesel energy. This is further illustrated in Figure 3.6 and Figure 3.7 which show the distribution of the charging and discharging energy over the yearlong and 1 month long (for January 2024) periods, respectively, for the different internal battery processes. For example, for the 1200 kW/4800 kWh battery, only 58.9% of the charging energy supplied by the curtailed renewable energy generation is stored in the battery. The remaining energy is used to reheat the battery or is lost due to the internal resistance of the battery and power converter. A similar pattern occurs during discharging, where only 72.7% of the total energy stored by the battery is used to offset the diesel energy. The remainder is lost due to self-discharge for battery heating or internal losses from the battery and power converter.

- Looking at the 1-month long results, absolute renewable energy increase is about 1.75 – 1.8 times greater than absolute diesel energy reduction for each battery size. This difference between RES and diesel energy changes is smaller than the observation made above for the yearlong simulation; this is because a greater portion of renewable energy absorbed by the battery is being stored in the battery as energy, as instead of being used for battery heating. Looking at Figure 3.6, we see that 25.9 - 27% of the energy absorbed by the battery is used for heating over the 1-month periods, whereas for the yearlong period this is 33.8 to 36.1%. During January, the battery is constantly in use, hence, it can maintain its minimum setpoint temperature via the battery ohmic losses during operation. They are only few standby periods, hence less opportunities for the battery to cool down when not in use, resulting in less energy required to actively heat the battery.

Table 3-6. Yearlong 'battery-only' results showing diesel reduction and reduced RES curtailment.

Battery Size	Diesel Reduction (kWh)	% Diesel Reduction	Renewable Energy Increase (kWh)	% Curtailment Reduction
240 kW	51,134	0.838%	110,992	2.06%
480 kW	100,020	1.639%	219,842	4.08%
720 kW	143,480	2.350%	322,698	5.99%
960 kW	181,901	2.980%	419,957	7.79%
1200 kW	223,182	3.656%	521,145	9.67%

Table 3-7. January 2024 'battery-only' results showing diesel reduction and reduced RES curtailment.

Battery Size	Diesel Reduction (kWh)	% Diesel Reduction	Renewable Energy Increase (kWh)	% Curtailment Reduction
240 kW	9,009	2.94%	15,701	1.90%
480 kW	16,664	5.43%	29,817	3.61%
720 kW	25,377	8.28%	45,160	5.46%
960 kW	33,047	10.78%	59,095	7.15%
1200 kW	41,301	13.47%	74,431	9.00%

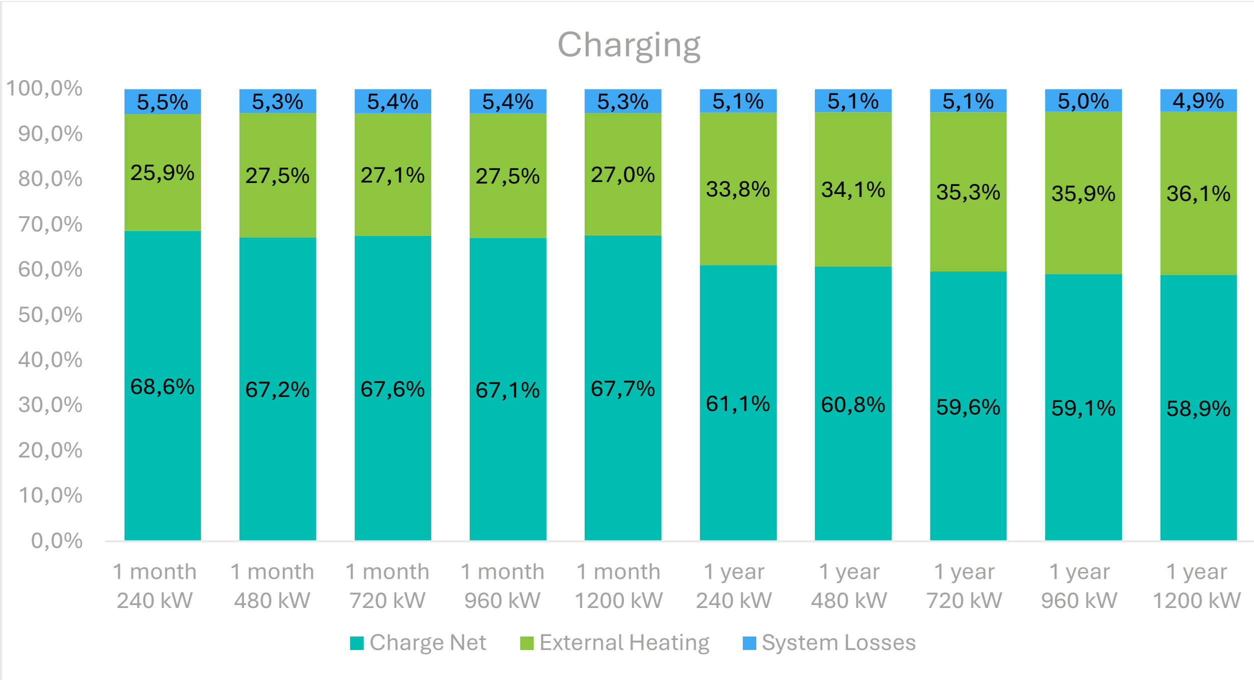

Figure 3.6 - Distribution of energy supplied to the battery by curtailed RES during charging. Includes net stored energy, external heating, and system losses.

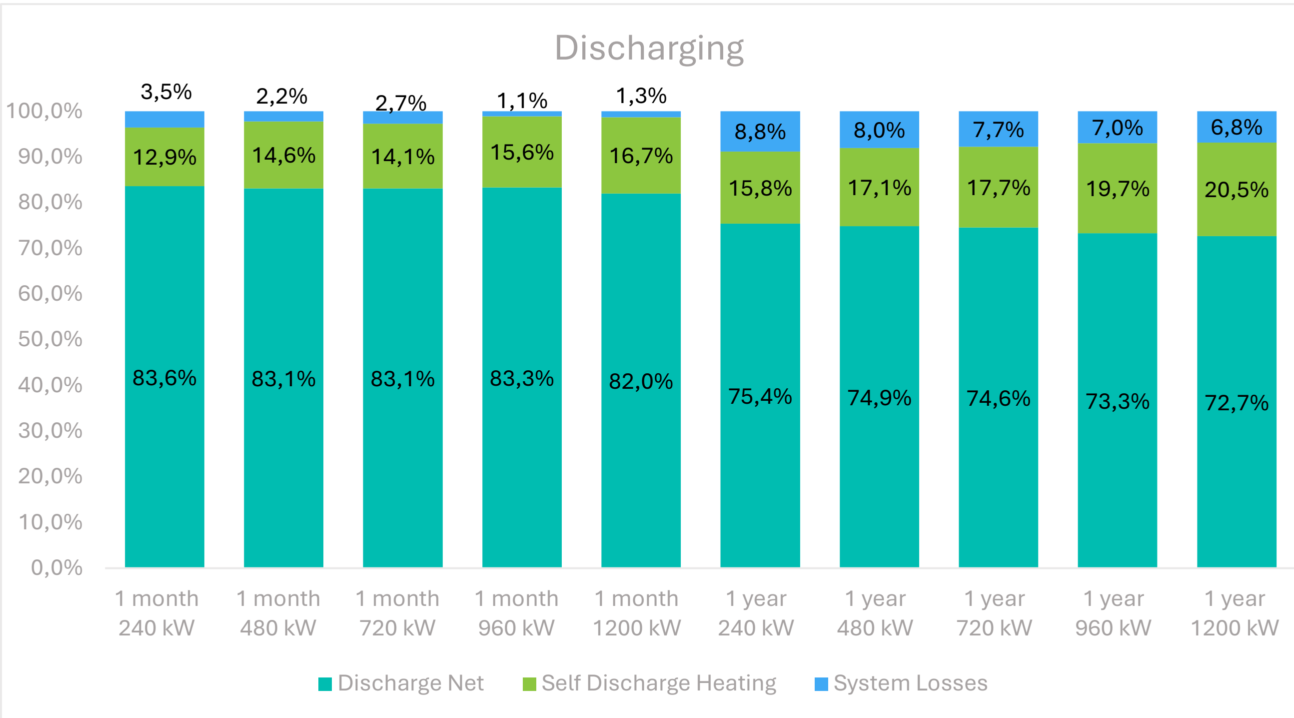

Figure 3.7 - Distribution of energy supplied by battery for energy offsetting diesel during discharging, including net discharging, self-discharge heating, and system losses.

3.5.2. HESS Performance Results

The results from the simulations are shown in Table 3-8 and Table 3-9 below, for case 1 and case 2, respectively. The results show the reduction in diesel usage and increase in renewable usage (reduction in curtailment) for the entire year.

Table 3-8 Summary of results for HESS, case 1.

Metric	BESS Size	SC Size					
		0 kW	1200 kW	2400 kW	3600 kW	4800 kW	6000 kW
Diesel Reduction (kWh) (%)	240 kW	51,134 (0.838%)	51,211 (0.839%)	51,235 (0.839%)	51,270 (0.840%)	51,297 (0.840%)	51,314 (0.841%)
	480 kW	100,020 (1.639%)	100,062 (1.639%)	100,114 (1.640%)	100,137 (1.640%)	100,161 (1.641%)	100,183 (1.641%)
	720 kW	143,480 (2.350%)	143,527 (2.351%)	143,569 (2.352%)	143,612 (2.353%)	143,636 (2.353%)	143,685 (2.354%)
	960 kW	181,901 (2.980%)	181,974 (2.981%)	182,030 (2.982%)	182,090 (2.983%)	182,146 (2.984%)	182,192 (2.985%)
	1200 kW	223,182 (3.656%)	223,285 (3.658%)	223,360 (3.659%)	223,485 (3.661%)	223,515 (3.662%)	223,655 (3.664%)
RES Curtail. Reduction (kWh) (%)	240 kW	110,992 (2.059%)	111,156 (2.062%)	111,230 (2.063%)	111,303 (2.064%)	111,364 (2.065%)	111,406 (2.066%)
	480 kW	219,842 (4.077%)	219,970 (4.080%)	220,087 (4.082%)	220,165 (4.083%)	220,233 (4.085%)	220,291 (4.086%)
	720 kW	322,698 (5.985%)	322,837 (5.988%)	322,955 (5.990%)	323,061 (5.992%)	323,139 (5.993%)	323,236 (5.995%)
	960 kW	419,957 (7.789%)	420,139 (7.792%)	420,286 (7.795%)	420,416 (7.798%)	420,548 (7.800%)	420,645 (7.802%)
	1200 kW	521,145 (9.666%)	521,380 (9.670%)	521,558 (9.674%)	521,785 (9.678%)	521,878 (9.679%)	522,110 (9.684%)

Table 3-9 Summary of results for HESS, case 2.

Metric	BESS Size	SC Size					
		0 kW	1200 kW	2400 kW	3600 kW	4800 kW	6000 kW
Diesel Reduction (kWh) (%)	240 kW	51,134 (0.838%)	50,463 (0.827%)	50,298 (0.824%)	50,223 (0.823%)	50,161 (0.822%)	50,103 (0.821%)
	480 kW	100,020 (1.639%)	99,228 (1.626%)	99,031 (1.622%)	98,953 (1.621%)	98,884 (1.620%)	98,800 (1.619%)
	720 kW	143,480 (2.350%)	142,601 (2.336%)	142,371 (2.332%)	142,257 (2.330%)	142,179 (2.329%)	142,113 (2.328%)
	960 kW	181,901 (2.980%)	180,998 (2.965%)	180,780 (2.962%)	180,672 (2.960%)	180,596 (2.958%)	180,491 (2.957%)
	1200 kW	223,182 (3.656%)	222,296 (3.642%)	222,079 (3.638%)	221,988 (3.637%)	221,963 (3.636%)	221,945 (3.636%)
RES Curtail. Reduction (kWh) (%)	240 kW	110,992 (2.059%)	111,531 (2.069%)	111,693 (2.072%)	111,792 (2.073%)	111,892 (2.075%)	111,991 (2.077%)
	480 kW	219,842 (4.077%)	220,264 (4.085%)	220,390 (4.088%)	220,497 (4.090%)	220,607 (4.092%)	220,681 (4.093%)
	720 kW	322,698 (5.985%)	323,171 (5.994%)	323,302 (5.996%)	323,403 (5.998%)	323,522 (6.000%)	323,614 (6.002%)
	960 kW	419,957 (7.789%)	420,483 (7.799%)	420,640 (7.802%)	420,749 (7.804%)	420,892 (7.806%)	420,971 (7.808%)
	1200 kW	521,145 (9.666%)	521,788 (9.678%)	521,981 (9.681%)	522,130 (9.684%)	522,343 (9.688%)	522,533 (9.692%)
SAFB (%)	240 kW	-	3.56%	5.92%	8.13%	10.09%	11.90%
	480 kW	-	3.50%	5.81%	8.00%	9.92%	11.66%
	720 kW	-	3.53%	5.86%	8.07%	9.98%	11.70%
	960 kW	-	3.53%	5.84%	8.04%	9.94%	11.67%
	1200 kW	-	3.54%	5.86%	8.05%	9.92%	11.60%

Using the equations summarized in Section 3.4.5, the renumeration for the reduction of diesel consumption and CO_2 emissions were calculated for the various HESS arrangements for Case 1 and are shown in Figure 3.8. Note that the median return values are shown for each HESS battery size, as adding and increasing the SC sizes for each arrangement causes a variation of up to ± €80. The 1-month renumeration was projected for 12 months to compare the best performing month with the overall annual performance. We can see that the results for the 1-month-projected-to-1-year outperform the actual 1 year by ~ 3 times as much, which reinforces our previous claim that a high amount of surplus is RES is required for the salt-based battery to be able to offset diesel consumption and obtain higher renumeration based on cost savings.

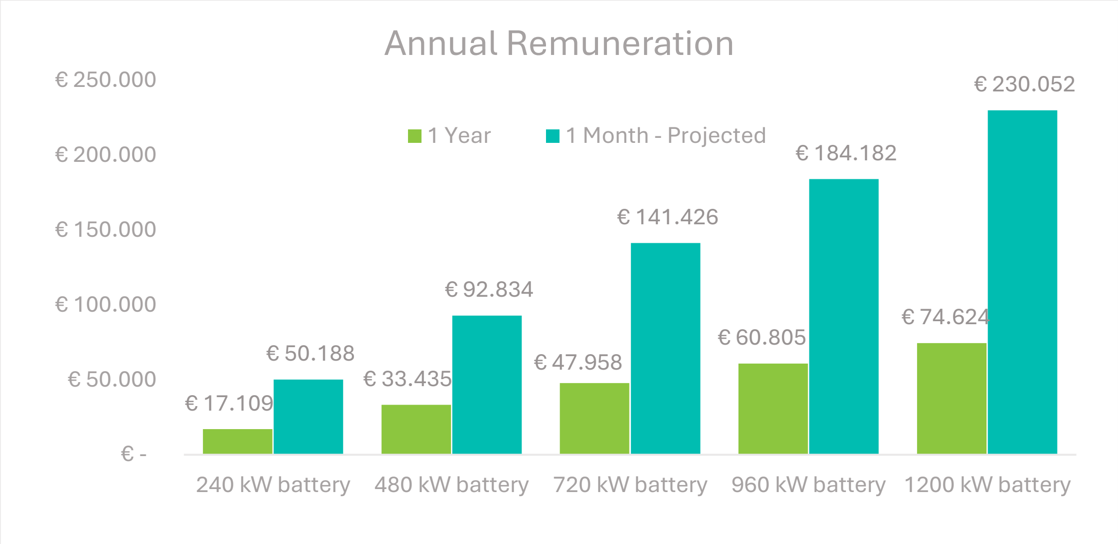

Figure 3.8 Case 1 median renumeration for battery only arrangement for 1 year and 1 month projected to 1 year.

Figure 3.9 below illustrates the annual remuneration earned by the SC for providing regulation services when assessing Case 2. As the size of the SC increases, the revenue from regulation also increases. This is expected, since a larger SC has greater capacity to inject or absorb energy, enabling it to smooth fluctuations more effectively and participate more frequently in regulation, resulting in higher compensation. Conversely, as the battery size increases, the remuneration received by the SC decreases. This occurs because a larger battery is more likely to fully offset periods of diesel generation, reducing the frequency and extent of fluctuations that the SC would need to regulate, thus lowering the SC's contribution and associated earnings.

Figure 3.10 shows the total renumeration received by each HESS arrangement, for reducing diesel and CO_2, and for providing regulation. These results correspond approximately as the some of the results in Figure 3.9 with the results for the 1- year renumeration for battery only scenarios as seen in Figure 3.8. We note that the results Figure 3.8 are for Case 1, and the reduced diesel has relatively minor discrepancies when compared to those of Case 2 (see Table 3-8 and Table 3-9). For increasing SC sizes, the renumeration increases, which is expected as more remuneration is received from the increase in regulation activity, similar to what was seen in Figure 3.9. However, this time, for increasing battery sizes, the remuneration also increases, which the opposite of what was seen in Figure 3.9. The remuneration received by the salt-based battery offsetting diesel use is ~ 1.7 – 3 times greater than the renumeration received for regulation, hence this dominates and is why we see increasing revenue for increasing battery sizes.

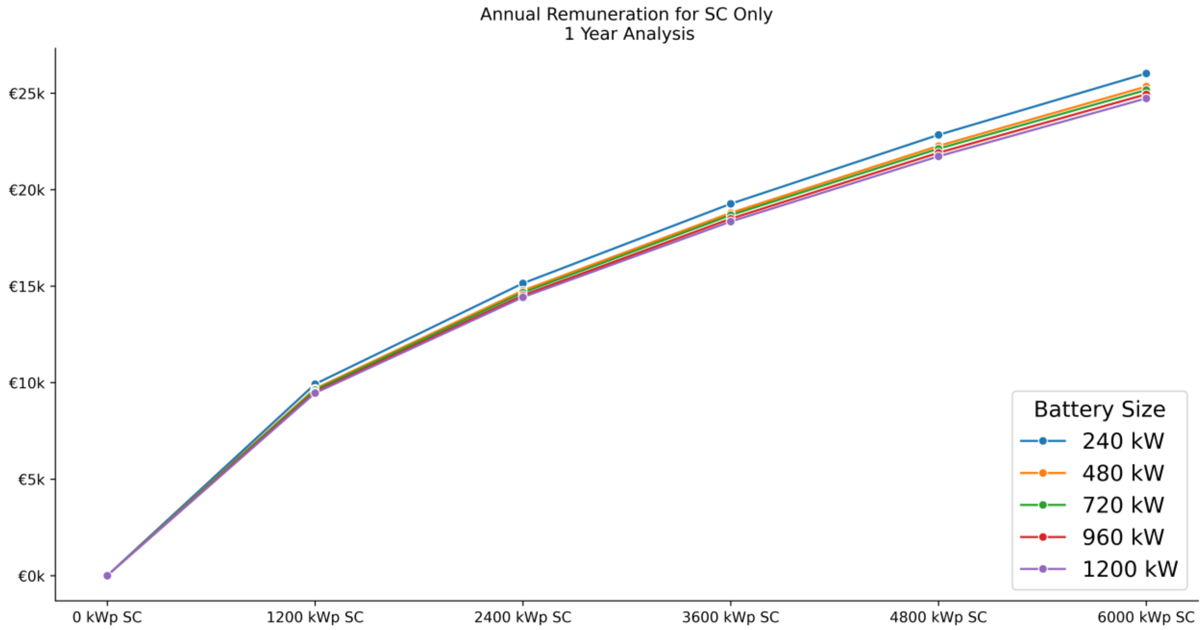

Figure 3.9 Case 2 renumeration for the regulation component only for a 1 year analysis.

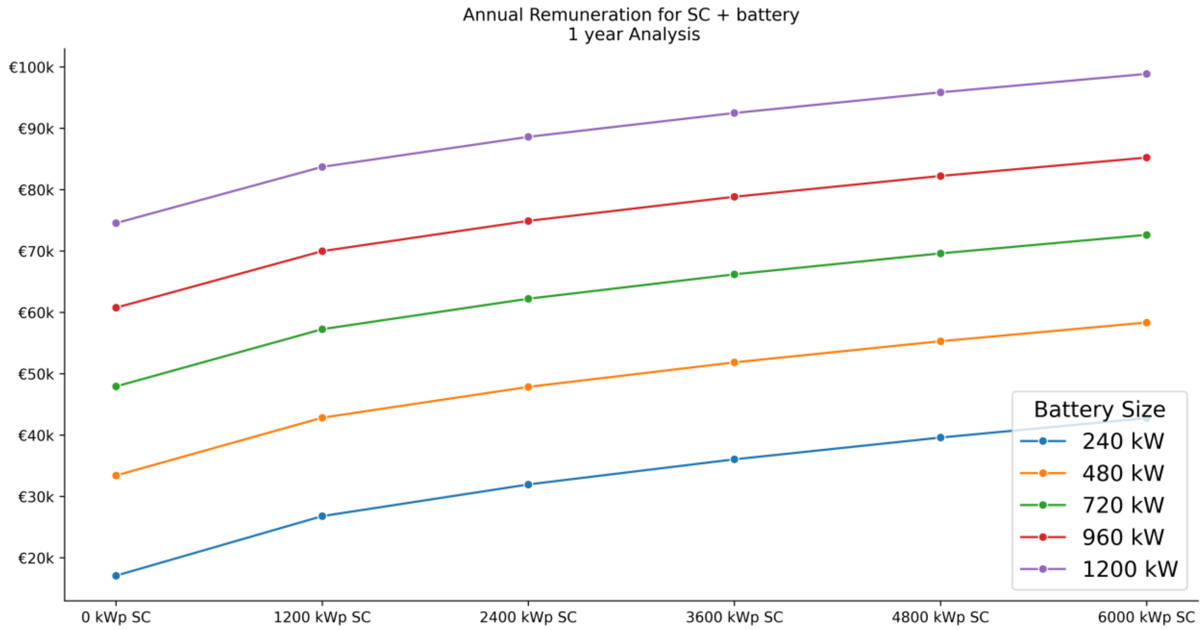

Figure 3.10 Case 2 total renumeration for the diesel reduction and regulation for a 1 year analysis.

Lastly, we show the same results, but for a 1-month-projected-to-1-year analysis for the month of January in Figure 3.11 and Figure 3.12. We see that the renumeration received for the regulation component is lower than the 1-year results as seen in Figure 3.9, by approximately 40%. This is because the month of January was not the best performing month for the SC, that is to say, there was relatively little need for regulation over this month compared to others;

therefore, less compensation was received for this activity. Despite this, the total renumeration was greater for 1-month-projected-to-1-year compared to the 1- year results. This aligns with our expectations, as we have already seen how this is the best performing month in terms of diesel reduction and that the income received by the battery-provided services dominates the total renumeration received.

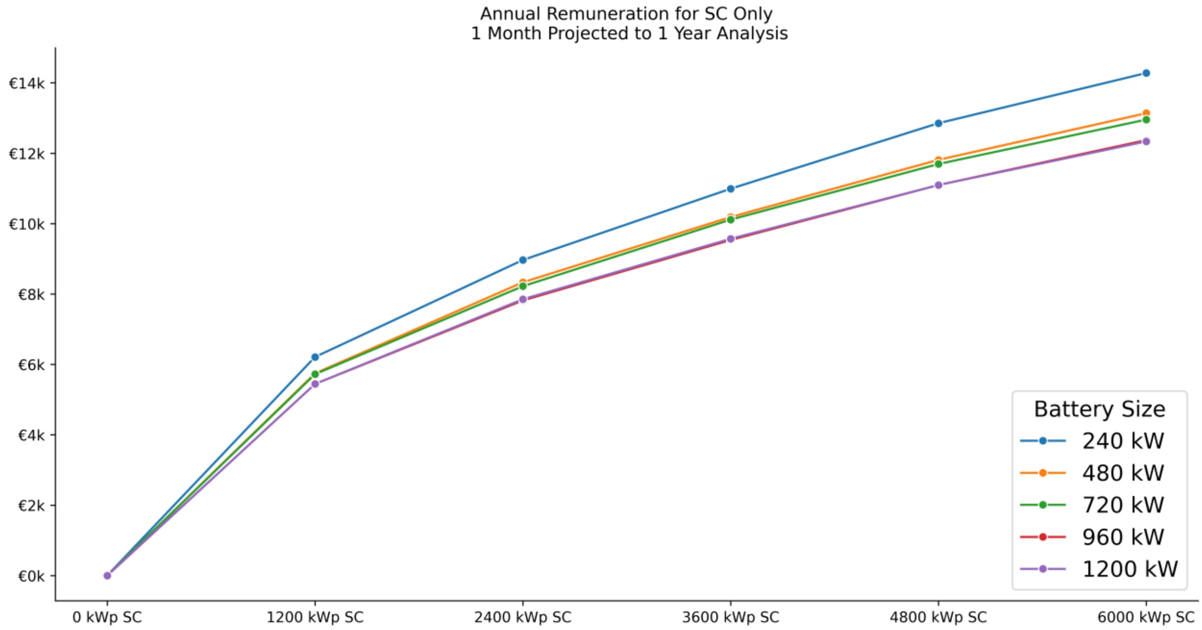

Figure 3.11 Case 2 renumeration for the regulation component only for a 1-month-projected-to-1-year analysis.

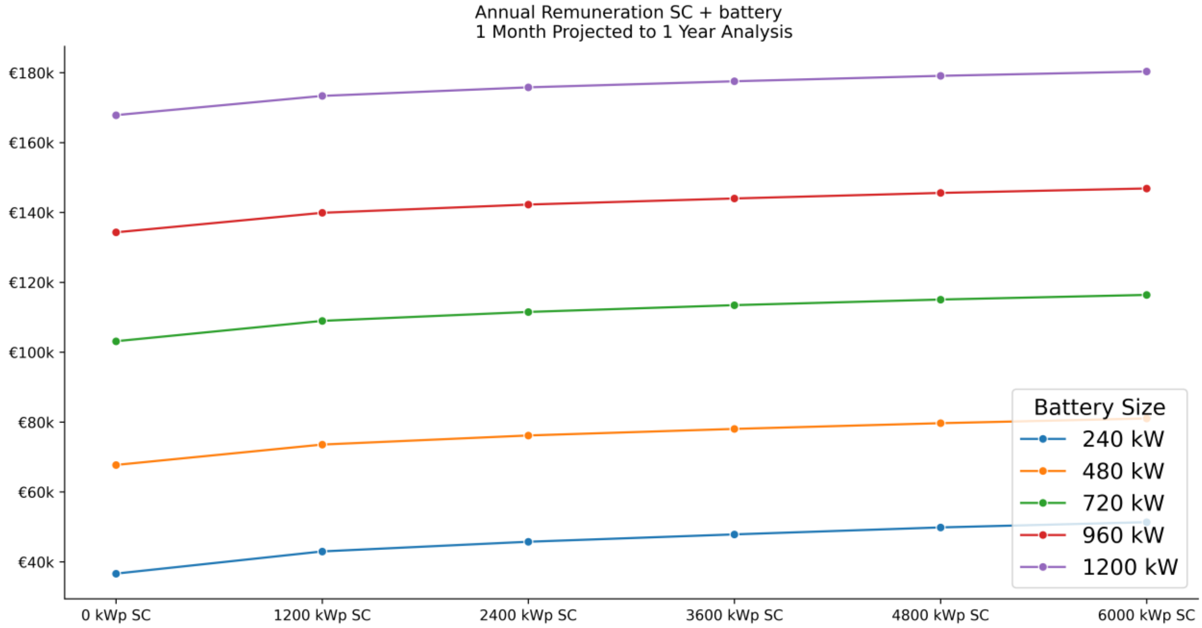

Figure 3.12 Case 2 total renumeration for the diesel reduction and regulation for a 1-month-projected-to-1-year analysis.

3.6. TECHNO-ECONOMIC ANALYSIS

3.6.1. Case 1 Results

Case 1 Results – 1 Year

NPV results were calculated for the different HESS arrangements, for project periods of 10, 15 and 20 years. The results are summarised in Figure 3.13 and given by the negative NPV values for all arrangements, the project is not economically viable under the assumptions used. For increasing battery sizes, we see more negative NPVs, outlining that the CAPEX dominates and future cashflows given by the diesel and CO_2 emission savings are not sufficient to offset the initial project costs. We do see as light improvement in NPV as we increase the assessment period, and the gains are more prominent for larger battery sizes. For example, the absolute NPV difference between the most negative NPV of 10 years, to the best NPV of 20 years for the 240 kW battery HESS arrangements vary by ~€54,000 to €63,000. For the largest battery of 1200 kW the NPVs vary by €297,000 to €306,000. With the addition of a supercapacitor into the arrangement, we see a sudden decrease in NPV, as can be seen by notable difference between the HESS with 0 kW SC and HESS with 1200 kW SC. Following this, the NPV decreases gradually with increasing SC size. This would be expected as we have seen in the diesel reduction results in Table 3-8 and Table 3-9, and the first year renumeration in Figure 3.8, that the SC provides little contribution to cost savings, hence the large CAPEX would offset cashflows acquired from the battery and SC contributions.

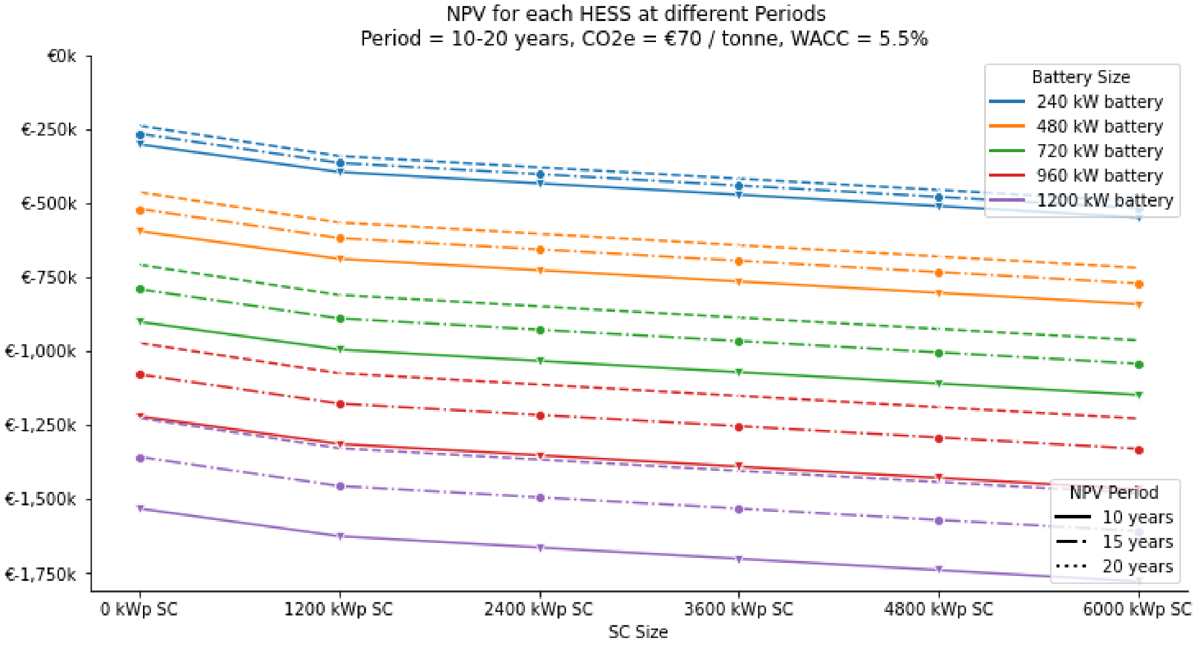

Figure 3.13 - NPV calculation for different HESS sizes for 10, 15, and 20-year project periods, with a battery CAPEX of €450/kWh.

The annual cost savings for each HESS is presented in the top left subplot in Figure 3.14, as a percentage of the total original annual diesel and CO_2 emission costs. The adjacent subplots show the minimum required annual cost savings each HESS would need to make NPV = 0, which corresponds to sufficient future cashflows that would allow the project to break even with the initial investment cost. To break even at NPV 20 years, cost savings must be increased by 2.2 to 3.5 times of the currently determined annual savings, and for NPV 10 years, cost savings must increase by 3.4 to 5.3 times.

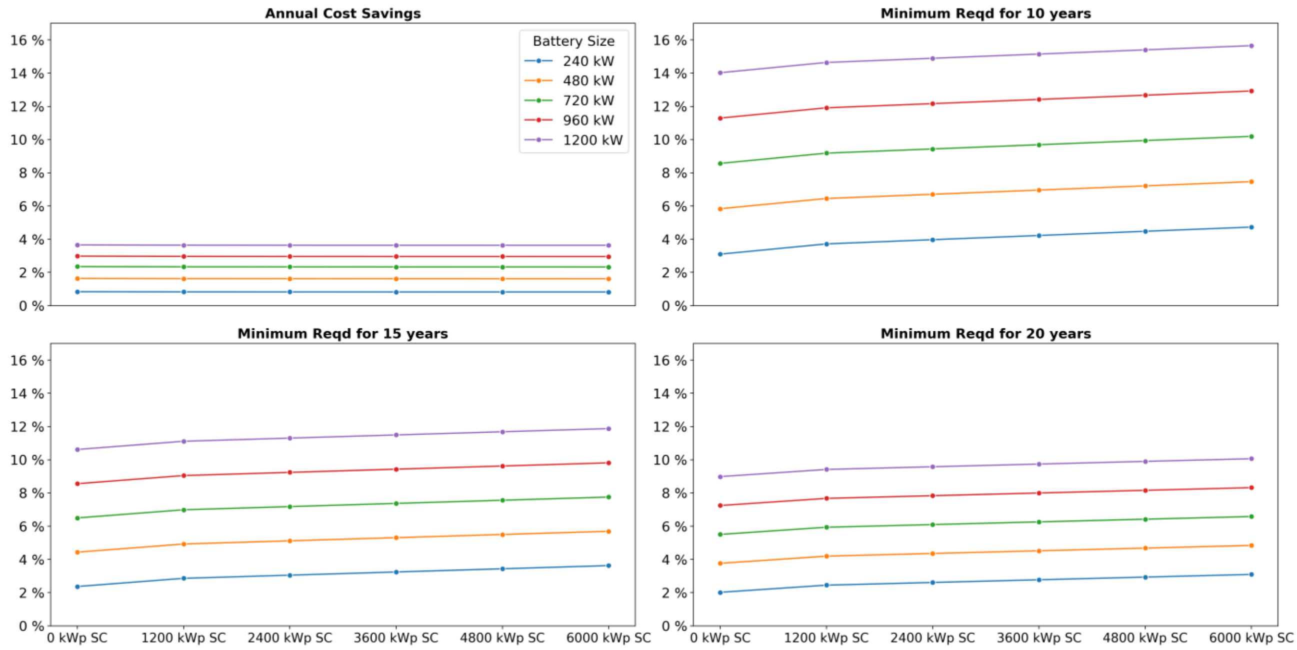

Figure 3.14 - Annual and required cost savings for diesel use and CO2 emissions to achieve NPV = 0 for 10, 15, and 20-year project periods

Figure 3.15 - Minimum shows the minimum specific battery costs, required to make the NPV = 0 for the 'battery-only' arrangement for different project periods. This assessment shows that the specific battery CAPEX must be reduced to €120 - €195 per kWh for the project to start to become economically viable. The current specific battery CAPEX used in the first NPV assessment was €450 / kWh, based on several studies, which is 2.3 - 3.75 times greater than the target. Forecasts anticipate that ZEBRA batteries will have a specific CAPEX of ~€350 per kWh by 2035 [30], which highlights that any expected CAPEX reduction in the near term is unlikely to impact project viability.

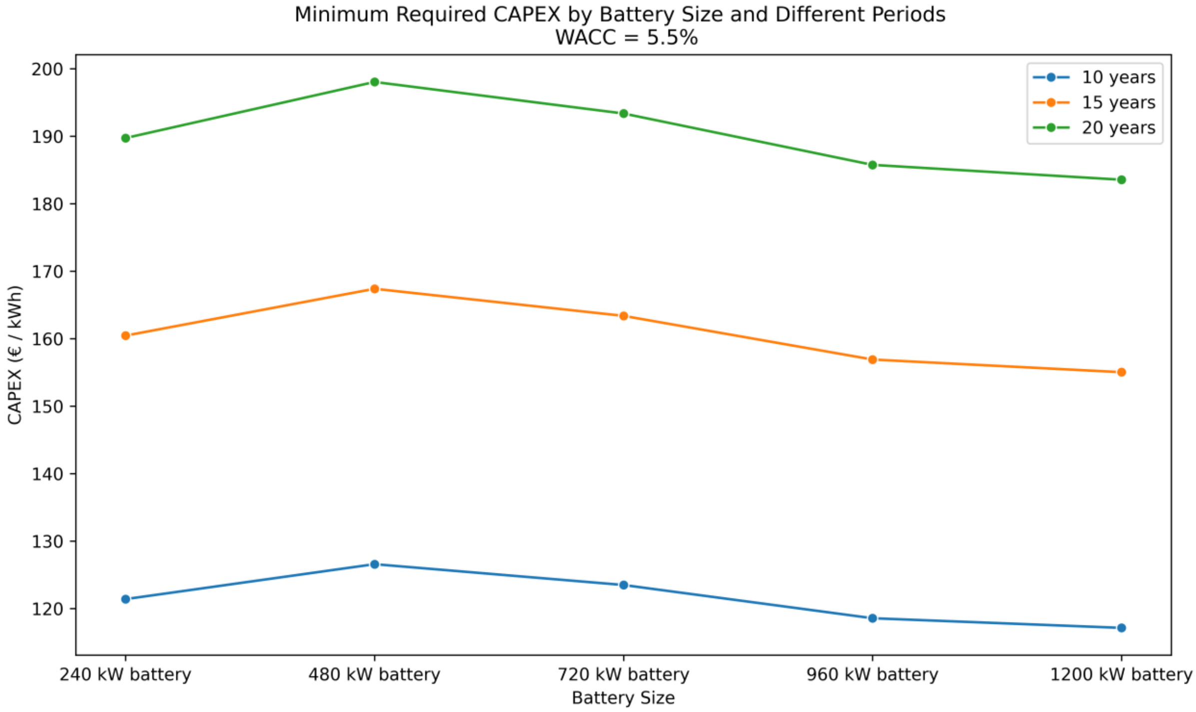

Figure 3.15 - Minimum battery costs to achieve NPV = 0 for 10, 15, and 20-year project periods.

Lastly, a CO_2 emission cost sensitivity analysis is carried out. So far, this techno-economic analysis has assumed a constant cost for CO_2 emissions at €70 per tonne. However, it is likey that over the 10 – 20 evaluation period, this could increase, therefore it is necessary to understand how this may impact the profitability of the project. Three additional NPV assessments were carried for different CO_2 emission cost projections, as shown in Figure 3.16. These scenarios are as follows

- Average 2025 - €70 per tonne, which has been used in the analysis thus far.
- Low projection - Emission costs will increase steadily at €1 per tonne
- Medium projection - Emission costs will increase steadily at €5 per tonne.
- High projection - Emission costs will increase rapidly up to €177 per tonne, as forecast by BloombergNef [31].Note that their forecast is only up to 2035, hence it was assumed that the costs would plateau following this year.

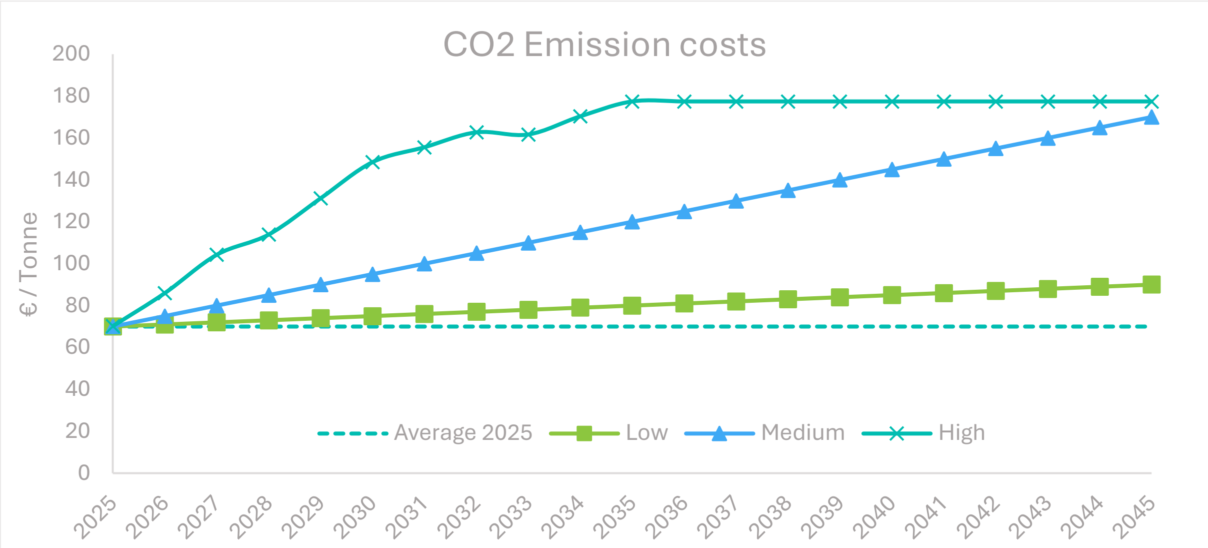

Figure 3.16 Projected CO2 emission costs

A sensitivity study was carried out to calculate NPV's for the three CO_2 emission cost projections, over a period of 10 – 20 years, and the results are shown in Figure 3.17 below. We can see that for each HESS and project period, the NPV increases as we move between the low CO_2 cost projection to the high CO_2 cost projection. This improves the NPV only slightly, and the same general trend can be observed, where the results are negative, and decreasing with battery size and with SC size. Despite adjusting the CO_2 emission costs, not enough returns are earned to make this a financially attractive project.

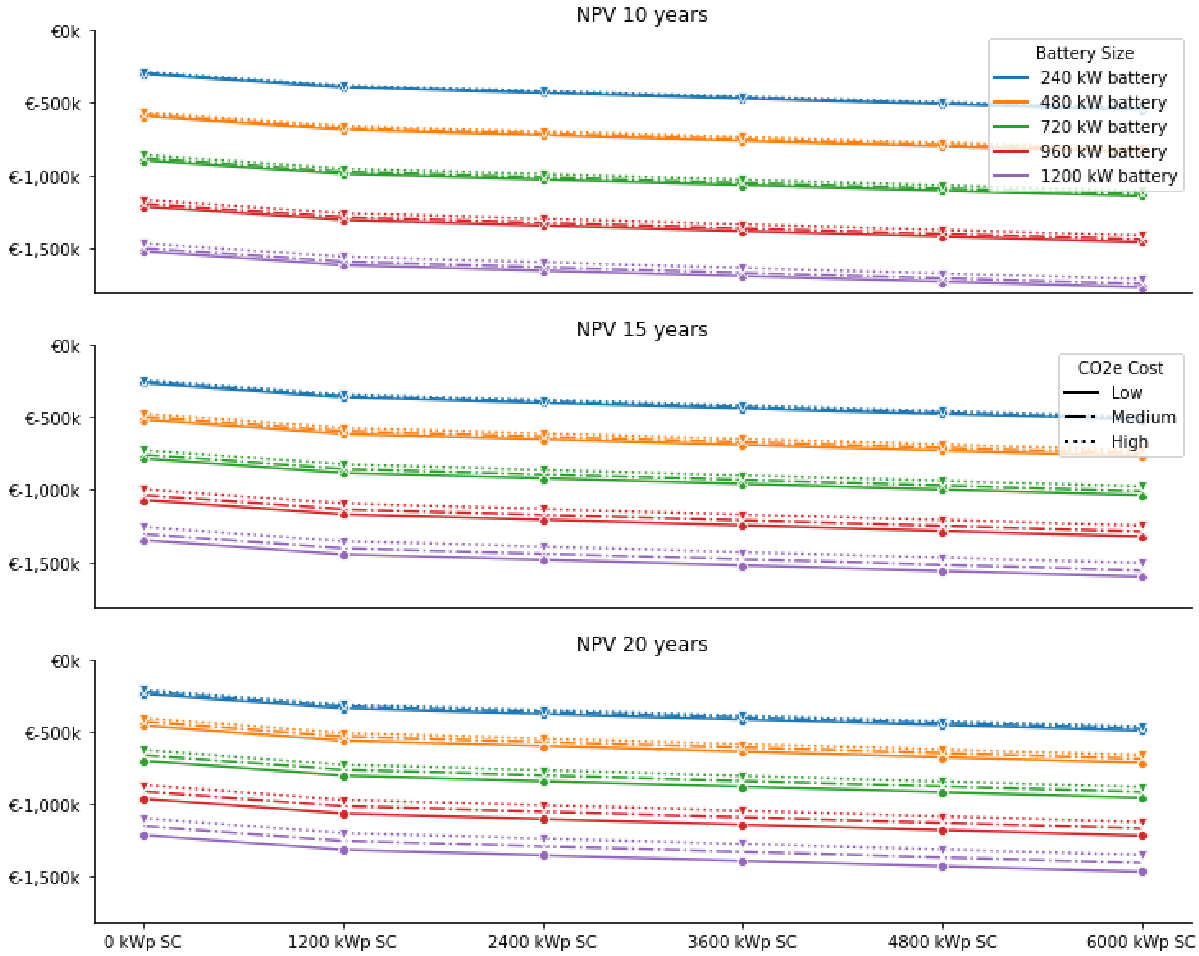

Figure 3.17 Sensitivity study

Case 1 Results – 1-Month projected to 1-year

An additional analysis was carried out using the renumeration results for the month of January, with corresponding annual revenue obtained by projecting for a 1-year period, as per Figure 3.8. As mentioned previously, January was the best performing month where the most diesel and CO_2 emissions were abated, as there was high availability of surplus RES, allowing the battery to operate frequently, maintain its temperature efficiently and maximize opportunities to displace diesel use. Therefore, it would be interesting to carry out a financial analysis for based on the period where the batteries operated under the most favorable conditions during the year.

An NPV analysis was carried out for each HESS over a period of 10 -20 years, using the January renumeration projected over a year long period. This was carried out using the three different CO_2 emission cost projections (low, medium and high) as per Figure 3.16. The NPV results are summarized in Figure 3.18. For this assessment, we see that the NPVs are better performing than for the 1- year assessment shown Figure 3.17, however with the NPV results still remain negative, with the exception of NPV 20 years with CO_2 emissions priced at medium and high cost projections. In these positive NPV cases, we see that cost savings from the CO_2 emissions and diesel reduction causes the future cashflows to dominate over the initial investment cost.

Looking at the NPV results for 20 years for the high CO_2 emission cost we see that the three largest batteries, 720 - 1200 kW, have a positive NPV with SC sizes up to 2400 kW – 3600 kW.

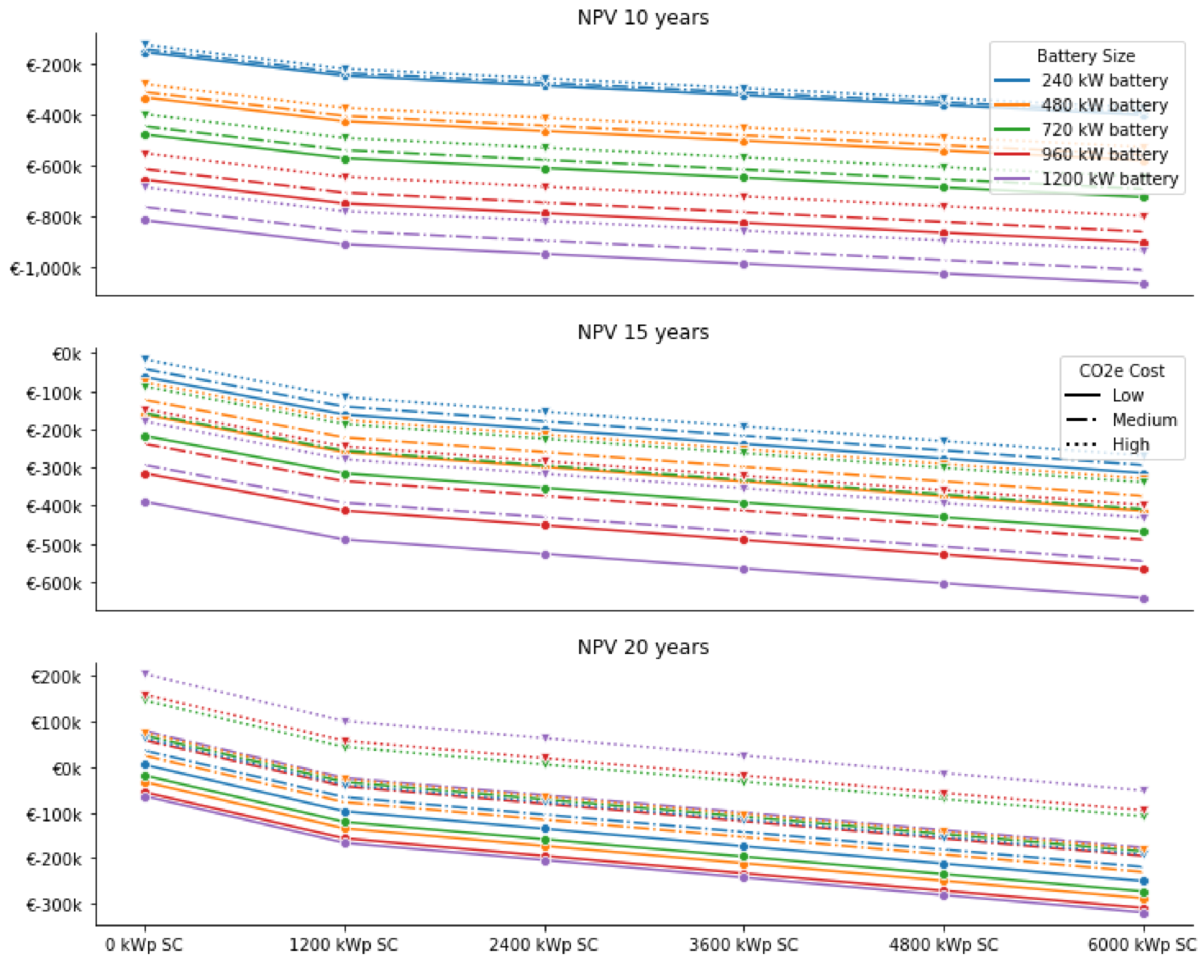

Figure 3.18 Sensitivity analysis for CO2 emission costs for 1-month-projected-to-1-year analysis

Figure 3.19. Minimum below shows the minimum specific battery CAPEX required by each battery size to achieve an NPV = 0 for the battery only scenarios for project periods of 10 – 20 years. We see that a smaller reduction would be required when compared to the corresponding results for the 1- year results as per Figure 3.15 - Minimum. For the 20- year period results specifically, the CAPEX would only need to be reduced by up to ~ € 25 per kWh. Additionally, we can see that the minimum CAPEX for project periods of 15 and 20 years is above the 2035 projected ZEBRA battery cost of €350 per kWh [30].

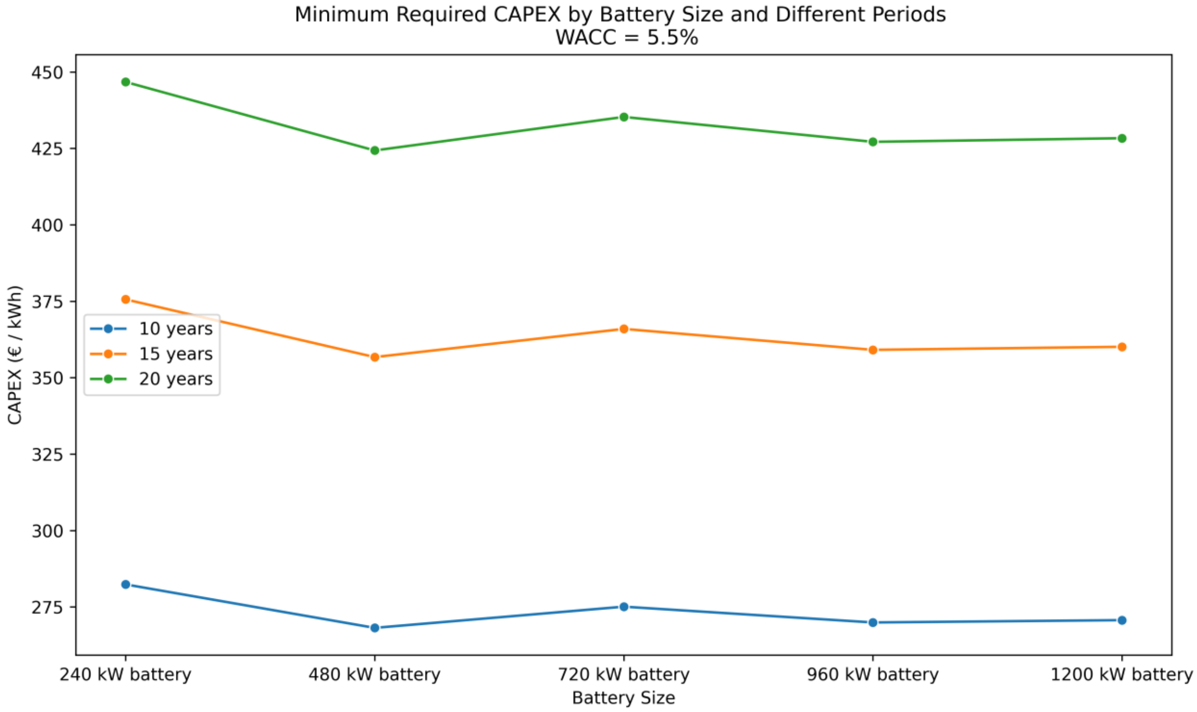

Figure 3.19. Minimum battery costs to achieve NPV = 0 for 10, 15, and 20-year project periods for a 1-month-projected-to-1-year-analysis.

3.6.2. Case 2 Results

An NPV assessment was carried out for the HESS arrangements for Case 2, using the renumeration as summarized in Figure 3.20 and Figure 3.21. Figure 3.20 shows the NPVs for the yearlong analysis, assessed at different project periods and for different CO_2 emission cost scenarios. Despite the added revenue for the SC regulation payment, all NPVs are negative as the CAPEX for the battery and SC dominate the future cashflows, hence there is no arrangement that would be economically viable. On the other hand, Figure 3.21 shows the NPV for the 1-month-projected-to-1-year analysis and we can see that there are several HESS arrangements with SC sizes between 0 - 3600 kW which have a positive NPV and hence are economically viable.

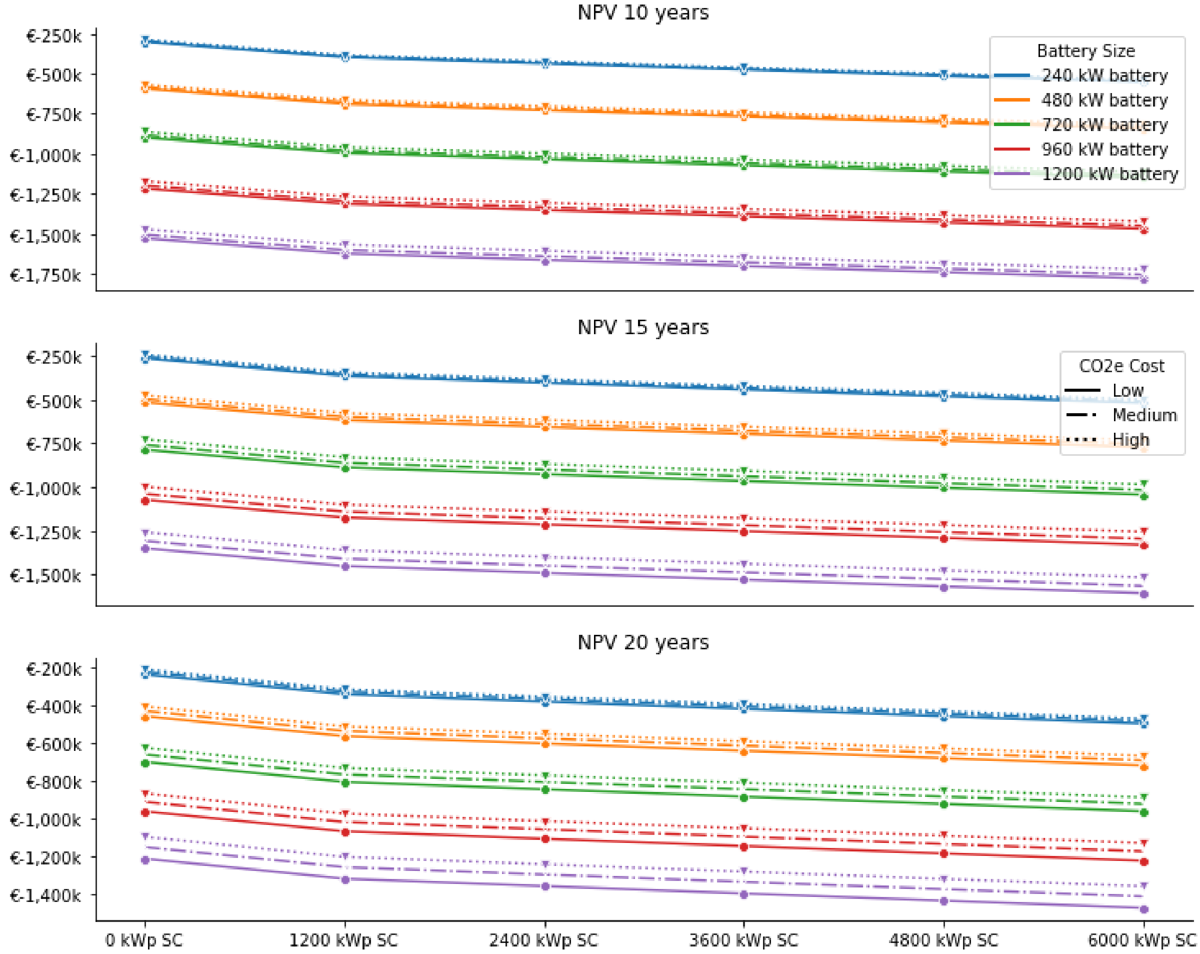

Figure 3.20 Case 2 NPV calculations using 1-year renumeration for different periods and CO2 emission costs

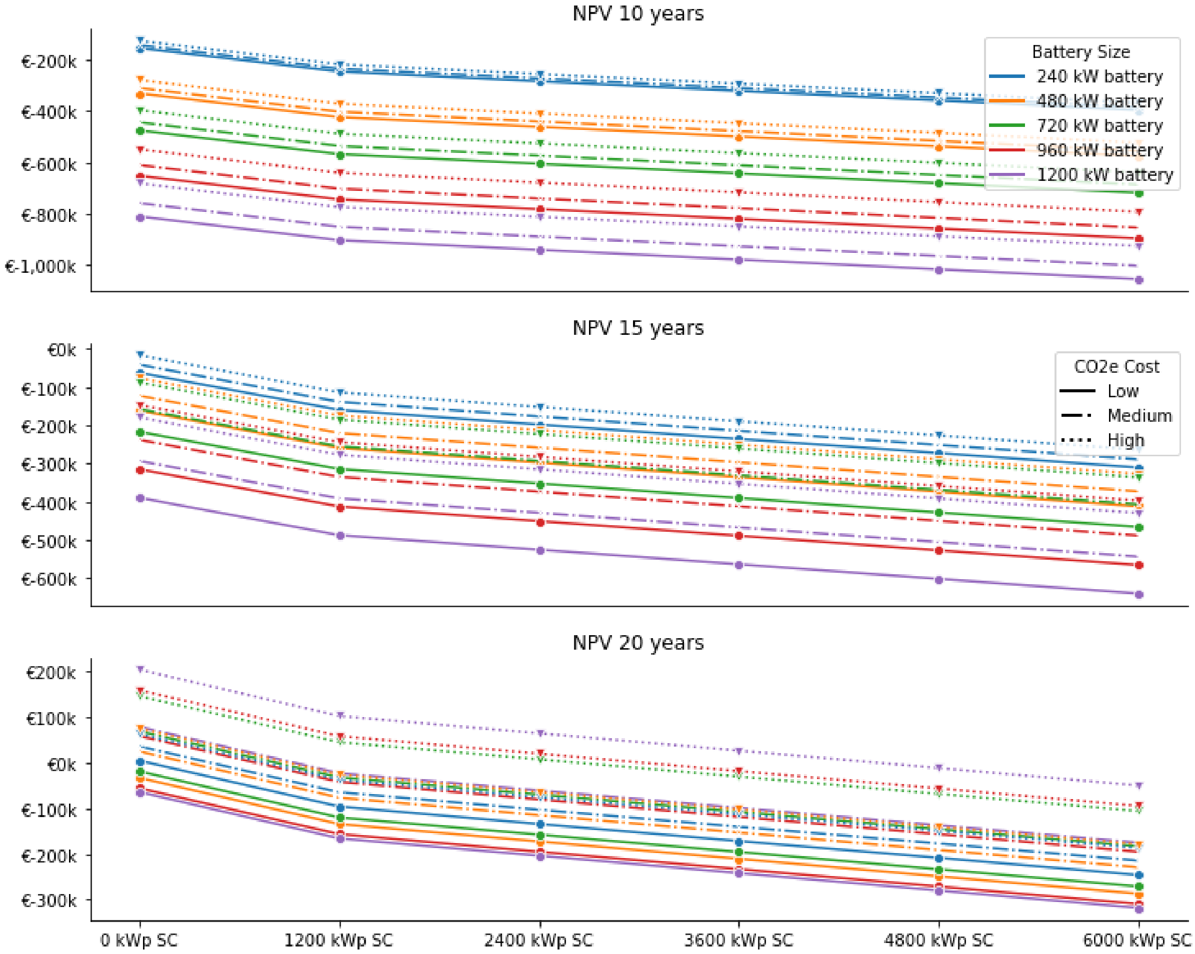

Figure 3.21 Case 2 NPV calculation using renumeration for 1-month-to-1-year, for different periods and CO2 emission costs

3.6.3. Summary of Results

Based on the results of the techno-economic analysis, none of the HESS configurations evaluated under Case 1 or Case 2 were found to be economically feasible within a one-year assessment period, as indicated by the NPV calculations. However, when extrapolating the performance observed in January, characterized by a high surplus of renewable energy, over a 20-year project horizon, several HESS configurations demonstrate economic viability. This holds particularly true under medium and high CO_2 emission cost scenarios, where avoided emissions contribute significantly to the overall financial return. These are summarised in Table 3-10 and ranked in best performing order based on NPV. Payback time and IRR have also been included in the summary.

Table 3-10 Summary of techno-economic sizing analysis for financially viable HESS arrangements for periods of 20 years, assessed at 1-month-projected-to-1-year.

BESS Size	SC Size	Case	CO2 e Scenario	NPV	Payback Time (Years)	IRR
1200 kW	0 kW	Case 1 & 2	High	€ 204,120	10.74	7.21%
960 kW	0 kW	Case 1 & 2	High	€ 158,981	11.29	6.53%
720 kW	0 kW	Case 1 & 2	High	€ 146,085	11.04	6.83%
1200 kW	1200 kW	Case 1	High	€ 102,569	11.24	6.59%
1200 kW	1200 kW	Case 2	high	€ 101,163	11.21	6.62%
1200 kW	0 kW	Case 1 & 2	Medium	€ 78,803	11.86	5.89%
480 kW	0 kW	Case 1 & 2	High	€ 75,304	11.86	5.89%
720 kW	0 kW	Case 1 & 2	Medium	€ 69,088	11.71	6.05%
1200 kW	2400 kW	Case 1	High	€ 64,774	12.17	5.57%
1200 kW	2400 kW	Case 2	high	€ 63,356	12.10	5.63%
240 kW	0 kW	Case 1 & 2	High	€ 63,262	11.90	5.84%
960 kW	0 kW	Case 1 & 2	Medium	€ 58,701	12.09	5.64%
960 kW	1200 kW	Case 1	High	€ 58,584	11.35	6.49%
960 kW	1200 kW	Case 2	high	€ 57,709	11.93	5.85%
720 kW	1200 kW	Case 1	High	€ 45,175	11.65	6.14%
720 kW	1200 kW	Case 2	high	€ 44,038	11.87	5.91%
240 kW	0 kW	Case 1 & 2	Medium	€ 35,936	11.84	5.94%
1200 kW	3600 kW	Case 1	High	€ 26,663	11.87	5.89%
1200 kW	3600 kW	Case 2	high	€ 25,076	11.87	5.88%
480 kW	0 kW	Case 1 & 2	Medium	€ 24,742	11.72	6.04%
960 kW	2400 kW	Case 1	High	€ 20,045	12.18	5.55%
960 kW	2400 kW	Case 2	high	€ 19,271	12.11	5.63%
720 kW	2400 kW	Case 1	High	€ 7,562	11.91	5.83%
720 kW	2400 kW	Case 2	high	€ 5,753	12.10	5.63%

3.6.4. Conclusion and Future works

The hybrid-storage assessment for Graciosa Island shows that salt-based batteries can meaningfully curb diesel use when renewable-energy (RES) surpluses are plentiful in the winter high-RES season, but they become almost idle during the summer period. In the January wind peak, surplus RES reached 826 MWh, about 2.4 times monthly diesel demand, and a 1200 kW / 4800 kWh battery displaced 41 MWh of diesel while recovering 74 MWh of curtailed wind and solar; roughly one-third of the stored energy was lost to self-heating and conversion, yet overall performance was robust. By contrast, in August and September curtailment virtually vanished, the battery cooled below its 265 °C set-point, and most of the scant surplus energy was consumed merely to reheat the battery, yielding negligible diesel savings. Comparing system configurations, Case 1 cuts annual diesel generation almost linearly with size, up to 223 MWh, or 3.7 % of yearly diesel, at 1200 kW, but never reaches positive NPV at today's capital costs. Case 2 improves power-quality metrics and trims curtailment marginally, yet it siphons some battery energy into regulation and raises CAPEX, so economic returns become still less attractive. Marginal diesel displacement flattens beyond roughly a 960 kW / 3.7 MWh battery, and sensitivity tests show that profitability emerges only when battery CAPEX falls below about €325 kWh^{-1} and when winter-season revenues (or a high CO_2 price) can be sustained throughout the year; under such optimistic assumptions, a 720-1200 kW battery without a large super-capacitor offers the highest NPV and a modest 7 % IRR. Adding a super-capacitor (Case 2) noticeably smooths fast fluctuations: The Smoothing and Fluctuation Benefit (SAFB) climbs from 0 % to almost 12 % as SC power rises from 0 to 6 MW. Yet every extra megawatt of SC shaves a little off diesel savings, for a 720-kW battery the yearly offset slips by ~1 % once a 6 MW SC is included, because some stored energy is now diverted into rapid regulation. The economics are harsher still: the SC costs € 32 kW^{-1} plus a € 40 000 installation fee, while regulation payments, though rising with SC size, remain only a third of total revenue and cannot overcome the higher CAPEX. Consequently, all SC-equipped layouts post negative NPVs in a normal year, and positive values emerge only when January-level revenues are projected across the year and CO_2 prices approach € 177 t^{-1}; under that optimistic scenario, batteries of 720-1200 kW coupled with SCs no larger than 2.4-3.6 MW return NPVs in the € 64-102 k range over 20 years. Taken together, the analysis points to a medium–large battery without, or with only a modest (≤2 MW) SC as the best compromise today: a 960-kW salt battery alone yields the highest diesel reduction per euro, while a 1200 kW unit maximises NPV once battery costs and carbon prices improve. Profitability nevertheless hinges on achieving lower storage CAPEX and capturing winter-season revenues year-round.

Future work should pivot from a single curtailment-driven lens to a scenario-oriented framework that sizes and dispatches storage for four realistic operating modes, self-consumption maximisation, diesel peak-shaving, high-power EV charging, and a future PV-dominated grid, while explicitly testing how the existing 2.6 MWh lithium-titanate pack is treated: left to handle fast frequency control alone, meshed with the new hybrid system on a shared DC bus, or retired in favour of a larger sodium or flow-battery plus super-capacitor stack. In parallel, the study should benchmark molten-salt cells against lower-temperature chemistries such as LFP, aqueous zinc, and flow batteries. Delivering these insights will require upgrading the present two-case genetic algorithm to a hierarchical optimiser that couples long-horizon mixed-integer sizing with a short-horizon dispatch agent capable of learning how to share duty cycles, heating losses, and reserve margins across all storage layers. Together, these enhancements would turn the current analysis into a flexible playbook for any mix of load growth, renewable expansion, and legacy-asset constraints on Graciosa or similar islanded microgrids.

4. CASE STUDY - GERMANY

4.1. INTRODUCTION

The Technology Center for Energy's (TZE) energy setup serves as a practical demonstration of battery-supported renewable integration. The site is interconnected with the public electricity grid. Nonetheless, the research institution has set ambitious objectives to enhance self-consumption of its on-site PV generation, optimize energy purchase costs, and leverage battery storage to mitigate peak demands. Particular attention is given to regulatory frameworks, electricity pricing, and technical constraints that can strongly shape the feasibility and economic performance of the HESS.

The TZE's facility is located in the municipality of Ruhstorf, situated in the Passau district in southern Germany and is tied into the municipal grid. It is a research institute of the Landshut University of Applied Sciences (ULA) that focusses on energy storage, smart grids, energy efficiency, energy management, hydrogen, bio-gas and other social or policy related topics. Various labs and research activities, such as battery and cell production and testing, hydrogen production and methanation, as well as offices make up a significant portion of the local energy demand profile. The site includes two PV plants, each managed via separate inverters, feeding into the facility's power network. While these solar installations aim to meet a large portion of daytime consumption, production intermittencies and the occasional mismatch between solar supply and campus loads require a robust energy management approach.

The research institute has some storage systems, including a HESS comprising of a Redox Flow battery (RFB) energy storage and Supercapacitor, a containerized RFB and a lithium-ion battery. Out of these three storage systems, lithium-ion battery is the active storage system and covers the storage requirements of the facility. This system stores surplus PV production at times of high generation (e.g., midday) and releases it to help with peak shaving or meeting evening/night loads. The resulting decreased dependence on external power purchases is intended to reduce operational costs and demonstrate next-generation energy solutions. Energy consumed is purchased at a wholesale rate that covers multiple public facilities. Any surplus generation that might be exported back into the grid is subject to feed-in tariffs determined by the year of PV plant commissioning. However, the facility generally has minimal excess due to sizeable on-site demand and the battery's ability to absorb extra production.

Core Objectives

The ensuing analysis focuses on determining optimal system sizing, dispatch strategies, and market participation scenarios for the Landshut campus. In particular, the study will explore:

- **Spot-Market Arbitrage and Feed-In Coordination:** Identifying times when it is profitable to charge the RFB from low-cost off-peak power (e.g., weekends) and discharge during more expensive peak hours or even export to the grid.
- **HESS Power and Energy Capacity Requirements:** Balancing the RFB's energy capacity with the Supercapacitors' high-power handling to align with campus load profiles.
- **Economic Viability and Sensitivity:** Reviewing how system performance changes in response to shifting wholesale electricity prices, feed-in tariff rates.
- **Demand-Charge Reduction:** Evaluating how best to deploy stored energy during peak usage times to minimize operational costs.

Accordingly, the forthcoming techno-economic assessment will concentrate on identifying the optimal sizing of both the RFB and the SC, with a strong focus on four key objectives: **minimizing grid-import costs**, **exploring arbitrage opportunities**, **ensuring the overall techno-economic feasibility under Germany's evolving tariff structure, maximizing PV self-consumption by charging HESS**. This includes evaluating the required power and energy capacities, load-following performance, and market-driven charging-discharging strategies. By capturing these interrelated parameters, campus load patterns, electricity pricing signals, and operational constraints, the analysis will illuminate how best to reduce energy expenditures and enhance renewable utilization in Landshut's campus environment, ultimately reinforcing the site's role as a sustainable, cost-effective energy system model.

Demand-Charge Reduction

Energy storage is widely recognized as a tool for peak shaving, which involves discharging stored energy during periods of highest demand to flatten the load profile. By reducing the peak power draw, facilities can avoid or lower demand charges on their utility bills, which are typically based on the maximum power usage over a billing period. In campus or commercial settings, a HESS that combines a RFB with SC can effectively smooth out short-lived spikes as well as sustained peaks. Similarly, the HyFlow project[32] at the University of Landshut exemplifies this approach: it targets a HESS that balances power demand "during critical grid conditions, e.g., during high load or generation peaks, whether for seconds or entire days," by harnessing the high-power capability of SCs and the high capacity of RFBs. This hybridization allows the system to absorb abrupt surges (for a few seconds) and also support longer peak periods, preventing peaks from exceeding certain thresholds[33]. The benefits of peak shaving with energy storage have been quantified, revealing that even a moderate deployment of distributed batteries (a few kWh per household) can halve the peak demand on residential feeders[34].

Behind-the-meter batteries have similarly been shown to cut peak demand, albeit to a more limited extent depending on sizing; an NREL analysis found that relatively small, short-duration lithium-ion systems could trim a facility's peak demand by about 2-3%, yielding notable demand-charge savings [35]. Real-world examples underscore the effectiveness of HESS for peak management. In one case study, a vanadium RFB was evaluated for a university library to avoid expensive demand charges, essentially shifting the library's HVAC and other loads off the grid during peak periods[36]. At utility scale, the world's largest flow battery installation in Dalian, China (100 - 200 MW scale), is explicitly used for peak shaving on the grid, buffering variability and reducing peak stress on the network[37]. These examples indicate that RFB-based systems can successfully mitigate peaks at both campus and grid levels. By shaving peak loads, institutions save on demand charges and defer capacity upgrades. Real-world applications and studies support that a well-sized HESS can significantly reduce peak demand, improve load factors, and cut utility costs by discharging during high-demand intervals and recharging when loads subside.

Spot-Market Arbitrage and Feed-In Coordination

HESS deployments can also participate in energy arbitrage[38], charging when electricity prices are low (or when there is excess generation) and discharging when prices are high. In deregulated European markets, this typically means drawing power or absorbing surplus renewables during off-peak hours (e.g. overnight or weekend periods with cheap energy) and then delivering power to cover loads or export to the grid during peak price hours (e.g. daytime peaks or early evening) [39]. The principle of arbitrage is to exploit price differentials: "store energy when rates are low, release it during high-rate periods." This can occur via direct spot market trading or time-of-use tariffs. For arbitrage purposes, a HESS with a long-life RFB is well-suited for daily cycling. RFBs can sustain numerous charge/discharge cycles with minimal degradation, making them ideal for this strategy. The integrated SC can support the RFB during de-rating periods by managing rapid charging and discharging, ensuring maximum energy utilization within the RFB's operational limits. The SC can handle rapid charging and discharging when the RFB is undergoing de-rating. If there is a price spike during this de-rating period, the SC can help absorb as much energy as possible, optimizing the use of the RFB for arbitrage purposes[12].

In the German context, feed-in coordination and market regulations play a crucial role in arbitrage strategies. Germany's Renewable Energy Act (EEG)[40] mandates that larger producers directly market their energy; for example, solar plants above 100 kW must sell on the market rather than receiving a fixed feed-in tariff[41]. This incentivizes using storage to optimize when to inject power into the grid. A case study on a Fraunhofer campus in Pfinztal, Germany, highlights leveraging a BESS to maximize revenue under dynamic pricing[42]: the BESS was optimized to charge on low-price weekends (or times of surplus renewable supply) and discharge during high-price weekday peaks. By coordinating with the spot market, the system can avoid feeding electricity into the grid when prices are depressed, instead storing it and only exporting (or reducing grid purchases) when market prices are favorable. This not only increases economic returns but also assists the grid by smoothing the demand-supply balance.

Research across Europe suggests that pure energy arbitrage with batteries has historically been marginal in profitability, but the potential is growing. A study evaluated arbitrage in several EU countries and found that under then-current conditions the net present value of a battery storage project for arbitrage alone was negative in most cases (e.g. around -€0.4 million NPV in the best cases like the UK/Ireland)[39]. This indicates that, with 2019 price spreads and battery costs, arbitrage barely failed to pay off. However, price volatility has increased in recent years, for instance, German wholesale electricity spiked to record highs in August 2022 (nearly €700/MWh)[43], improving the outlook for arbitrage revenues. Moreover, stacking arbitrage with other services (Grid services, or capacity market payments) can turn storage investments into economic[44]. Studies have also modeled feed-in tariff integration, showing that when feed-in remuneration is low, a battery should store surplus PV and time-shift its export to achieve higher effective prices or avoid curtailment[45]. In summary, literature indicates that RFB-based HESS can perform spot-market arbitrage and coordinated feed-in management, but economic success depends on market price spreads and smart control. HESS can capitalize on multiple value streams by charging the RFB with cheap renewable excess. This stored energy can then be used to shave the facility's peak, saving on demand charges, or sold on the intraday market during price surges. With appropriate energy management, such as predictive control to charge and discharge at optimal times[46], and under favorable market conditions, arbitrage can significantly reduce energy costs for an energy community or even generate revenue by selling power at peak prices[47].

HESS Sizing

Determining the optimal power and energy capacity of each component in a hybrid RFB+SC system is crucial to meet load-following requirements efficiently. It is widely recognized that in a hybrid storage system, the two components should be sized to complement their respective strengths: the RFB (or a battery) is best suited for storing and delivering energy over extended periods, while the SC is designed to handle short-duration, high-power demands. An effective sizing approach is to separate the demand profile by timescale: high-frequency, short-term fluctuations (lasting seconds to a minute) are handled by the SC, and lower-frequency, longer-lasting demand variations are met by the battery. By "filtering" the load or renewable output in this way, the SC can buffer rapid transients (preventing the battery from experiencing steep charge/discharge ramps), and the RFB can be devoted to slower load-following and energy shifting. This division of labor not only ensures the load is met at all times but also extends the life of the battery by avoiding strain from fast cycling[12].

Several studies propose methodologies for optimal HESS sizing. In[48] the study formulated a multi-objective optimization (using an improved partial swarm algorithm) to find the optimal capacity ratio between a battery and SC in a microgrid HESS, aiming to minimize power fluctuations and system cost. Their results showed that with the right sizing and control strategy, the HESS smoothed out nearly all high-frequency power oscillations, avoided battery overstrain, and even reduced overall cost by ~4.3% compared to a non-optimized case.

In practical terms, the optimal sizing often means the SC has a much higher power rating relative to its energy capacity. For example, one design for an industrial microgrid HESS pairs a vanadium RFB (providing the energy store) with a supercapacitor bank that holds only a small amount of energy. This underscores that the SC may be sized for power on the order of the battery's power, but with a tiny fraction of the energy, essentially dedicated to handling surges of a few seconds. Meanwhile, the RFB's energy tank is sized to several hours of the load, but its power converter might be smaller because the SC covers the spikes[46].

To determine sizing needs in any facility, one of the practical ways is to consider the specific load profile and use cases considering sizing methodologies that iterate between technical constraints and economic targets[49]. Key considerations include the peak power magnitude and duration, the typical daily load variation, and any rapid events like elevator or EV charger inrushes[50]. An optimal HESS will have sufficient SC capacity (power and short-term energy) to manage the facility's fast transients (maintaining power quality during, for example, a large motor startup or a sudden PV output drop). Simultaneously, the RFB component must be sized with enough energy to sustain longer load-following operation, for example, supplying evening peak demand for a few hours or bridging a cloudy lull in PV output, and enough power to meet the bulk of the demand once transients are handled[12].

Economic Viability and Sensitivity

The techno-economic feasibility of hybrid storage systems is a recurrent theme in many studies [50][51]. While HESS promise technical advantages, their economic viability depends on multiple factors, capital costs, electricity price dynamics, use-case stacking, and component degradation[52]. Studies generally find that hybridizing an RFB with a high-power device (SC or even a lithium battery) yields both technical and economic benefits: by extending the RFB's lifetime and efficiency, the hybrid can lower the levelized cost of storage over the system's life[53]. Key performance indicators for economic analysis include the system's ability to reduce energy costs (through arbitrage or peak shaving), its upfront CAPEX and ongoing OPEX (including maintenance and any electrolyte replacement costs for RFBs), and the degradation rates of components (which affect how often expensive replacements are needed).

One major factor is the spread between low and high electricity prices, as this determines arbitrage revenue. If typical peak/off-peak spreads are narrower, returns diminish; conversely, more volatile markets (or added value from grid services) improve profitability[54]. The studies confirm this: the profitability of battery storage in European arbitrage was found to be marginal under 2019 price conditions, but is expected to turn positive as battery costs decline and price volatility increases[39]. Another critical factor is battery degradation and lifespan. Because RFBs feature long cycle life and decoupled energy capacity (electrolyte volume) from power (stack size), they can sustain daily cycling for 20+ years. However, capacity fade can still occur in stacks or pumps over time. Incorporation of VRFB efficiency curves and capacity loss into an arbitrage optimization model, showing that neglecting degradation would overestimate revenue properly accounting for fade helped identify an optimal operating strategy that balances immediate profits with long-term capacity retention[55]. This implies that an economically optimized HESS might sometimes operate conservatively (e.g. avoiding deep discharge of the RFB or reserving some electrolyte capacity) to prolong its life, ultimately yielding better lifecycle economics [56].

4.2. DESCRIPTION OF SYSTEM AND DATA INSIGHTS

Currently, the campus of the Technology Center for Energy (TZE) belonging to ULA incorporates two separate photovoltaic (PV) plants. The first is a rooftop PV plant with a peak production capacity of nearly 27.44 kW and the second is a Carport PV plant with a peak production capacity of 10.8 kW. For research and demonstration purposes, TZE has 2 RFBs, out of which one is a test-bench and works as a HESS in conjunction with a supercapacitor, and the other is a containerized system. The test-bench can generate a maximum power of 30 kW, with the help of a RFB, with a configuration of 5 kW / 10 kWh and a SC, with a configuration of 25 kW / 300 kJ. The containerized RFB, which is placed below the Carport PV system has the following configuration: 10 kW/100kWh and is not in active operation due to the high self-consumption. The facility has a Lithium-ion battery, that has a total capacity of approximately 92 kWh and is currently the only active storage system. The whole facility is grid connected and fulfills excess energy requirements from the grid.

The setup allows ULA to significantly increase on-site solar utilization and reduce reliance on the municipal grid. Although the campus already mitigates a portion of its peak demand through these PV installations, it still faces times of either surplus power or high load requirements. The high capacity of the storage system provides extended-duration storage (e.g., storing midday production for later use). By utilizing the storage systems, the campus aims to optimize self-consumption of solar energy, reduce the energy consumption from the grid, and advance TZE's broader research mission in battery and energy network innovation.

The energy generation data of the two PV plants is captured with a resolution of one second and is stored in separate files of '.csv' format. The structure of both the data files is the same. Both have two columns, namely 'ts' and 'power'. The 'ts' column contains the date and time details captured in the local Time Zone in ISO 8601 format without microseconds, for example 2020-07-10 15:00:00. The 'power' column contains the AC power generated by the PV plant at the respective time in watts (W).

The energy consumption data of the facility is also captured with a resolution of one second and stored in '.csv' format. The columns present in the energy consumption data file are the following: 'ts', 'power', 'frequency', 'U1_Real', 'U2_Real', 'U3_Real', 'U1_Im', 'U2_Im', 'U3_Im', 'I1_Real', 'I2_Real', 'I3_Real', 'I1_Im', 'I2_Im', 'I3_Im'. The 'ts' and 'power' columns are the same as the columns for the energy generation data for the PV plants. The U*_Real is the real voltage in volts (V) and U*_Im is the imaginary voltage in volts (V), in the three phases at the respective time, where * denotes the phase 1, 2 or 3. Similarly, I*_Real and I*_Im is the respective real and imaginary current in amperes (A) in the phases 1, 2 or 3 at the respective time.

4.3. METHODOLOGY

This section details how the optimal HESS size and operating strategy are established for the demo site of Technology Centre for Energy campus of University of Landshut (ULA). The analysis re-uses the multi-period optimization framework, workflow and component models explained in D2.2[1], while Appendix 1 gathers the sizing specifics. These elements are adapted to ULA's grid-connected, PV-rich setting and its unique technical, economic and regulatory constraints. The key steps are summarized below, follow the same logic as the Gracíolica case, but with data sources, constraints and objective functions tuned to the German context.

4.3.1. Data Collection and Scenario Definition

In this case study, two PV systems, local loads, and the public grid are interconnected. One year of load and PV production data, provided at second-by-second intervals, is utilized as input for the optimization process. This high-resolution data was averaged to hourly intervals to establish the baseline for long-term energy optimization of the RFB, including use cases such as energy trading and arbitrage. To address the RFB's power de-rating limits, minute-based data aggregated from the second-by-second dataset is used to optimize the integration of a SC. This ensures the SC effectively compensates for the RFB's limitations, particularly during high-power demand windows, by enhancing power responsiveness. Additionally, wholesale electricity prices for grid energy purchases and applicable feed-in tariffs for potential energy exports were incorporated into the optimization framework. Finally, second-by-second data was employed to demonstrate the full capabilities of the HESS in peak shaving during power spikes. This high-resolution simulation provides a clear contrast with HESS behavior under minute-based control, illustrating the system's superior performance in managing rapid power fluctuations and maintaining power quality.

Various Scenarios are considered for this case study, starting to focus on reducing campus peak loads to lower demand charges through peak shaving and demand management. Explore the cost-effectiveness of buying energy at off-peak/low-tariff times (weekends, nights) and discharging during peak or high-tariff periods through spot-market (or tariff-based) arbitrage. Increase on-site self-consumption of solar energy by storing midday excess and shifting it to periods of higher campus demand through PV integration. Evaluate selling small surpluses to the grid under the local feed-in tariff structure if they remain after meeting campus loads and battery charging.

4.3.2. HESS components models

In this case study, the HESS was comprised of a vanadium RFB, as well as a supercapacitor. This section will provide a brief description of these technologies, and further details can be found in the deliverable document D2.2[1], which elaborates on the technical constraints and the equations used to model these technologies. Table 4-1 below summarises the RFB model parameters and Table 3-2 in Section 3.4.2 summarises the parameters used for the supercapacitor.

Table 4-1 Summary of RFB model parameters

Parameter	Value
Cells per Stack	48 cells
Cell membrane area	1628 cm2
Membrane area sepcific resistance	1.6/1.4 ohm cm2 (discharge/charge)
Nominal Power / Max Power per cell stack	8.35 kW / 12.5 kW
SOC Limits	10 - 80%
Terminal voltage limit during charging	1.5 V per cell and occurs at ~ 46% SOC
Terminal Current Limit	167 A
Vanadium ion concentration in electrolyte	1.6 Mol /L
Degradation	0.002% per cycle (assuming 20% degradation after 10,000 cycles)
Capacity fade due to crossover	0.215% per cycle[57]
Capacity fade due to electrolyte imbalance	0.055% per cycle [57]
Overall Capacity fade	0.27% per cycle

A total of 18 RFB sizes were assessed, corresponding to a combination of 3 different battery power ratings and 6 different total storage capacities. The power rating and storage capacities are summarised in Table 4-2. The power maximum power rating was adjusted by increasing the number of cells in series. As per Table 4-1, we see that one stack in the RFB model used corresponds to 48 cells, and therefore RFB power sizes of 12.5 kW and 25 kW correspond to 1 and 2 cell stacks, respectively. The 18.75 kW RFB corresponds to 1.5 stacks, and it is understanding that this is a non-standard size that may not be possible to procure for the VRFB make that our model is based on. However, this has been included in the assessment to allow for a more detailed assessment on how increasing power rating will affect the overall performance and techno-economics.

Table 4-2. Summary of total storage capacities and power rating used for the different RFB sizes

Storage Size Range			Power Size Range	
Total Storage Capacity	**Usable Capacity**	**Tank Volume**	**Maximum Rated Power**	**No. of Cells**
60 kWh	42 kWh	2,000 L	12.5 kW	48
90 kWh	63 kWh	3,000 L		
120 kWh	84 kWh	4,000 L	18.75 kW	72
150 kWh	105 kWh	5,000 L		
180 kWh	126 kWh	6,000 L	25 kW	96
240 kWh	168 kWh	8,000 L		

For each of the 18 RFBs, an HESS simulation was performed using 5 different SC sizes; this corresponded to a total of 90 HESS arrangements that were assessed. The SC sizes are summarised in Table 4-3 and they correspond to a multiple of SC submodules connected in series. As mentioned in Section 3.4.2, the SC sizes correspond to their peak available power (kWp).

Table 4-3 Summary of SC sizes used in the HESS assessment

Table 4-3**Peak Power**	**No. in Series & Parallel**
20 kWp	1 s, 1 p
40 kWp	2 s, 1 p
60 kWp	3 s, 1 p
80 kWp	4 s, 1 p
100 kWp	5 s, 1 p

Charging/discharge and profiles are shown for the different battery sizes in Figure 4.1 to Figure 4.3. The power profile shows the total power absorbed by the battery during charging from 10% SOC, from time = 0 to 50 hours, when charging at its rated power. Subsequently, the rated discharged by the battery from 80% SOC. This illustrates the power derating that occurs in the RFB during charging, which occurs to maintain the cell voltage below 1.5 V, as discussed in deliverable D2.2 [1]. We can see the implications this would have on the battery charging time, and how it differs from the discharging time. For example, for the 12.5 kW / 60 kWh RFB, charging from 10 to 80% SOC takes up to 8 hours, where as during discharge it takes~ 3 hours. The 12.5 kW / 60 kWh RFB, this may be seen as a 3 hour battery, given by its P rate to Storage Size ratio; however it is important to note that this applies to the discharging and the charging time takes over 2 times. This is consistent with other RFB sizes where charging time is 2-2.5 times longer than discharging time.

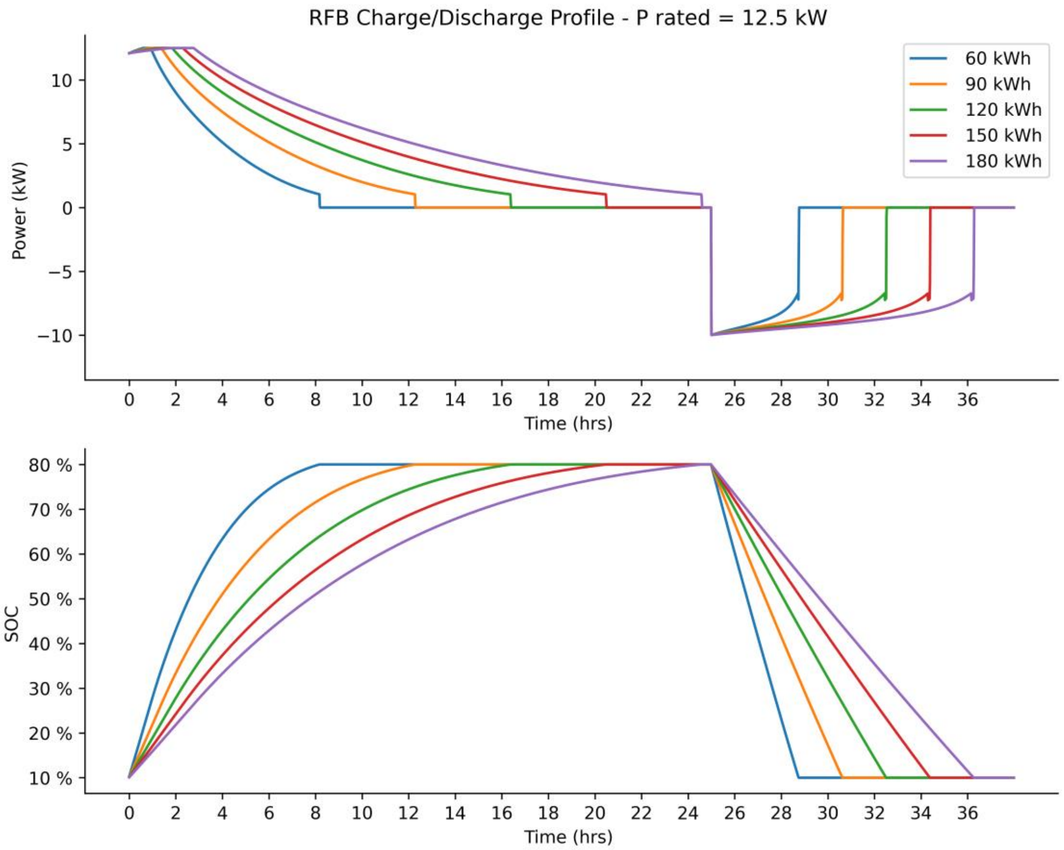

Figure 4.1 Charge/discharge curve and SOC profile for different RFB storage sizes with rated power of 12.5 kW

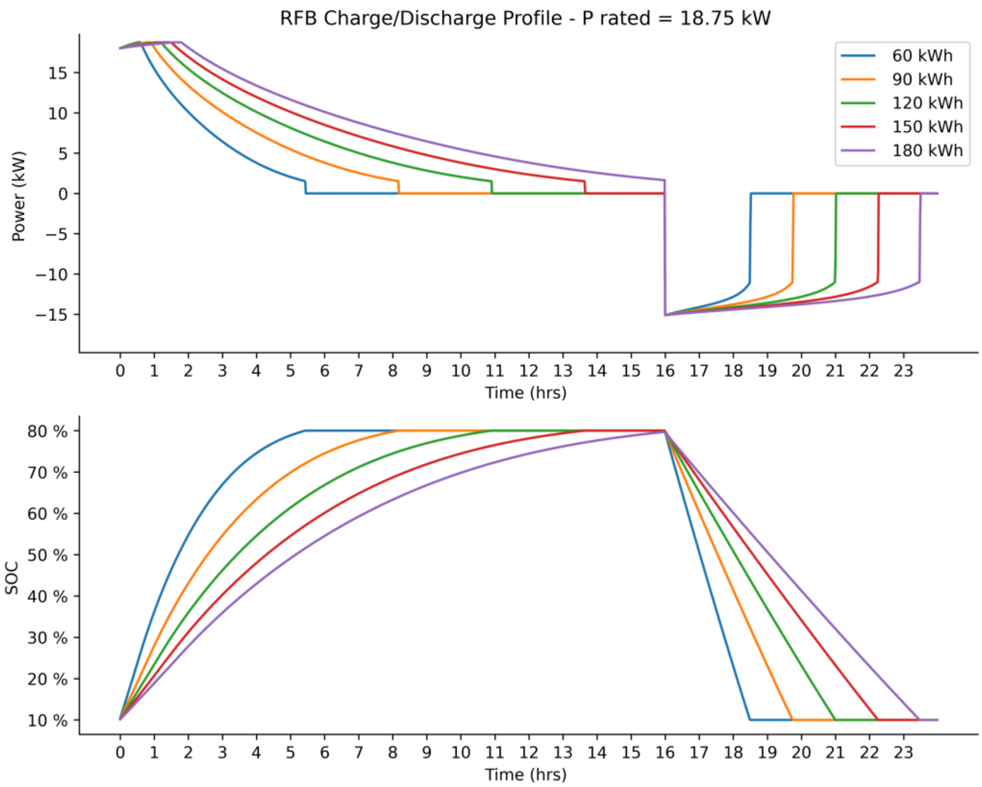

Figure 4.2 Charge/discharge curve and SOC profile for different RFB storage sizes with rated power of 18.75 kW

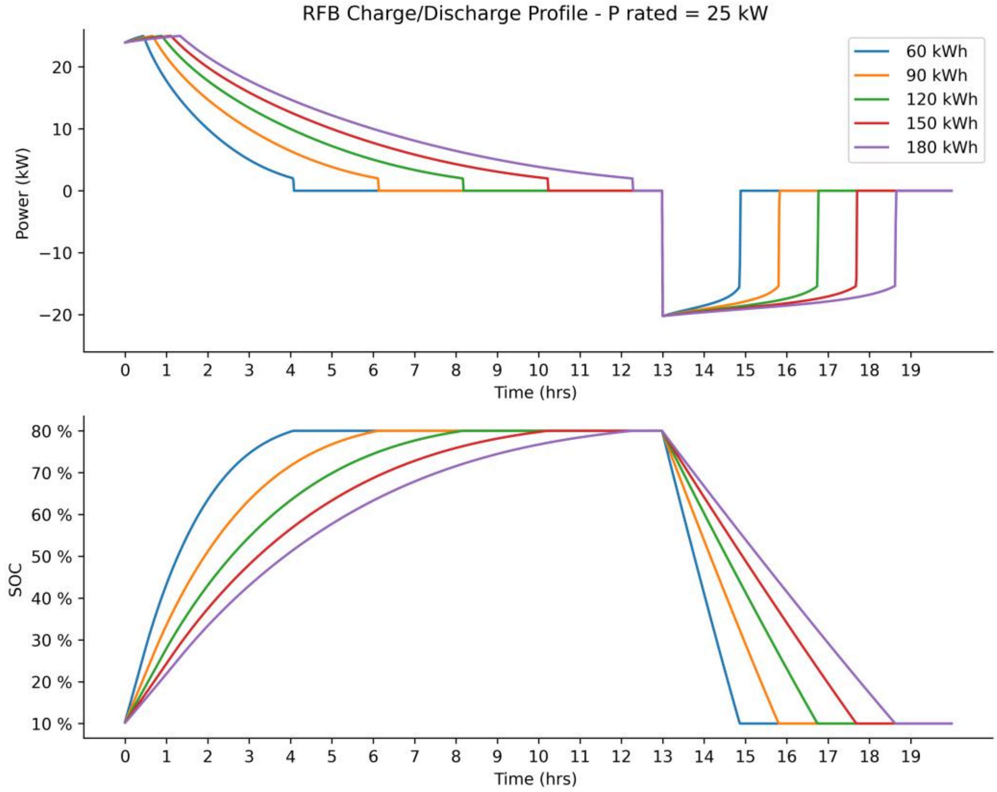

Figure 4.3 Charge/discharge curve and SOC profile for different RFB storage sizes with rated power of 25 kW

4.3.3. Operational constraints

RFB and SC

No additional site-specific operational constraints were defined for the RFB and SC. Refer to the default technological parameters summarized in Table 3-2 in Section 3.4.2 for SC parameters and Table 4-1 for the RFB parameters.

Grid Import and Export

As mentioned above, the whole facility of the Technology Center of Energy of the Landshut University of Applied Sciences (ULA) is grid connected and must adhere to the general regulations of the network operator in terms of energy consumption and feed-in. These constraints can be expressed as per equations (26) to (28), with the relevant variables defined below.

- $P_{\text{buy}}(t)$: Power imported from the grid at time t [kW]
- $P_{\text{sell}}(t)$: Power exported to the grid at time t [kW]
- $P_{\text{PV}}^{\max}$: Combined peak power of the PV systems [kW]
- $P_{\text{grid}}^{\max}$: Maximum allowed grid import power [kW]

No simultaneous import and export, as per equation (26).

$$P_{\text{buy}}(t) \cdot P_{\text{sell}}(t) = 0, \quad \forall t \tag{26}$$

The maximum energy that is supposed to be fed in by the facility is limited by the combined peak power of both the PV plants. Also, as with every other grid connected facility, there is a maximum limit of the power that can be consumed from the grid at any given time. Maximum feed-in (export) power limited by PV capacity are defined by equation (27).

$$P_{sell}(t) \leq P_{PV}^{max}, \quad \forall t \tag{27}$$

Lastly, the maximum import (consumption) power limited by grid contract, as per equation (28).

$$P_{buy}(t) \leq P_{grid}^{max}, \quad \forall t \tag{28}$$

4.3.4. Objective Function

RFB Objective Function

The objective function is to minimize the cost of electricity used by the facility over a designated time horizon. This is carried out by optimizing charging the discharging schedule of the RFB as per the objective function in equation (29) below, along with the supporting equations (30) and (31). A brief summary of the desired optimized RFB behaviour is as follows:

- RFB will recharge by purchasing electricity from the grid at the lowest price period of the day, or it will utilize surplus PV generation.
- RFB will discharge to offset the load during high priced electricity periods during the day, or it will discharge to export and sell power to the grid.

$$\min[CT] = min\left[\sum_{t=1}^{T}\left(C_{buy}(t) \cdot P_{imp}(t) - C_{sell} \cdot P_{exp}(t)\right) \Delta t\right] \tag{29}$$

Where:

$$P_{imp}(t) = \begin{cases} |P_L(t) + P_{RFB}(t) + P_{PV}(t)|, & if\,|P_L(t) + P_{RFB}(t)| \geq |P_{PV}(t)| \\ 0\quad, & if\,|P_L(t) + P_{RFB}(t)| < |P_{PV}(t)| \end{cases} \tag{30}$$

$$P_{exp}(t) = \begin{cases} P_{PV}(t) + P_{RFB}(t) + P_L(t), & if |P_{PV}(t) + P_{RFB}(t)| \geq |P_L(t)| \\ 0, & if |P_{PV}(t) + P_{RFB}(t)| < |P_L(t)| \end{cases} \quad (31)$$

- $P_{\text{imp}}(t)$ is the power imported or purchased from the grid at time t [kW].
- $P_{exp}(t)$ is the power exported or sold to the grid at time t [kW].
- $P_{RFB}(t)$ is the charge power (negative) or discharge power (positive) of the RFB at time t [kW].
- $P_L(t)$ is the facility's power consumption or load at time t, and is negative [kW].
- $P_{PV}(t)$ is the power generated by the PV plant at time t [kW].
- CT is the total cost of electricity over the time horizon T [€].
- $C_{buy}(t)$ is the dynamic purchase price of electricity at time t [€/kWh].
- C_{sell} is the feed in tariff to sell electricity back to the grid and this is 0.0688 €/kWh.
- Δt is the time step for the assessment.

Two cases were assessed in this case study, as summarized below:

- Case 1 with two requirements:
  I. Charge and discharge the RFB in an optimum way to offset electricity usage during high-price periods or sell back to the grid.
  II. The RFB must recharge during to its maximum SOC on weekends.

- Case 2 with one requirement:
  I. Charge and discharge the RFB in an optimum way to offset electricity usage during high-price periods or sell back to the grid.

Requirement I. for Case 1 and Case 2 is the same and is already accounted for by the objective function equation (29); however, for requirement II. We must elaborate the objective function even further. We do this by adding a penalty fee for when the RFB is deviates from this requirement. The updated objective function is shown in equation (32).

$$\min[CT] = min\left[\sum_{t=1}^{T}\left(\left[C_{buy}(t) \cdot P_{imp}(t) - C_{sell} \cdot P_{exp}(t)\right]\Delta t - PF\right)\right] \quad (32)$$

Where:

$$PF = \begin{cases} 0.5 \cdot C_{penalty} \cdot [SOC_{max} - SOC(t = 24hr)], & if\ Day = Saturday \\ C_{penalty} \cdot [SOC_{max} - SOC(t = 24hr)], & if\ Day = Sunday \\ 0, & if\ Day = Weekday \end{cases} \quad (33)$$

- PF is the penalty fee charged.

- SOC_{max}, is the maximum RFB SOC.
- $SOC(t = 24hr)$ is the average SOC of the RFB during the last hour of the day.
- $C_{penalty}$ is the penalty weight.

SC Objective Function

The supercapacitor is intended to support the RFB by enhancing recharging performance and increasing PV self-consumption. It will charge using excess PV power during periods when the RFB is scheduled to recharge but is unable to fully utilize the available PV energy due to charging limitations imposed by cell voltage constraintsas discussed in Section 4.3.2 and Figure 4.1 to Figure 4.3. In periods where the RFB is recharging well below its charging power limits, the SC will discharge and supply additional charging power to the RFB. By adjusting the imported and exported power calculated in equations (30) and(31), using equations (34) and (35) below, using a temporal resolution of 1 minute.

$$P_{imp,adjusted}\,(t) = P_{imp}(t) - P_{SC} \quad if\ P_{SC} > 0 \tag{34}$$

$$P_{exp,adjusted}\,(t) = P_{exp}(t) + P_{SC} \quad if\ P_{SC} < 0 \tag{35}$$

4.3.5. Techno-Economic Modeling

Similar to the Portugal case study, the techno-economic assessment for each HESS for the current case was based on an NPV analysis. To do so, an annual revenue was calculated for each HESS arrangement, and this was based on the electricity cost savings that were achieved for each system. The cost savings were the difference between the facility's original total cost of electricity and the new total cost of electricity, achieved by implementing the HESS. This is summarised in equation (36), and the new total cost, CT_{New}, was determined using the optimization function in equations (29), (30) and (31). The degraded cashflow in is then calculated, similar to the Portugal Case Study in Section 3.4.5, using a degradation rate of 0.002% per cycle; this rate corresponds to a permanent capacity loss 20% after 10,000 battery cycles..

$$CF_{in} = CT_{original} - CT_{New} \tag{36}$$

$$CF_{in,degraded} = CF_{in}\left[1 - (Y - 1)n_{cyc,R\,FB}\delta_{RFB}\right] \tag{37}$$

A similar NPV calculation was used as per the Portugal Case Study, and this general equation is summarised in equation (38). For a full description of the parameters used in this equation, refer to sub-section 3.4.5 where NPV is first introduced in this report.

$$NPV = \sum_{Y=1}^{N} \frac{CF_{in,degraded} - CF_{Out}}{(1 + WACC)^{Y}} - CAPEX_{HESS} \quad (38)$$

The inputs for the NPV calculation are described by equations (39) to (43) below.

$$CF_{out} = OPEX_{RFB} + OPEX_{SC} \quad (39)$$

$$OPEX_{RFB} = OPEX_{mix} \cdot n_{mixing} + OPEX_{Rebalance} \cdot n_{reb} \quad (40)$$

$$OPEX_{mix} = 0.5 \cdot S_{RFB} \cdot C_{buy,ave} + C_{labor,mix} \cdot t_{mixing} \quad (41)$$

$$OPEX_{Rebalance} = (\beta \cdot S_{RFB} + E_{pump}) \cdot C_{buy,ave} + C_{labour,reb} \cdot t_{reb} \quad (42)$$

$$CAPEX_{HESS} = S_{RFB} \cdot CAPEX_{RFB} + S_{SC} \cdot CAPEX_{SC} + CAPEX_{SC,install} \quad (43)$$

Where:

- $CT_{original}$ is the original annual total cost of electricity in the facility
- CT_{New} is the new annual total cost of electricity in the facility with the HESS
- $n_{cyc,R\,FB}$, is the number of battery cycles in 1 year.
- δ_{RFB}, is the RFB degradation rate (see Table 4-6) [% / cycle].
- N is the project period and corresponds to the expected lifetime of the HESS where it still generates revenue (see Table 4-6).
- Y is the assessment interval, and corresponds to 1 year, (see Table 4-6).
- $WACC$ is the weighted average cost of capital (see Table 4-6).
- $OPEX_{RFB}$ is the RFB OPEX and dependent on the number of electrolyte rebalancing and mixing activities that occur in a year (see Table 4-5) [€/activity]
- n_{mix} is the number of mixing activities carried out in one year.
- $C_{labor,mix}$ is the labor cost for the mixing activity. It is assumed this can be carried out by an inhouse technician (see Table 4-6) [€ / hr].
- n_{reb} is the number of rebalancing activities carried out in one year.
- $C_{labor,reb}$ is the labor cost for the rebalancing activity and it is assumed this is carried out by an outside specialist (see Table 4-6) [€ / hr]
- t_{mixing} and t_{reb} is the time to carryout mixing or rebalancing activity, respectively [hr]
- E_{pump} is the energy used by the pumps during rebalancing procedure [kWh]
- β, amount of degradation allowed before rebalancing (20 %)
- $C_{buy,ave}$ median cost of electricity over the year (€0.08 / kWh)
- $OPEX_{SC}$ is the annual SC OPEX (see Table 4-6).
- S_{RFB} is the battery size in terms of energy storage capacity [kWh]
- S_{SC} is the SC size in terms of maximum power output [kW]

- $CAPEX_{RFB}$ is the specific RFB cost as summarized in Table 4-4, and already accounts for installation cost. Specific cost was determined based on [56]which considers both power rating and total storage capacity of the RFB.
- $CAPEX_{SC}$ is the specific SC cost (see Table 4-6).
- $CAPEX_{SC,install}$ is the SC installation cost (see Table 4-6).

The NPV calculation in equation (38) must be modified to take consider the capacity fade of the battery due to the electrolyte decay, which has been discussed in detail in deliverable D2.2 [1]. This will affect the performance of the RFB and hence have a direct impact on the revenue it can generate. The effects of capacity fade is already considered in the RFB model and therefore represented accordingly in the first year cashflow and NPV for 1 year; however, we cannot use the same cashflow for every year, as that would incorrectly assume that capacity fade of the battery is the same every year. Although the capacity fade mechanism stays consistent and follows the same pattern, the initial and final values for the RFBs final capacity are different for each year of the NPV assessment. This is illustrated more clearly in Figure 4.4. To manage this, we adapt the equation (38), and scale the daily revenue (or incoming cashflow) to remove the daily effects of the capacity fade that occur in first year, and add the forecasted daily capacity fade affects for the relevant year. The adjust incoming cashflow is shown in equation (44) and this is used in place of CF_{in} in equation (37), to determine the NPV using (38).

$$CF_{in,adjusted}\,(Y = n) = \sum_{d=1}^{365} \left(CF_{in,daily}(d) \cdot \frac{\mu_{daily}(Y = n,\ d)}{\mu_{daily}(Y = 1, d)} \right) \tag{44}$$

Where:

- n is the year number in the NPV assessment period.
- d is the day number in the year.
- $CF_{in,daily}$ is the daily revenue or incoming cashflow [€]
- μ_{daily} is the factor of RFB remaining capacity due to the fading mechanisms. Where the μ_{daily} is used for years greater than 1, this is forecasted [%].

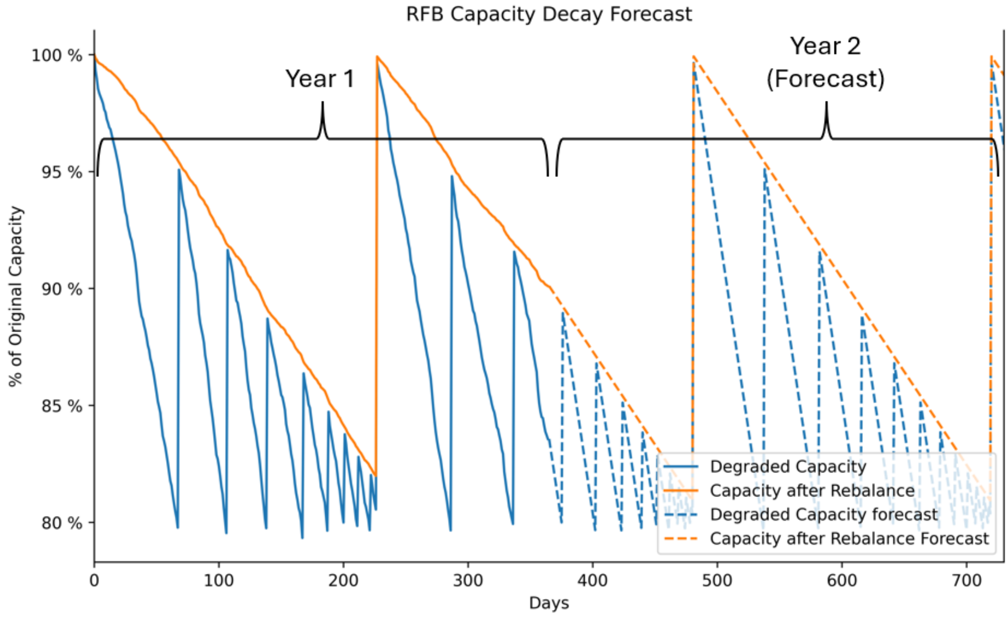

Figure 4.4 Example of the RFB capacity fade for two years

Table 4-4 Specific RFB CAPEX for each battery size

Total Storage Capacity	Maximum Power Rating		
	12.5 kW	18.75 kW	25 kW
60 kWh	€ 483 / kWh	€ 593 / kWh	€ 697 / kWh
90 kWh	€ 389 / kWh	€ 462 / kWh	€ 532 / kWh
120 kWh	€ 342 / kWh	€ 397 / kWh	€ 449 / kWh
150 kWh	€ 314 / kWh	€ 358 / kWh	€ 400 / kWh
180 kWh	€ 295 / kWh	€ 332 / kWh	€ 367 / kWh
240 kWh	€ 272 / kWh	€ 299 / kWh	€ 325 / kWh

Table 4-5 RFB OPEX for mixing and rebalancing for 1 maintenance activity

Metric	Battery Size	Power Rating		
		P = 25 kW	P = 18.75 kW	P = 12.5 kW
Mix cost	60 kWh RFB	€ 38	€ 50	€ 74
	90 kWh RFB	€ 58	€ 76	€ 112
	120 kWh RFB	€ 77	€ 101	€ 149
	150 kWh RFB	€ 96	€ 126	€ 186
	180 kWh RFB	€ 115	€ 151	€ 223
	240 kWh RFB	€ 154	€ 202	€ 298
Service Cost	60 kWh RFB	€ 230	€ 240	€ 259
	90 kWh RFB	€ 245	€ 259	€ 288
	120 kWh RFB	€ 260	€ 279	€ 318
	150 kWh RFB	€ 275	€ 299	€ 347
	180 kWh RFB	€ 290	€ 319	€ 376
	240 kWh RFB	€ 320	€ 358	€ 435

Table 4-6 Summary parameters used in the NPV calculation

Parameter	Description	Value
$CAPEX_{SC}$	SC specific cost	€32 /kW
$CAPEX_{SC,install}$	SC installation cost	50% of SC CAPEX
$OPEX_{SC}$	SC annual OPEX	€200 / year
N	Project lifetime	10 – 20 years
$WACC$	Weighted average cost of capital	6.6 %
δ_{RFB}	Battery degradation rate	0.002% / cycle
β	Allowable maximum capacity loss due to fade before rebalancing is required	20 %

4.4. BATTERY AND HESS PERFORMANCE RESULTS

4.4.1. TZE Power Profile

TZE is coupled to a 40 kWp PV system, which can supplement and offset some of the energy demand of the facility. Figure 4.5. and Figure 4.6 below shows examples of the 1- year data used in our analysis and depict the power profile of the university over a 24 - hour period during winter and summer seasons. The profiles correspond to the total load or power demand for the university, the power generated by the PV system, and the netload, which corresponds to the sum of the total load and PV generation. Where netload is positive, a surplus of PV power is generated, this is sold to the grid at the specified feed-in tariff.

Table 4-7 Summary of the total PV energy generated and exported

Parameters	Absolute Energy	% of Total PV
Total PV Energy Generated	27,127 kWh	-
Total PV Energy Exported	6,588 kWh	24.3%
Total PV Energy Consumed	20,540 kWh	75.57 %

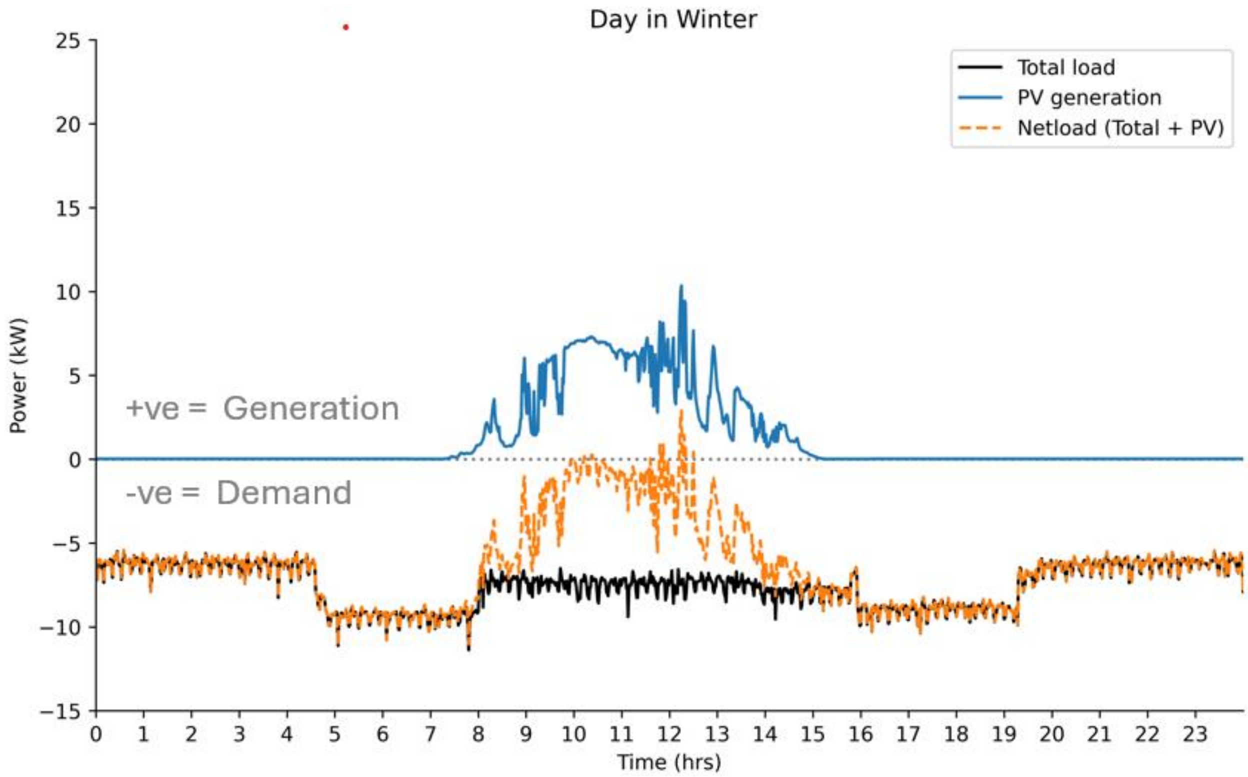

Figure 4.5. Actual power profile of TZE over a 24-hour - Winter period.

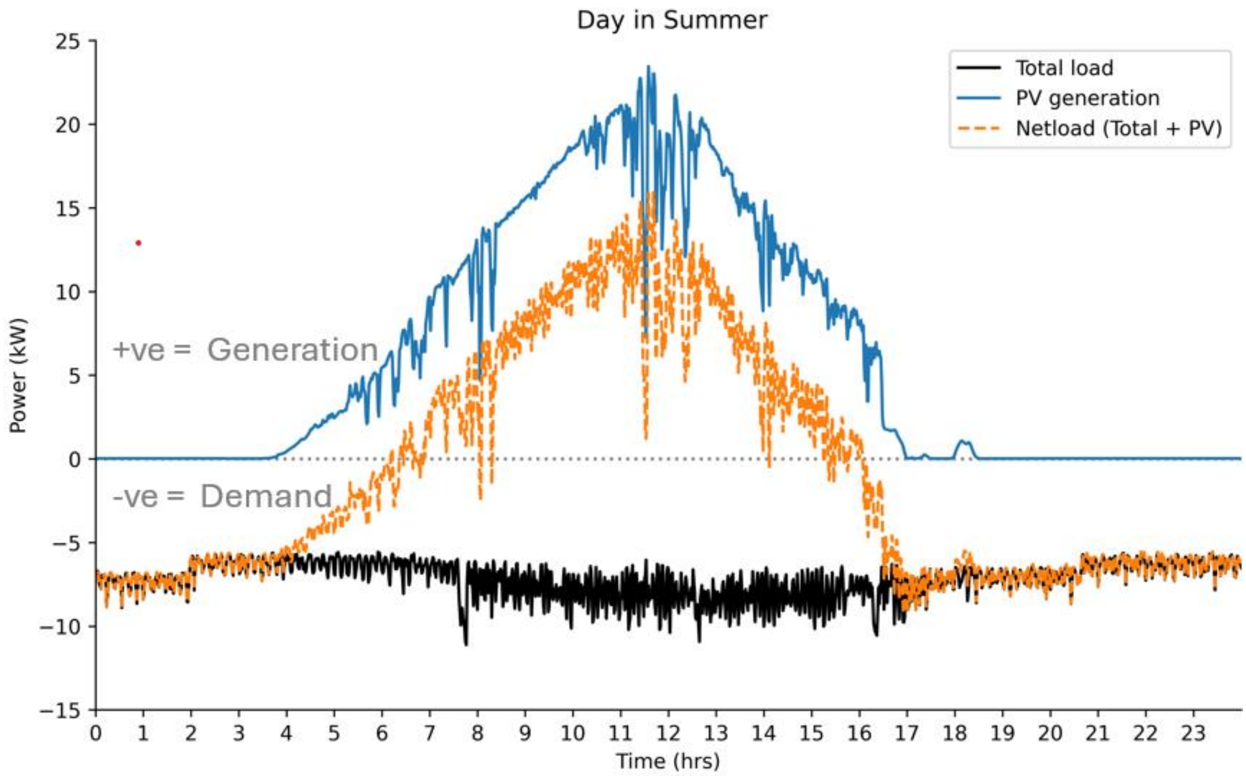

Figure 4.6 Actual power profile of TZE over a 24-hour - Summer period.

With the RFB, excess PV solar can be stored by using it to recharge the battery. The RFB can then discharge at a later time to help reduce the netload and decrease the power consumption of the university, performing a load shifting mechanism. The RFB will also take advantage of the electricity prices which vary over the course of the day, such that it will recharge when prices are low, and discharge to reduce the netload during high price periods and therefore will reduce the cost of energy for the facility. Figure 4.7. shows an example of the variance of the purchase price of electricity over a 24-hour period, for a day in winter and a day in summer. During the day in winter, we can see how the RFB could recharge over the low price periods during the first 6 hours and then discharge at about 15:00 to 21:00 when electricity is most expensive, to reduce electricity usage during these price periods. The summer day pricing illustrates how the daily pricing can change over the year, and how price can fall below negative in some cases.

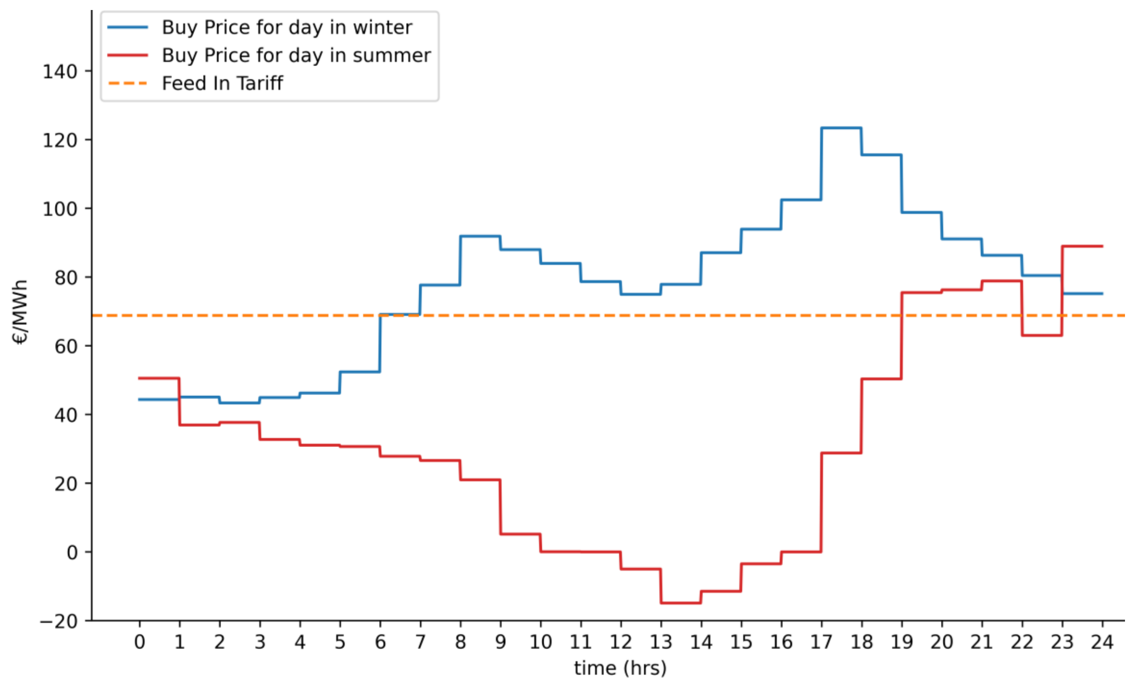

Figure 4.7. Example of variance of electricity price over a 24-hour period for a day in winter and in summer.

4.4.2. Battery Performance

Example of Optimized Performance

Figure 4.8 below shows an example of an optimized RFB operation, when incorporated with the facility over a sample 24-hour period. The plots show the original and now RFB augmented netload, the RFB charging/discharging profile and corresponding SOC, and the corresponding energy prices for each hour. This illustrates how the RFB is optimized to recharge during low electricity price periods, which will increase the netload during this time; and discharge to reduce the facility's netload during high electricity price periods.

Time 0 - 6 hours:

- At the beginning of the period, the RFB is at its lowest SOC of 10 %.
- The electricity prices are at the lowest range, compared to the remainder of the day.
- At time = 2 hours, the RFB recharges, using the low-price electricity. The new netload increases in magnitude as the facility is drawing power from the grid to recharge the RFB and meet their energy needs. The load increase is from 10 kW to ~17 - 20 kW.
- The battery recharges to 50% SOC.

Time 6 - 9 hours:

- Electricity prices increase and reach some of the highest rates for the day.
- The battery stops recharging and now discharges to offset the decrease the original netload from ~ 10 kW to ~2.5 to 5 kW. This reduces the facility’s energy consumption over this high electricity priced period.
- The battery discharges to 15% SOC.

Time 9 - 15 hours:

- Electricity prices decrease and reach a medium price range for the day during this period.
- The RFB is on standby for the first hour, and then once electricity prices decrease even further, it starts to recharge and reaches a SOC of 50%.
- As seen with time 0 – 6 hours, the netload increases as the facility is consuming power to recharge the RFB and to use for their utilities.

Time 15 - 19 hours:

- The electricity prices reach another high price period for the day.
- The battery discharges to reduce the netload during this high price period and brings its magnitude down from ~10 kW to 0 to 2 kW.

Time 19 - 24 hours:

- Battery has discharged to its minimum SOC and remains on standby for the remainder of the day, except for a brief activity during time = 20 – 21.5 hours.

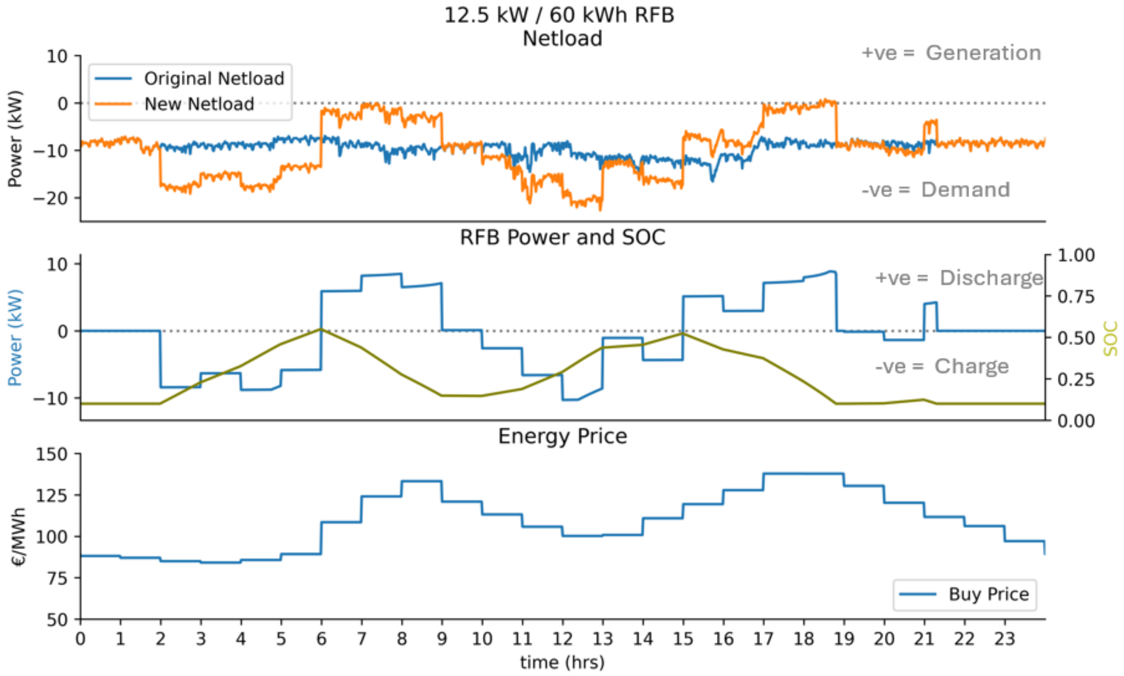

Figure 4.8. An example of an optimized 12.5 kW / 60 kWh RFB operation

Comparing the Performance for the Different Cases

Figure 4.9 and Figure 4.10 show the one-week average performance of the 12.5 kW/ 60 kWh battery for case 1 and case 2. In general, we can see that the case 1 weekday

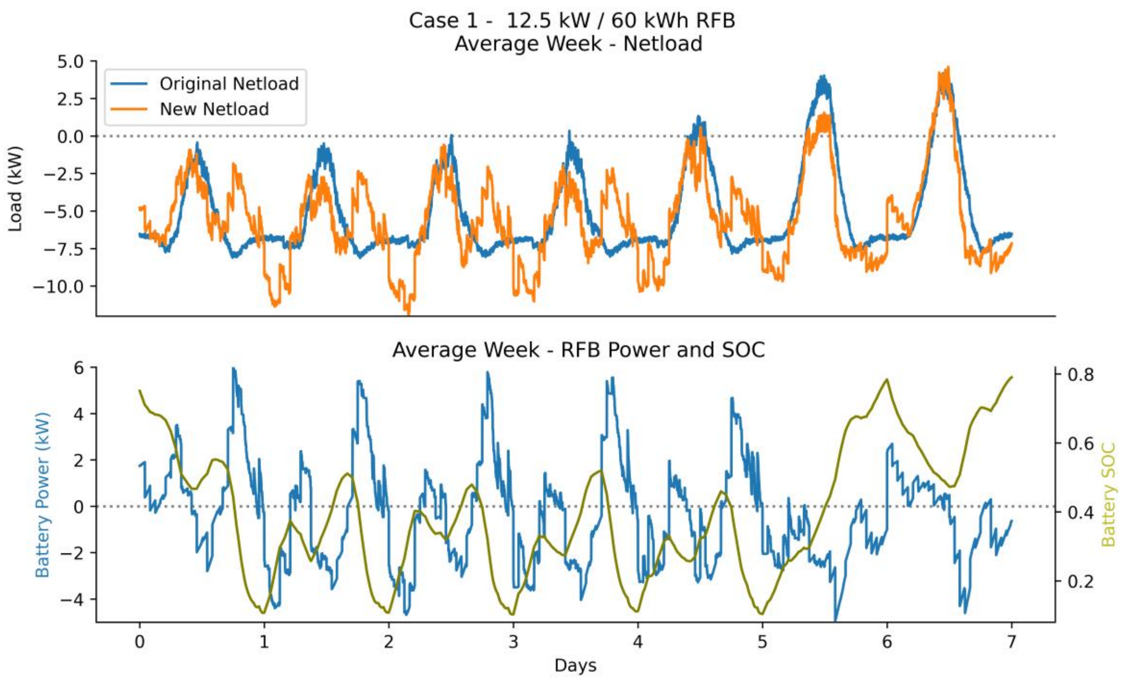

Figure 4.9 One-week average profile for a 12.5 kW / 60 kW RFB for case 1

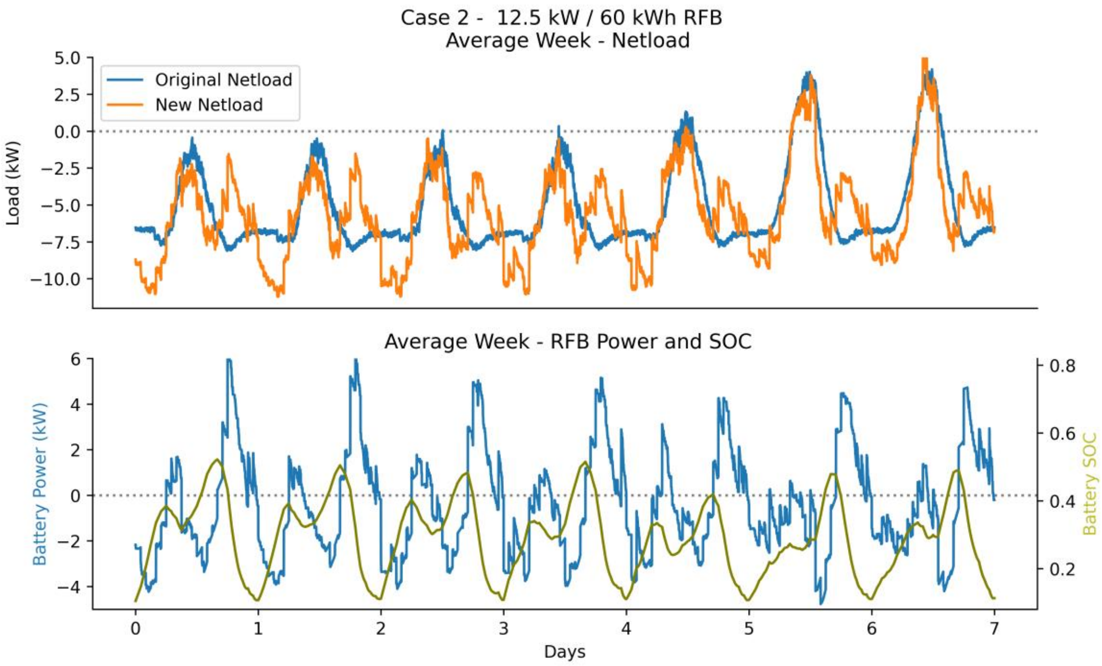

Figure 4.10 One-week average profile for a 12.5 kW / 60 kW RFB for case 2

Battery Electrolyte Degradation

Figure 4.11 and Figure 4.12 below show the RFB capacity degradation due to electrolyte decay for a 1 year period for 12.5 kW / 60 kWh and 25 kW / 60 kWh RFBs. By comparing low and high power-rated RFBs, we can observe how power rating influences battery cycling, degradation, and consequently the frequency of mixing and rebalancing required to maintain system performance. A higher power-to-capacity ratio results in a greater number of cycles, as the RFB can more readily cycle through its full energy capacity. This increased cycling leads to accelerated degradation. We see over the course of the year, the 25 kW/ 60 kW battery goes through ~500 cycles and requires a rebalancing activity after the maximum storage capacity reaches its minimum limit at approximately 225. The 12.5 kW / 60 kWh RFB does not go through a sufficient number of cycles for rebalancing to occur.

Table 4-8 summarizes of the number of battery cycles, mixing activities and rebalancing activities over the 1-year period. When the number of mixing or rebalancing activities is less than one, the value indicates how close the RFB is to requiring that activity.

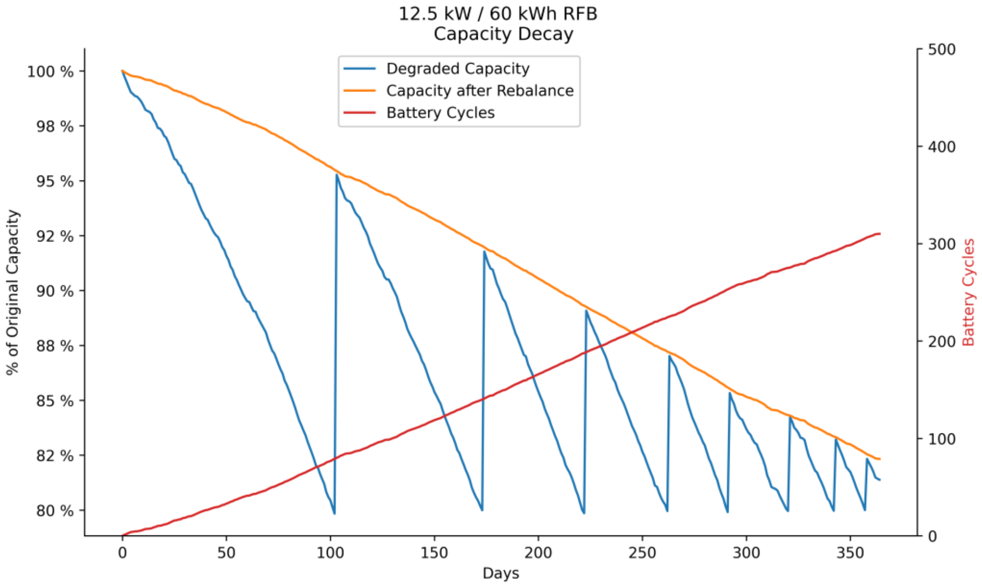

Figure 4.11. Example of cycle-based capacity decay for a 12.5 kW / 60 KWh RFB for a 1 year analysis

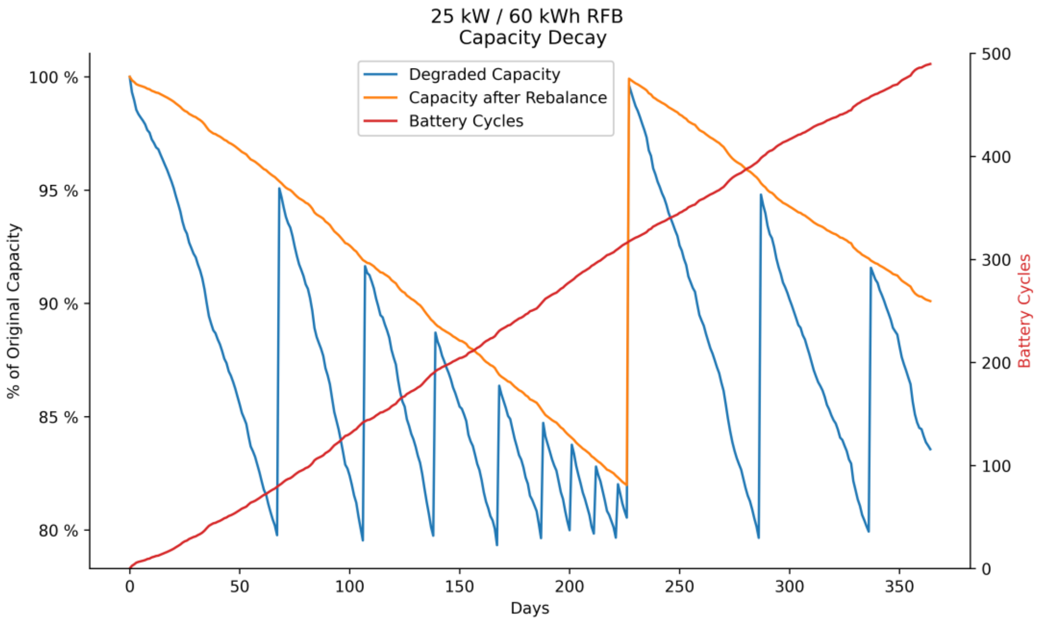

Figure 4.12 Example of cycle-based capacity decay for a 25 kW / 60 KWh RFB for a 1 year analysis

Table 4-8 Summary of rebalancing and mixing activites after 1 year, with values averaged for Case 1 and Case 2

Result	Batter Storage Capacity	P = 25 kW		P = 18. 75 kW		P = 12.5 kW	
		Case 1	Case 2	Case 1	Case 2	Case 1	Case 2
Battery Cycles	60 kWh RFB	489	490	399	412	307	310
	90 kWh RFB	360	372	296	299	206	214
	120 kWh RFB	286	289	230	230	159	157
	150 kWh RFB	234	242	187	183	132	125
	180 kWh RFB	203	202	155	153	113	108
	240 kWh RFB	153	150	120	113	88	78
No. of Mixing Activities	60 kWh RFB	11	11	10	10	8	8
	90 kWh RFB	9	9	7	7	3	3
	120 kWh RFB	6	6	4	4	2	2
	150 kWh RFB	4	4	2	2	1	1
	180 kWh RFB	3	3	2	2	1	1
	240 kWh RFB	2	2	1	1	1	1
No. of Rebalance Activities	60 kWh RFB	1	1	1	1	0.13	0.12
	90 kWh RFB	1	1	0.16	0.15	0.42	0.39
	120 kWh RFB	0.19	0.18	0.34	0.34	0.55	0.55
	150 kWh RFB	0.34	0.31	0.47	0.48	0.62	0.64
	180 kWh RFB	0.42	0.43	0.56	0.56	0.68	0.69
	240 kWh RFB	0.56	0.57	0.66	0.68	0.75	0.78

Battery Only Annual Returns

The reduced annual energy cost and corresponding gross annual savings for each battery are summarized in Table 4-9 and Table 4-10 below, for case 1 and case 2, respectively. Cost savings occur for all cases and battery sizes, which amount to €128 to €505, corresponding to 4.3 to 12 % savings as the original annual energy cost is € 4,214. We see that the results in Case 2 give greater cost savings than Case1, indicating that the Case 2 scheme was better performing. We note again that for Case 1 our objective function forces the battery to recharge such that, at the end of Saturday it is desired to have a SOC > 50% and at the end of Sunday the SOC = 80%. Figure 4.13 to Figure 4.15 show the weekend charging and SOC profiles for different RFB storage sizes, for different rated power. Looking at Figure 4.13, we can see that the smaller RFB's (60 – 120 kWh), are able to fully recharge over the first 24 hours of the weekend, owing to their smaller storage sizes. This also gives them the opportunity to discharge over the course of the weekend, to either offset times of high volume or high-cost energy use, or to sell back to the grid, allowing for some savings to be made. This is clearly seen in the SOC dip occurring between, 24 – 36 hours. Immediately after this dip, the smaller RFBs continue to charge by to meet their recharging obligation by hour 48. The larger batteries on the other hand are unable to carry out any energy trading during the weekend, as their large size and relatively low power rating requires the full period of the weekend. This long recharging period is also compounded by the RFB's derating that occurs during charging, as shown in Figure 4.1 to Figure 4.3 in Section 4.3.2. Figure 4.14 and Figure 4.15 show the weekend charging results for the RFBs with a rated power of 18.75 kW and 25 kW. In these We can see how the larger RFB's (150 – 240 kWh) can recharge quicker, compared to to the 12.5 kW battery, due to their higher rated power and hence can participate in energy trading during the weekend period; however, there is still a very clear distinction between the larger and smaller sized RFBs, as the smaller RFBs can also take advantage of the high power to enhance their energy trading and increase energy savings.

Another interesting observation is the Case 2 annual cost saving, particularly when comparing the 12.5 kW RFB results to the 18.75 and 25 kW RFB results. The 18.75 and 25 kW RFB results show that generally, the cost savings increase as the RFB storage capacity increases. This would be expected, as with more storage capacity, the RFB is capable of trading more energy and offsetting the facility's load for longer, resulting in more costs saved. The 12.5 kW RFB, however, shows an inverse trend. To explain this, we look at the power, SOC and efficiency profile for the 12.5 kW RFBs in Figure 4.16, below. For all RFB sizes, we see that the charging efficiency is ~85.5% at the beginning of the cycle, and increases non-linearly to a maximum of 89% once a 60 % SOC is reached, and then proceeds to decrease to 88% once the full SOC is reached. Due to the low charging rate, it can take 8 to 14 hours for these RFBs to recharge, and because the RFB charging/discharging schedule was optimized for a 24 hour period, the RFBs with larger storage capacities are less likely to recharge to a SOC of 50 – 70 % where the charging higher efficiencies occur. Therefore, it can be stated that for the RFBs with a rated power of 12.5 kW, higher losses would be expected during charging with increasing battery storage capacity, and hence lower annual cost savings. The 18.75 kW and 25 kW RFBs can recharge at a higher rate, therefore they can maintain SOC of 50 – 70% at the higher charging efficiencies and are not as sensitive to these charging losses. However, they are still impacted by this mechanism which can help explain why the best annual savings occur for the 180 kWh RFB, instead of the 240 kWh size.

There is a clear trend when adjusting the storage capacity or when adjusting the power capacity, which would be expected, as either of these parameters will have a direct impact on the battery performance. Table 4-9 summarizes the absolute difference between annual cost savings for a changing storage capacity at a fixed rated power, and for a changing rated power for a fixed storage capacity; and it also shows the relative spread of the difference range.

Table 4-9 Battery only annual cost savings for case 1

Metric	Battery Storage Size	P rated = 25 kW	P rated = 18.75 kW	P rated = 12.5 kW
Absolute Savings	60 kWh	€ 358	€ 299	€ 216
	90 kWh	€ 399	€ 312	€ 203
	120 kWh	€ 402	€ 283	€184
	150 kWh	€ 378	€ 272	€ 164
	180 kWh	€ 357	€ 275	€ 170
	240 kWh	€ 318	€ 243	€ 190
% Savings	60 kWh	8.5%	7.1%	5.1%
	90 kWh	9.5%	7.4%	4.8%
	120 kWh	9.5%	6.7%	4.4%
	150 kWh	9.0%	6.5%	3.9%
	180 kWh	8.5%	6.5%	4.0%
	240 kWh	7.5%	5.8%	4.5%

Table 4-10 Battery only annual cost savings for case 2

Metric	Battery Storage Size	P rated = 25 kW	P rated = 18.75 kW	P rated = 12.5 kW
Absolute Savings	60 kWh	€ 396	€ 356	€ 268
	90 kWh	€ 465	€ 384	€ 269
	120 kWh	€ 489	€ 380	€ 264
	150 kWh	€ 491	€ 394	€ 243
	180 kWh	€ 513	€ 394	€ 232
	240 kWh	€ 487	€ 388	€ 219
% Savings	60 kWh	9.4%	8.4%	6.4%
	90 kWh	11.0%	9.1%	6.4%
	120 kWh	11.6%	9.0%	6.3%
	150 kWh	11.6%	9.4%	5.8%
	180 kWh	12.2%	9.4%	5.5%
	240 kWh	11.6%	9.2%	5.2%

Table 4-11 Difference in annual energy cost savings with changing battery storage capacity and rated battery power.

Cases	Adjusted Battery Parameter	Absolute Difference Between Possible Annual savings	Relative Spread of Annual Savings
Case 1	Storage Capacity	€52 - €84	23 % - 28 %
	Rated Power	€127 - €218	49 % - 78 %
Case 2	Storage Capacity	€39 - €116	10 % - 25 %
	Rated Power	€128-€280	38 % - 74%

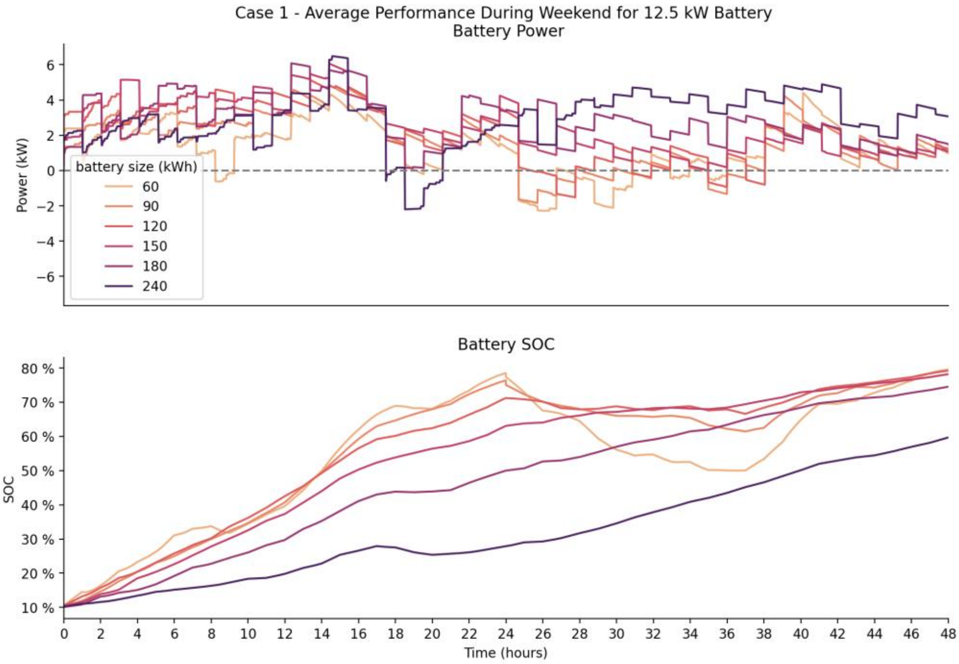

Figure 4.13 Average RFB power and SOC profile during the weekend for RFB's with different storage capacities and fixed rated power at 12.5 kW.

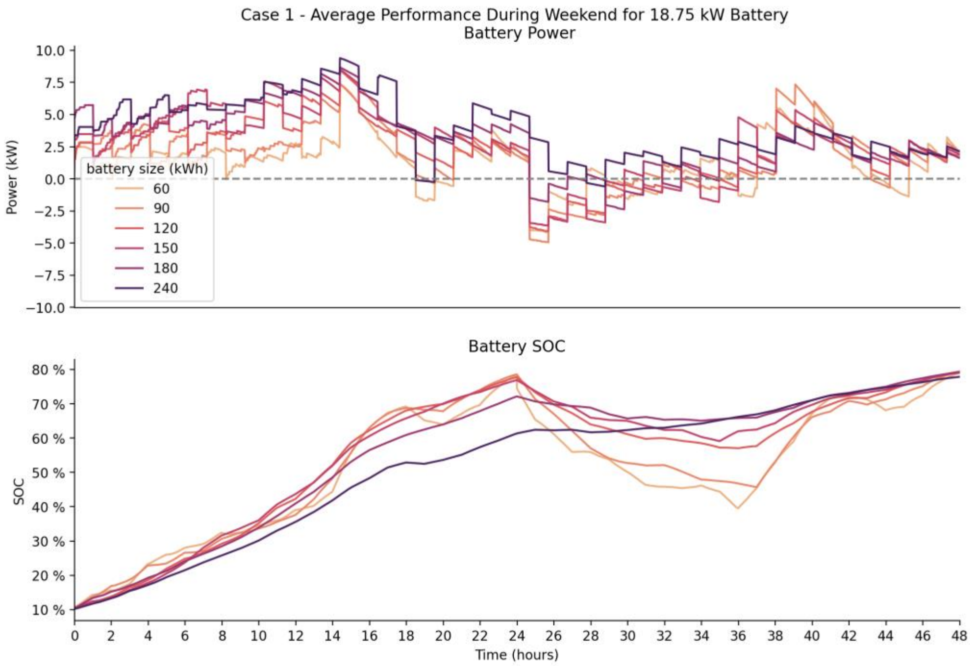

Figure 4.14 Average RFB power and SOC profile during the weekend for RFB's with different storage capacities and fixed rated power at 18.75 kW.

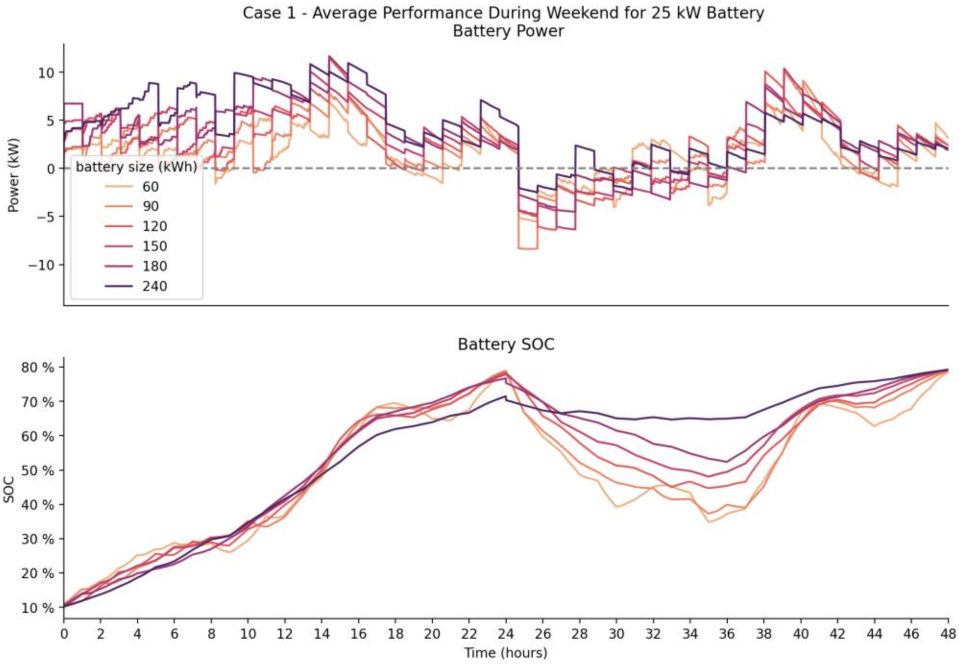

Figure 4.15 Average RFB power and SOC profile during the weekend for RFB's with different storage capacities and fixed rated power at 25 kW.

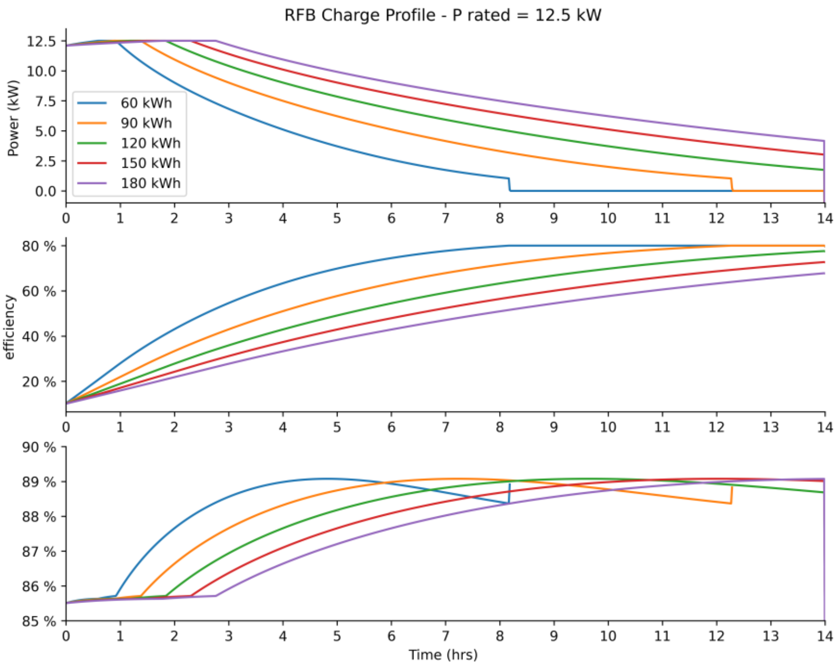

Figure 4.16 Power, SOC and efficiency profile for the 12.5 kW RFB during recharging.

Figure 4.17 shows the cumulative sum of energy purchased and energy sold to the grid during the year for each RFB by rated power. For each power rating (12.5 – 25 kW), the RFB energy trading has been averaged across all storage capacity sizes (60 – 240 kWh), and the error bars represent one standard deviation. Figure 4.17 shows the cumulative energy trading cost, for each average RFB size by power rating, which corresponds to the cumulative sum of energy sold multiplied by feed in tariff; and energy purchased multiplied by the corresponding spot market price. These graphs also show the original data without a RFB in the arrangement. The following observations can be made from this graph:

12.5 kWh RFB:

- The energy sold to grid is similar to the original profile, indicating that the 12.5 kWh sells very little surplus energy to the grid. This is due to the low power rating of the battery, which is sufficient to only offset the original netload of the facility.
- The with this RFB arrangement, a greater energy volume than the original arrangement, as per Figure 4.17; however, the optimized RFB buys this additional energy when it is at a lower cost and discharges to offset the load during high priced periods. We therefore see a lower cost from buying energy, compared to the original, in Figure 4.18.
- We conclude that for the 12.5 kWh RFB, the cost savings occur is mainly due buying energy from the grid and discharging to offset the load.

18.75 kW RFB:

- A significant amount of energy is sold back to the grid, as the power rating of the RFB allows for offsetting the load with additional surplus that can be sold at the feed in tariff.
- As per the 12.5 kWh RFB, greater volumes of energy are purchased, as seen by Figure 4.17; however the cumulative cost from buying (as per Figure 4.18), is less than the original cost. This indicates that the RFB purchases power at lower price periods and discharges during higher priced periods to offset the load and reduce the costs incurred. This is similar to the 12.5 kWh RFB, however, the cumulative cost is greater and closer to the original cost in comparison as this size RFB is capable of purchasing greater volumes of energy.
- The cost savings acquired for the 18.75 kWh is a balanced mechanism, where it is offsetting the load during high priced energy periods using the RFB stored energy, which was purchased during low priced energy periods.

25 kW RFB:

- A significant amount of energy is sold back to the grid, as the power rating of the RFB allows for offsetting the load with additional surplus that can be sold at the feed in tariff.
- A large volume of energy is purchased as seen in Figure 4.17. In Figure 4.18 we see that the cumulative cost of purchased energy is now greater than the original cost, which differs from the 12.5 kW and 18.75 kW RFBs. Although this battery is also carrying out offsetting, such high volumes of energy are purchased, that cost savings cannot be attributed to this mechanism.
- The cost savings for this battery are acquired from selling electricity to the grid.

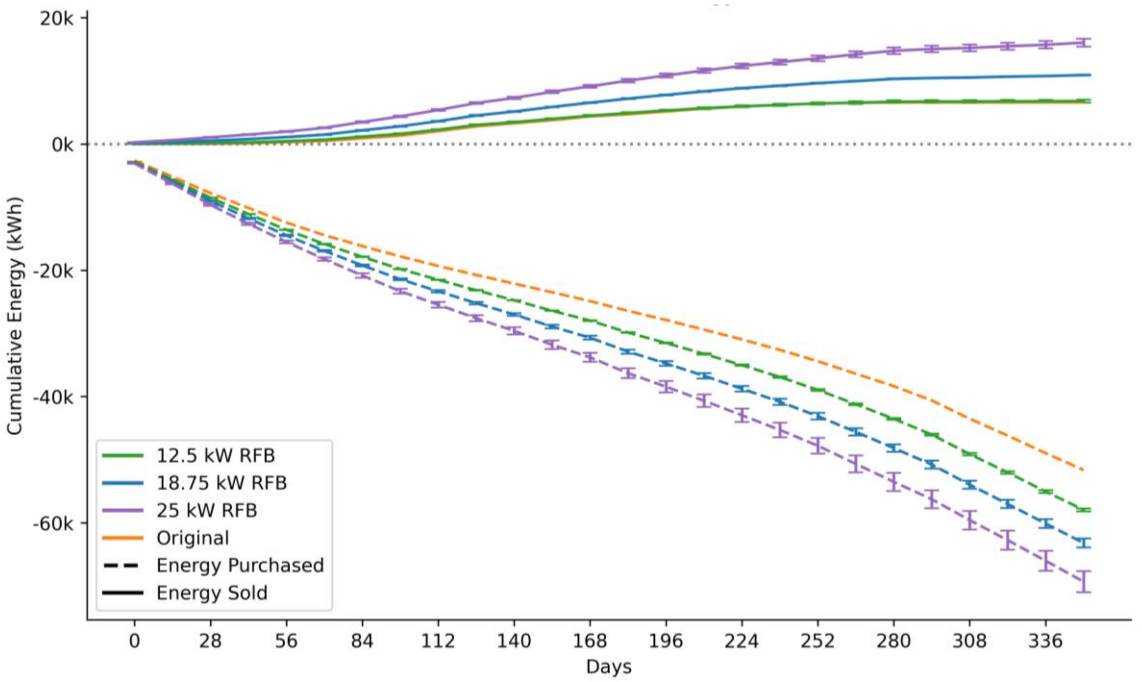

Figure 4.17 Average cumulative sum of energy purchased and sold annually for each RFB size by power rating

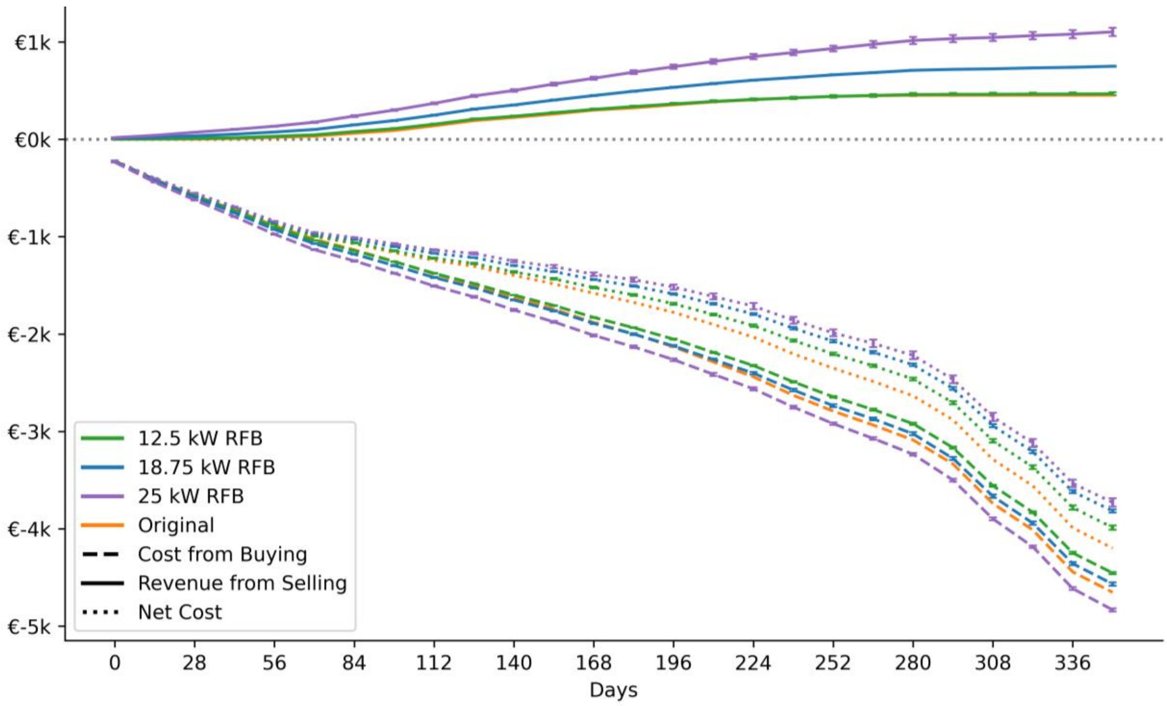

Figure 4.18 Average cumulative sum of annual cost and revenue for energy purchased and sold, respectively for each RFB size by power rating.

4.4.3. HESS Performance

Case 1 Results

Figure 4.19 shows the change in annual savings between 12.5 kW RFB only case, and the HESS arrangements when the 20 kWp to 100 kWp SCs are added to the system. By adding a SC capacitor into the system, the annual savings decrease by ~ 0.6 % when using the 20 kWp SC, to ~1.8 % when using the 100 kWp. In the HESS arrangement, the SC is designed to support the RFB by storing surplus PV power when the RFB is already charging at its maximum capacity due to derating. The SC then discharges to recharge the RFB, helping to avoid grid electricity purchases. However, this surplus PV would otherwise be exported to the grid, generating revenue through the feed-in tariff. By diverting this energy, the SC reduces export revenue—effectively cannibalizing it. As a result, the SC's contribution is offset by the loss in export income, which explains the observed decrease in annual savings.

Figure 4.20 shows how the annual PV self-consumption increases for each HESS system when coupled to a 12.5 kW RFB, and is a percentage of the total PV energy consumed in Table 4-7 in Section 4.4.1. This provides a clearer illustration of how the SC increases PV self-consumption and hence decreases the exported PV, therefore decreasing the revenues obtained for the RFB only case.

Figure 4.19 and Figure 4.20 show the results for the HESS with the 12.5 kW RFB for Case 1, however, the general impact of the SC is representative for the 18.75 kW and 25 kW RFBs. The annual savings results for all HESS are shown in Table 4-12, and the PV self-consumption results in Table 4-13 .

Based on these results, we can conclude that the SC has no added benefit to the overall cost savings. Although the SC improves PV self-consumption, this is at the expense of the revenue generated from exported surplus PV. The assistance that the SC provides to the RFB during charging is insufficient to provide an overall benefit.

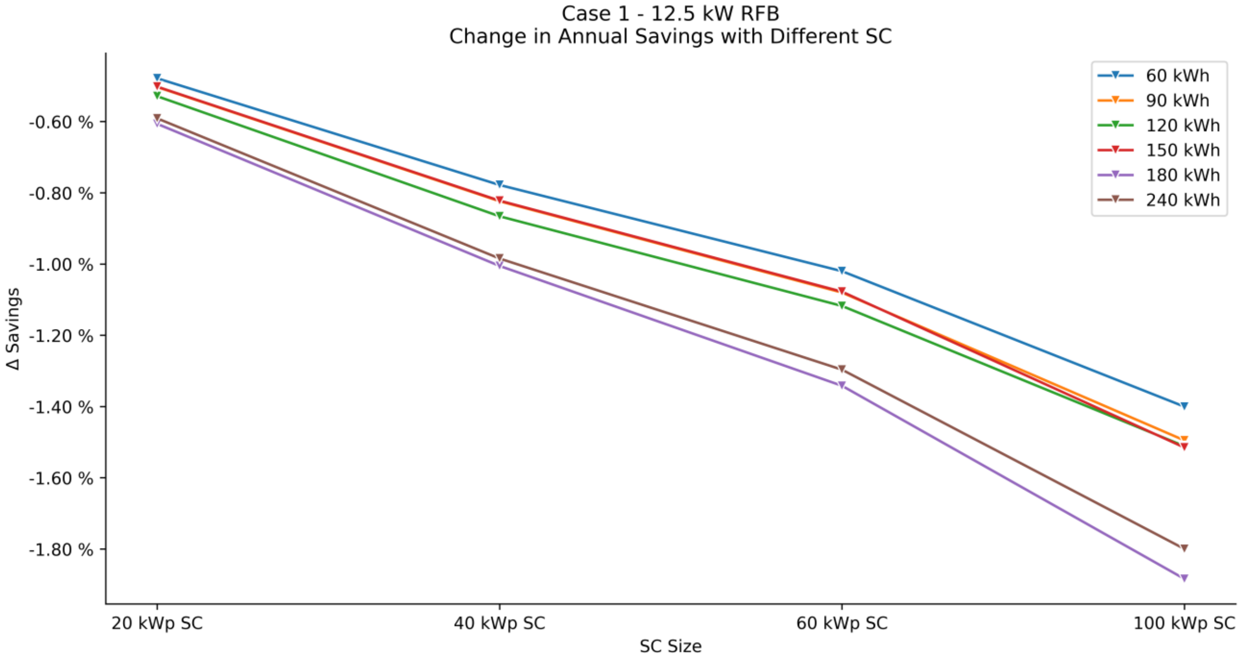

Figure 4.19 Change in annual savings for the 12.5 kW RFBs with different SC sizes

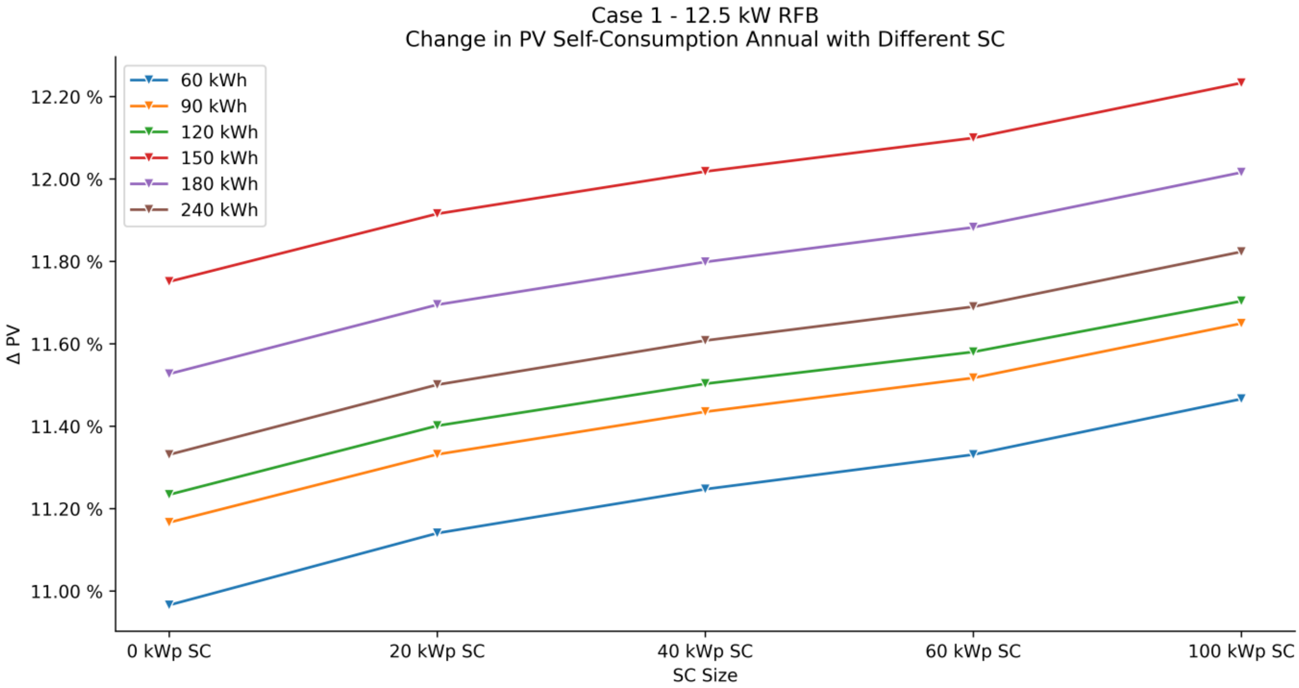

Figure 4.20 Change in annual PV self-consumption for the 12.5 kW RFBs with different SC sizes

Table 4-12 Annual savings increase for each HESS for Case 1

Battery Size	SC Size				
	0 kWp	20 kWp	40 kWp	60 kWp	100 kWp
12.5 kW / 60 kWh	€ 216 (5.13%)	€ 215 (5.10%)	€ 214 (5.08%)	€ 213 (5.06%)	€ 212 (5.04%)
12.5 kW / 90 kWh	€ 203 4.81%	€ 201 4.78%	€ 200 4.76%	€ 200 4.74%	€ 199 4.71%
12.5 kW / 120 kWh	€ 184 (4.36%)	€ 182 (4.32%)	€ 181 (4.30%)	€ 180 (4.28%)	€ 179 (4.25%)
12.5 kW / 150 kWh	€ 164 (3.90%)	€ 163 (3.87%)	€ 162 (3.84%)	€ 161 (3.82%)	€ 160 (3.79%)
12.5 kW / 180 kWh	€ 170 (4.02%)	€ 168 (3.98%)	€ 167 (3.96%)	€ 166 (3.94%)	€ 165 (3.91%)
12.5 kW / 240 kWh	€ 190 (4.52%)	€ 189 (4.48%)	€ 188 (4.45%)	€ 187 (4.43%)	€ 185 (4.40%)
18.75 kW / 60 kWh	€ 299.32 (7.10%)	€ 298.21 (7.08%)	€ 297.43 (7.06%)	€ 296.80 (7.04%)	€ 295.74 (7.02%)
18.75 kW / 90 kWh	€ 311.69 (7.40%)	€ 310.66 (7.37%)	€ 309.97 (7.35%)	€ 309.40 (7.34%)	€ 308.40 (7.32%)
18.75 kW / 120 kWh	€ 282.98 (6.71%)	€ 281.78 (6.69%)	€ 280.97 (6.67%)	€ 280.29 (6.65%)	€ 279.13 (6.62%)
18.75 kW / 150 kWh	€ 272.38 (6.46%)	€ 271.16 (6.43%)	€ 270.33 (6.41%)	€ 269.64 (6.40%)	€ 268.47 (6.37%)
18.75 kW / 180 kWh	€ 274.97 (6.52%)	€ 273.74 (6.49%)	€ 272.90 (6.48%)	€ 272.21 (6.46%)	€ 271.02 (6.43%)
18.75 kW / 240 kWh	€ 243.19 (5.77%)	€ 241.78 (5.74%)	€ 240.85 (5.71%)	€ 240.07 (5.70%)	€ 238.78 (5.67%)
25 kW / 60 kWh	€ 358.21 (8.50%)	€ 357.32 (8.48%)	€ 356.62 (8.46%)	€ 356.01 (8.45%)	€ 354.90 (8.42%)
25 kW / 90 kWh	€ 399.38 (9.48%)	€ 398.50 (9.46%)	€ 397.83 (9.44%)	€ 397.25 (9.43%)	€ 396.20 (9.40%)
25 kW / 120 kWh	€ 401.74 (9.53%)	€ 400.86 (9.51%)	€ 400.19 (9.50%)	€ 399.63 (9.48%)	€ 398.63 (9.46%)
25 kW / 150 kWh	€ 377.58 (8.96%)	€ 376.67 (8.94%)	€ 376.01 (8.92%)	€ 375.44 (8.91%)	€ 374.43 (8.88%)
25 kW / 180 kWh	€ 357.33 (8.48%)	€ 356.39 (8.46%)	€ 355.69 (8.44%)	€ 355.09 (8.43%)	€ 354.05 (8.40%)
25 kW / 240 kWh	€ 317.88 (7.54%)	€ 316.86 (7.52%)	€ 316.13 (7.50%)	€ 315.52 (7.49%)	€ 314.46 (7.46%)

Table 4-13 Annual PV self-consumption increase for each HESS for Case 1

Battery Size	SC Size				
	0 kWp	20 kWp	40 kWp	60 kWp	100 kWp
12.5 kW / 60 kWh	2,132 kWh (10.38%)	2,169 kWh (10.56%)	2,192 kWh (10.67%)	2,210 kWh (10.76%)	2,239 kWh (10.90%)
12.5 kW / 90 kWh	2,297 kWh (11.18%)	2,335 kWh (11.37%)	2,357 kWh (11.48%)	2,375 kWh (11.56%)	2,404 kWh (11.70%)
12.5 kW / 120 kWh	2,363 kWh (11.50%)	2,401 kWh (11.69%)	2,424 kWh (11.80%)	2,441 kWh (11.89%)	2,469 kWh (12.02%)
12.5 kW / 150 kWh	2,519 kWh (12.26%)	2,560 kWh (12.46%)	2,585 kWh (12.59%)	2,605 kWh (12.68%)	2,635 kWh (12.83%)
12.5 kW / 180 kWh	2,552 kWh (12.43%)	2,588 kWh (12.60%)	2,610 kWh (12.71%)	2,627 kWh (12.79%)	2,655 kWh (12.93%)
12.5 kW / 240 kWh	2,516 kWh (12.25%)	2,552 kWh (12.43%)	2,575 kWh (12.54%)	2,594 kWh (12.63%)	2,623 kWh (12.77%)
18.75 kW / 60 kWh	2,342 kWh (11.4%)	2,371 kWh (11.5%)	2,390 kWh (11.6%)	2,404 kWh (11.7%)	2,429 kWh (11.8%)
18.75 kW / 90 kWh	2,923 kWh (14.2%)	2,952 kWh (14.4%)	2,971 kWh (14.5%)	2,987 kWh (14.5%)	3,013 kWh (14.7%)
18.75 kW / 120 kWh	2,900 kWh (14.1%)	2,932 kWh (14.3%)	2,953 kWh (14.4%)	2,969 kWh (14.5%)	2,997 kWh (14.6%)
18.75 kW / 150 kWh	2,911 kWh (14.2%)	2,940 kWh (14.3%)	2,959 kWh (14.4%)	2,974 kWh (14.5%)	3,000 kWh (14.6%)
18.75 kW / 180 kWh	3,020 kWh (14.7%)	3,051 kWh (14.9%)	3,071 kWh (15.0%)	3,087 kWh (15.0%)	3,115 kWh (15.2%)
18.75 kW / 240 kWh	2,998 kWh (14.6%)	3,031 kWh (14.8%)	3,053 kWh (14.9%)	3,071 kWh (14.9%)	3,100 kWh (15.1%)
25 kW / 60 kWh	2,499 kWh (12.2%)	2,523 kWh (12.3%)	2,541 kWh (12.4%)	2,555 kWh (12.4%)	2,581 kWh (12.6%)
25 kW / 90 kWh	2,827 kWh (13.8%)	2,852 kWh (13.9%)	2,870 kWh (14.0%)	2,885 kWh (14.0%)	2,910 kWh (14.2%)
25 kW / 120 kWh	3,034 kWh (14.8%)	3,057 kWh (14.9%)	3,073 kWh (15.0%)	3,087 kWh (15.0%)	3,111 kWh (15.1%)
25 kW / 150 kWh	3,238 kWh (15.8%)	3,263 kWh (15.9%)	3,280 kWh (16.0%)	3,295 kWh (16.0%)	3,319 kWh (16.2%)
25 kW / 180 kWh	3,317 kWh (16.1%)	3,343 kWh (16.3%)	3,362 kWh (16.4%)	3,378 kWh (16.4%)	3,406 kWh (16.6%)
25 kW / 240 kWh	3,367 kWh (16.4%)	3,393 kWh (16.5%)	3,412 kWh (16.6%)	3,427 kWh (16.7%)	3,453 kWh (16.8%)

Case 2 Results

Similar results are presented for Case 2 in Figure 4.21, Figure 4.22, Table 4-14 and Table 4-15, like for Case 1. The same observations are, as per Case 1, where the SC improves PV self-consumption, however there is no added benefit to the overall cost savings.

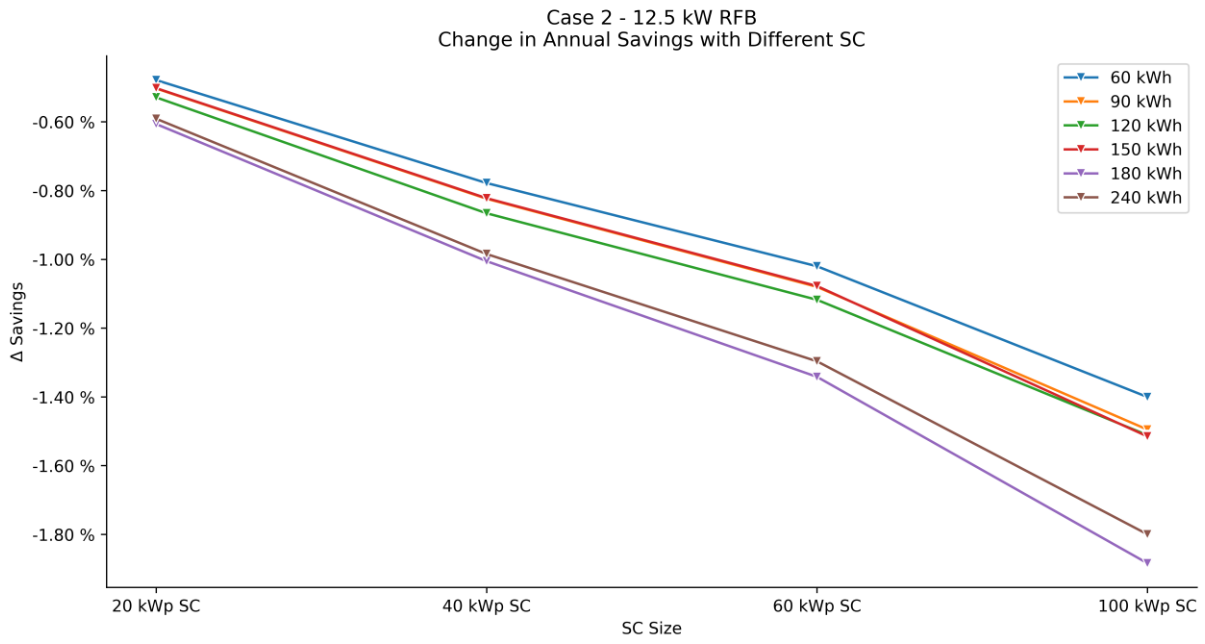

Figure 4.21. Change in annual savings for the 12.5 kW RFBs with different SC sizes

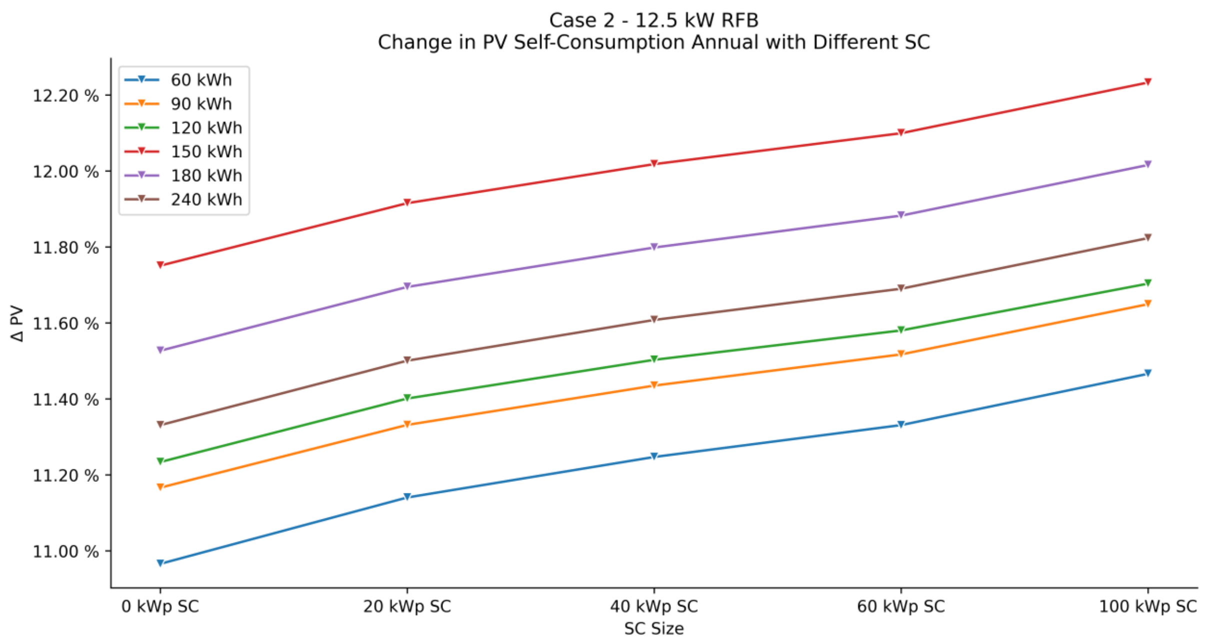

Figure 4.22 Change in annual PV self-consumption for the 12.5 kW RFBs with different SC sizes

Table 4-14 Annual savings increase for HESS arrangements for Case 2

Battery Size	SC Size				
	0 kWp	20 kWp	40 kWp	60 kWp	100 kWp
12.5 kW / 60 kWh	€ 268 (6.36%)	€ 267 (6.33%)	€ 266 (6.31%)	€ 265 (6.29%)	€ 264 (6.27%)
12.5 kW / 90 kWh	€ 269 6.38%	€ 268 6.35%	€ 267 6.33%	€ 266 6.31%	€ 265 6.28%
12.5 kW / 120 kWh	€ 264 (6.25%)	€ 262 (6.22%)	€ 261 (6.20%)	€ 261 (6.18%)	€ 260 (6.16%)
12.5 kW / 150 kWh	€ 243 (5.76%)	€ 241 (5.73%)	€ 241 (5.71%)	€ 240 (5.69%)	€ 239 (5.67%)
12.5 kW / 180 kWh	€ 232 (5.52%)	€ 231 (5.48%)	€ 230 (5.46%)	€ 229 (5.44%)	€ 228 (5.41%)
12.5 kW / 240 kWh	€ 219 (5.19%)	€ 217 (5.16%)	€ 216 (5.14%)	€ 216 (5.12%)	€ 215 (5.09%)
18.75 kW / 60 kWh	€ 355.94 (8.45%)	€ 354.94 (8.42%)	€ 354.27 (8.41%)	€ 353.70 (8.39%)	€ 352.73 (8.37%)
18.75 kW / 90 kWh	€ 384.22 (9.12%)	€ 383.21 (9.09%)	€ 382.52 (9.08%)	€ 381.91 (9.06%)	€ 380.82 (9.04%)
18.75 kW / 120 kWh	€ 379.66 (9.01%)	€ 378.63 (8.98%)	€ 377.90 (8.97%)	€ 377.28 (8.95%)	€ 376.20 (8.93%)
18.75 kW / 150 kWh	€ 394.10 (9.35%)	€ 393.06 (9.33%)	€ 392.31 (9.31%)	€ 391.66 (9.29%)	€ 390.55 (9.27%)
18.75 kW / 180 kWh	€ 394.45 (9.36%)	€ 393.31 (9.33%)	€ 392.53 (9.31%)	€ 391.87 (9.30%)	€ 390.71 (9.27%)
18.75 kW / 240 kWh	€ 388.50 (9.22%)	€ 387.41 (9.19%)	€ 386.65 (9.17%)	€ 386.01 (9.16%)	€ 384.87 (9.13%)
25 kW / 60 kWh	€ 396.44 (9.41%)	€ 395.50 (9.38%)	€ 394.79 (9.37%)	€ 394.16 (9.35%)	€ 393.02 (9.32%)
25 kW / 90 kWh	€ 464.76 (11.03%)	€ 463.92 (11.01%)	€ 463.24 (10.99%)	€ 462.64 (10.98%)	€ 461.54 (10.95%)
25 kW / 120 kWh	€ 488.77 (11.60%)	€ 487.99 (11.58%)	€ 487.39 (11.56%)	€ 486.84 (11.55%)	€ 485.86 (11.53%)
25 kW / 150 kWh	€ 490.63 (11.64%)	€ 489.78 (11.62%)	€ 489.14 (11.61%)	€ 488.57 (11.59%)	€ 487.55 (11.57%)
25 kW / 180 kWh	€ 512.80 (12.17%)	€ 512.00 (12.15%)	€ 511.36 (12.13%)	€ 510.81 (12.12%)	€ 509.82 (12.10%)
25 kW / 240 kWh	€ 487.45 (11.57%)	€ 486.51 (11.54%)	€ 485.80 (11.53%)	€ 485.18 (11.51%)	€ 484.11 (11.49%)

Table 4-15 Annual PV self-consumption increase for each HESS for Case 2.

Battery Size	SC Size				
	0 kWp	20 kWp	40 kWp	60 kWp	100 kWp
12.5 kW / 60 kWh	2,252 kWh (10.97%)	2,288 kWh (11.14%)	2,310 kWh (11.25%)	2,327 kWh (11.33%)	2,355 kWh (11.47%)
12.5 kW / 90 kWh	2,294 kWh (11.17%)	2,328 kWh (11.33%)	2,349 kWh (11.43%)	2,366 kWh (11.52%)	2,393 kWh (11.65%)
12.5 kW / 120 kWh	2,307 kWh (11.23%)	2,342 kWh (11.40%)	2,363 kWh (11.50%)	2,379 kWh (11.58%)	2,404 kWh (11.70%)
12.5 kW / 150 kWh	2,414 kWh (11.75%)	2,447 kWh (11.92%)	2,469 kWh (12.02%)	2,485 kWh (12.10%)	2,513 kWh (12.23%)
12.5 kW / 180 kWh	2,368 kWh (11.53%)	2,402 kWh (11.69%)	2,423 kWh (11.80%)	2,441 kWh (11.88%)	2,468 kWh (12.02%)
12.5 kW / 240 kWh	2,327 kWh (11.33%)	2,362 kWh (11.50%)	2,384 kWh (11.61%)	2,401 kWh (11.69%)	2,429 kWh (11.82%)
18.75 kW / 60 kWh	2,444 kWh (11.9%)	2,472 kWh (12.0%)	2,491 kWh (12.1%)	2,506 kWh (12.2%)	2,532 kWh (12.3%)
18.75 kW / 90 kWh	2,624 kWh (12.8%)	2,651 kWh (12.9%)	2,668 kWh (13.0%)	2,683 kWh (13.1%)	2,709 kWh (13.2%)
18.75 kW / 120 kWh	2,786 kWh (13.6%)	2,814 kWh (13.7%)	2,832 kWh (13.8%)	2,848 kWh (13.9%)	2,874 kWh (14.0%)
18.75 kW / 150 kWh	2,896 kWh (14.1%)	2,922 kWh (14.2%)	2,939 kWh (14.3%)	2,954 kWh (14.4%)	2,979 kWh (14.5%)
18.75 kW / 180 kWh	2,961 kWh (14.4%)	2,989 kWh (14.5%)	3,007 kWh (14.6%)	3,022 kWh (14.7%)	3,049 kWh (14.8%)
18.75 kW / 240 kWh	2,874 kWh (14.0%)	2,902 kWh (14.1%)	2,921 kWh (14.2%)	2,937 kWh (14.3%)	2,964 kWh (14.4%)
25 kW / 60 kWh	2,435 kWh (11.9%)	2,459 kWh (12.0%)	2,476 kWh (12.1%)	2,490 kWh (12.1%)	2,515 kWh (12.2%)
25 kW / 90 kWh	2,858 kWh (13.9%)	2,882 kWh (14.0%)	2,899 kWh (14.1%)	2,913 kWh (14.2%)	2,938 kWh (14.3%)
25 kW / 120 kWh	3,220 kWh (15.7%)	3,242 kWh (15.8%)	3,258 kWh (15.9%)	3,272 kWh (15.9%)	3,296 kWh (16.0%)
25 kW / 150 kWh	3,094 kWh (15.1%)	3,116 kWh (15.2%)	3,132 kWh (15.2%)	3,146 kWh (15.3%)	3,170 kWh (15.4%)
25 kW / 180 kWh	2,914 kWh (14.2%)	2,935 kWh (14.3%)	2,951 kWh (14.4%)	2,964 kWh (14.4%)	2,987 kWh (14.5%)
25 kW / 240 kWh	3,244 kWh (15.8%)	3,267 kWh (15.9%)	3,284 kWh (16.0%)	3,297 kWh (16.1%)	3,322 kWh (16.2%)

4.4.4. TECHNO-ECONOMIC ANALYSIS

Figure 4.23 to Figure 4.25 show the NPV results for the various HESS arrangements, for both Case 1 and Case 2, assessed over periods of 10 – 20 years. In all cases we can see that the NPV are negative, ranging from - €47,000 to -€90,000, and NPV decreases with increasing battery size, increasing SC size and increasing project period. The last point is interesting, as typically, NPV is expected to increase with a longer project period, as an extended timeframe allows for more opportunities to generate revenue. This increased cash inflow helps offset the initial investment cost and move the project toward the breakeven point, improving overall profitability. However, the annual revenue for the different RFB sizes varies between €164 to €512, and this is significantly lower than the annual HESS OPEX, which is can range at about €100 - €1,300 (depending on the year and size) for the RFB and €200 for the SC. Due to this, the HESS generate a negative annual cashflow.

Figure 4.26 to Figure 4.28 show the NPV calculations for the same HESS arrangements as per, with the OPEX neglected from the annual cashflow to understand how this may impact the results. Although the resultant NPVs are still highly negative, there are some noticeable differences compared to the NPVs shown in Figure 4.23 to Figure 4.25, such as:

- All NPVs are slightly more positive than before, ranging from -€25,000 to -€80,000.
- By ignoring the OPEX, the annual cashflow is always positive, hence we see an increasing NPV with increasing project period, as typically expected.
- Comparing the NPV across different project durations for the same HESS configuration shows a notably narrower range of results. This would be expected as the annual cashflow, which is only the revenue in this case, is > 1% of the HESS CAPEX; hence a significantly longer period would be required for the cashflow to offset the initial investment in a meaningful way.

The NPV analysis shows highly negative values for all HESS arrangements. This due the high CAPEX and high OPEX compared to the revenue achieved by each system. For this case study, an RFB is not a financially viable investment as it does not generate enough returns to offset the outgoing costs or the initial investment.

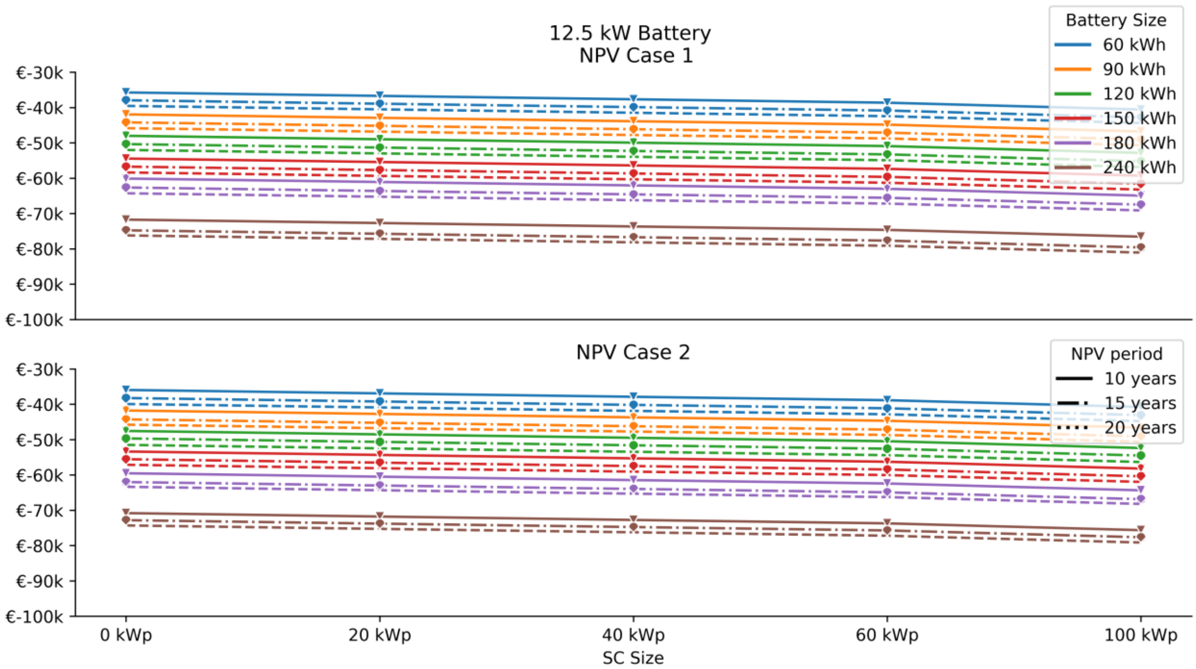

Figure 4.23 NPV results for different HESS combinations using a 12.5 kW RFB

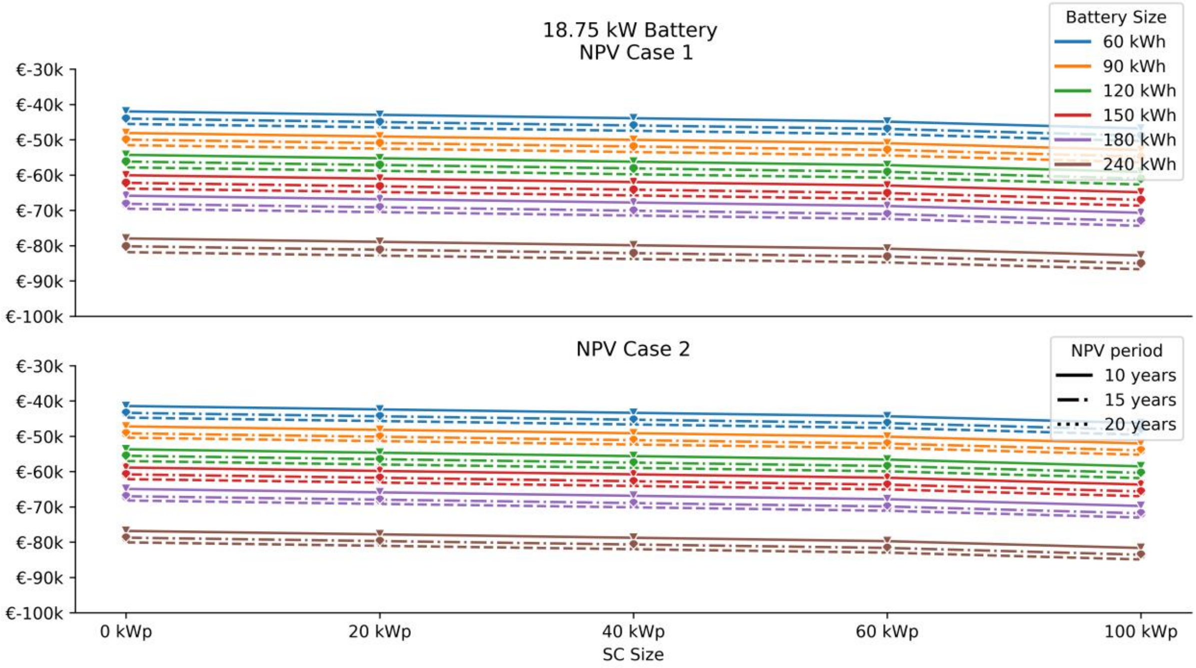

Figure 4.24 NPV results for different HESS combinations using a 18.75 kW RFB

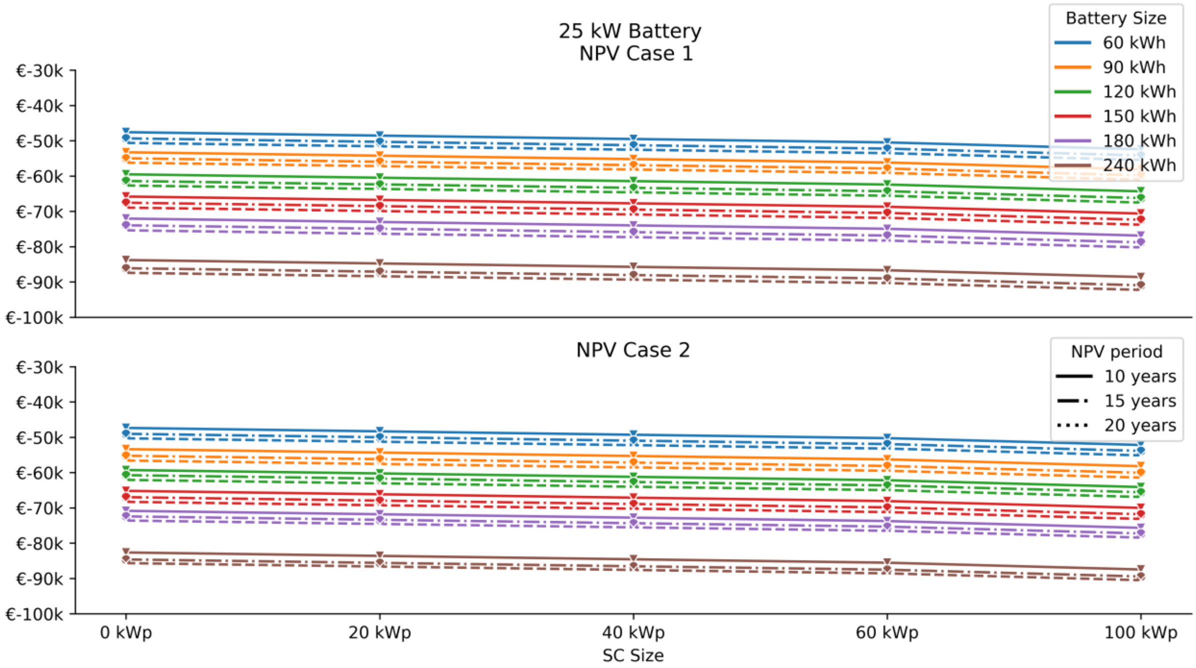

Figure 4.25 NPV results for different HESS combinations using a 25 kW RFB

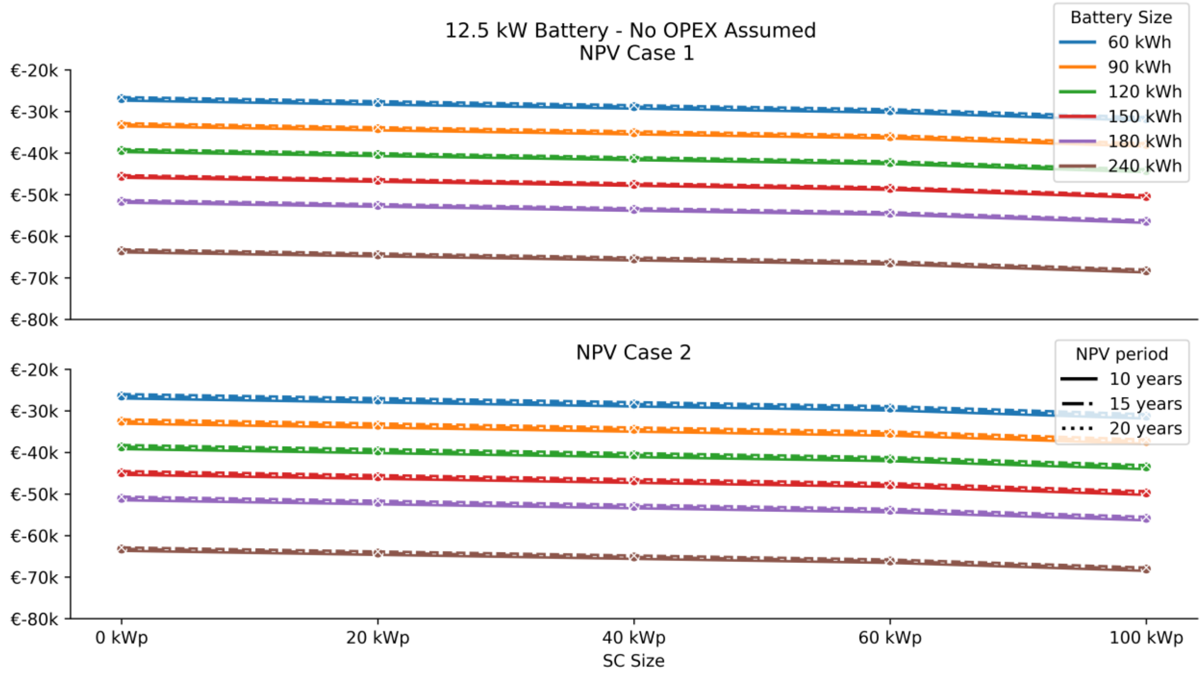

Figure 4.26 NPV results for different HESS combinations using a 12.5 kW RFB, ignoring OPEX in cashflow calculations.

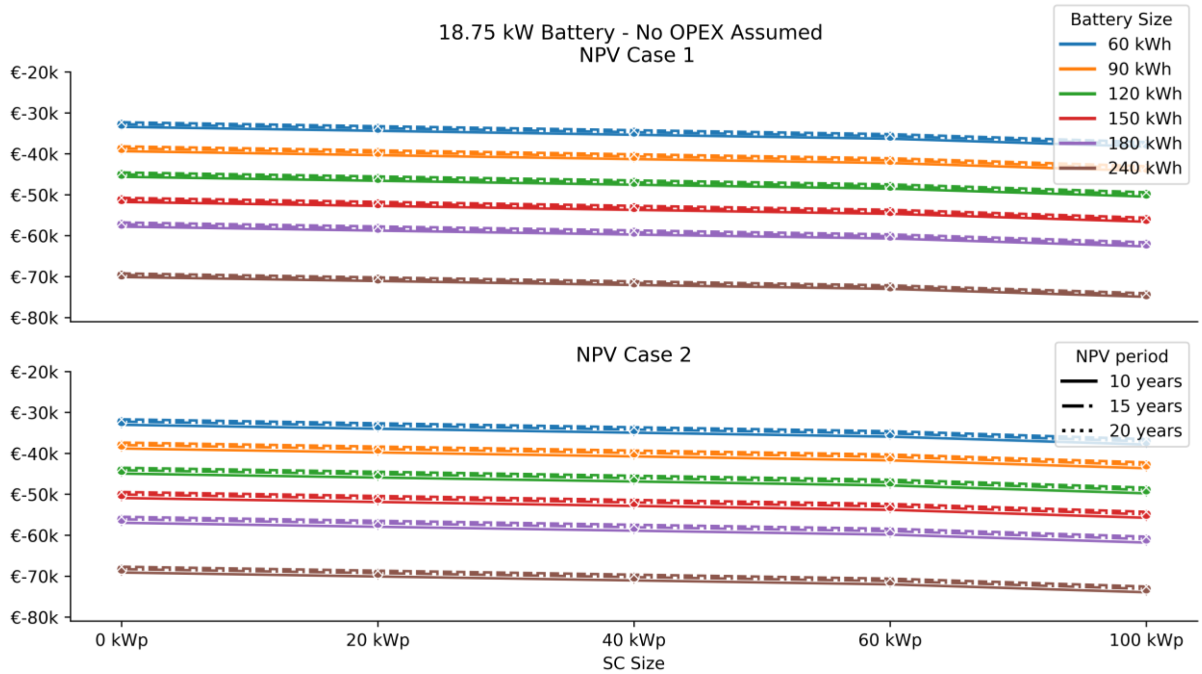

Figure 4.27 NPV results for different HESS combinations using a 18.75 kW RFB, ignoring OPEX in cashflow calculations.

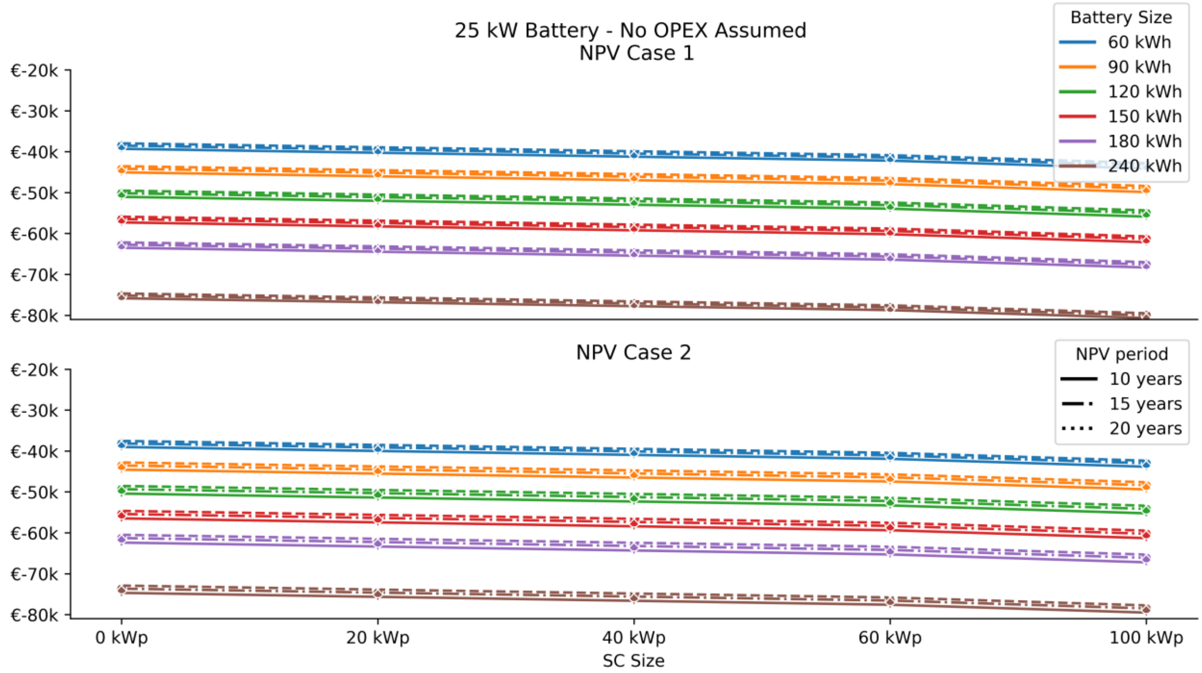

Figure 4.28 NPV results for different HESS combinations using a 25 kW RFB, ignoring OPEX in cashflow calculations.

4.5. CONCLUSION & DISCUSSION

The Germany case study, based at the TZE campus of Landshut University, provides an insightful evaluation of the techno-economic feasibility of implementing a HESS composed of a Vanadium RFB and a SC. The facility integrates renewable energy generation via rooftop and carport PV systems and actively seeks to enhance energy self-sufficiency, cost efficiency, and grid interaction through advanced storage solutions.

The analysis suggests that combining RFB and SC technologies can offer complementary benefits. The RFB provides long-duration energy storage, helping to shift loads and take advantage of lower electricity prices. Meanwhile, the SC contributes by handling short bursts of high-power demand and supporting the RFB during recharge phases, particularly where quick response is needed. While the overall impact of hybridization is moderate, it does contribute to improved load following, increasing self-consumption of PV, and some reduction in peak demand.

From a technical standpoint, the HESS succeeded in reducing grid imports during high-price periods and utilizing low-price or surplus PV energy during off-peak hours. The RFB was consistently optimized to recharge during low-tariff periods and discharge during peak-price periods, yielding savings through both demand-charge reduction and time-based arbitrage. The SC enhanced fast responsiveness, smoothed net loads, and assist on the RFB by absorbing powers from PV and accelerating recharge. The study emphasizes the importance of high-resolution energy data and flexible operation strategies. By leveraging lower timeframe simulations, the analysis captured more dynamics of the energy system and identified opportunities for peak charging within that timeframe, which would be missed in lower-resolution models.

Economically, the NPV analysis revealed that carefully sized HESS configurations can yield positive financial outcomes, particularly under scenarios with high electricity price volatility, appropriate feed-in tariffs, and reduced capital costs for RFBs. However, profitability remains sensitive to system sizing, component degradation (especially electrolyte decay in the RFB), and operating strategies. The study highlighted that failing to account for degradation can lead to overestimations in revenue, underscoring the importance of lifecycle-aware optimization.

All in all, this study underscores that a well-sized HESS can significantly enhance the technical performance of renewable-integrated facilities. While current cost structures still pose barriers to widespread adoption, ongoing reductions in storage CAPEX, coupled with increasing electricity price volatility, position HESS as a promising asset for smart campuses, microgrids, and energy communities aiming for decarbonization and cost efficiency.

5. CASE STUDY - ITALY

5.1. INTRODUCTION

Italy operates a complex electricity market structure, including Day-Ahead market, (Mercato del Giorno Prima (MGP)), Intraday market (Mercato Infragiornaliero (MI)), Balancing market (Mercato di Bilanciamento (MB)), specific ancillary services (Mercato dei Servizi di Dispacciamento (MSD)) like Fast Reserve (FR) market, and Capacity market (Mercato della Capacità (MC)) all utilized by the Italian System Operator, Terna[58], to procure the resources that it requires for managing and monitoring the system.

The MGP is Italy's main wholesale electricity market where participants submit bids to buy or sell electricity for each hour of the following day. It ensures efficient matching of supply and demand and sets the baseline for scheduling electricity production and consumption. The MI allows participants to adjust their electricity positions after the Day-Ahead Market closes to reflect updated forecasts or unforeseen events. It operates in multiple sessions daily and helps improve real-time system efficiency and reliability. This market has evolved into a hybrid model combining continuous trading with auctions, allowing participants to adjust positions closer to real-time.

The MSD, managed by Terna, secures resources to ensure grid reliability through congestion resolution, reserve provision, and balancing. It includes both a planning phase and a real-time Balancing Market, with bids selected based on system needs. The MB is the real-time component of the MSD, where Terna corrects imbalances by dispatching flexible resources on short notice. It ensures supply and demand are matched in real-time to maintain grid stability. It also remunerates both capacity availability and energy activation for services like frequency restoration (aFRR, mFRR) and replacement reserves (RR). The MC incentivizes investments in generation and storage by awarding long-term contracts to ensure availability during system stress. Participants receive fixed payments and must return surplus profits if market prices exceed a certain level. The Fast Reserve market provides ultra-fast balancing services from flexible technologies like batteries to maintain frequency stability during sudden imbalances. Resources are selected through tenders and respond within seconds, supporting a resilient, renewable-powered grid.

Optimizing the operation of a HESS across these multiple, interconnected markets presents a significant challenge. Operators must decide how to allocate the HESS capacity (both power and energy) among different revenue streams (energy arbitrage, balancing capacity/energy payments, FR remuneration) while respecting the technical limitations of the BESS and SC components and adhering to complex market rules. This section of the report summarizes case studies investigating the co-optimization strategies and economic viability of a HESS participating in the Italian MGP, MI, MB, and FR markets, simultaneously.

5.2. PURPOSE OF THE CASE STUDY

The primary purpose of these case studies is to:

- Evaluate the economic feasibility of investing in and operating a HESS (BESS + SC) within the current Italian electricity market framework.
- Develop and analyze optimal operational strategies for the HESS to maximize profitability by simultaneously participating in the MGP, MI, MB, and the FR services.
- Quantify the potential revenue streams from each market (MGP/MI arbitrage, MB capacity/energy, FR capacity remuneration) and assess the benefits of revenue stacking.
- Investigate the technical challenges and operational constraints associated with managing the HESS state (SOC, degradation) while meeting the demanding requirements of services like Fast Reserve and respecting grid/market limitations.
- Understand the interplay between the BESS and SC components in providing different market services effectively.

While existing research has explored the participation of BESS or SC individually in various electricity markets, and some studies have examined HESS in ancillary service provision, specific analyses focusing on the co-optimization of HESS across the full spectrum of relevant Italian markets (MGP, MI, MB, and specifically the FR product) remain relatively limited. This literature review synthesizes key findings from published papers, mainly focusing on the participation of Microgrids (MGs) and Energy Storage Systems (ESS) in multiple electricity markets.

The economic potential of BESS in the day-ahead and automatic frequency restoration reserves (aFRR) markets was evaluated in [59] using an agent-based model. The study showed better economic prospects in 2030 compared to 2019, with a projected shift in revenue sources from reserve to day-ahead markets. [60] proposed a general payoff model to assess BESS utilization in European markets. While energy arbitrage was found unviable in most regions, frequency regulation services, especially in Central Western and Northern Europe, remained promising.

A techno-economic study of a 2 MW/2 MWh BESS in the Italian market, conducted in [61], examined auxiliary consumption, SOC, SoH, and RTE across 2019, 2020, and 2022 price scenarios. It found that CAPEX is a key driver of economic viability, emphasizing the impact of price fluctuations on investment returns. A modeling study in [62] explored BESS participation in fast frequency regulation and the balancing market in Italy. It found that stacking services (e.g., fast reserve and replacement reserve) across the year improves both investment returns and operational efficiency.

In [63], machine learning and deep learning techniques were applied to forecast zonal prices and bid acceptance in DAM and XBID markets. The results highlighted XBID's competitiveness and underscored the importance of capacity payments to ensure BESS viability. [64] conducted a comprehensive study assessing the profitability of various ESS technologies (PHS, CAES, HES, FES, LBS, CSP-TES) using a joint clearing model for energy and ancillary services. The findings support the economic viability of ESS in frequency regulation markets, highlighting the importance of location and system flexibility.

A bi-level model, proposed in [65], examined the joint optimization of ESS location and size in centralized electricity markets. It applied a rate-of-return constraint and analyzed the impact of regulation market policies, which is conceptually relevant for large-scale HESS planning. [66] presented an ADP-based strategy for pumped hydro storage. It found that integrated day-ahead and intraday trading outperforms single-market or sequential strategies, underlining the importance of accurate price forecasting.

A multistage stochastic optimization model was proposed in [67]for a Virtual Power Plant (VPP) comprising wind, PV, and BESS. It demonstrated that full participation in DA, ID, and balancing markets improves profitability and reduces imbalance costs. A similar multistage optimization model for a wind+BESS VPP in [[68] showed additional economic benefits when including ancillary service markets, reinforcing the value of broader multi-market participation.

[69]proposed a multi-market bidding strategy for grid-side BESS operating as independent market participants. The study confirmed the economic advantage of engaging in both day-ahead and intraday markets. [70] used a Markov Decision Process (MDP)-based model with reinforcement learning to optimize trading decisions for energy storage in the European intraday market, offering a scalable and adaptive approach for microgrid operations.

In [71], a planning model for aggregated DERs following a price-maker strategy was proposed. The study emphasized the benefits of market-aware aggregation under price uncertainty.

An optimal management strategy for integrated PV+BESS systems, introduced in [72] , demonstrated that droop-based primary frequency regulation and market-based energy delivery can be jointly achieved through a two-level stochastic control architecture. A hierarchical Energy Management System (EMS) was developed in [73]for a PV-BESS system participating in Italian electricity markets. The study showed the effectiveness of forecast-driven scheduling in maximizing profits and ensuring reliable operation. In [74], a hybrid neural network methodology improved 24-hour-ahead PV power forecasting in microgrids, enhancing bidding strategies in the DA and ID markets.

[75]offered strategic recommendations that stressed the importance of regulatory clarity and appropriate incentives to support BESS deployment in deregulated electricity markets such as Italy's. A unified planning framework for coordinated RES+ESS investment was presented in [76]. The study concluded that combining market revenue with financial incentives can fully cover investment costs, offering important insights for national energy planning. A probabilistic bidding optimization approach for aggregators, incorporating flexible demand, renewable generation, and forecast uncertainty, was proposed in [77]. The study showed that this approach yields better results than deterministic strategies in day-ahead and intraday markets.

5.3. METHODOLOGY DESCRIPTION

The solution methodology developed for optimizing the operation of the microgrid and determining optimal asset sizes addresses the multifaceted challenges of long-term planning, forecast uncertainty, and sequential electricity market participation. It combines a rolling horizon simulation with a multi-stage market-clearing structure (Day-Ahead, Intra-Day, and Balancing markets), embedded within a sizing loop that evaluates discrete BESS and SC capacity combinations to identify the most profitable configuration over the system's lifetime. This integrated framework supports detailed techno-economic analysis by capturing both operational dynamics and investment trade-offs, allowing for the evaluation of storage system configurations in terms of capital costs, flexibility, and market revenues.

The increasing penetration of distributed energy resources, such as solar and wind, alongside advances in storage technologies, is reshaping the electricity landscape. Microgrids, localized systems capable of operating in both grid-connected and islanded modes, offer enhanced reliability, resilience, and local optimization of energy resources. Their economic viability, however, depends heavily on effective management of internal power flows and strategic participation in electricity markets.

Electricity markets typically clear in a sequential fashion, starting with the Day-Ahead market, followed by Intra-Day and Balancing markets, enabling market participants to adjust their strategies as forecasts improve. Simultaneously, grid operators procure ancillary services like Fast Reserve to ensure system stability, offering additional revenue streams for flexible assets such as batteries and supercapacitors.

Optimizing microgrid design thus requires the selection of storage capacities that strike a balance between capital investment and operational value. Mathematical optimization models serve as a robust tool for addressing this challenge, enabling comprehensive evaluation of operational strategies, system sizing, and market interactions under realistic technical and regulatory constraints.

The Procedure

The procedure works through a combination of techniques:

Rolling Horizon Simulation: To overcome the computational challenges of optimizing over an extended period (e.g., a year) and to manage decreasing forecast accuracy over time, a rolling horizon strategy is used. The total simulation duration is divided into shorter, consecutive planning periods. The optimization model is solved for each of these periods sequentially. A crucial aspect is the seamless transition of the system state between periods; the final state of key dynamic variables (like energy levels in storage systems and DG status/output) at the end of one planning period becomes the initial state for the next. The length of the planning period involves a trade-off: a longer period allows for a broader look-ahead but relies on less accurate long-term forecasts, while a shorter period uses more accurate short-term forecasts but can lead to decisions that are not purely optimal for the overall system. An end-of-horizon target for storage energy levels is often included to encourage storage systems to maintain a reasonable state of charge, mitigating the "drain-down" effect and promoting better performance in subsequent periods.

Sequential Market Stages: Within each planning period of the rolling horizon, the optimization problem is solved multiple times to reflect the chronological nature of electricity market participation and the refinement of forecasts over time. This approach models the decision-making process of a market participant who first commits to the Day-Ahead market based on early forecasts, then adjusts their position in the Intra-Day market with updated information, and finally participates in the Balancing Market based on near real-time conditions and system needs, including ancillary services like Fast Reserve.

Day-Ahead (DA) Stage: The optimization model is initially solved using the earliest available forecasts for PV generation, Load, and market prices relevant for the DA stage, covering the entire planning period. Decision variables related to downstream markets (MI, MB) are typically constrained or fixed to zero. The results determine the optimal DA energy bids and provide a preliminary operational schedule.

Intra-Day (ID) Stage: Following the DA solve, the optimal DA energy bids are fixed as hard constraints. Updated forecasts for PV, Load, and MI prices, which are typically more accurate, are loaded. Market variables for MB remain fixed to zero. The model is re-solved with these updated inputs and constraints, focusing on using the flexibility of storage, DG, and ID market participation to adjust to updated forecasts and minimize deviations from the initial DA schedule. The results determine the optimal ID energy bids and further refine the operational schedule.

Balancing Market (MB) Stage: In the final market stage, the optimal DA and ID energy bids determined in the previous stages are fixed as hard constraints. The latest, most accurate forecasts for PV, Load, and MB prices are used. Market variables for MB capacity offers are released and optimized, subject to capacity and energy availability constraints and the FR provision constraints. The model is solved one final time for the period. This stage captures the value of offering capacity in the balancing market and the operational adjustments needed to meet these commitments and provide FR services. The results from this MB stage represent the final realized operational decisions for the period.

Sizing Optimization: The overall framework also includes an outer loop for sizing optimization to determine the economically optimal sizes for the BESS and SC power capacities from a predefined set of potential options. This is achieved by embedding the rolling horizon, multi-stage operational simulation within an enumeration loop that iterates through all possible design configurations. Instead of continuous optimization, this approach evaluates a discrete set of commercially available or technically feasible sizes for BESS and SC power capacities. For each combination of candidate sizes, a unique system configuration is defined and evaluated. For this analysis, the energy capacities of the storage systems are directly linked to their power capacities based on assumed characteristics, simplifying the sizing problem. The nominal BESS energy capacity is assumed to be proportional to its power capacity based on a fixed discharge duration, while the nominal SC energy capacity is linked to its power capacity via a fixed power-to-energy ratio.

Post-Processing and Analysis: After simulating all predefined BESS and SC capacity combinations, key financial metrics are calculated for each configuration to evaluate its economic viability over an assumed project lifetime. These metrics include CAPEX for the BESS and SC components based on unit costs for the chosen capacities, Simulated Operational Profit (the total profit generated from market operations and operational costs over the simulated period), Estimated Annual Operational Profit (scaled from the simulated profit), Annualized Capital Expenditure (EAC) (spreading the total CAPEX over the project lifetime), Net Annual Profit (the estimated annual profit after accounting for the cost of capital), NPV and IRR (standard financial metrics to evaluate overall project viability). The configuration that yields the highest Net Annual Profit is identified as the economically optimal size within the evaluated set.

For the identified optimal configuration, the detailed results from the final stage of each period solved during the rolling horizon simulation are collected and concatenated into a single, continuous time series covering the entire simulation horizon. A comprehensive set of KPIs is calculated based on these aggregated results to provide a detailed quantitative evaluation of the microgrid's technical and economic performance. These KPIs include both economic indicators (like revenue contributions, profitability indices, and payback periods) and operational indicators (quantifying asset utilization, load satisfaction, and grid interaction).

Finally, effective visualization techniques are used to interpret the large volume of results and communicate findings. This includes plots for sizing analysis (e.g., profit landscapes, profit vs. power/CAPEX) and time-series operational plots for the optimal configuration (e.g., input data profiles, market transactions, asset dispatch, SOC, variable evolution across stages), as well as plots from the high-resolution FR event simulation. These analyses and visualizations collectively provide a deep understanding of the optimal system design, its expected financial performance, operational behavior, and technical capability to provide dynamic grid services.

5.4. MATHEMATICAL FORMULATION

This section presents the mixed-integer linear programming (MILP) model developed to optimize the short-term scheduling of a grid-connected PV micro-grid equipped with a battery energy storage system (BESS), a super-capacitor bank (SC), and a Diesel Generator (DG). The system interacts with multiple electricity markets including the Day-Ahead market (MGP), Intra-day market (MI), and Balancing market (MSD). The goal is to determine the optimal dispatch of all components to minimize total operational costs while ensuring system constraints and market rules are satisfied.

5.4.1. Problem Formulation

During every hourly interval of a 24-hour planning horizon, the operator must decide how much power to buy or sell on several electricity markets, how to charge or discharge each storage device, and when to start or stop the diesel unit. The single objective is to maximize total profit: market revenues, capacity payments, and reserve payments are added, while fuel costs, degradation costs, and capital recovery charges are subtracted. Time is represented by the set T, which contains all the numbered intervals in the horizon. For example, if the horizon covers one day with hourly resolution, $T = \{1, \dots, 24\}$. A special index t = 0 refers to the system state immediately before the horizon starts. The constant Δt gives the duration of each interval (e.g., one hour), and |T| denotes the total number of intervals.

a) Sets

- H: Set of hours in the planning horizon $(h = 1, \dots, H_{sim})$. H_{sim} is total simulation hours.
- h: Index for a specific hour, $h \in H$.

b) Parameters

- $P_{\mathrm{PV}\_forecast}(h)$: Forecasted PV power generation for hour h [kW].
- $P_{Load}(h)$: Forecasted internal load demand for hour h [kW].
- $P^{buy}_{Grid\_max}, P^{sell}_{Grid\_max}$: Maximum power import from or export to the grid capacity [kW].
- $\lambda_{\mathrm{MGP}}(h)$: Forecasted Day-Ahead Market (MGP) price for hour h [EUR/MWh].
- $\lambda_{\mathrm{MI}}(h)$: Forecasted Intraday Market (MI) average price for hour h [EUR/MWh].
- $\lambda^{up}_{\mathrm{MB}\_cap}(h)$: Forecasted Balancing Market (MB) upward capacity price for hour h [EUR/MW].
- $\lambda^{down}_{\mathrm{MB}\_cap}(h)$: Forecasted Balancing Market (MB) downward capacity price for hour h [EUR/MW].
- $\lambda^{up}_{\mathrm{MB}\_en}(h)$: Forecasted MB upward energy price per hour h [EUR/MWh].
- $\lambda^{down}_{\mathrm{MB}\_en}(h)$: Forecasted MB downward energy price per hour h [EUR/MWh].
- $p^{up}_{\mathrm{MB}\_act}(h), p^{down}_{\mathrm{MB}\_act}(h)$: Estimated MB activation probability per hour h [p.u.].
- $P_{\mathrm{FR}\_commit}(h)$: Committed Fast Reserve capacity for hour h [kW].
- $\lambda^{hourly}_{\mathrm{FR}\_cap}$: Fast Reserve capacity remuneration price [EUR/MWh].
- $I_{\mathrm{FR}}(h)$: Binary indicator: 1 if hour h is within an FR commitment period, 0 otherwise.
- $T_{\mathrm{FR}\_SC\_pulse}$: Duration of SC pulse for FR support [h].
- $T_{\mathrm{FR\_BESS}\_ramp}$: Duration of BESS ramp for FR support [h].
- $E^{up}_{\mathrm{FR}\_SC\_pulse}(h) = P_{\mathrm{FR}\_commit}(h) \cdot T_{\mathrm{FR}\_SC\_pulse} / \eta_{\mathrm{SC\_dc}}$: Minimum SC energy buffer required for upward FR during hour h [kWh].
- $E^{down}_{\mathrm{FR}\_SC\_pulse}(h) = P_{\mathrm{FR}\_commit}(h) \cdot T_{\mathrm{FR}\_SC\_pulse} \cdot \eta_{\mathrm{SC\_ch}}$: Minimum SC energy headroom for downward FR during hour h [kWh].
- $E^{up}_{\mathrm{FR\_BESS}\_ramp}(h) = 0.5 \cdot P_{\mathrm{FR}\_commit}(h) \cdot T_{\mathrm{FR\_BESS}\_ramp} / \eta_{dc}$: Minimum BESS energy buffer required for upward FR ramp during hour h [kWh].
- $E^{down}_{\mathrm{FR\_BESS}\_ramp}(h) = 0.5 \cdot P_{\mathrm{FR}\_commit}(h) \cdot T_{\mathrm{FR\_BESS}\_ramp} \cdot \eta_{ch}$: Minimum BESS energy headroom for downward FR ramp during hour h [kWh].
- T_{MB_dur}: Assumed duration for MB activation energy calculation (e.g., 0.25 h).

- $C_{Curt}^{penalty}$: Penalty cost for PV curtailment [EUR/kWh].
- $bigM$: A large constant value used in Big-M method for logical constraints.
- $P_{\text{BESS}\_ch\_max}, P_{\text{BESS}\_dc\_max}$: Max BESS charge/discharge power [kW].
- E_{BESS_max}: Nominal BESS energy capacity [kWh].
- SoC_{min}, SoC_{max}: Minimum/Maximum BESS SOC limits relative to E_{BESS_max} [p.u.].
- $E_{\text{BESS}\_min} = SoC_{min} \cdot E_{\text{BESS}\_max}$: Minimum allowed BESS energy level [kWh].
- $E_{\text{BESS}\_max\_actual} = SoC_{max} \cdot E_{\text{BESS}\_max}$: Maximum usable BESS energy level [kWh].
- η_{ch}, η_{dc}: BESS charging/discharging efficiencies [p.u.].
- $E_{\text{BESS}\_initial}$: Initial energy in BESS at simulation start ($h = 1$) [kWh].
- E_{BESS_target}: Target BESS energy at planning horizon end ($h = H_{sim}$) [kWh].
- C_{deg}^{BESS}: Estimated BESS degradation cost per unit of energy throughput [EUR/kWh].
- $P_{\text{SC}\_ch\_max}, P_{\text{SC}\_dc\_max}$: Maximum SC charging/discharging power capacity [kW].
- E_{SC_max}: Nominal SC energy capacity, used as reference for SOC calculation [kWh].
- $SoC_{\text{SC}\_min}, SoC_{\text{SC}\_max}$: Minimum/Maximum SC SOC limits relative to E_{SC_max} [p.u.].
- $E_{\text{SC}\_min} = SoC_{\text{SC}\_min} \cdot E_{\text{SC}\_max}$: Minimum allowed SC energy level [kWh].
- $E_{\text{SC}\_max\_actual} = SoC_{\text{SC}\_max} \cdot E_{\text{SC}\_max}$: Maximum usable SC energy level [kWh].
- $\eta_{\text{SC}\_ch}, \eta_{\text{SC}\_dc}$: SC charging/discharging efficiencies [p.u.].
- $E_{\text{SC}\_initial}$: Initial energy in SC at simulation start ($h = 1$) [kWh].
- E_{SC_target}: Target SC energy at planning horizon end ($h = H_{sim}$) [kWh].
- C_{deg}^{SC}: Estimated SC degradation cost per unit of energy throughput [EUR/kWh].
- $P_{\text{DG}}^{min}, P_{\text{DG}}^{max}$: Minimum and maximum DG power output when operational [kW].
- $RU_{\text{DG}}, RD_{\text{DG}}$: DG Ramp-up and Ramp-down rate limits [kW/h].
- $SU_{\text{DG}}, SD_{\text{DG}}$: DG Startup ramp power limit and Shutdown ramp power limit [kW].
- $SUC_{\text{DG}}, SDC_{\text{DG}}$: DG Startup and Shutdown costs per event [EUR].
- $Cost_{fuel}^{var}$: DG variable fuel cost per unit of energy generated [EUR/ kWh].
- $Cost_{fuel}^{fixed}$: DG fixed operational cost per hour when running [EUR/h].
- $T_{\text{DG}}^{up}, T_{\text{DG}}^{down}$: Minimum Up-Time and Down-Time for DG, expressed in hours.
- $u_{\text{DG}}(0)$: Initial ON/OFF status of DG (1 if ON, 0 if OFF) before hour $h = 1$.
- $P_{\text{DG}}(0)$: Initial power output of DG [kW] before hour $h = 1$.

c) Decision Variables

- $P_{\text{MGP}}^{buy}(h), P_{\text{MGP}}^{sell}(h)$: Power bought from/sold to MGP for hour h [kW].
- $P_{\text{MI}}^{buy}(h), P_{\text{MI}}^{sell}(h)$: Power bought from/sold to MI for hour h [kW].
- $P_{PV\_curt}(h)$: Power curtailed from PV generation during hour h [kW].
- $P_{\text{BESS}}^{ch}(h), P_{\text{BESS}}^{dc}(h)$: BESS charging/discharging power during hour h [kW].
- $E_{\text{BESS}}(h)$: Energy stored in BESS at the end of hour h [kWh].
- $u_{\text{BESS}\_ch}(h), u_{\text{BESS}\_dc}(h) \in \{0,1\}$: Binary variables indicating BESS charging/discharging state in hour h.
- $P_{\text{SC}}^{ch}(h), P_{\text{SC}}^{dc}(h)$: SC charging/discharging power during hour h [kW].

- $E_{\mathrm{SC}}(h)$: Energy stored in SC at the end of hour h [kWh].
- $u_{\mathrm{SC}\_ch}(h), u_{\mathrm{SC}\_dc}(h) \in \{0,1\}$: Binary variables indicating SC charging/discharging state in hour h.
- $P^{up}_{\mathrm{MB}\_cap}(h), P^{down}_{\mathrm{MB}\_cap}(h)$: Upward/downward balancing capacity for MB [kW].
- $u^{buy}_{grid}(h), u^{sell}_{grid}(h) \in \{0,1\}$: Binary variables for grid power import/export per h.
- $P_{\mathrm{DG}}(h)$: Power output of DG during hour h [kW].
- $u_{\mathrm{DG}}(h) \in \{0,1\}$: Binary variable: 1 if DG is ON during hour h, 0 otherwise.
- $v_{\mathrm{DG}}(h) \in \{0,1\}$: Binary variable: 1 if DG starts up at the beginning of hour h, 0 otherwise.
- $w_{\mathrm{DG}}(h) \in \{0,1\}$: Binary variable: 1 if DG shuts down at the beginning of hour h, 0 otherwise.

d) Objective Function

The objective is to maximize the total economic profit over the planning horizon (H_{sim} hours). Note $\Delta t = 1$ hour is implicit.

$$\begin{aligned}
\text{Maximize: } \sum_{h=1}^{H_{sim}} [& \big(\lambda_{\mathrm{MGP}}(h)P^{sell}_{\mathrm{MGP}}(h) - \lambda_{\mathrm{MGP}}(h)P^{buy}_{\mathrm{MGP}}(h)\big)/C_{factor} \\
& +\big(\lambda_{\mathrm{MI}}(h)P^{sell}_{\mathrm{MI}}(h) - \lambda_{\mathrm{MI}}(h)P^{buy}_{\mathrm{MI}}(h)\big)/C_{factor} \\
& +\big(\lambda^{up}_{\mathrm{MB}_cap}(h)P^{up}_{\mathrm{MB}_cap}(h) + \lambda^{down}_{\mathrm{MB}_cap}(h)P^{down}_{\mathrm{MB}_cap}(h)\big)/C_{factor} \\
& +(p^{up}_{\mathrm{MB}_act}(h)\lambda^{up}_{\mathrm{MB}_en}(h)P^{up}_{\mathrm{MB}_cap}(h) \\
& \qquad +p^{down}_{\mathrm{MB}_act}(h)\lambda^{down}_{\mathrm{MB}_en}(h)P^{down}_{\mathrm{MB}_cap}(h))/C_{factor} \\
& +\big(\lambda^{hourly}_{\mathrm{FR}_cap}P_{\mathrm{FR}_commit}(h)I_{\mathrm{FR}}(h)\big)/C_{factor} \\
& -\big(Cost^{var}_{fuel} \cdot P_{\mathrm{DG}}(h) + Cost^{fixed}_{fuel} \cdot u_{\mathrm{DG}}(h)\big) \\
& -SUC_{\mathrm{DG}} \cdot v_{\mathrm{DG}}(h) - SDC_{\mathrm{DG}} \cdot w_{\mathrm{DG}}(h) \\
& -C^{\mathrm{BESS}}_{deg}\big(P^{ch}_{\mathrm{BESS}}(h) + P^{dc}_{\mathrm{BESS}}(h)\big) \\
& -C^{\mathrm{SC}}_{deg}\big(P^{ch}_{\mathrm{SC}}(h) + P^{dc}_{\mathrm{SC}}(h)\big) \\
& -C^{penalty}_{Curt} \cdot P_{PV_curt}(h)]
\end{aligned} \tag{45}$$

Where $C_{factor} = 1000$. Revenues/costs are summed hourly.

e) Constraints

- *Power Balance Constraint*

Ensures hourly energy balance (Power * 1 hour).

$$\left(P_{\mathrm{PV}_{forecast}}(h) - P_{PV_{curt}}(h)\right) + P_{\mathrm{BESS}}^{dc}(h) + P_{\mathrm{SC}}^{dc}(h) + P_{\mathrm{DG}}(h)$$
$$+P_{\mathrm{MGP}}^{buy}(h) + P_{\mathrm{MI}}^{buy}(h) =$$
$$P_{Load}(h) + P_{\mathrm{BESS}}^{ch}(h) + P_{\mathrm{SC}}^{ch}(h) + P_{\mathrm{MGP}}^{sell}(h) + P_{\mathrm{MI}}^{sell}(h) \tag{46}$$

- *PV Curtailment Constraint*

Limits PV curtailment based on hourly forecast.

$$0 \le P_{PV\_curt}(h) \le P_{PV\_forecast}(h) \tag{47}$$

- *BESS Constraints*

Energy dynamics: Links energy level between consecutive hours.

$$E_{\mathrm{BESS}}(h) = E_{\mathrm{BESS}}(h-1) + \left(P_{\mathrm{BESS}}^{ch}(h)\eta_{ch} - P_{\mathrm{BESS}}^{dc}(h)/\eta_{dc}\right) \quad \forall h > 1 \tag{48}$$

$$E_{\mathrm{BESS}}(1) = E_{\mathrm{BESS}\_initial} + \left(P_{\mathrm{BESS}}^{ch}(1)\eta_{ch} - P_{\mathrm{BESS}}^{dc}(1)/\eta_{dc}\right)$$

State of Charge (SOC) limits: Applied hourly.

$$E_{\mathrm{BESS}\_min} \le E_{\mathrm{BESS}}(h) \le E_{\mathrm{BESS}\_max\_actual} \tag{49}$$

Charging/Discharging power limits: Applied hourly.

$$0 \le P_{\mathrm{BESS}}^{ch}(h) \le P_{\mathrm{BESS}\_ch\_max} \cdot u_{\mathrm{BESS}\_ch}(h)$$
$$0 \le P_{\mathrm{BESS}}^{dc}(h) \le P_{\mathrm{BESS}\_dc\_max} \cdot u_{\mathrm{BESS}\_dc}(h) \tag{50}$$

Mutually exclusive operation: Applied hourly.

$$u_{\mathrm{BESS}\_ch}(h) + u_{\mathrm{BESS}\_dc}(h) \le 1 \tag{51}$$

End-of-horizon target SOC: Applied at the last hour.

$$E_{\mathrm{BESS}}(H_{sim}) \ge E_{\mathrm{BESS}\_target} \tag{52}$$

Binary nature of control variables:

$$u_{\mathrm{BESS}\_ch}(h), u_{\mathrm{BESS}\_dc}(h) \in \{0,1\} \tag{53}$$

- *Supercapacitor (SC) Constraints*

Energy dynamics:

$$E_{\text{SC}}(h) = E_{\text{SC}}(h-1) + \left(P_{\text{SC}}^{ch}(h)\eta_{\text{SC}\_ch} - P_{\text{SC}}^{dc}(h)/\eta_{\text{SC}\_dc}\right) \quad \forall h > 1 \tag{54}$$

$$E_{\text{SC}}(1) = E_{\text{SC}\_initial} + \left(P_{\text{SC}}^{ch}(1)\eta_{\text{SC}\_ch} - P_{\text{SC}}^{dc}(1)/\eta_{\text{SC}\_dc}\right) \tag{55}$$

State of Charge (SOC) limits:

$$E_{\text{SC}\_min} \leq E_{\text{SC}}(h) \leq E_{\text{SC}\_max\_actual} \tag{56}$$

Charging/Discharging power limits:

$$\begin{gathered} 0 \leq P_{\text{SC}}^{ch}(h) \leq P_{\text{SC}\_ch\_max} \cdot u_{\text{SC}\_ch}(h) \\ 0 \leq P_{\text{SC}}^{dc}(h) \leq P_{\text{SC}\_dc\_max} \cdot u_{\text{SC}\_dc}(h) \end{gathered} \tag{57}$$

Mutually exclusive operation:

$$u_{\text{SC}\_ch}(h) + u_{\text{SC}\_dc}(h) \leq 1 \tag{58}$$

End-of-horizon target SOC:

$$E_{\text{SC}}(H_{sim}) \geq E_{\text{SC}\_target} \tag{59}$$

Binary nature of control variables:

$$u_{\text{SC}\_ch}(h), u_{\text{SC}\_dc}(h) \in \{0,1\} \tag{60}$$

- *Grid Connection Constraints*

Grid import/export limits:

$$\begin{gathered} P_{\text{MGP}}^{buy}(h) + P_{\text{MI}}^{buy}(h) + P_{\text{MB}\_cap}^{down}(h) \leq P_{Grid\_max}^{buy} \cdot u_{grid}^{buy}(h) \\ P_{\text{MGP}}^{sell}(h) + P_{\text{MI}}^{sell}(h) + P_{\text{MB}\_cap}^{up}(h) \leq P_{Grid\_max}^{sell} \cdot u_{grid}^{sell}(h) \end{gathered} \tag{61}$$

Mutually exclusive grid operation:

$$u_{grid}^{buy}(h) + u_{grid}^{sell}(h) \leq 1 \tag{62}$$

Restrictions during FR commitment ($I_{FR}(h) = 1$):

$$\begin{gathered} P_{\text{MGP}}^{buy}(h) \leq bigM \cdot (1 - I_{FR}(h)) \\ P_{\text{MGP}}^{sell}(h) \leq bigM \cdot (1 - I_{FR}(h)) \\ P_{\text{MI}}^{buy}(h) \leq bigM \cdot (1 - I_{FR}(h)) \\ P_{\text{MI}}^{sell}(h) \leq bigM \cdot (1 - I_{FR}(h)) \end{gathered} \tag{63}$$

Binary and non-negativity constraints:

$$u_{grid}^{buy}(h), u_{grid}^{sell}(h) \in \{0,1\}$$
$$P_{\mathrm{MGP}}^{buy}(h), P_{\mathrm{MGP}}^{sell}(h) \geq 0 \tag{64}$$
$$P_{\mathrm{MI}}^{buy}(h), P_{\mathrm{MI}}^{sell}(h) \geq 0$$

- *Balancing Market (MB) Capacity Constraints*

Non-negativity of offered capacity:

$$P_{\mathrm{MB}\_cap}^{up}(h) \geq 0$$
$$P_{\mathrm{MB}\_cap}^{down}(h) \geq 0 \tag{65}$$

Power reserve availability (BESS-based, outside FR periods):

$$P_{\mathrm{BESS}}^{dc}(h) + P_{\mathrm{MB}\_cap}^{up}(h) \leq P_{\mathrm{BESS}\_dc\_max} \cdot (1 - I_{FR}(h))$$
$$P_{\mathrm{BESS}}^{ch}(h) + P_{\mathrm{MB}\_cap}^{down}(h) \leq P_{\mathrm{BESS}\_ch\_max} \cdot (1 - I_{FR}(h)) \tag{66}$$

Energy reserve availability for MB duration (BESS-based, outside FR periods):

$$E_{\mathrm{BESS}}(h) - \frac{P_{\mathrm{MB}\_cap}^{up}(h)}{\eta_{dc}} \cdot T_{MB\_dur} \geq E_{\mathrm{BESS}\_min} \quad (\text{if } I_{FR}(h) = 0) \tag{67}$$
$$E_{\mathrm{BESS}}(h) + P_{\mathrm{MB}\_cap}^{down}(h) \cdot \eta_{ch} \cdot T_{MB\_dur} \leq E_{\mathrm{BESS}\_max\_actual} \quad (\text{if } I_{FR}(h) = 0)$$

No MB bids during FR provision:

$$P_{\mathrm{MB}\_cap}^{up}(h) \leq bigM \cdot (1 - I_{FR}(h))$$
$$P_{\mathrm{MB}\_cap}^{down}(h) \leq bigM \cdot (1 - I_{FR}(h)) \tag{68}$$

- *Fast Reserve (FR) Constraints*

Active only when $I_{FR}(h) = 1$, ensuring hourly capacity and energy reservation.

Power reservation for FR:

$$P_{\mathrm{SC}}^{dc}(h) \leq P_{\mathrm{SC}\_dc\_max} - P_{\mathrm{FR}\_commit}(h)$$
$$P_{\mathrm{SC}}^{ch}(h) \leq P_{\mathrm{SC}\_ch\_max} - P_{\mathrm{FR}\_commit}(h)$$
$$P_{\mathrm{BESS}}^{dc}(h) \leq P_{\mathrm{BESS}\_dc\_max} - P_{\mathrm{FR}\_commit}(h) \tag{69}$$
$$P_{\mathrm{BESS}}^{ch}(h) \leq P_{\mathrm{BESS}\_ch\_max} - P_{\mathrm{FR}\_commit}(h)$$

Energy buffer reservation for FR:

$$E_{\mathrm{SC}}(h) \geq E_{SC\_min} + E_{\mathrm{FR}\_SC\_pulse}^{up}(h)$$
$$E_{\mathrm{SC}}(h) \leq E_{SC\_max\_actual} - E_{\mathrm{FR}\_SC\_pulse}^{down}(h)$$
$$E_{\mathrm{BESS}}(h) \geq E_{BSS\_min} + E_{\mathrm{FR}\_\mathrm{BESS}\_ramp}^{up}(h) \tag{70}$$
$$E_{\mathrm{BESS}}(h) \leq E_{BSS\_max\_actual} - E_{\mathrm{FR}\_\mathrm{BESS}\_ramp}^{down}(h)$$

- *Diesel Generator (DG) Constraints*

Power output limits:

$$P_{\mathrm{DG}}^{min} \cdot u_{\mathrm{DG}}(h) \leq P_{\mathrm{DG}}(h) \leq P_{\mathrm{DG}}^{max} \cdot u_{\mathrm{DG}}(h) \tag{71}$$

Status change logic (startup/shutdown):

$$\begin{aligned} &v_{\mathrm{DG}}(h) - w_{\mathrm{DG}}(h) = u_{\mathrm{DG}}(h) - u_{\mathrm{DG}}(h-1) \quad \forall h > 1 \\ &v_{\mathrm{DG}}(1) - w_{\mathrm{DG}}(1) = u_{\mathrm{DG}}(1) - u_{\mathrm{DG}}(0) \quad \text{for } h = 1 \\ &v_{\mathrm{DG}}(h) + w_{\mathrm{DG}}(h) \leq 1 \end{aligned} \tag{72}$$

Ramp rate limits ($\Delta t = 1$ hour):

$$\begin{aligned} P_{\mathrm{DG}}(h) - P_{\mathrm{DG}}(h-1) &\leq RU_{\mathrm{DG}} \cdot u_{\mathrm{DG}}(h-1) + SU_{\mathrm{DG}} \cdot v_{\mathrm{DG}}(h) \quad \forall h > 1 \\ P_{\mathrm{DG}}(1) - P_{\mathrm{DG}}(0) &\leq RU_{\mathrm{DG}} \cdot u_{\mathrm{DG}}(0) + SU_{\mathrm{DG}} \cdot v_{\mathrm{DG}}(1) \quad \text{for } h = 1 \\ P_{\mathrm{DG}}(h-1) - P_{\mathrm{DG}}(h) &\leq RD_{\mathrm{DG}} \cdot u_{\mathrm{DG}}(h) + SD_{\mathrm{DG}} \cdot w_{\mathrm{DG}}(h) \quad \forall h > 1 \\ P_{\mathrm{DG}}(0) - P_{\mathrm{DG}}(1) &\leq RD_{\mathrm{DG}} \cdot u_{\mathrm{DG}}(1) + SD_{\mathrm{DG}} \cdot w_{\mathrm{DG}}(1) \quad \text{for } h = 1 \end{aligned} \tag{73}$$

Minimum up-time and down-time (in hours):

$$\begin{aligned} &\sum_{k=h}^{h+T_{\mathrm{DG}}^{up}-1} u_{\mathrm{DG}}(k) \geq T_{\mathrm{DG}}^{up} \cdot v_{\mathrm{DG}}(h) \quad \forall h \in \{1, \dots, H_{sim} - T_{\mathrm{DG}}^{up} + 1\} \\ &\sum_{k=h}^{h+T_{\mathrm{DG}}^{down}-1} (1 - u_{\mathrm{DG}}(k)) \geq T_{\mathrm{DG}}^{down} \cdot w_{\mathrm{DG}}(h) \quad \forall h \in \{1, \dots, H_{sim} - T_{\mathrm{DG}}^{down} + 1\} \end{aligned} \tag{74}$$

Binary nature of control variables:

$$u_{\mathrm{DG}}(h),\ v_{\mathrm{DG}}(h),\ w_{\mathrm{DG}}(h) \in \{0,1\} \tag{75}$$

5.4.2. Post-Processing: Techno-Economic Analysis

This section describes the calculation of key metrics based on the hourly optimal solution (*). Parameters are the same as in the sub-hourly version, but their interpretation aligns with hourly resolution. H_{sim} remains the total number of hours simulated.

5.4.2.1. Economic Key Performance Indicators (KPIs)

a) CAPEX

Calculated identically using optimal P^{opt} and E^{opt}.

$$\begin{aligned} Cost_{CAPEX}^{\mathrm{BESS,opt}} &= C_p^{\mathrm{BESS}} \cdot P_{\mathrm{BESS}}^{\mathrm{opt}} + C_e^{\mathrm{BESS}} \cdot E_{\mathrm{BESS}}^{\mathrm{opt}} \\ Cost_{CAPEX}^{\mathrm{SC,opt}} &= C_p^{\mathrm{SC}} \cdot P_{\mathrm{SC}}^{\mathrm{opt}} + C_e^{\mathrm{SC}} \cdot E_{\mathrm{SC}}^{\mathrm{opt}} \\ Cost_{CAPEX}^{Total,\mathrm{opt}} &= Cost_{CAPEX}^{\mathrm{BESS,opt}} + Cost_{CAPEX}^{\mathrm{SC,opt}} \end{aligned}$$

b) EAC

Calculated identically using total CAPEX, discount rate r, and lifetime L.

$$EAC = Cost_{CAPEX}^{Total,\text{opt}} \cdot \frac{r(1+r)^L}{(1+r)^L - 1}$$

c) Simulated Operational Profit

Summation over hours (H_{sim}), $\Delta t = 1$ hour is implicit.

$$Rev_{DA}^{*} = \sum_{h=1}^{H_{sim}} \left(\lambda_{\text{MGP}}^{*}(h) P_{\text{MGP}}^{sell,*}(h) - \lambda_{\text{MGP}}^{*}(h) P_{\text{MGP}}^{buy,*}(h)\right) / C_{factor}$$

$$Rev_{ID}^{*} = \sum_{h=1}^{H_{sim}} \left(\lambda_{\text{MI}}^{*}(h) P_{\text{MI}}^{sell,*}(h) - \lambda_{\text{MI}}^{*}(h) P_{\text{MI}}^{buy,*}(h)\right) / C_{factor}$$

$$Rev_{MB_{c}ap}^{*} = \sum_{h=1}^{H_{sim}} \left(\lambda_{\text{MB}_{c}ap}^{up,*}(h) P_{\text{MB}_{c}ap}^{up,*}(h) + \lambda_{\text{MB}_{c}ap}^{down,*}(h) P_{\text{MB}_{c}ap}^{down,*}(h)\right) / C_{factor}$$

$$Rev_{MB_{e}n}^{*} = \sum_{h=1}^{H_{sim}} \left(p_{\text{MB}_{a}ct}^{up}(h) \lambda_{\text{MB}_{e}n}^{up,*}(h) P_{\text{MB}_{c}ap}^{up,*}(h) + p_{\text{MB}_{a}ct}^{down}(h) \lambda_{\text{MB}_{e}n}^{down,*}(h) P_{\text{MB}_{c}ap}^{down,*}(h)\right) / C_{factor}$$

$$Rev_{FR}^{*} = \sum_{h=1}^{H_{sim}} \left(\lambda_{FR_{c}ap}^{hourly} P_{FR_{c}ommit}^{*}(h) I_{FR}^{*}(h)\right) / C_{factor}$$

$$Cost_{DG}^{*} = \sum_{h=1}^{H_{sim}} \left(Cost_{fuel}^{var} \cdot P_{\text{DG}}^{*}(h) + Cost_{fuel}^{fixed} \cdot u_{\text{DG}}^{*}(h) + SUC_{\text{DG}} \cdot v_{\text{DG}}^{*}(h) + SDC_{\text{DG}} \cdot w_{\text{DG}}^{*}(h)\right)$$

$$Cost_{Deg}^{*} = \sum_{h=1}^{H_{sim}} \left(C_{deg}^{\text{BESS}} \left(P_{\text{BESS}}^{ch,*}(h) + P_{\text{BESS}}^{dc,*}(h)\right) + C_{deg}^{\text{SC}} \left(P_{\text{SC}}^{ch,*}(h) + P_{\text{SC}}^{dc,*}(h)\right)\right)$$

$$Cost_{Curt}^{*} = \sum_{h=1}^{H_{sim}} \left(P_{PV_{c}urt}^{*}(h) \cdot C_{Curt}^{penalty}\right)$$

$$Profit_{OP,sim}^{*} = \left(Rev_{DA}^{*} + Rev_{ID}^{*} + Rev_{MB_{c}ap}^{*} + Rev_{MB_{e}n}^{*} + Rev_{FR}^{*}\right) - \left(Cost_{DG}^{*} + Cost_{Deg}^{*} + Cost_{Curt}^{*}\right)$$

d) Annual Operational Profit

Calculated identically by scaling $Profit_{OP,sim}^{*}$.

$$Profit_{OP,ann}^{*} = Profit_{OP,sim}^{*} \cdot \frac{365 \times 24}{H_{sim}} \quad (\text{if } H_{sim} > 0)$$

e) Net Annual Profit

Calculated identically.

$$Profit_{Net,ann}^{*} = Profit_{OP,ann}^{*} - EAC$$

f) Net Present Value (NPV)

Calculated identically using $Profit_{Net,ann}^{*}$ and $Cost_{CAPEX}^{Total,\text{opt}}$.

$$NPV = -Cost_{CAPEX}^{Total,\text{opt}} + \sum_{y=1}^{L} \frac{Profit_{Net,ann}^{*}}{(1+r)^y}$$

g) Internal Rate of Return (IRR)

Calculated identically. Solved for r_{IRR}:

$$0 = -Cost_{CAPEX}^{Total,\text{opt}} + \sum_{y=1}^{L} \frac{Profit_{Net,ann}^{*}}{(1+r_{IRR})^y}$$

h) Levelized Cost of Storage (LCOS) for BESS

Calculations adapted for hourly summation.

$$Dis_{sim}^{\mathrm{BESS},*} = \sum_{h=1}^{H_{sim}} P_{\mathrm{BESS}}^{dc,*}(h) \quad [\mathrm{kWh}]$$

$$Thr_{sim}^{\mathrm{BESS},*} = \sum_{h=1}^{H_{sim}} \left(P_{\mathrm{BESS}}^{ch,*}(h) + P_{\mathrm{BESS}}^{dc,*}(h)\right) \quad [\mathrm{kWh}]$$

$$LCOS^{\mathrm{BESS}} = \frac{Cost_{LT}^{\mathrm{BESS},*}}{Dis_{LT}^{\mathrm{BESS},*}} (\text{if } Dis_{LT}^{\mathrm{BESS},*} > 0), [\mathrm{EUR/kWh\ discharged}]$$

5.4.2.2. Operational KPIs

i) BESS Depth of Discharge (DOD):

$$DoD_{\mathrm{BESS}}^{*}(\%) = \frac{\max_h\left(E_{\mathrm{BESS}}^{*}(h)\right) - \min_h\left(E_{\mathrm{BESS}}^{*}(h)\right)}{E_{\mathrm{BESS}}^{\mathrm{opt}}} \times 100\%$$

j) BESS/SC Annual Energy Throughput:

$$Thr_{\mathrm{ann}}^{\mathrm{BESS},*} = \left(\sum_h \left(P_{\mathrm{BESS}}^{\mathrm{ch},*}(h) + P_{\mathrm{BESS}}^{\mathrm{dc},*}(h)\right)\right) \cdot \frac{ScaleFactor_{\mathrm{ann}}}{C_{\mathrm{factor}}} [\mathrm{MWh/annum}]$$

$$Thr_{\mathrm{ann}}^{\mathrm{SC},*} = \left(\sum_h \left(P_{\mathrm{SC}}^{\mathrm{ch},*}(h) + P_{\mathrm{SC}}^{\mathrm{dc},*}(h)\right)\right) \cdot \frac{ScaleFactor_{\mathrm{ann}}}{C_{\mathrm{factor}}} [\mathrm{MWh/annum}]$$

k) Annual Diesel Fuel Consumption:

$$Fuel_{\mathrm{DG,ann}}^{*} = \left(\sum_h P_{\mathrm{DG}}^{*}(h)\right) \cdot FuelCon_{\mathrm{SDG}} \cdot ScaleFactor_{\mathrm{ann}} [\mathrm{L/annum}]$$

l) RES Contribution to Load:

$$RESContrib_{Load}^{*}(\%) = \frac{\sum_h \left(P_{\mathrm{PV}\_forecast}(h) - P_{PV\_curt}^{*}(h)\right)}{\sum_h P_{Load}(h)} \times 100\%$$

m) Diesel Contribution to Load:

$$DGContrib_{Load}^{*}(\%) = \frac{\sum_h P_{\mathrm{DG}}^{*}(h)}{\sum_h P_{Load}(h)} \times 100\%$$

n) ESS Discharge Contribution to Load:

$$ESS\_DC\_Contrib_{Load}^{*}(\%) = \frac{\sum_h \left(P_{\mathrm{BESS}}^{dc,*}(h) + P_{\mathrm{SC}}^{dc,*}(h)\right)}{\sum_h P_{Load}(h)} \times 100\%$$

o) Self-Sufficiency Rate (SSR):

$$SSR^*(\%) = \frac{\sum_h \left(P^*_{\mathrm{PV\_}net}(h) + P^*_{\mathrm{DG}}(h) + P^{dc,*}_{\mathrm{BESS}}(h) + P^{dc,*}_{\mathrm{SC}}(h) \right)}{\sum_h P_{Load}\,(h)} \times 100\%$$

Where $P^*_{\mathrm{PV\_}net}(h) = P_{\mathrm{PV\_}forecast}(h) - P^*_{PV\_curt}(h)$.

p) Diesel Generator Capacity Factor (DGCF):

$$DGCF^*(\%) = \frac{\sum_h P^*_{\mathrm{DG}}\,(h)}{P^{max}_{\mathrm{DG}} \cdot H_{sim}} \times 100\% \quad (\text{if } P^{max}_{\mathrm{DG}} \cdot H_{sim} > 0)$$

q) Potential RES Curtailment Factor:

$$RESCurtFactor^*(\%) = \frac{\sum_h P^*_{PV\_curt}\,(h)}{\sum_h P_{\mathrm{PV\_}forecast}\,(h)} \times 100\% \quad (\text{if denominator} > 0)$$

r) BESS Round-Trip Efficiency (RTE):

$$RTE^*_{\mathrm{BESS}}(\%) = \frac{\sum_h P^{dc,*}_{\mathrm{BESS}}\,(h)}{\sum_h P^{ch,*}_{\mathrm{BESS}}\,(h)} \times 100\% \quad (\text{if denominator} > 0)$$

s) BESS State of Charge (SOC) Utilization:

$$SOCUtil^*_{\mathrm{BESS}}(\%) = \frac{\max_h(E^*_{\mathrm{BESS}}(h)) - \min_h(E^*_{\mathrm{BESS}}(h))}{E_{\mathrm{BESS\_}max\_actual} - E_{\mathrm{BESS\_}min}} \times 100\% \quad (\text{if denominator} > 0)$$

t) Average FR Power (in FR Hours):

$$P^*_{\mathrm{FR},avg} = \frac{\sum_{h|I^*_{FR}(h)=1} P^*_{\mathrm{FR\_}commit}\,(h)}{\sum_{h|I^*_{FR}(h)=1} 1} \quad [\mathrm{kW}] \quad (\text{if active FR hours} > 0)$$

u) BESS Energy Capacity Factor:

$$ECF^*_{\mathrm{BESS}}(\%) = \frac{\frac{1}{H_{sim}} \sum_h E^*_{\mathrm{BESS}}\,(h)}{E^{\mathrm{opt}}_{\mathrm{BESS}}} \times 100\%$$

v) BESS Equivalent Full Cycles (EFC) per year:

$$EFC^*_{\mathrm{BESS,ann}} = \frac{Thr^{\mathrm{BESS},*}_{\mathrm{ann}} \cdot C_{factor}}{2 \cdot E^{\mathrm{opt}}_{\mathrm{BESS}}} \quad [\text{cycles/year}]$$

w) SC Energy Buffer Ratio:

$$BufferRatio^*_{\mathrm{SC}}(\%) = \frac{\frac{1}{H_{sim}} \sum_h E^*_{\mathrm{SC}}\,(h)}{E^{\mathrm{opt}}_{\mathrm{SC}}} \times 100\%$$

x) Cost per Cycle (BESS Degradation):

$$\mathrm{Cost}_{\mathrm{PerCycle}^*_{\mathrm{BESS}}} = \frac{\mathrm{Cost}_{\mathrm{BESS,sim}^*_{\mathrm{Deg}}} \cdot \mathrm{ScaleFactor}_{\mathrm{ann}}}{\mathrm{EFC}^*_{\mathrm{BESS,ann}}}, \quad [\mathrm{EUR/cycle}], \quad (\text{if } \mathrm{EFC}^*_{\mathrm{BESS,ann}} > 0)$$

Where $Cost_{Deg}^{\text{BESS},sim,*} = \sum_h C_{deg}^{\text{BESS}} \left(P_{\text{BESS}}^{ch,*} + P_{\text{BESS}}^{dc,*}\right)$ is the total BESS degradation cost during the simulation.

y) Annual CO_2 Emissions from Diesel:

$$CO2_{\text{DG,ann}}^{*} = \left(\sum_h P_{\text{DG}}^{*}(h)\right) \cdot EF_{\text{DG}} \cdot ScaleFactor_{ann} \quad \left[\text{ton CO}_2/\text{year or kg CO}_2/\text{year}\right]$$

5.5. SIMULATION RESULTS

5.5.1. Case A: Low Horizon Case

5.5.1.1. System Description

a) System Data and Simulation Context

The simulation environment models a grid-connected microgrid with access to various electricity markets.

- **Load and PV Data:** The system includes a 1500 kW PV array. Load profiles exhibit typical daily variations with a base load of 40 kW and peaks up to 50 kW, featuring morning (11:00) and evening (20:00) peak consumption periods. PV generation follows a typical daily pattern, peaking midday, while load shows variations with morning and evening peaks. Market prices (DA, ID, MB capacity) exhibit volatility, presenting opportunities for arbitrage and strategic reserve offerings.

- **Simulation Periods:** To capture seasonal variability, the system is simulated over three carefully selected distinct 2-day periods in 2024 Italian market data:
  - Period 1: February 5th - February 6th
  - Period 2: June 3rd - June 4th
  - Period 3: October 7th - October 8th

- **Market Prices:** The simulation incorporates real hourly price data for Day-Ahead (MGP), Intra-Day (MI), and Balancing Market (MB) upward and downward capacity for the North Zone [78] in Italy electricity market. MB energy prices are derived as a fraction of MB capacity prices. These prices exhibit typical market volatility, creating opportunities for strategic arbitrage and service provision.
  - **Grid Connection:** The microgrid can import or export up to 5 MW from/to the main utility grid.
  - **Sizing Options:** BESS power capacities tested included [500, 1000, 1500, 2000, 2500, 3000, 5000] kW, each with a 4-hour discharge duration. Concurrently, SC power capacities were varied across [50, 100, 150, 200, 250, 300] kW, with a fixed power-to-energy ratio. This multi-dimensional sizing sweep allowed for a thorough exploration of the performance landscape.

The operational strategy is determined through a sequential optimization across Day-Ahead, Intra-Day, and Balancing Market stages, with provisions for FR ancillary service participation. Each stage optimizes the dispatch for a 24-hour horizon, considering updated forecasts for PV generation and load, and prevailing market prices. The objective function at each stage is to maximize the net operational profit, defined as total revenues from market participation (energy sales, capacity payments for MB and FR) minus total operational costs (fuel for DG, degradation of BESS and SC, and a penalty cost for PV curtailment). The optimization is performed using Python's optimization libraries, with results from one stage informing the fixed parameters of the subsequent stage.

b) Components Data

The microgrid comprises the following key dispatchable and non-dispatchable assets presented in Table 5-1 and Table 5-2.

Table 5-1: Hybrid Energy Storage System (HESS) Parameters

Parameter	**BESS (VRFB) Value**	**Supercapacitor (SC) Value**	**Unit**	**Notes**
Power Options Simulated	*Varies (e.g., 500-5000)*	*Varies (e.g., 50-300)*	kW	Sizing optimization range
Discharge Duration	4	N/A (Uses PE Ratio)	hours	BESS specific
Power-to-Energy (PE) Ratio	N/A	30	hoursseconds	30s discharge
Charge Efficiency	0.85	0.98	-	
Discharge Efficiency	0.85	0.98	-	
Minimum SOC	0.2 (20%)	0.3 (30%)	-	Fraction of nominal/reference capacity
Maximum SOC	0.8 (80%)	0.9 (90%)	-	Fraction of nominal/reference capacity
Initial SOC Ratio (per period)	0.3 (30%)	0.3 (30%)	-	Start state for each new simulation period
Degradation Cost	0.005	0.03667 (calculated)	€/kWh- throughputthruput	
CAPEX	350	1000	€/kW	

Parameter	BESS (VRFB) Value	Supercapacitor (SC) Value	Unit	Notes
(Power)				
CAPEX (Energy)	400	15000	€/kWh	

Note: SC degradation cost is calculated based on reference parameters and lifetime cycles. SC CAPEX (Energy) is notably high.

Table 5-2: Diesel Generator (DG) Parameters

Parameter	Value	Unit
Minimum Power	100	kW
Maximum Power	1000	kW
Ramp-Up Rate	200	kW/hr
Ramp-Down Rate)	200	kW/hr
Start-Up Ramp	700 (0.7*Pmax)	kW
Shut-Down Ramp	400 (0.4*Pmax)	kW
Start-Up Cost	53	€
Shut-Down Cost	30	€
Variable Fuel Cost	0.35	€/kWh
Fixed Fuel Cost (per hour ON)	10	€/hr
Minimum Up Time	3	hours
Minimum Down Time	2	hours
Initial Status (per period)	Off (0)	-
Initial Power (per period)	0	kW

c) FR Commitment and Parameters

The system also has the capability to participate in the FR market. The commitment to FR is determined dynamically based on an hourly indicator derived from a pre-generated daily FR schedule.

- FR Schedule Generation: For each simulated day, an FR participation window is randomly generated. This window is defined by a start hour (between 11:00 and an hour ensuring the duration fits before 21:00) and a duration (randomly chosen from 2, 3, or 4 hours).

- FR Committed Power: For a given hour, the system commits a fixed amount of power for FR service. This committed power is calculated as: FR_Commit_Power = 0.3 * min (BESS_Power_Rating, SC_Power_Rating) For instance, with a 3000kW BESS and 50kW SC, the FR_Commit_Power would be 0.3 * 50kW = 15 kW.

- FR Revenue: Revenue from FR is based on an hourly capacity payment (60 €/MW/h or 0.06 €/kW/h) multiplied by the committed power.

- Energy Headroom for FR: When FR is committed, specific constraints ensure sufficient energy is reserved in both BESS and SC to deliver this service if activated:

  - Energy needed from SC for a short pulse response (30 seconds).
  - Energy headroom needed in SC to absorb for a short pulse.
  - Energy needed from BESS for a sustained ramp (5 minutes).
  - Energy headroom needed in BESS to absorb for a sustained ramp. These energy reservation constraints can influence the storage dispatch strategy, potentially requiring charging even at unfavorable prices to maintain FR readiness.

5.5.1.2. Results Analysis

The following sections detail the operational behavior and market interactions of the best-identified configuration (3000kW BESS, 50kW SC) based on the simulated periods.

a) Input Data Profiles and Forecast Evolution (PV and Load)

The simulation utilizes dynamic input data, including PV generation forecasts, load demand profiles, and various electricity market prices (DA, ID, MB capacity). The Figure 5.1 plot illustrates typical daily patterns for these inputs across the simulated periods. PV generation follows a clear daily cycle, peaking midday, while load demand shows distinct morning and evening peaks. Market prices exhibit characteristic volatility, which the optimization model aims to exploit. The period labels (P1, P2, P3) on the plot clearly delineate the start and end dates of each distinct simulation segment, aiding in the interpretation of results across different seasonal conditions.

The Figure 5.2 showcases the sequential updating of forecasts as the operational horizon approaches real-time. The Day-Ahead (DA) forecasts provide the initial baseline. Intra-Day (ID) forecasts offer refinements, and finally, the Balancing Market (MB) stage operates on the most current forecasts. This sequential refinement allows the system to adapt its dispatch strategy to improving forecast accuracy.

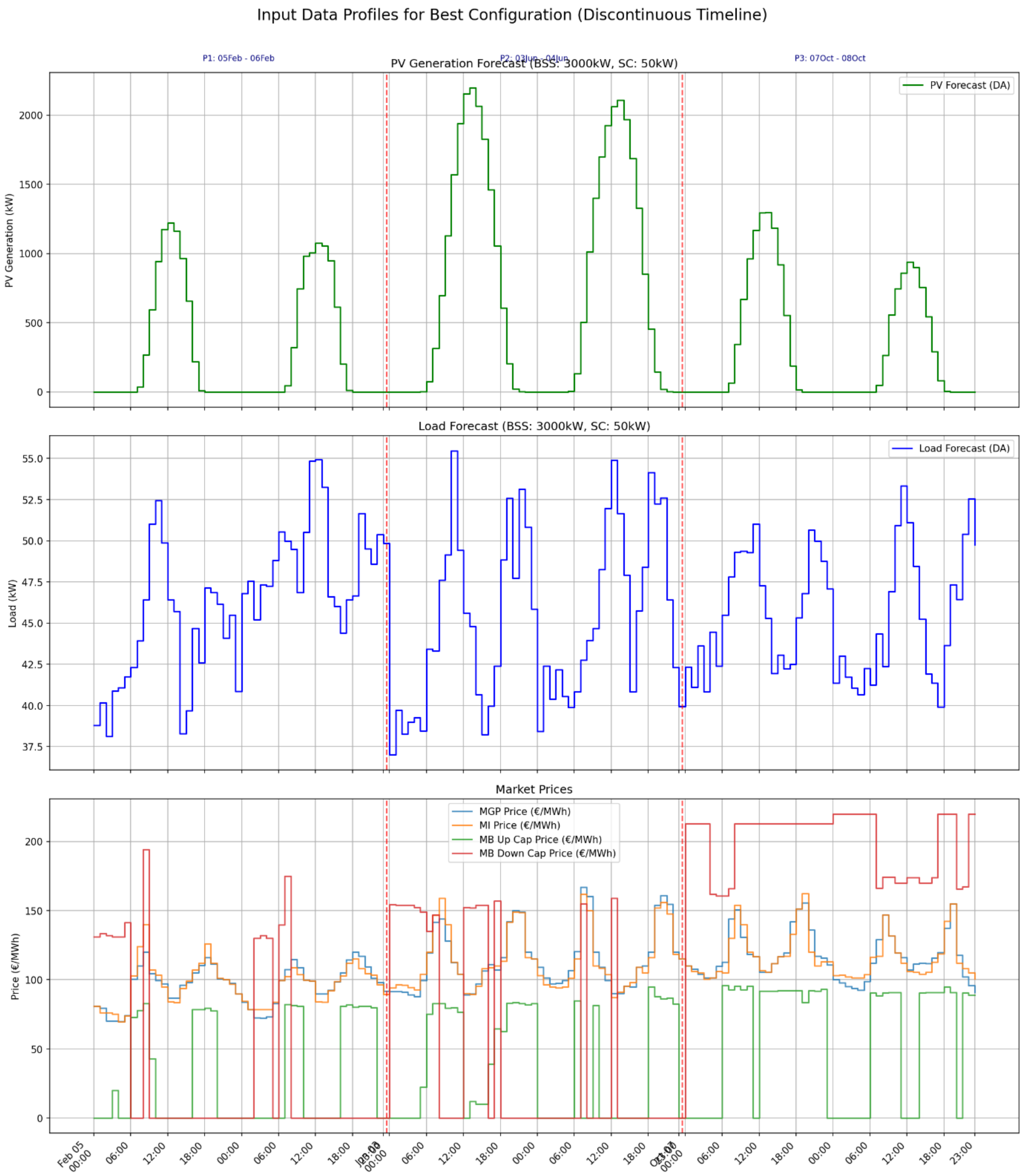

Figure 5.1 Input Data Profiles

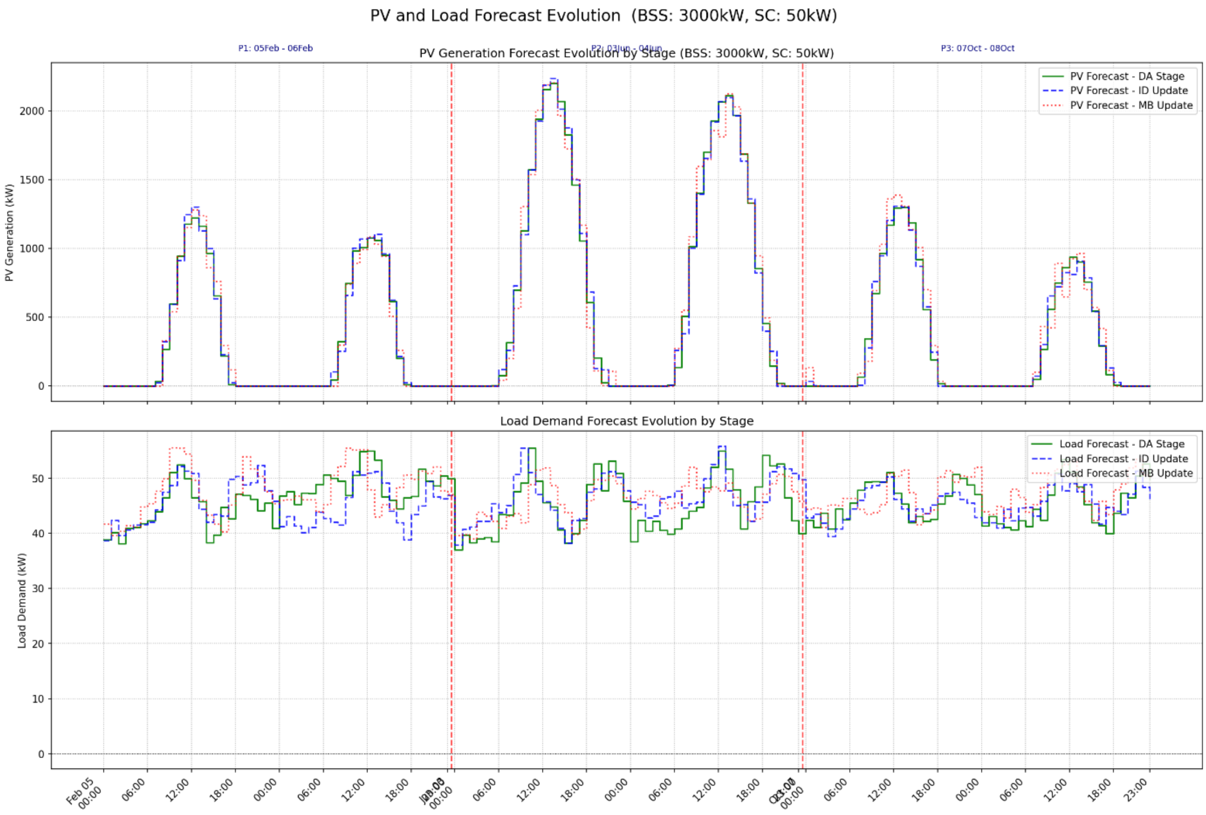

Figure 5.2 PV and Load Forecast Evolution

- **Market Interaction Stages**

Market Interaction plots are presented in Figure 5.3:

DA Market Transactions (Top Panel): The system demonstrates active and strategic participation in the DA market. Significant energy sales to the grid are consistently observed during midday hours across all three periods, aligning with peak PV generation. Conversely, energy purchases from the grid occur during early morning and late evening hours when PV generation is absent and load needs to be met or storage needs to be charged optimally based on DA prices. The magnitude of these transactions underscores the system's capacity to act as a significant player in the DA market.

ID Incremental Transactions (Middle Panel): This panel reveals the corrective actions and opportunistic trading in the ID market. Compared to the DA stage, ID transactions are generally of smaller volume and appear more sporadic. For instance, in P1 (Feb 05-06), there are minor incremental sales (light green, negative) during PV hours and small incremental purchases (salmon, positive) during evening hours. Similar corrective buys and sells are seen in P2 and P3, indicating the system is fine-tuning its energy position based on updated forecasts and ID market price signals, often to reduce imbalances or capture marginal profit opportunities not available or foreseen in the DA stage.

Combined Net Grid Interaction by Market Stage (Bottom Panel): This panel provides a synthesized view of the microgrid's net energy position and MB flexibility. The Net Grid (DA Only) (grey dotted line) shows the initial net commitment from the DA market. The Net Grid (DA+ID Energy) (black solid line) represents the refined net energy position after Intra-Day market adjustments. This line clearly shows large net exports during peak PV production across all periods and significant net imports during early morning or late evening hours.

The Potential Max Import (w/ MB Down) (dashed sky blue line) and Potential Max Export (w/ MB Up) (dashed light coral line) illustrate the total range of grid interaction if the offered MB capacities were fully activated on top of the DA+ID energy schedule. For example, during the midday PV peak on Feb 05 (P1), the system is already a large net exporter from DA/ID; the MB upward capacity offers the potential for even greater export. Conversely, during the morning hours of June 03, when the system is a net importer from DA/ID, the MB downward capacity offers the potential for even greater import (or reduced net export if it were exporting). This visualization underscores the significant operational flexibility and market leverage provided by the 3000kW BESS in the balancing market.

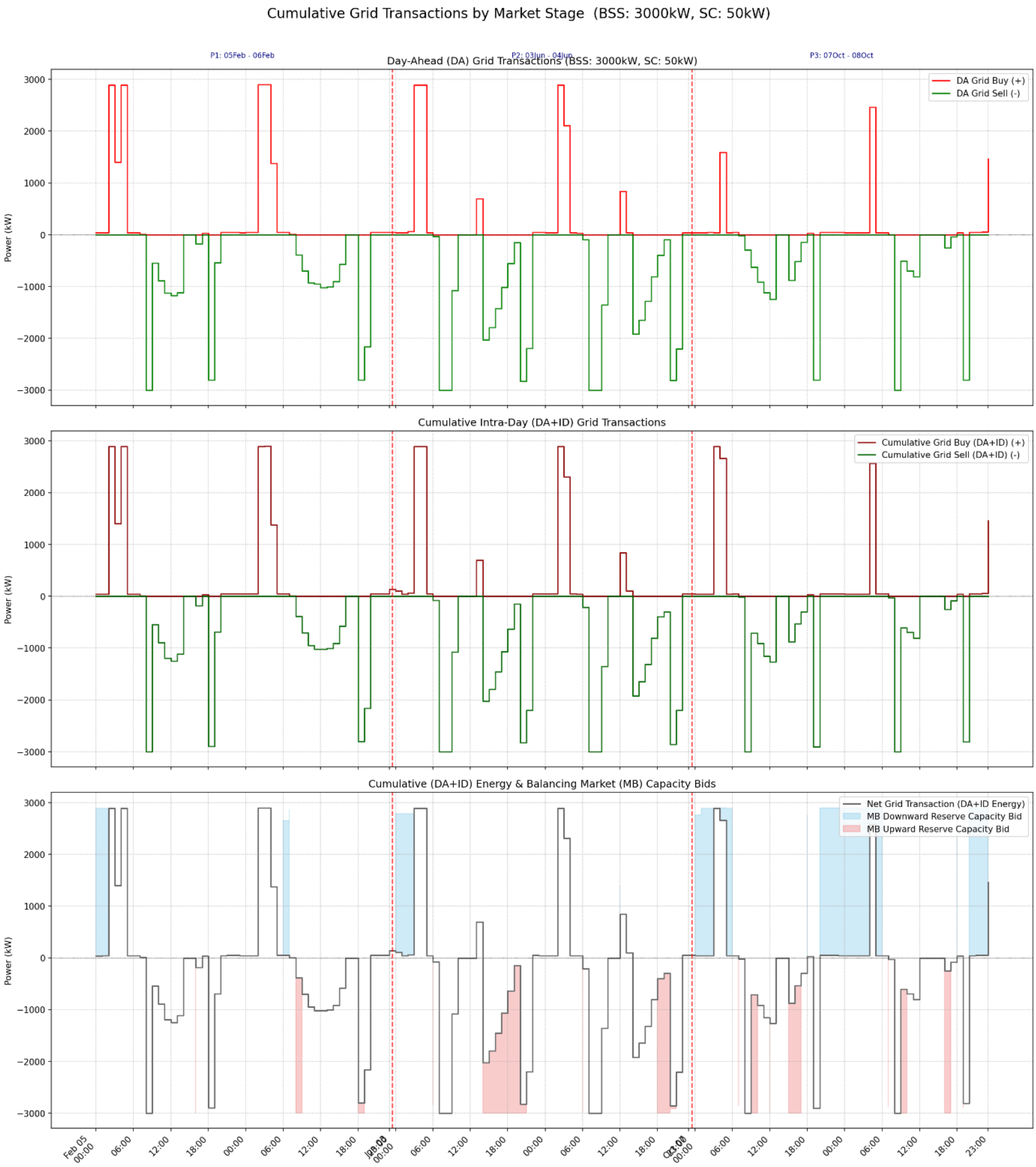

Figure 5.3 Market Transactions

b) **Dispatch & SOC Summaries**

Figure 5.4 provide detailed hourly dispatch plots for each asset alongside storage SOC for DA, ID, and MB stages. We analyze the MB Stage plot for the 3000kW BSS / 50kW SC configuration as it represents the final operational plan.

- **Market Price Context (Top Panel):** MB Up and Down Capacity Prices are displayed, providing the economic signals that guide the system's MB capacity offering strategy.

These prices fluctuate, indicating varying values for upward and downward flexibility throughout the simulated periods.

- **System Dispatch & Net Grid Interaction (Middle Panel):**
    - **Load:** Exhibits typical daily demand patterns with distinct peaks.
    - **Net PV (Gen - Curt):** Significant PV generation is available during daylight hours and is either self-consumed, used for storage charging, or exported. PV curtailment is minimal (around 1.6% based on KPIs), indicating effective utilization of renewable energy.
    - **DG Power:** The Diesel Generator is dispatched by the MB stage primarily during periods of high net demand that cannot be economically or technically met by storage discharge or pre-committed grid imports alone, or when its operation is necessary to fulfill reserve requirements while other assets are constrained. For this configuration, DG plays a notable role, contributing significantly to the energy mix when conditions necessitate its use.
    - **BESS Charge/Discharge:** The BESS serves as the primary workhorse for energy shifting and market arbitrage. It charges substantially during high PV periods or when net grid import costs (from DA/ID) are low, often reaching its power limit. Conversely, it discharges heavily to meet evening load peaks or to export energy when grid sale prices (factored into the net grid transaction or MB energy opportunities) are high. The dispatch closely follows price signals and PV availability.
    - **SC Charge/Discharge:** The Supercapacitor displays characteristic behavior of extremely rapid, high-power charges and discharges. While its total energy throughput is relatively small, these bursts are critical for its role in providing rapid FR response and potentially smoothing very short-term power imbalances. This activity is often dictated by FR commitment constraints that require specific energy headroom.
    - **Net Grid Trans. (MB) (+ for Buy) :** This crucial line depicts the net energy exchange position that was *settled in the Day-Ahead and Intra-Day markets*. The MB stage optimization then uses local assets (BESS, SC, DG) to meet the final load forecast, considering this pre-established net grid flow. The plot shows substantial net grid sales during PV peak hours and significant net grid purchases during periods of low PV and high demand.
    - **FR Market Exclusivity:** Notably, during hours where Fast Reserve (FR) is committed, the optimization model enforces rules that prevent simultaneous energy transactions in the Day-Ahead and Intra-Day markets (i.e., buy/sell variables are effectively zero due to active constraints). This ensures dedicated

availability for FR. The Balancing Market capacity bids during such hours would then be made with the HESS capacity remaining after FR commitments.

- **Energy Storage SOC (Bottom Panel):**
    - **BESS SOC:** The BESS SOC cycles extensively and effectively between its operational minimum of 20% and maximum of 80%, demonstrating active energy arbitrage and load shifting capabilities. It generally aims to meet the 30% end-of-day SOC target. However, the optimization may prioritize immediate high-profit discharge opportunities or ensuring FR energy readiness over strictly adhering to a gradual path towards this target, provided it always respects the 20% minimum limit during intra-day operation. The start of each new 2-day simulation period correctly shows the BESS SOC resetting to its defined initial charge of approximately 30%.
    - **SC SOC:** The SC SOC operates dynamically within its 30% to 90% window. It exhibits very rapid full charges to its maximum and subsequent discharges, particularly aligned with periods of FR commitment. This behavior is consistent with its role in maintaining precise energy headroom required for the high-power, short-duration pulse response expected from the SC for FR services. Similar to the BESS, each new period begins with the SC SOC reset to its initial 30% state.

The interplay between these dispatch decisions and SOC management, guided by evolving market prices and forecasts, highlights the sophisticated strategy employed by the optimization to maximize the microgrid's operational profit.

Dispatch & SoC Summary (Net Grid) - Stage: DA (BSS: 3000kW, SC: 50kW) - Stage: DA

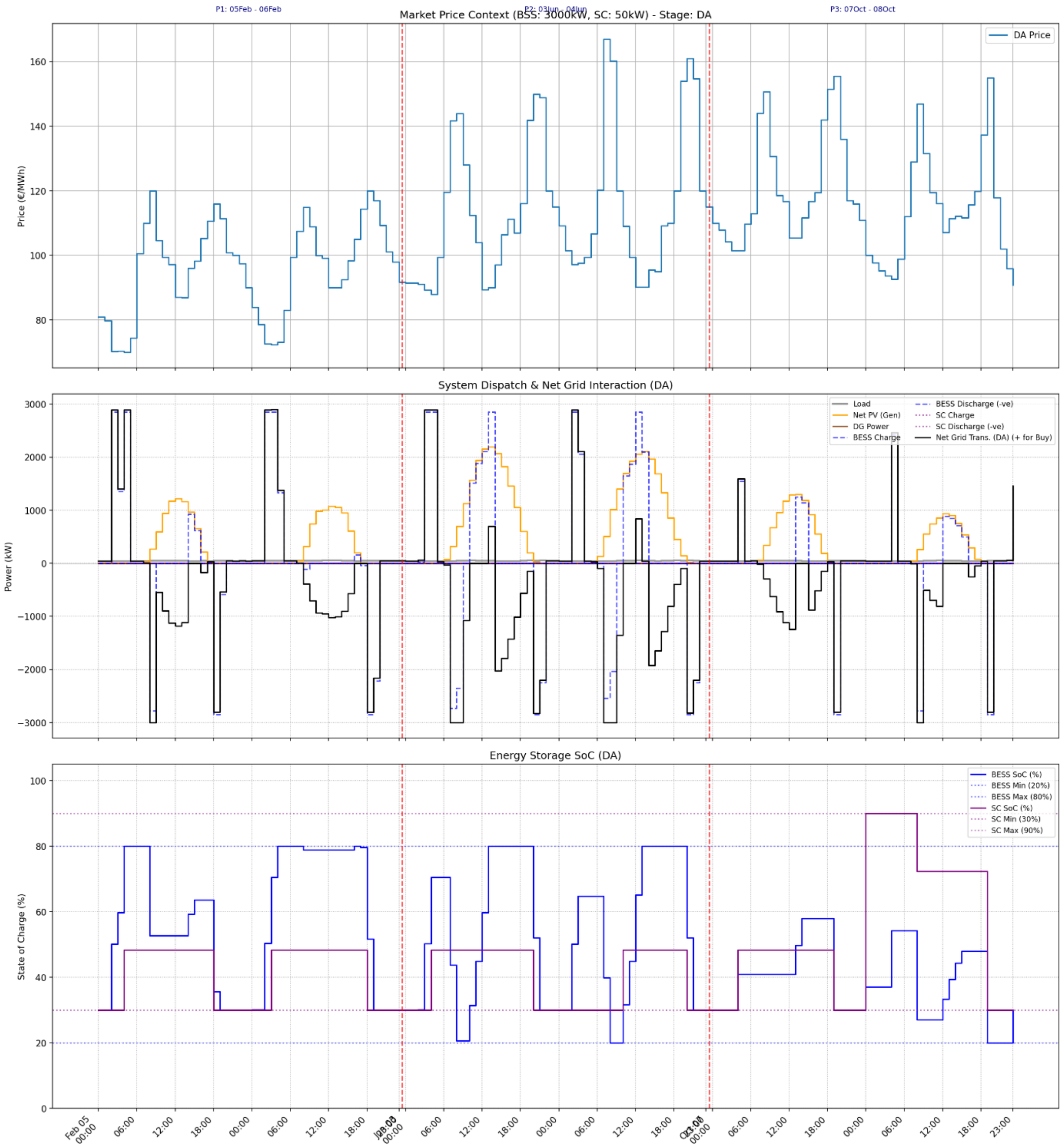

Dispatch & SoC Summary (Net Grid) - Stage: ID (BSS: 3000kW, SC: 50kW) - Stage: ID

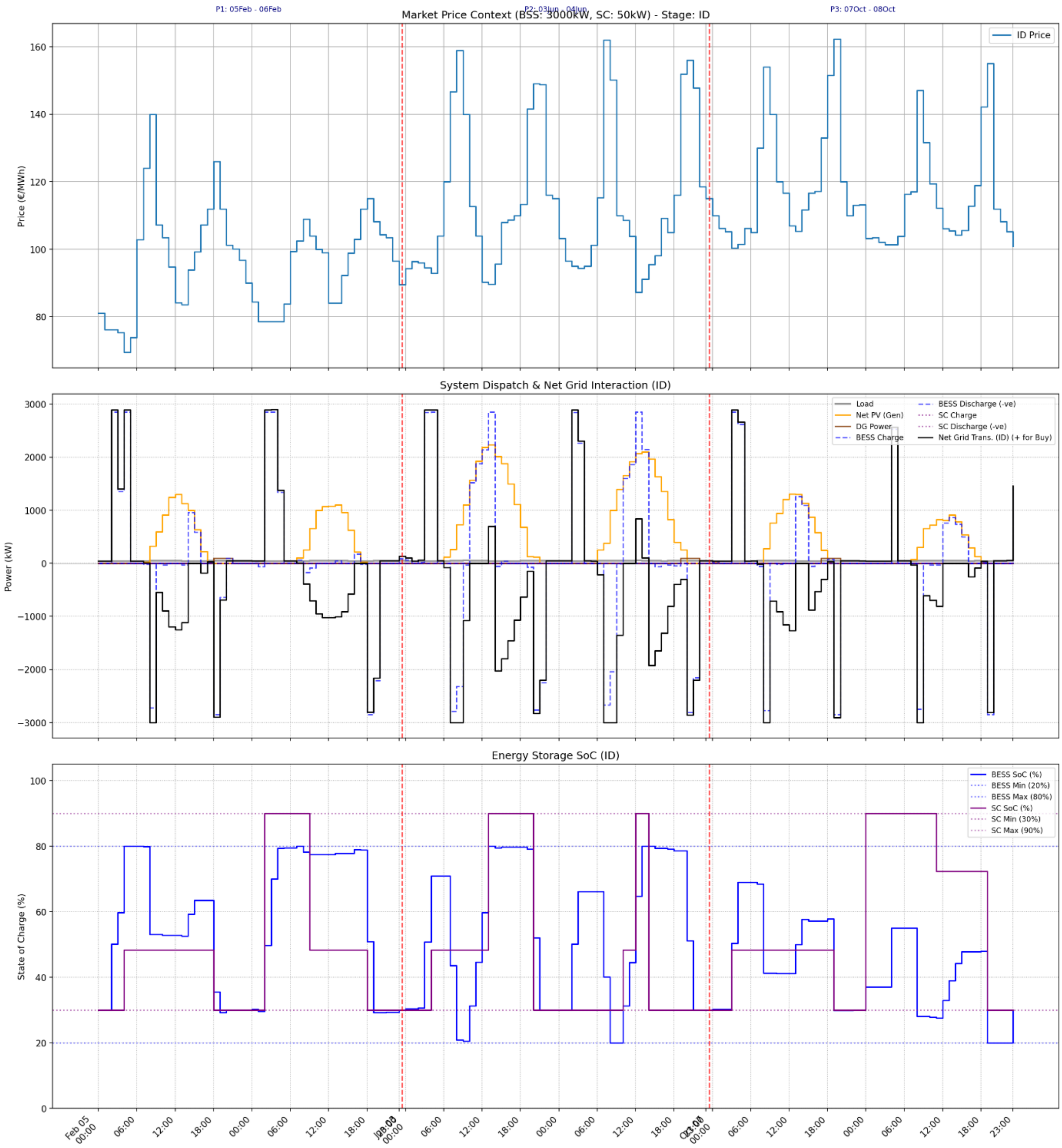

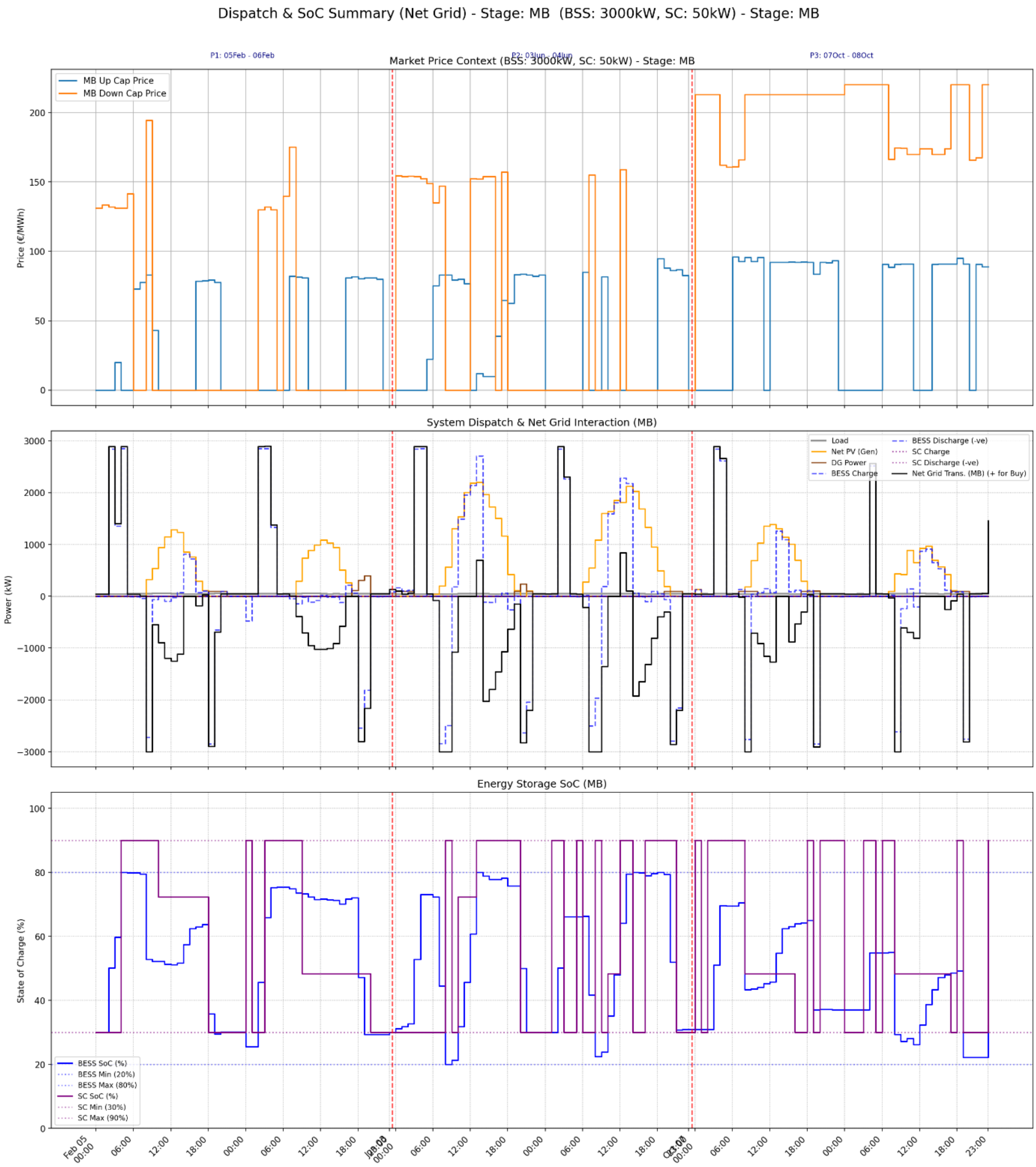

Figure 5.4 Dispatch & SOC Summaries

c) FR Event Simulation

To evaluate the dynamic response capabilities of the HESS, a detailed simulation of a FR activation event was conducted. The Figure 5.5 plot illustrates the system's behavior during a representative 5-minute upward FR event (requiring power discharge) at a selected hour. For this specific event simulation, an FR commitment was intentionally chosen to be a significant portion of the smaller storage asset's power rating (e.g., 90% of the 50kW SC capacity, resulting in a 45kW commitment in the example plot) to clearly visualize the distinct roles and coordinated response of the BESS and SC.

As shown in the plot, the target power requested by the grid (black dashed line) initiates at this committed level and decays linearly to zero over the 5-minute event duration. The total power delivered by the HESS (red solid line) accurately tracks this decaying target profile. The SC (blue dotted line) demonstrates its high-power capability by delivering the initial, rapid burst of power, fulfilling its role for the first 30 seconds. Following this initial pulse, the BESS (green dashed line) seamlessly ramps up its discharge to sustain the FR delivery for the remainder of the event, showcasing its capability for more sustained energy provision.

The corresponding SOC panel illustrates the energy dynamics. The SC SOC (left axis) shows a rapid but relatively small decrease in percentage during its high-power pulse, reflecting its smaller energy capacity but high power density. Conversely, the BESS SOC (right axis) exhibits a more gradual decline as it contributes a larger volume of energy over the sustained ramp period. Both storage units operate well within their defined SOC minimum and maximum limits throughout the event, confirming the HESS's technical ability to reliably deliver the committed FR service according to the designed response profile. This detailed event simulation complements the broader economic optimization by verifying the physical capabilities underpinning the system's participation in fast-acting ancillary services.

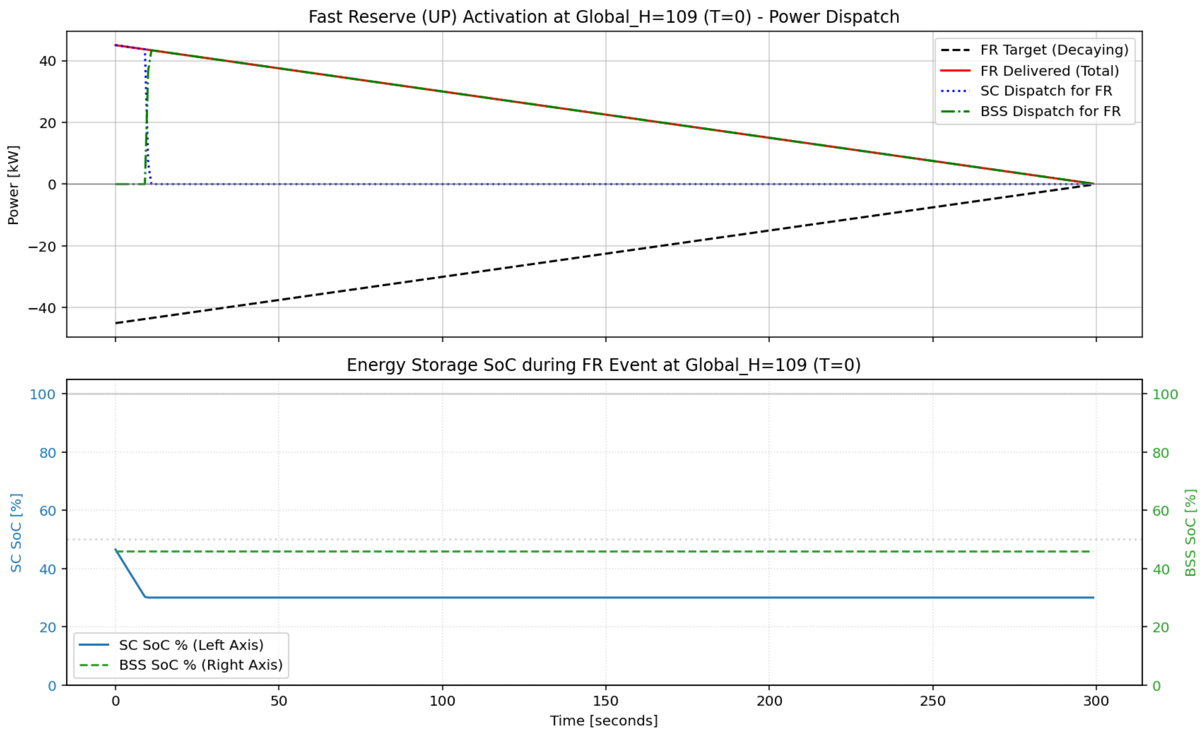

Figure 5.5 Fast Reserve (UP) Activation Simulation

5.5.1.3. Techno-Economic Performance Analysis

The techno-economic viability of the HESS within the microgrid is a primary focus of this investigation. To assess this, various BESS and SC capacities were simulated, and their performance is evaluated here considering both the initial CAPEX and the operational profits generated through multi-market participation. The baseline economic assumptions for this core analysis include a project lifetime of 15 years and a discount rate of 8%.

The Figure 5.6 scatter plot, provides a foundational view of project feasibility. Each point represents a unique BSS/SC sizing configuration resulting from the optimization studies. The x-axis displays the Equivalent Annual Cost, which effectively annualizes the total upfront CAPEX over the project's lifetime, factoring in the chosen discount rate. The y-axis quantifies the average annual operational profit generated by each respective configuration; this profit is determined by annualizing the net operational earnings (market revenues less direct operational expenses from the simulation model) achieved across several representative periods and then averaging these outcomes. The red dashed "Breakeven Line," where Operational Profit precisely equals EAC, serves as a critical benchmark: configurations plotted above this line are projected to yield a positive net annual profit, signifying their financial attractiveness. The plot clearly demonstrates that a significant number of simulated configurations surpass this breakeven threshold. It also visually underscores that while larger BESS capacities generally achieve higher operational profits, these larger systems concurrently incur substantially higher EACs, thereby highlighting the crucial trade-off between operational earning potential and the magnitude of upfront investment. The optimal configurations will be those that find the most favorable balance, maximizing the positive difference between operational profit and EAC.

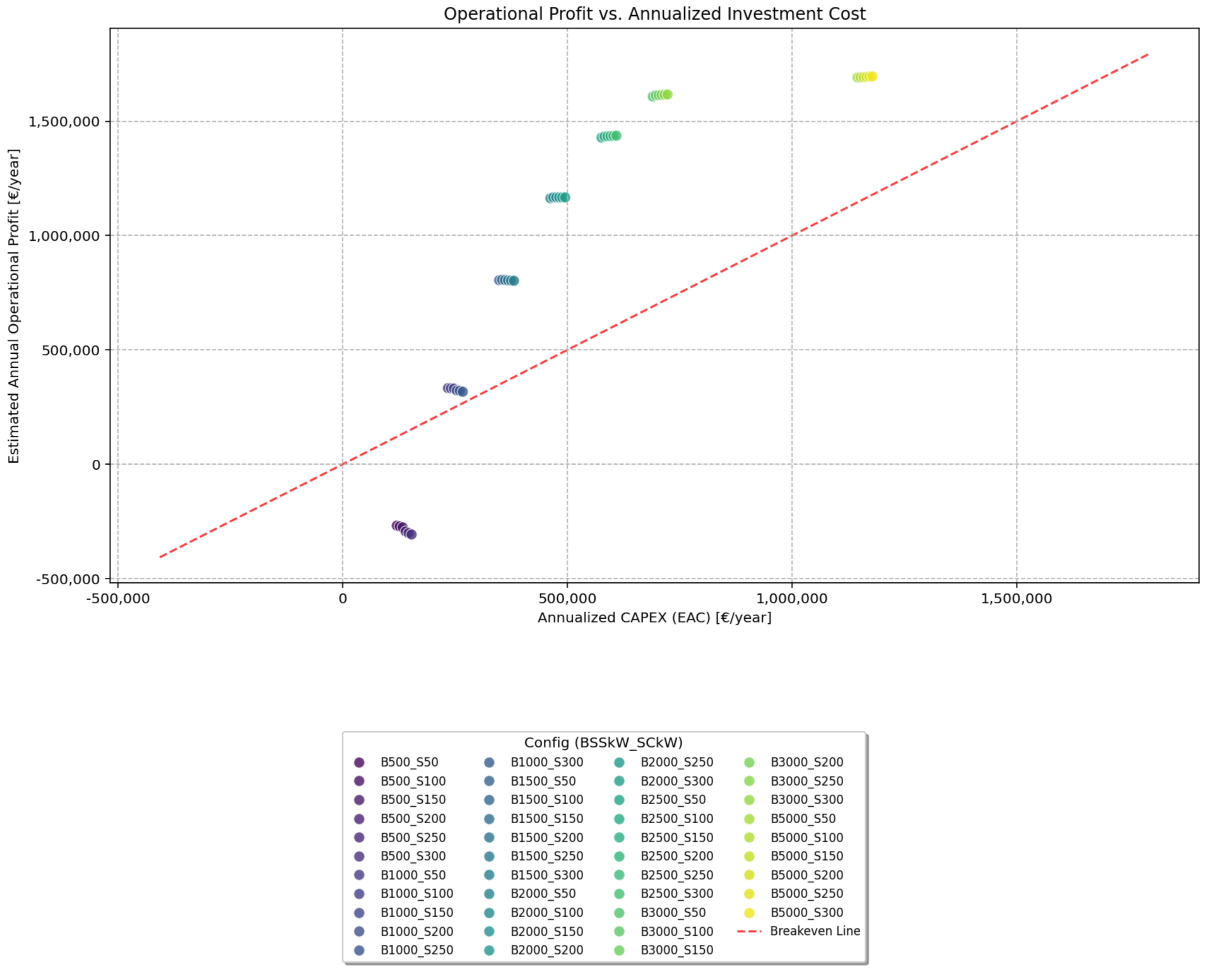

Figure 5.6 Operational Profit vs. Annualized Investment Cost (Case A)

Figure 5.7 offers a gridded visualization of the final net annual profit (calculated as Annual Operational Profit minus EAC) for each simulated BESS/SC combination. The color intensity directly corresponds to profitability, with brighter yellow hues indicating higher net annual profits. This plot clearly reveals that for the tested SC capacities, ranging from 50kW to 300kW, the net annual profit landscape is predominantly shaped by the BESS capacity, likely due to the BESS's significant role in bulk energy management and its larger contribution to total system CAPEX.

Profitability demonstrates a robust upward trend as BESS power scales from 500kW up to an optimal region around 3000kW. To illustrate, for a constant 50kW SC, increasing the BESS from 500kW (yielding a net annual profit of approximately €357,820) to 1500kW (net annual profit of €718,897) results in more than a twofold increase in net profit. This favorable trend continues, culminating in the B3000_S50 configuration achieving the highest observed net profit of €1,088,906 in this analysis. However, for BESS capacities extending beyond 3000kW, such as the 5000kW option (e.g., B5000_S50 showing a net profit of €700,636), the heatmap suggests a plateauing and subsequent decline in net profit. This indicates that for very large

BESS installations, the escalating annualized capital costs may begin to outweigh the marginal gains in operational profit.

In contrast, the variation in SC capacity within the tested range (50kW to 300kW) exerts a less dramatic influence on the overall net annual profit compared to BESS sizing. While subtle, there appears to be a slight preference for smaller SCs (50kW to 150kW) when paired with the larger, more profitable BESS configurations, if the sole objective is maximizing this net annual profit figure. This might suggest that the primary economic benefits captured by the SC in this specific model setup (which includes FR capacity revenue) are largely realized even with smaller SC sizes, and increasing SC capacity further adds proportionally more to the CAPEX than it contributes to the overall net profit through bulk energy operations.

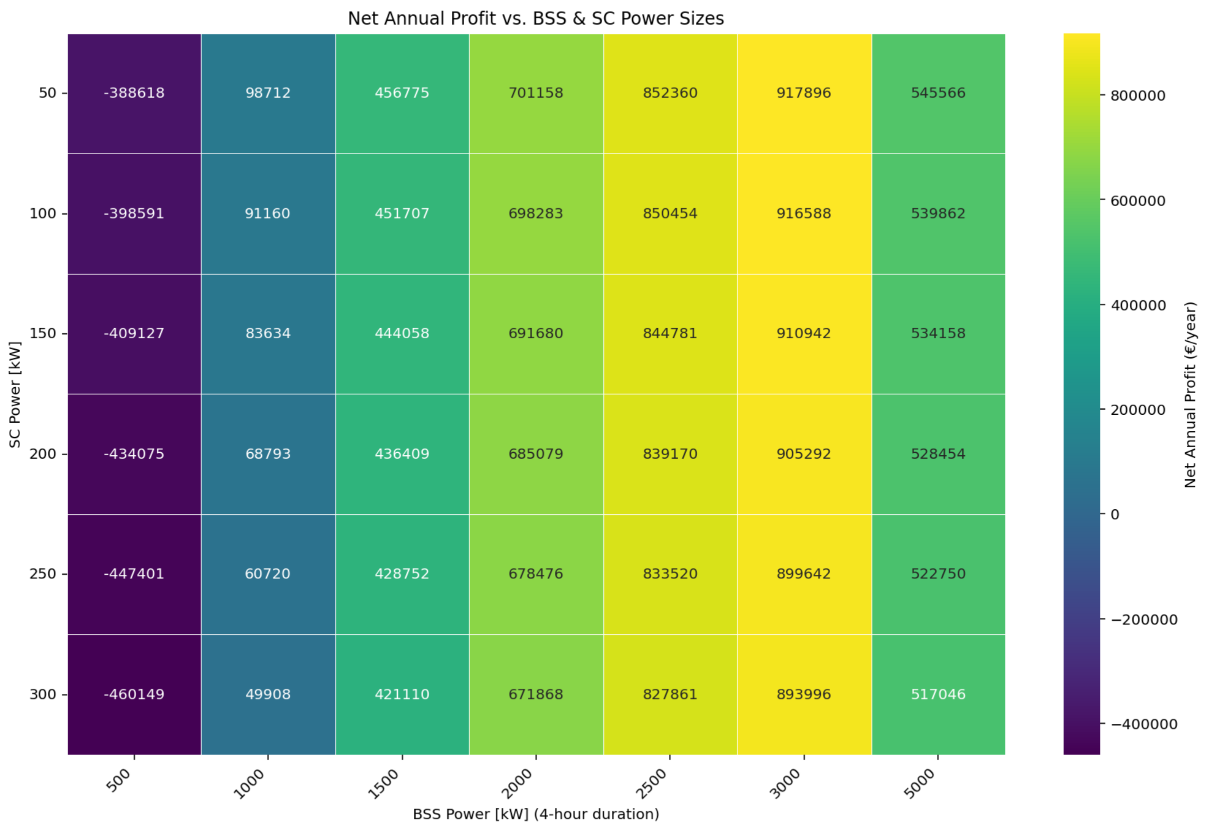

Figure 5.7 Net Annual Profit vs. BSS & SC Power Sizes (Case A)

The Figure 5.8 plot provides a three-dimensional perspective of the heatmap data, further emphasizing the "hill" of profitability. The visual peak of this landscape clearly aligns with BESS capacities in the 2500kW to 3000kW range when paired with smaller SC sizes (50kW to 150kW). The "Best Found" marker, corresponding to the B3000_S50 configuration based on maximizing the baseline net annual profit, is appropriately positioned at or near this summit. This three-dimensional representation is particularly useful for intuitively understanding how net profit responds to simultaneous changes in both BSS and SC capacities. Furthermore, it graphically underscores a key insight: while a single sizing combination might emerge as mathematically optimal under the baseline assumptions, a broader plateau or region of near-optimal configurations often exists, offering valuable flexibility in practical system design where factors such as capital constraints, risk tolerance, or specific service requirements might influence the final selection.

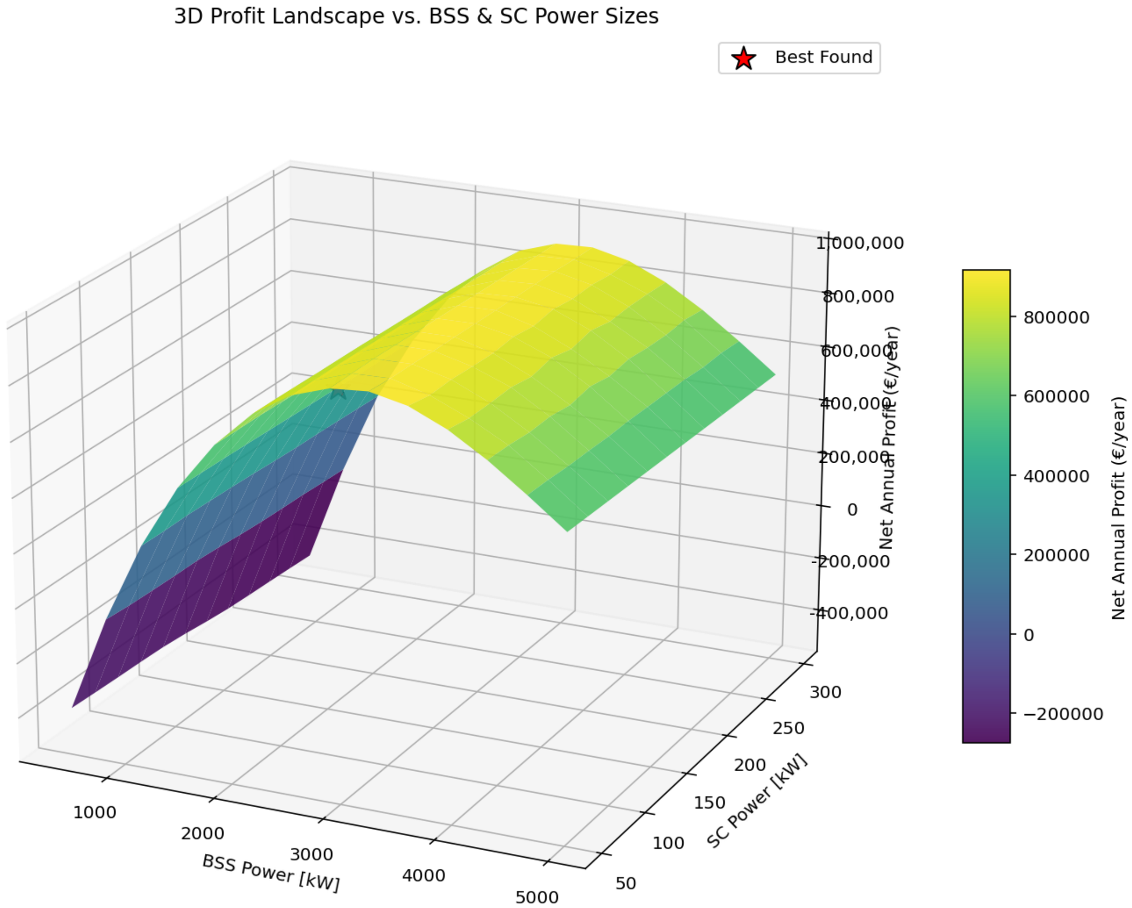

Figure 5.8 3D Profit Landscape vs. BSS & SC Power Sizes (Case A)

To further dissect these relationships, the line plot in Figure 5.9 specifically illustrates the impact of BESS capacity on net annual profit for several discrete SC sizes. Each colored line corresponds to a fixed SC capacity, tracing profitability as BESS capacity varies. A consistent pattern emerges across all SC lines: they exhibit a distinct concave (or inverted U-shape) profile. Net annual profit rises sharply with increasing BESS capacity in the lower ranges, indicative of the significant value derived from larger energy storage for arbitrage and market services. This rise typically peaks for a BESS capacity around 3000 kW, after which profitability tends to plateau and then decline as the annualized cost of even larger BESS capacities begins to outweigh incremental operational gains.

This plot compellingly demonstrates that, for the range of SC sizes tested (50kW to 300kW), the BESS capacity yielding the maximum net annual profit consistently hovers around the 3000 kW mark. Furthermore, it highlights that the variance in *peak* profitability across these different

SC sizes is relatively modest. For instance, when paired with the optimal 3000 kW BESS, the net annual profit only fluctuates from approximately €1.07M (with a 300kW SC) to €1.09M (with a 50kW SC). This observation reinforces the earlier finding that BESS sizing is the more dominant factor influencing overall net annual profit in this particular system configuration and market context, compared to the SC sizing within the range explored.

.

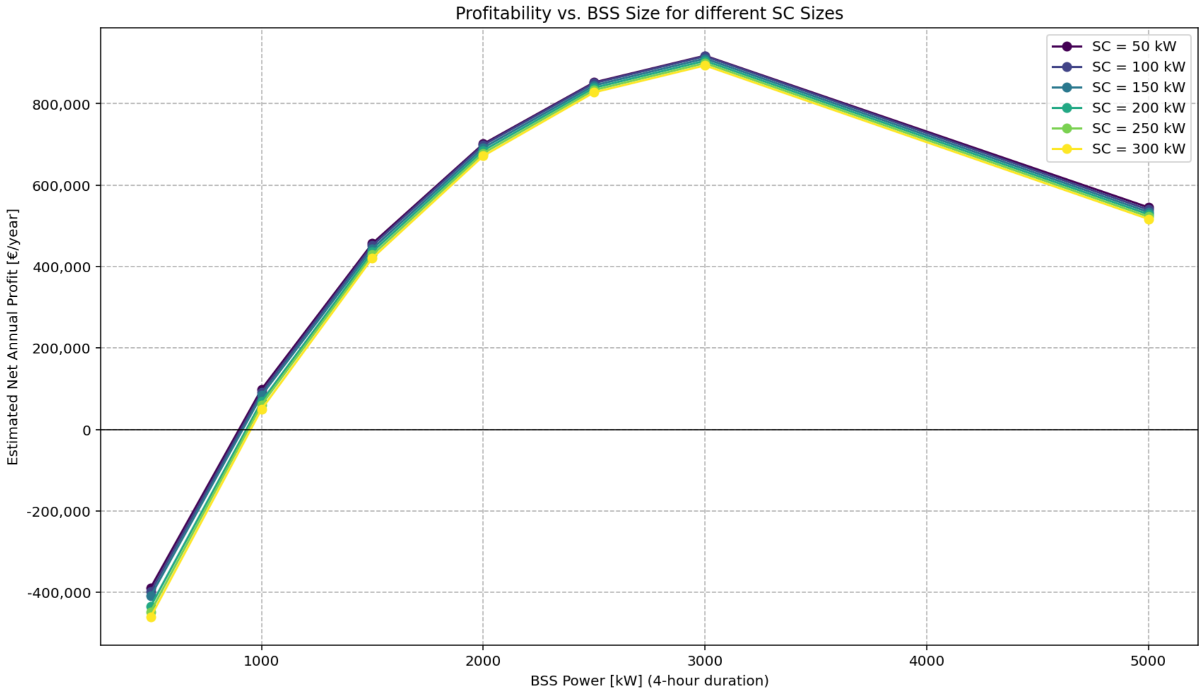

Figure 5.9 Profitability vs. BSS Size for different SC Sizes (Case A)

Finally, the scatter plot in Figure 5.10 directly juxtaposes the achieved net annual profit against the required total upfront investment (Total System CAPEX) for each simulated BESS/SC configuration. The general trend observed is that as the total system CAPEX increases (points shifting to the right on the x-axis, primarily driven by larger BESS capacities), the estimated net annual profit also tends to rise. However, this relationship clearly exhibits diminishing marginal returns, where each additional unit of investment yields progressively smaller increases in profit, especially at higher CAPEX levels.

The data points form distinct clusters, generally grouped by BESS size, with variations within each cluster reflecting the more modest CAPEX impact of different SC sizes. The upper-left envelope of these points effectively traces a "Pareto front," representing the set of most efficient investments, those achieving the highest net annual profit for a given level of CAPEX. While the B3000_S50 configuration (approximately €1.09M net profit for a ~€5.9M CAPEX) is identified as yielding one of the highest absolute net profits, the plot also illuminates other strategic options. For instance, a configuration like B2500_S50, offering a slightly lower net profit (e.g., potentially around €1.03M, based on interpolations from the heatmap data) but at a notably reduced CAPEX (approximately €4.9M), might present a more attractive return-on-investment profile or be a more suitable choice if initial capital outlay is a significant constraint.

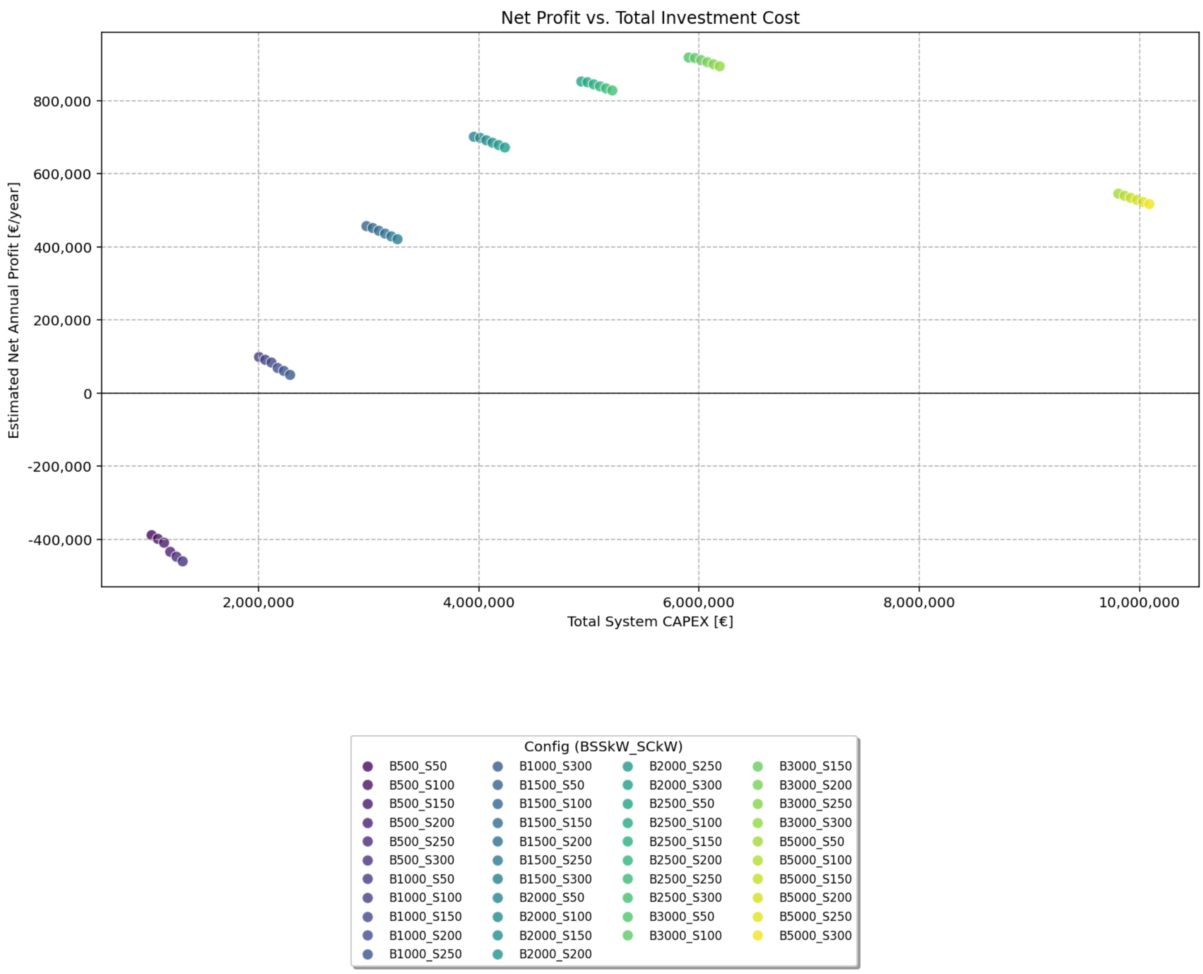

Figure 5.10 Net Profit vs. Total Investment Cost (Case A)

Collectively, these techno-economic plots indicate that while a 3000kW BSS paired with a 50kW SC emerges as the configuration maximizing the baseline net annual profit in this study, a broader range of BSS capacities (notably 2000kW to 3000kW) coupled with smaller SCs (50kW to 150kW) also deliver robust financial performance. The substantial positive net annual profit for these configurations, often exceeding €800,000 to €1,000,000 per year, demonstrates the system's strong capability to generate economic value significantly above its annualized investment and operational costs through strategic multi-market participation. Ultimately, the final selection of an "optimal" system in a real-world deployment would likely involve a holistic assessment, considering these quantitative results alongside specific investor risk preferences, capital availability, and the nuanced operational and strategic benefits of different SC sizes for specialized grid services like Fast Reserve, whose full value might not be entirely encapsulated by the overall net profit metric alone.

5.5.1.4. KPIs Calculation

The operational performance of the best-identified configuration (3000kW BSS, 50kW SC) is further explained by key performance indicators, derived from the MB stage results and annualized from the extended 6-day simulation across three representative periods. These results are presented in Table 5-3.

Table 5-3 Calculated KPIs for Case A

Economic Metrics						
Metric Description	Net Annual Profit	NPV	LCOE	Self Sufficiency Percentage	Annual Operational Emissions	Simple Payback Period
Value	1,607,920.56 €	7,856,711.74 €	1.7	1626.70%	-857,262.21 kg CO_2-eq	3.67 years
Metric Description	Profitability Index	Project IRR	LCOS BESS	Total Lifecycle Cost (PV)	BESS Cost per Cycle	
Value	2.33%	26.42%	0.24	10,456,108.52 €	120.00 €	
Technical Metrics						
Metric Description	Avg FR Committed Power	Sim Peak Grid Demand	RES Curtailment Factor	ESS Discharged Contribution to Load	DG Contribution to Load	RES Contribution to Load
Value	15.00 kW	2897.46 kW	1.61%	642.77%	45.36%	938.58%
Metric Description	BESS ECF	BESS EFC (Annual)	BESS DOD Mean	SC Energy Buffer Ratio		
Value	50.77%	263.61	60.00%	96.49%		
Energy Metrics						
Metric Description	Total Sim Load	Sim DG Energy	Sim BESS Throughput	Annual BESS Throughput	Lifetime Energy Delivered	Lifetime Total BESS Discharge for LCOS
Value	6,759.40 kWh	3,066.04 kWh	104,000.79 kWh	6,326.71 MWh	6,167,953.16 kWh	39,639,381.07 kWh
Other Metrics						
Metric Description	BESS Total Lifecycle Cost for LCOS	BM Capacity Revenue Contribution	BM Energy Revenue Contribution	DA Revenue Contribution	FR Revenue Contribution	ID Revenue Contribution
Value	9,586,819.35 €	71.43%	5.02%	22.91%	0.05%	0.59%
Revenue Stack – Simulation Period						

Metric Description	BM Capacity Market Revenue	BM Energy Market Revenue	Curtailment Cost	DA Market Revenue	FR Market Revenue	ID Market Revenue
Value	21,405.45 €	1,505.32 €	1,035.93 €	6,864.25 €	13.50 €	177.08 €
Metric Description	Net Operational Profit	Total Cost of Diesel Generator	Total Degradation Cost	Total Gross Market Revenue	Total Operational Cost	
Value	26,431.57 €	1,977.11 €	520.99 €	29,965.60 €	3,534.03 €	
Revenue Stack – Annual						
Metric Description	Annual BM Capacity Market Revenue	Annual BM Energy Market Revenue	Annual Curtailment Cost	Annual DA Market Revenue	Annual FR Market Revenue	Annual ID Market Revenue
Value	1,302,164.86 €	91,573.82 €	63,019.00 €	417,575.45 €	821.25 €	10,772.17 €
Metric Description	Annual Net Operational Profit	Annual Total Cost of Diesel Generator	Annual Total Degradation Cost	Annual Total Gross Market Revenue	Annual Total Operational Cost	
Value	1,607,920.56 €	120,274.49 €	31,693.50 €	1,822,907.55 €	214,987.00 €	

The optimized 3000 kW BSS and 50 kW SC configuration demonstrates good financial performance, achieving a remarkable 26.42% IRR with a rapid 3.67-year payback period. This configuration excels in market participation, generating €1.82 million in annual gross revenue against €214,987 in operational costs, resulting in a substantial €1.61 million annual net profit and €7.86 million NPV. The revenue diversification is strategically focused on balancing market capacity services (71.43%) and day-ahead market operations (22.91%), reflecting an optimization strategy that prioritizes high-value grid services. The profitability index of 2.33% and low LCOS of 0.24 €/kWh further underscore the superior economic efficiency of this system configuration.

From a technical perspective, the system shows a high battery utilization while maintaining the a 60% depth of discharge management strategy. The supercapacitor utilization is extremely high at 96.49% energy buffer ratio, despite the smaller SC capacity. The high self-sufficiency (1,626.70%) and renewable contribution metrics (938.58%) indicate substantial energy export and relative to the low local load, with the system effectively participating across multiple markets while experiencing minimal renewable curtailment (1.61%).

5.5.1.5. Discussion and Conclusion

The simulation results for a grid-connected microgrid featuring a 3000kW/12000kWh BESS and a 50kW SC demonstrate strong potential for profitability and positive environmental impact. The system achieves an average net annual profit of approximately €1.09 million by strategically participating in DA, ID, MB, and FR markets. This profitability is driven by significant operational profits that comfortably exceed the EAC.

The operational strategy involves active utilization of the BESS for energy arbitrage and load shifting, complemented by the SC's role in rapid response services (likely FR). The low PV curtailment and high effective utilization of PV (indicated by high self-sufficiency and ESS contribution beyond local load) highlight the system's capability to integrate renewable energy effectively. The negative lifecycle carbon emissions and a very short carbon payback time further emphasize the environmental benefits of such a system, primarily through the displacement of higher-carbon grid electricity.

While the 3000kW BSS / 50kW SC configuration performs very well under the baseline economic assumptions, the "true" optimal solution is sensitive to variations in CAPEX, discount rates, and project lifetimes, as would be explored in a full sensitivity analysis.

- **Lower CAPEX:** If capital costs for BESS or SC were lower (e.g., through technological advancements or subsidies), even larger systems might become more profitable, or the profitability of the current optimal would further increase.
- **Higher CAPEX:** Conversely, increased CAPEX would reduce net profits and potentially shift the optimal sizing towards smaller systems.
- **Discount Rate & Lifetime:** Higher discount rates or shorter lifetimes increase the EAC, making it harder for operational profits to yield a positive net profit. Longer lifetimes and lower discount rates would improve the financial attractiveness.

The sizing plots provided (heatmap, 3D landscape) suggest that there's a "sweet spot" for BESS sizing. Beyond a certain capacity, the incremental operational profit may not justify the incremental CAPEX. SC's optimal size is likely more strongly tied to the specific revenue potential from FR and its contribution to overall system efficiency or BESS longevity (not explicitly modeled here beyond basic degradation).

5.5.2. Case B: Extended Horizon Case

5.5.2.1. System Description

a) System Data

The simulation environment models a grid-connected microgrid with access to various electricity markets.

- **Load and PV Data, Market Prices, Grid Connection, and Sizing Options:** These parameters are drawn from the same underlying datasets and maintain the same limits as in the Case Study A.

- **Simulation Periods:** This study employs an Extended Case Study design, simulating one representative week (7 days) from each month of 2024. The selected periods are:
  - P1: Jan 08-14, P2: Feb 05-11, P3: Mar 11-17, P4: Apr 08-14,
  - P5: May 06-12, P6: Jun 03-09, P7: Jul 01-07, P8: Aug 12-18,
  - P9: Sep 09-15, P10: Oct 07-13, P11: Nov 04-10, P12: Dec 02-08.

  This totals 84 simulated days, providing a more comprehensive basis for annual extrapolations compared to previous limited-duration studies.

b) Components Data

The core asset parameters are consistent with previous analyses detailed in Table 5-1 and Table 5-2. The key difference for this detailed report section is the focus on the **BSS: 3000kW, SC: 100kW** configuration, which emerged as optimal from the extended sizing simulations.

5.5.2.2. Results Analysis

The following analyses pertain to the B3000kW_S100kW configuration over the 84 simulated days.

a) Input Data (PV and Load)

The PV and Load Forecast Evolution plot (see Figure 5.11) now displays the PV, Load, and Market Price data spanning the twelve 7-day periods. The period labels (P1-P12) clearly shows each simulated month's representative week. This extended view allows for a better appreciation of seasonal trends in PV output (higher in summer months like P8-Aug), load variations, and market price dynamics throughout the year. The greater diversity of conditions in this extended dataset provides a more robust foundation for evaluating the system's long-term operational strategy.

Figure 5.11 PV and Load Forecast Evolution (Case B)

b) Market Interaction Stages

Figure 5.12 displays the market interactions in three stages:

DA Market: Large volume energy purchases and sales persist, driven by PV availability and price arbitrage opportunities.

ID Market: Incremental adjustments continue to refine the DA position.

MB Capacity Bids: The system frequently offers close to its 3000 kW BESS capacity for both upward and downward reserves, maximizing potential capacity revenue.

Combined Net Grid Interaction: The system consistently acts as a net exporter during daylight hours with high PV, and a net importer during nighttime or low PV periods. The MB capacity offerings provide a wide band of operational flexibility around the DA+ID energy commitments. The patterns observed in the 6-day study are largely reinforced over the extended 84-day simulation, demonstrating a robust market participation strategy.

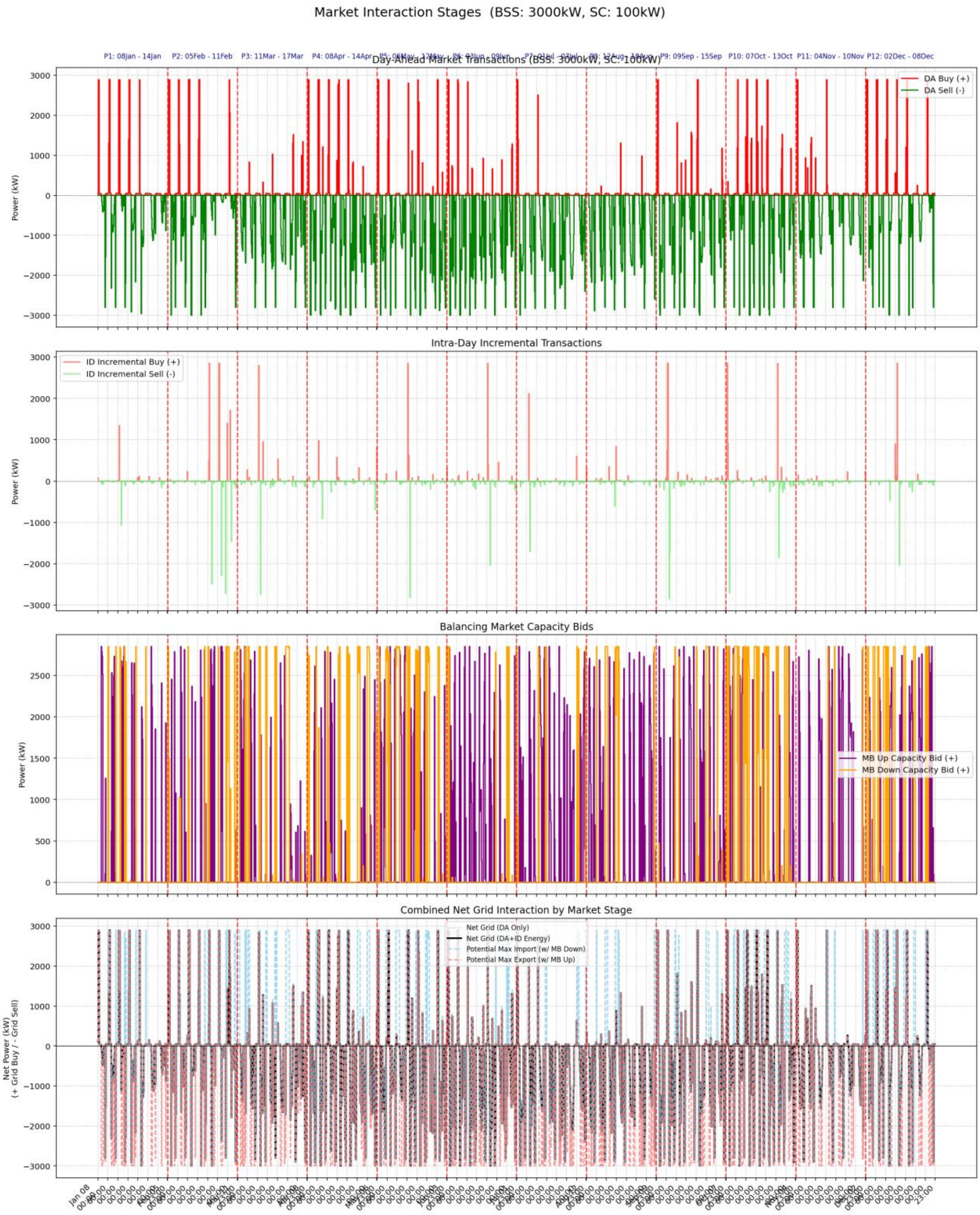

Figure 5.12 Market Transactions (Case B)

c) Dispatch & SOC Summaries

Analyzing the representative Figure 5.4 (for B3000kW_S100kW over 84 days):

- **System Dispatch:** The BESS remains the primary asset for bulk energy shifting, charging extensively from PV and discharging to meet load or export. The DG continues to operate during periods of energy deficit or high market prices when storage is constrained. The **100kW SC** (compared to 50kW in the previous detailed analysis) shows similar rapid charge/discharge behavior linked to FR commitments; while its power rating is higher, its energy throughput relative to the BESS remains small, emphasizing its role in power-intensive services. The larger SC capacity means a higher FR power commitment (0.3 * 100kW = 30kW vs. 15kW with the 50kW SC), potentially leading to more FR revenue if market prices for this service are favorable.

- **Energy Storage SOC:** BESS SOC behavior is consistent withCase A, actively cycling within its 20%-80% limits and resetting to ~30% for each new 7-day period. The SC SOC also shows dynamic cycling between its 30%-90% limits, often driven by FR energy headroom requirements. The larger SC capacity means that satisfying the energy headroom for a 30kW FR commitment is still a small fraction of its reference energy capacity (100kW * (30/3600)hr / (0.9-0.3) = 1.389 kWh), allowing it to comfortably meet these FR needs

.

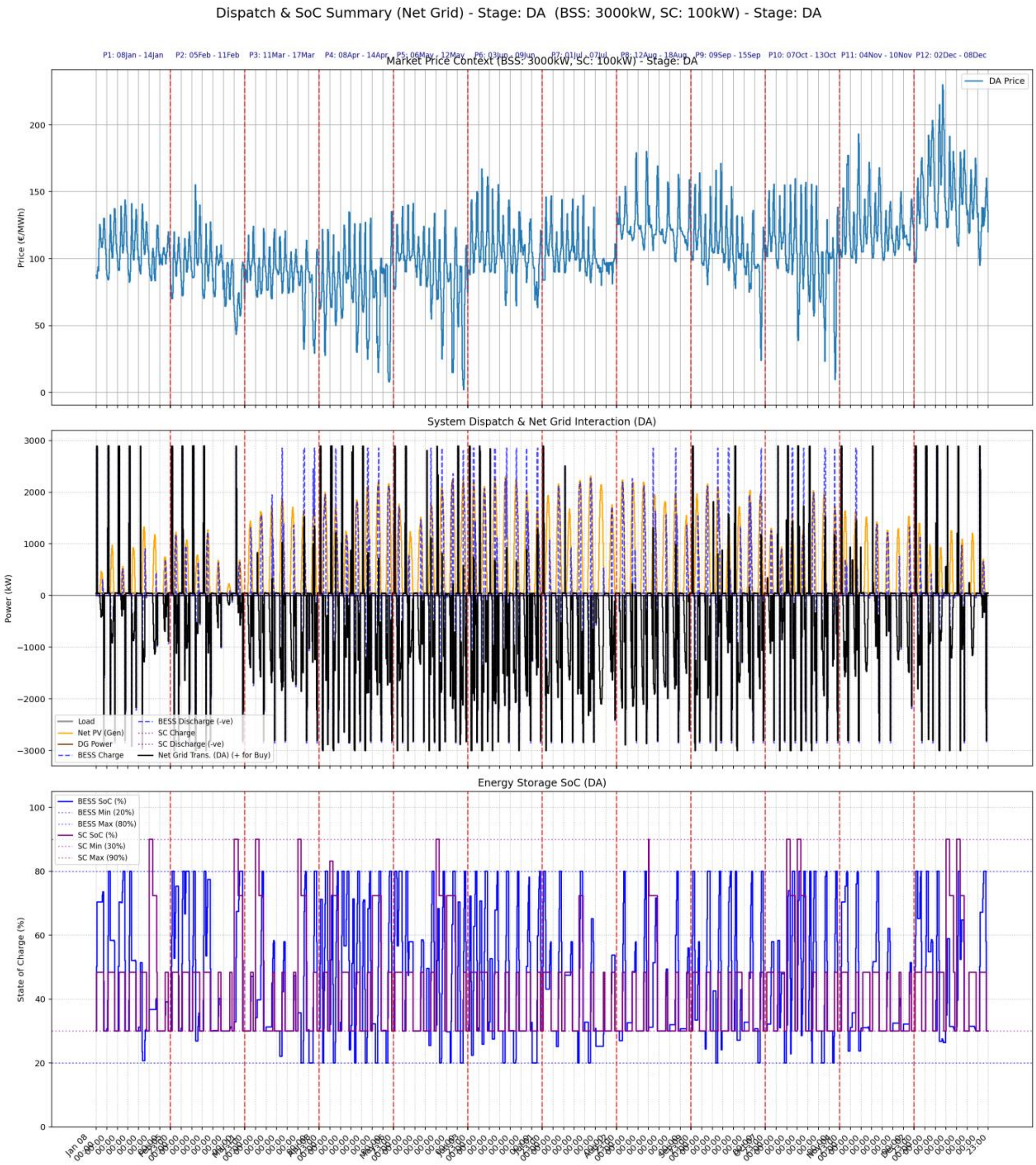
Dispatch & SoC Summary (Net Grid) - Stage: DA (BSS: 3000kW, SC: 100kW) - Stage: DA
Market Price Context (BSS: 3000kW, SC: 100kW) - Stage: DA
P1: 08Jan - 14Jan
P2: 05Feb - 11Feb
P3: 11Mar - 17Mar
P4: 08Apr - 14Apr
P5: 06May - 12May
P6: 03Jun - 09Jun
P7: 01Jul - 07Jul
P8: 12Aug - 18Aug
P9: 09Sep - 15Sep
P10: 07Oct - 13Oct
P11: 04Nov - 10Nov
P12: 02Dec - 08Dec
DA Price
Price (€/MWh)
System Dispatch & Net Grid Interaction (DA)
Power (kW)
Load
Net PV (Gen)
DG Power
BESS Charge
BESS Discharge (-ve)
SC Charge
SC Discharge (-ve)
Net Grid Trans. (DA) (+ for Buy)
Energy Storage SoC (DA)
State of Charge (%)
BESS SoC (%)
BESS Min (20%)
BESS Max (80%)
SC SoC (%)
SC Min (30%)
SC Max (90%)

Dispatch & SoC Summary (Net Grid) - Stage: ID (BSS: 3000kW, SC: 100kW) - Stage: ID

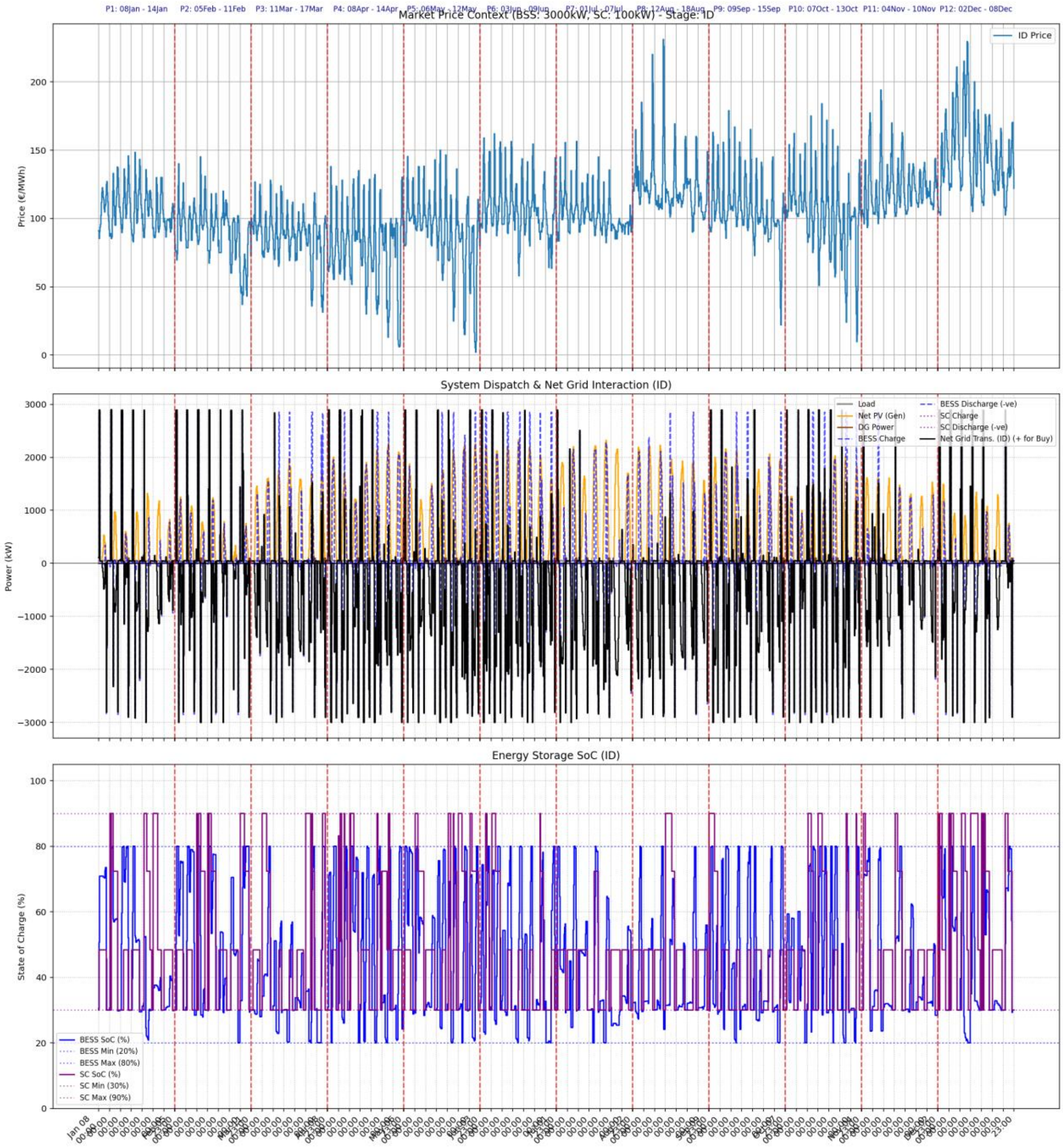

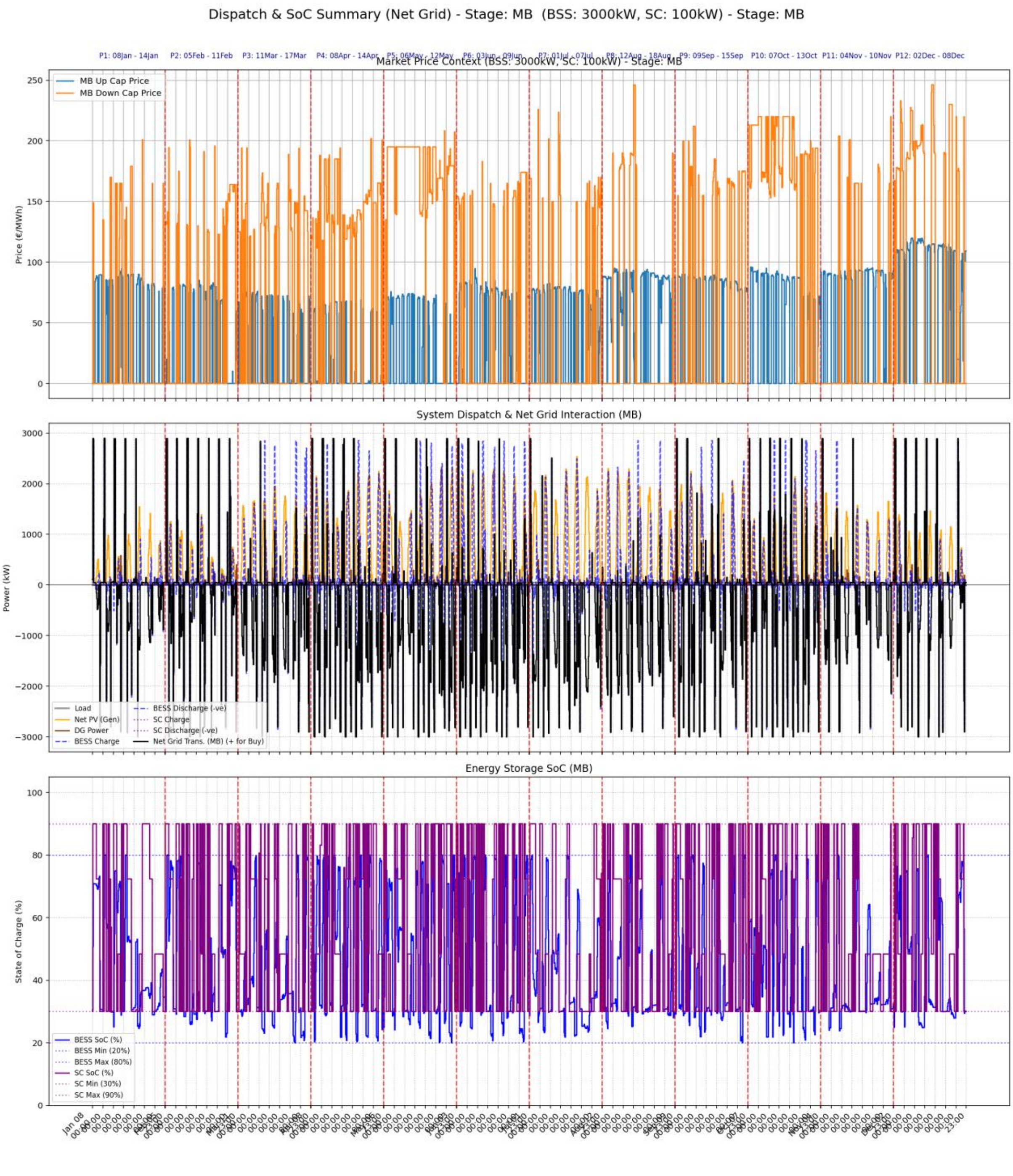

Figure 5.13 Dispatch & SOC Summaries (Case B)

5.5.2.3. Techno-Economic Performance Analysis

The Figure 5.14 (Operational Profit vs. Annualized Investment Cost) provides a foundational view of project feasibility across the spectrum of simulated HESS configurations. Each point on the scatter plot represents a unique BSS/SC sizing combination. The x-axis quantifies the Equivalent Annual Cost (EAC), which translates the total upfront CAPEX into an equivalent annual cost over the 15-year project lifetime at an 8% discount rate. The y-axis shows the corresponding average annual operational profit achieved by that configuration through multi-market participation, as derived from the 84-day extended simulation. The red dashed "Breakeven Line" (where Operational Profit equals EAC) signifies the point of zero net profit.

The configurations plotted above this line are economically viable, generating sufficient operational profit to cover their annualized capital costs and yield a net positive return. The plot clearly demonstrates that a substantial number of configurations, particularly those involving larger BESS capacities (2000kW and above), comfortably surpass this breakeven threshold. This indicates that leveraging larger storage capacities tends to unlock higher operational profits, primarily through enhanced capabilities for energy arbitrage and ancillary service provision. However, it's also evident that these higher operational profits come at the cost of increased EAC, underscoring the critical trade-off between earning potential and upfront investment.

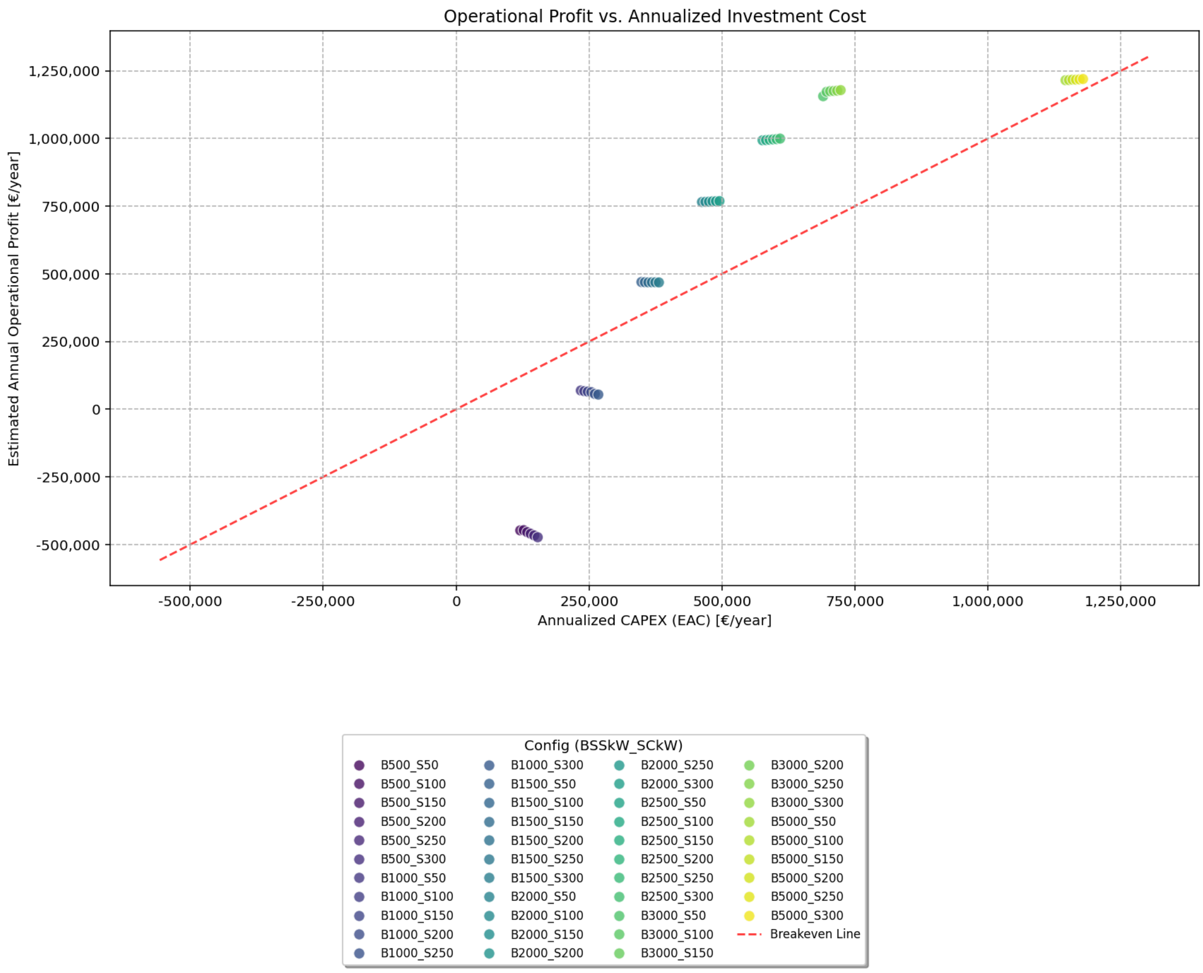

Figure 5.14: Operational Profit vs. Annualized Investment Cost (Case B)

The heatmap in Figure 5.15 presents a gridded, color-coded view of the net annual profit for all simulated BESS and SC capacity combinations. Brighter yellow areas signify higher profitability, while darker purple areas indicate lower or negative net profits. This plot confirms the trends observed in the line and 3D plots: optimal BESS capacity lies in the 2500kW to 3000kW range. For instance, the B3000kW row shows peak profits around €466k-€476k when paired with SCs from 50kW to 200kW. For any given BESS capacity, the variation in net profit due to SC size changes (rows in the heatmap) is generally less pronounced than the variation seen when changing BESS capacity (columns). For example, with a 1500kW BESS, net profit ranges from about €107k (SC=150kW) to €121k (SC=50kW). In contrast, with a 50kW SC, net profit ranges from -€567k (BSS=500kW) to a peak of €466k (BSS=3000kW), before dropping to €69k (BSS=5000kW). This underscores the BESS's primary role in driving overall energy market profitability. The heatmap is particularly effective for quickly identifying regions of high performance and understanding the relative sensitivity of net profit to changes in either storage component's size.

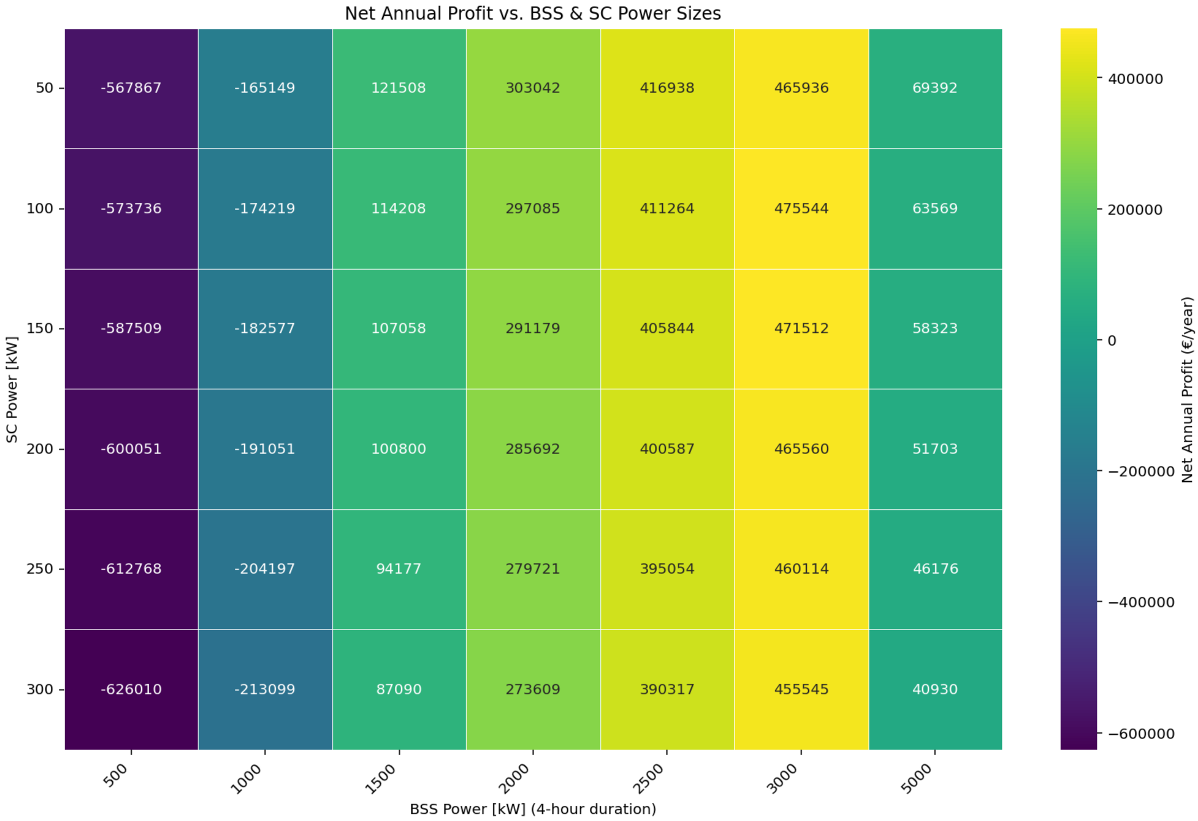

Figure 5.15 Net Annual Profit vs. BSS & SC Power Sizes (Case B)

The 3D Profit Landscape plot (Figure 5.16) offers a volumetric representation of the net annual profit as a function of both BESS power and SC power. This visualization provides an intuitive understanding of the combined impact of sizing both storage components. The "hill" of profitability is clearly discernible, with its peak or plateau located in the region of higher BESS capacities (around 2500kW to 4000kW, visually peaking near 3000kW) and across the range of SC capacities, though tending towards smaller SC sizes for the absolute peak. The "Best Found" marker (indicating the B3000kW_S100kW configuration based on the provided log for highest net profit among configurations with *this specific SC parameter set*) is situated prominently on this profitable plateau. The surface illustrates how profit changes smoothly or sharply as one moves away from this optimal region. For example, decreasing BESS power from the peak results in a steeper decline in profit than moderately increasing or decreasing SC power from its optimal pairing. This plot is particularly valuable for understanding the sensitivity of net profit to simultaneous variations in both storage dimensions and for identifying broader regions of robust, near-optimal performance rather than focusing solely on a single point estimate.

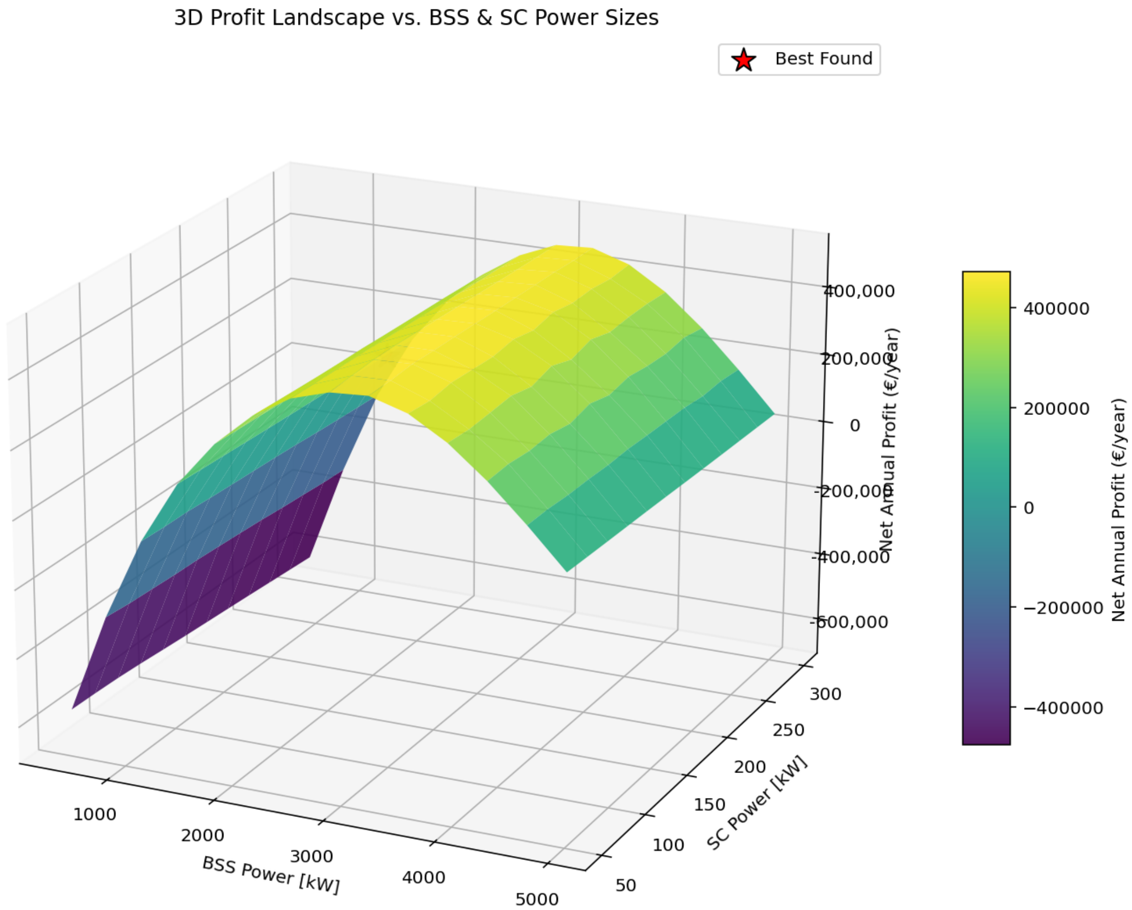

Figure 5.16 3D Profit Landscape vs. BSS & SC Power Sizes (Case B)

Figure 5.17 (Profitability vs. BESS Size for different SC Sizes) shows the HESS performance by illustrating how net annual profit changes with increasing BESS capacity, for several discrete SC power ratings (each represented by a different colored line). A consistent and clear trend is observable across all SC sizes: the net annual profit initially rises sharply as BESS capacity increases from 500kW. This demonstrates the significant value larger BESS capacities bring through increased energy arbitrage opportunities and greater participation in capacity-based markets. The profitability curves for all SC sizes peak for a BESS capacity of approximately 3000kW. Beyond this point, further increases in BESS capacity (e.g., to 5000kW) lead to a marked decline in net annual profit, as the substantial increase in annualized BESS CAPEX outweighs the marginal additional operational profits. A key insight from this plot is the relatively small spread between the lines representing different SC capacities, particularly at the peak BESS performance. For instance, at 3000kW BESS, the net annual profit across SC sizes from 50kW to 300kW varies only modestly (e.g., the heatmap showed a range of ~€455k to ~€475k with B3000kW based on different data). This strongly suggests that while optimal BESS sizing is critical for maximizing net profit, the choice of SC capacity (within the tested range) has a comparatively smaller impact on this specific overall financial metric, though its role in specific services like FR remains vital.

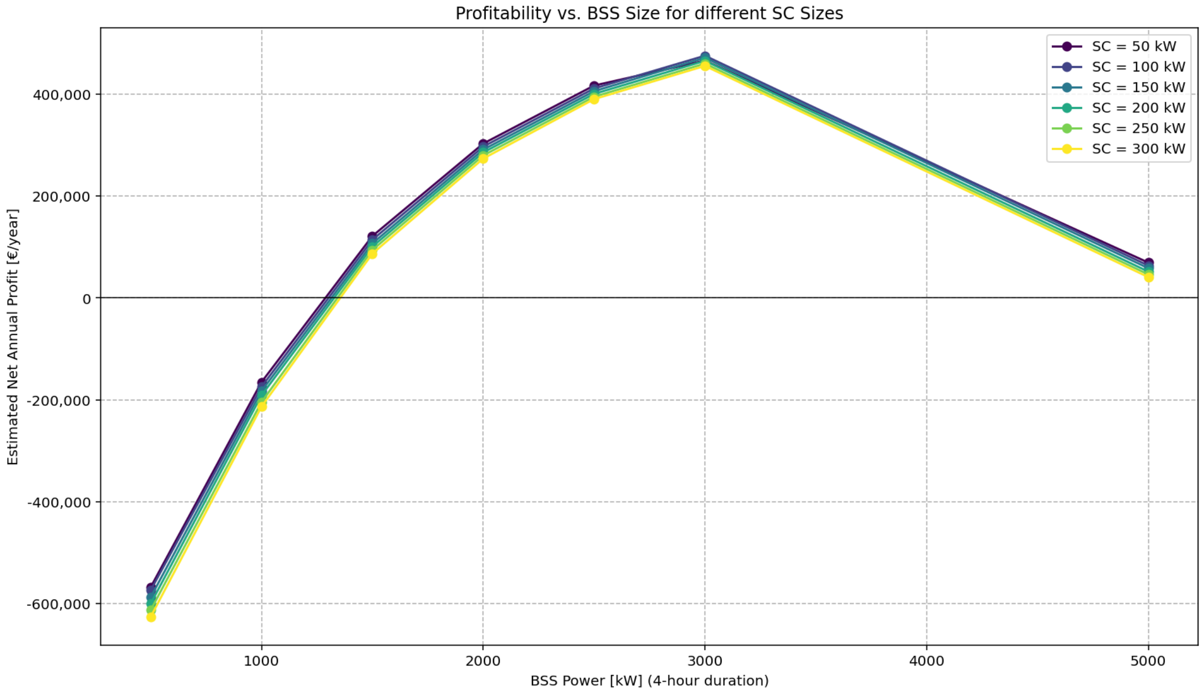

Figure 5.17 Profitability vs. BSS Size for different SC Sizes (Case B)

Figure 5.18 (Net Profit vs. Total Investment Cost) directly relates the estimated net annual profit to the total system CAPEX for each configuration. As total system CAPEX increases (predominantly due to larger BESS installations, shifting points to the right), there is a general trend of increasing net annual profit up to a certain investment level. Beyond this point, typically for the largest BESS sizes (e.g., 5000kW), the net annual profit begins to decline, indicating that the incremental operational benefits no longer justify the substantial increase in capital cost and its associated annualized burden. The configurations form distinct clusters, mainly grouped by BESS size, with variations within each cluster representing different SC capacities. The "efficient frontier" of this plot (the upper-left envelope of points) would highlight configurations offering the best net profit for a given level of investment. The B3000kW_S100kW configuration, with a total CAPEX of approximately €5.96 million, achieves a net annual profit of around €475,544, positioning it as a highly profitable option, though not necessarily the one with the absolute highest profit on this specific chart if other SC sizes paired with 3000kW BESS performed slightly better (as suggested by the heatmap). This plot is instrumental in identifying configurations that balance high profitability with manageable upfront capital outlay, a crucial consideration for investment decisions.

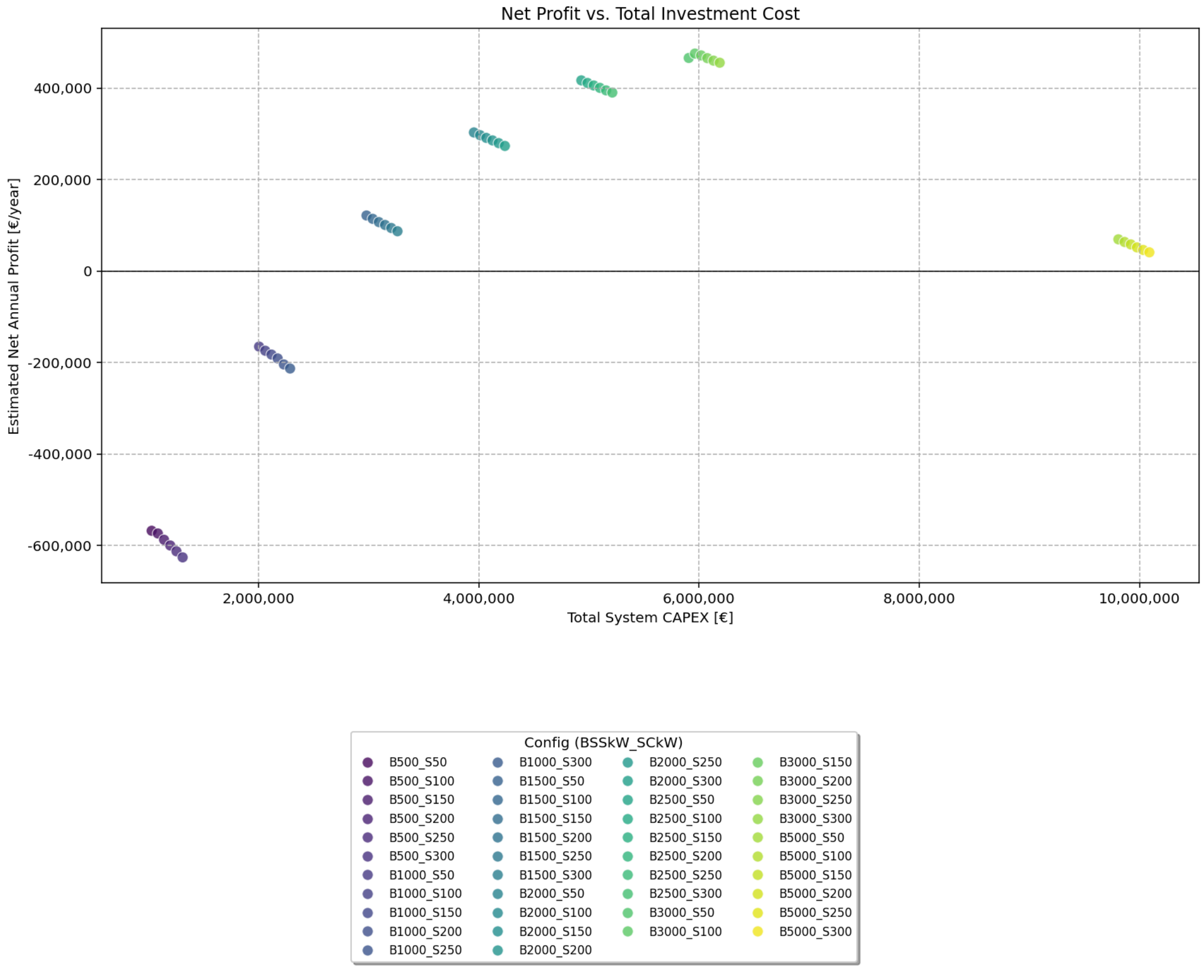

Figure 5.18 Net Profit vs. Total Investment Cost (Case B)

Collectively, these techno-economic plots indicate that while the configuration of a 3000kW BESS paired with a 100kW SC yielded the highest net annual profit (€475,544) in the specific detailed run for this extended case study analysis, the broader sizing exploration suggests optimal BESS capacity is robustly situated in the 2500kW to 3000kW range. Within this range, smaller SC capacities (50kW to 150kW) tend to yield slightly higher overall net annual profits, suggesting that the incremental CAPEX of larger SCs is not always fully compensated by increased operational profit from bulk energy services or the modeled FR revenues alone. The final selection of an "optimal" system should balance this maximized net profit with considerations of capital availability, investor risk appetite, and the strategic value of enhanced ancillary service capabilities offered by larger SCs.

5.5.2.4. KPIs Calculation

The KPIs, annualized from the 84-day extended simulation for the B3000kW_S100kW configuration are presented in Table 5-4.

Table 5-4 Final KPIs for Best Configuration for Case 2 (Best final configuration: BSS=3000, SC=100)

Economic Metrics						
Metric Description	Net Annual Profit	NPV	LCOE	Self Sufficiency %	Simple Payback Period	Profitability Index
Value	1,172,140.53 €	4,070,411.92 €	1.75 €/kWh (assumed)	1713.37%	5.09 years	1.68%
Metric Description	LCOS BESS	BESS Cost per Cycle	Project IRR			
Value	0.29€/kWh	120€	18.02%			
Technical Metrics						
Metric Description	Avg FR Committed Power	Sim Peak Grid Demand	RES Curtailment Factor	ESS Discharge Contribution to Load	DG Contribution to Load	RES Contribution to Load
Value	30 kW	2897.73 kW	1.34%	575.5%	38.03%	1099.85%
Metric Description	BESS ECF	BESS EFC Annual	BESS DOD Mean	SC Energy Buffer Ratio		
Value	44.38%	221.43 Cycles/year	60%	93.36%		
Energy Metrics						
Metric Description	Total Simulated Load	Simulated BESS Throughput	Annual BESS Throughput	Simulated DG Energy	Lifetime Energy Delivered	Lifetime Total BESS Discharge for LCOS
Value	89,022.63 kWh	1,223,033.90 kWh	5,314.37 MWh	33,851.08 kWh	5,802,367.83 kWh	33,382,518.38 kWh
Other Metrics						
Metric Description	BESS Total Lifecycle Cost PV for LCOS	BM Capacity Revenue Contribution	BM Energy Revenue Contribution	DA Revenue Contribution	FR Revenue Contribution	ID Revenue Contribution

Value	9,586,819.35 €	63.57%	4.65%	31%	0.15%	0.64%
Revenue Stack (Simulation)						
Metric Description	BM Capacity Market Revenue	BM Energy Market Revenue	Curtailment Cost	DA Market Revenue	FR Market Revenue	ID Market Revenue
Value	197,191.58€	14,429.48€	13,313.18€	96,160.54€	451.8€	1,973.60€
Metric Description	Net Operational Profit	Diesel Generator Cost	Degradation Cost	Total Gross Market Revenue	Total Operational Cost	
Value	269,752.89€	21,003.88€	6,137.06€	310,207.01€	40,454.12€	
Revenue Stack (Annual)						
Metric Description	Annual BM Capacity Market Revenue	Annual BM Energy Market Revenue	Annual Curtailment Cost	Annual DA Market Revenue	Annual FR Market Revenue	Annual ID Market Revenue
Value	856,844.36€	62,699.54€	57,848.95€	417,840.46€	1,963.18€	8,575.77€
Metric Description	Annual Net Operational Profit	Annual DG Cost	Annual Degradation Cost	Annual Gross Market Revenue	Annual Operational Cost	
Value	1,172,140.53 €	91,266.85€	26,666.98€	1,347,923.31 €	175,782.78€	

The optimized hybrid energy storage configuration (3000 kW BSS, 100 kW SC) demonstrates exceptional financial and environmental performance, achieving an IRR of 18.02% with a 5.09-year payback period. This configuration's robust economics stem from its sophisticated market participation strategy, with 63.57% of revenue derived from balancing market capacity services and 31% from day-ahead market operations, generating €1.35 million in annual gross revenue against €175,783 in operational costs. The system's strong financial metrics (€4.07 million NPV, 1.68% profitability index) indicate this is not merely an environmentally-driven investment but a financially sound one that significantly exceeds typical investment hurdle rates.

The technical performance metrics reveal a highly utilized battery system (221.43 annual equivalent full cycles) with effective depth of discharge management (60% mean DOD) and excellent supercapacitor utilization (93.36% energy buffer ratio). However, the high self-sufficiency (1,713%) and renewable contribution metrics (1,100%) values are due to the system’s high exports to the grid and low local load requirements. These high percentages reflect a system optimized for market participation rather than purely self-consumption, enabling it to capture revenue across multiple market segments while maintaining minimal renewable curtailment (1.34%).

5.5.2.5. Case Comparison

The transition from the Low Horizon Case Study (which simulated 6 carefully selected days) to the more comprehensive Extended Case Study (spanning 84 days across twelve representative weeks) revealed an adjustment in the projected average annualized operational profit. For instance, while the Case A indicated an annualized operational profit around €1.78 million for a 3000kW BESS configuration (paired with a 50kW SC), the Extended Case Study yielded an average of €1,172,141 for a similar 3000kW BESS (paired with a 100kW SC). This highlights the impact of broader temporal representation on performance metrics. Several factors contribute to this observed difference in average annualized operational profit when moving from a shorter, potentially more selective simulation to a longer, more diverse one, even with comparable primary storage (BESS) capacities:

a) Representativeness of Simulated Periods:
- Case A (6 days total): The three 2-day periods selected for this case might have coincidentally captured days with particularly favorable market conditions for profit generation (e.g., high price volatility for arbitrage, good PV generation aligning with high prices, lucrative FR/MB opportunities). When these "good" days are annualized, they project a very high annual profit.
- Case B (84 days total): Simulating one week from each month provides a much broader and likely more realistic sample of operational conditions throughout a year. This will inevitably include:
  - Days with lower price volatility, reducing arbitrage profit.
  - Days with poor PV generation coinciding with low prices (less opportunity to sell surplus).
  - Periods where load patterns are less favorable for storage cycling.
  - Months with generally lower market prices or fewer ancillary service calls.
- The average performance over these 84 diverse days is expected to be more moderate than an average based on a few potentially cherry-picked or simply fortunate days.

b) Impact of SC Size (50kW vs. 100kW) on Overall System Operation:
- Stricter Operational Constraints: Committing more power to FR means more energy needs to be reserved in the SC (and potentially BESS as a backup or for longer FR delivery parts). This might reduce the flexibility of the HESS for other markets (DA, ID, energy part of MB) during FR active hours. If the profit from those other markets is higher than the incremental FR revenue, the net effect could be lower overall profit.
- The SC also has higher degradation costs per cycle if it's larger and cycling similarly. SC degradation cost depends on the SC's CAPEX relative to its lifetime throughput. A larger SC might have a different (not necessarily higher or lower without recalculating) SC degradation cost if power and energy components of its CAPEX scale differently.

c) Annualization of Less Profitable Days:
- The Extended Case will include more "average" or even "bad" days from a profitability perspective. When the operational profit from these less profitable days (or days with

small losses) is annualized, it contributes a smaller positive (or a negative) figure to the overall average.

- The Low Horizon Case might have missed these less favorable day types.

d) Different "Optimal" Strategies for Different Periods:

- The optimization strategy for a cold winter week with low PV and high heating load will be very different from a sunny summer week with high PV and AC load. The profitability of these strategies will vary. The Extended Case captures more of this strategic diversity and its impact on average profit.

In essence, the "average annual operational profit" from the Extended Case Study (€1,172,141) is a more realistic and conservative estimate of the system's true annual earning potential precisely because it's based on a much wider and more diverse set of operating conditions, since it takes into account above mentioned various conditions.

The higher value from Case A (€1,780,172) suggests that the 6 days chosen for that study were, on average, more profitable than a typical day across the entire year. This isn't necessarily "wrong" for those specific 6 days, but it highlights the danger of extrapolating too much from very short simulation periods.

To further underline the influence of selected simulation periods and prevailing market conditions on projected economic outcomes, an additional case study (Case C) was conducted. This scenario also comprised 6 total simulation days but utilized different representative 2-day periods: March 11-12, July 1-2, and November 4-5, 2024. The key sizing evaluation plots for this scenario are presented below.

The Figure 5.19 plot for this scenario again shows multiple configurations achieving operational profits above their annualized capital costs. However, the overall magnitude of operational profits for any given CAPEX level appears generally lower than in the Case Study B (which used 84 days) and potentially different from the Case A. This suggests that the market conditions or PV/load profiles during these March, July, and November days were, on average, less conducive to high operational profit generation compared to the other simulated sets of days.

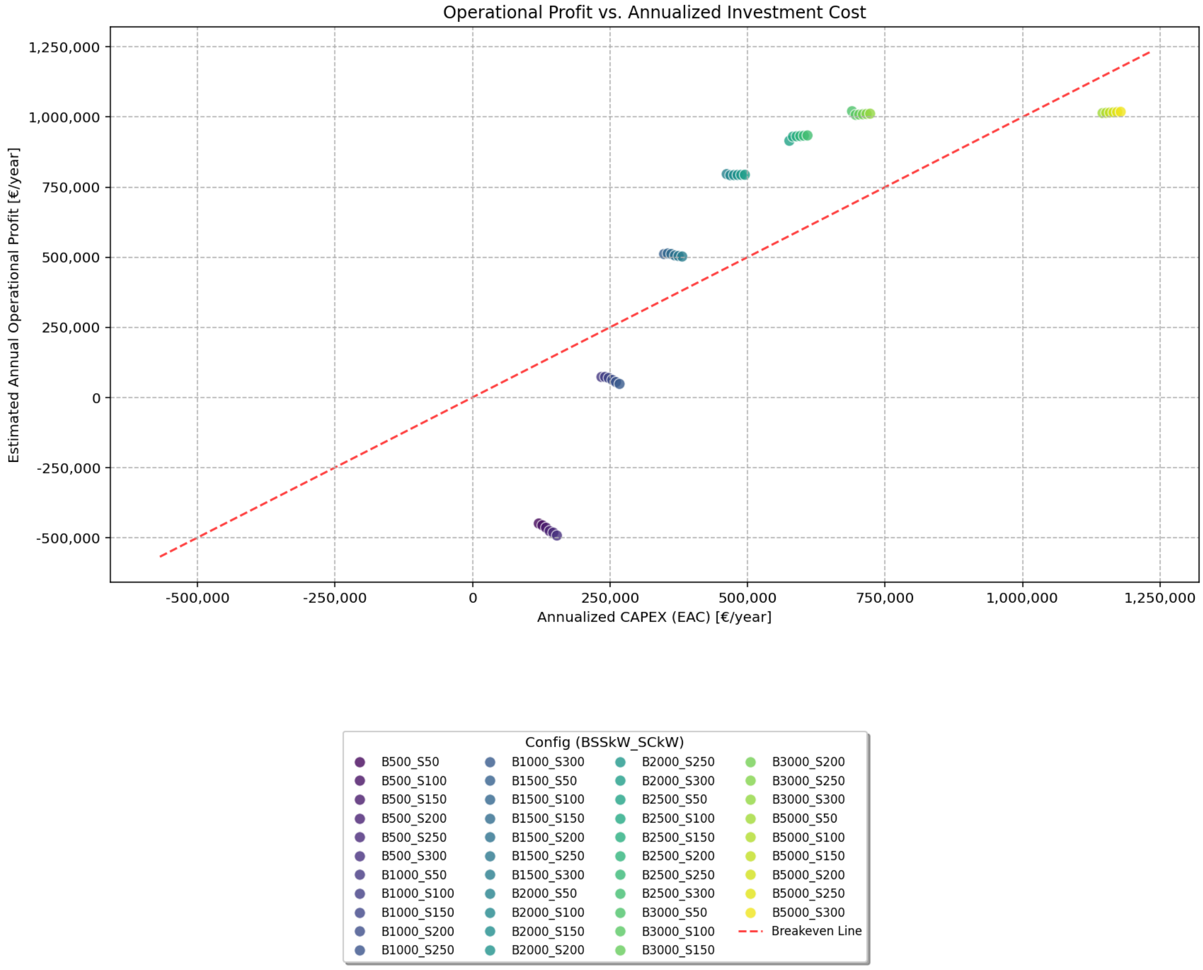

Figure 5.19 Operational Profit vs. Annualized Investment Cost (Case C)

Consequently, the "Net Profit vs. Total Investment Cost" plot for Case C (Figure 5.20) reflects this. While a similar pattern of increasing net profit with CAPEX (up to a point) is observed, the peak net annual profits achieved are visibly lower than those seen in the Extended Case study's sizing plots. Several configurations that were significantly profitable in the Extended Case might now appear closer to the breakeven point or even yield negative net annual profits, highlighting the sensitivity of net returns to the specific days chosen for simulation and annualization. For example, the larger BESS configurations (e.g., 5000 kW) which showed some positive net profit in the previous heatmap, now exhibit more pronounced negative net profits in this scenario.

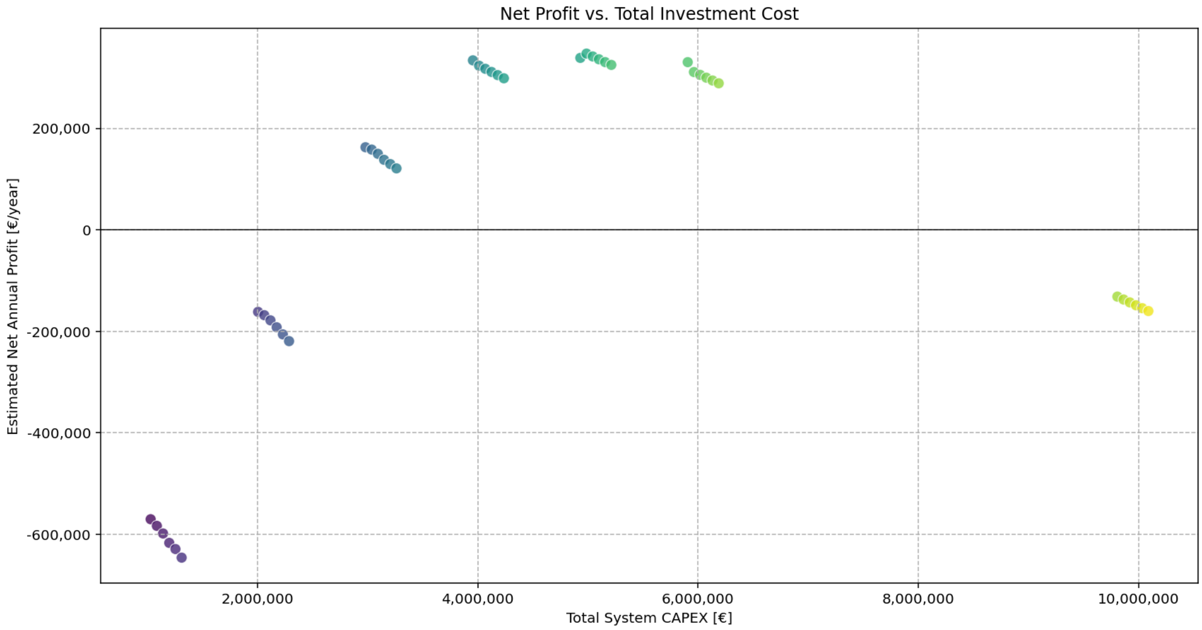

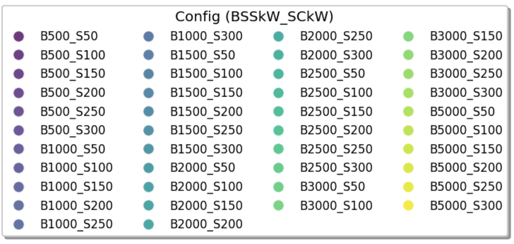

Figure 5.20 Net Profit vs. Total Investment Cost (Case C)

The "Profitability vs. BSS Size for different SC Sizes" plot for Case C (Figure 5.21) reinforces this observation. The characteristic inverted U-shape is present, but the peak of the curves (maximum net annual profit) is lower, occurring around a BESS size of 2500-3000 kW, but with a maximum net annual profit potentially in the range of €400,000-€500,000, compared to peaks closer to €900,000-€1,000,000 in the sizing plots derived from the Extended Case. The decline in profitability for BESS sizes beyond 3000 kW is also steeper. The relative insensitivity to SC size for a given BESS capacity appears to hold, similar to previous observations.

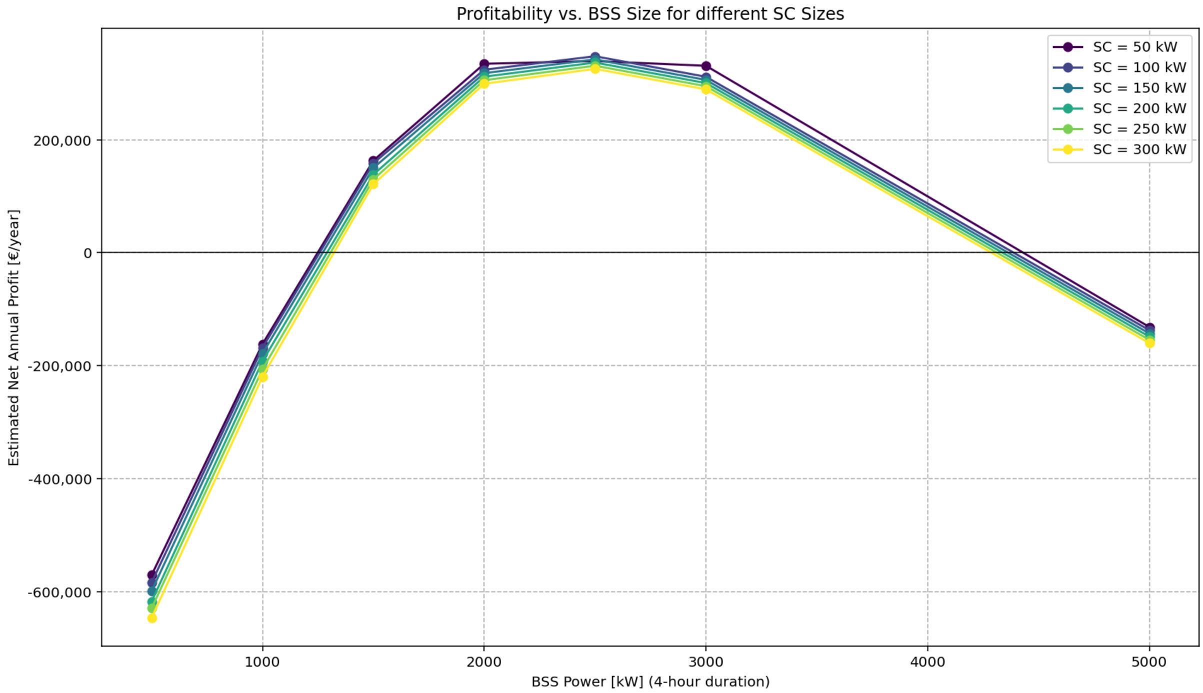

Figure 5.21 Profitability vs. BSS Size for different SC Sizes (Case C)

This brief analysis of Case C, utilizing a different set of 6 representative days, clearly demonstrates the significant influence that the choice of simulation periods—and thereby the specific market prices, PV availability, and load patterns encountered—has on the projected techno-economic outcomes. While the general trends in how BESS and SC sizing affect profitability may remain similar (e.g., an optimal BESS size exists, SC impact on overall net profit is secondary), the absolute values of operational and net profits can vary considerably. This underscores the importance of simulating over a diverse and sufficiently long set of periods, as done in the Extended Case Study B, to derive more robust and reliable annualized performance metrics for investment decision-making and system design. Short, selective simulations can provide useful operational insights but may lead to overly optimistic or pessimistic financial projections if the chosen days are not broadly representative.

5.5.2.6. Discussion and Conclusion

The extended 84-day simulation study provides a more robust validation of the techno-economic and environmental performance of the HESS-integrated microgrid. The B3000kW_S100kW configuration demonstrates substantial profitability, achieving an average net annual profit of approximately €475,544. This result, while positive, is moderated compared to extrapolations from shorter simulation periods, highlighting the importance of comprehensive seasonal analysis. The system continues to show its strength in maximizing PV utilization, actively participating in multiple electricity markets, and significantly contributing to grid decarbonization with a rapid carbon payback time and substantial negative lifecycle emissions.

Comparison with results from sizing plots (which likely used a consistent methodology across all configurations for the 84-day extended run) suggests that while the B3000kW BESS is near the optimal size, a 50kW SC might yield slightly higher net annual profits than a 100kW SC, primarily due to lower upfront CAPEX and potentially lower degradation costs unless FR revenues specifically favor the larger SC significantly. The optimal SC size is thus highly sensitive to its specific service revenue streams and its impact on overall system costs.

The findings emphasize that while a specific configuration can be identified as "best" based on a single metric under baseline assumptions, a range of HESS sizes can deliver strong performance. The choice in a real-world scenario should weigh the projected net profit against upfront investment, operational complexity, and the specific values attributed to different ancillary services. The current modeling framework provides a powerful tool for such decision-making, and further refinement of KPI calculations (EFC, DG capacity factor.)

6. CASE STUDY - TUNISIA

6.1. INTRODUCTION

The electricity grid in Tunisia is well established and extends across the entire country, despite the limited availability of primary energy resources. Electricity generation in Tunisia still largely relies on fuel and gas turbines. However, the government is making significant efforts to decarbonize the grid by promoting renewable energy sources.

As a demonstration site, an industrial facility in Tunisia has been selected. This site has already installed a PV power plant on-site to maximize self-consumption. To provide context for this type of system in Tunisia, here is a brief overview: industrial and tertiary consumers connected to the medium-voltage (MV) grid are allowed to install PV plants without any capacity limit. However, they are not permitted to inject more than 30% of their production into the grid. Moreover, the feed-in tariff for the energy sold back to the grid is only 20% of the purchase price from the grid. This makes local energy storage a much more attractive option, as storing excess energy for later use can generate significantly more value than feeding it into the grid.

6.2. PURPOSE OF THE CASE STUDY

The African case study highlights how a HESS specifically combining a VRFB with a SC, can optimize energy costs and enhance system performance. The VRFB provides long-duration energy storage, while the supercapacitor ensures fast response to power fluctuations. By analysing system sizing, operational behaviour, and techno-economic outcomes, the case study aims to:

- Quantify the reduction in grid dependence and energy costs.
- Assess the role of the supercapacitor in mitigating peak demand.
- Demonstrate the technical feasibility and economic viability of integrating HESS.
- Deliver insights and recommendations that could inform and strengthen Tunisia's regulatory framework, once energy storage is permitted.

Quantify the reduction in grid dependence and energy costs

By integrating a HESS combining a VRFB and a supercapacitor into an industrial PV system, the site significantly reduces its reliance on grid electricity. Since net billing in Tunisia allows only up to 30% of the PV generation to be sold back, and at only 20% of the purchase tariff, storing this surplus energy for later use becomes more profitable than feeding it into the grid. This leads to a measurable decrease in energy imports from the utility and a reduction in overall energy costs, especially during peak tariff hours. Simulations and operational data can quantify this impact by comparing the system's grid consumption and cost profile before and after HESS integration.

Assess the role of the supercapacitor in mitigating peak demand

Supercapacitors, due to their high-power density and fast response, are ideal for handling short-term, high-power demands, such as equipment start-ups or transient loads. In this use case, the supercapacitor smooths out demand spikes that would otherwise lead to increased peak charges or draw expensive electricity from the grid. By mitigating these peaks, the supercapacitor extends battery life (by offloading sudden power bursts from the VRFB) and enhances the site's load profile — reducing both operational stress on the grid and associated peak demand charges, where applicable

Evaluate the technical feasibility and economic viability of integrating HESS

The Tunisian industrial demo case provides a valuable opportunity to evaluate both the technical feasibility and the economic viability of integrating a HESS. Technically, the combination of a VRFB and a supercapacitor delivers a robust solution that offers long-duration energy storage alongside fast power response well-suited to the dynamic load profiles of industrial facilities. Economically, the ability to store surplus PV energy instead of selling it back at a low feed-in rate and to discharge during peak consumption periods translates into substantial energy cost savings and a higher return on investment. Furthermore, the long cycle life and modular nature of VRFBs contribute to a favourable total cost of ownership compared to conventional lithium-ion technologies.

Deliver insights and recommendations that could inform and strengthen Tunisia's regulatory framework, once energy storage is permitted

This case study generates concrete data and insights that can inform future energy policy and storage regulation in Tunisia. It highlights the limitations of the current net billing scheme in incentivizing renewable adoption and the economic benefits that storage could unlock for industries aiming to maximize self-consumption. The results could support proposals for regulatory reforms, such as allowing behind-the-meter storage, redefining self-consumption incentives, and enabling participation of storage assets in grid services or demand response. These findings could be valuable in shaping a storage-inclusive legal framework aligned with Tunisia's national energy transition objectives.

6.3. Case study and data description

Currently, the industrial facility has a 1,200 kWp rooftop PV system installed. In 2024, the total energy demand reached 4,707 MWh, while the PV system generated 1,886 MWh, covering approximately 40.1% of the total energy needs. However, due to consumption patterns and grid constraints, only 28% of the site's energy demand was directly supplied by the PV system, with the remainder drawn from the grid. Over the year, 70% of the PV generation was self-consumed on-site, while the remaining 30% was exported to the grid.

As shown in Figure 6.1, the self-consumption profile closely follows the trend of the site's electricity demand from the grid. The energy produced by the on-site PV system over the year forms a distinct seasonal curve, with lower generation during the winter months (beginning and end of the year) and a pronounced peak during the summer months, when solar irradiance is highest.

August experienced the highest demand of the year, with 643,621 kW, of which 72.1% was imported from the grid. During this month, 90.8% of the energy generated by the PV plant was self-consumed, resulting in a surplus of 9.2%.

May recorded the lowest consumption of the year, with a demand of 284,470 kW. During this month, 37.1% of the energy consumed was supplied by the PV plant, which accounted for 49.1% of the energy produced on-site, leaving a surplus of 50.9% that was injected into the grid. This month saw the highest percentage of energy generated by the PV plant used for self-consumption, as well as the highest surplus of the year at 50.9%. Notably, May was the only month in which the PV plant generated more energy than was consumed from the grid.

July had the highest generation from the PV plant, at 229,143 kW, and the second highest demand of the year. The PV plant provided 33.9% of the total energy demand, with 80.4% of the generated energy being used for self-consumption and the remaining 22.8% being injected into the grid.

November had the lowest generation from the PV plant, with 71.4% of the generated energy used for self-consumption and 28.6% injected into the grid. During this month, the PV plant provided 22.5% of the energy demand.

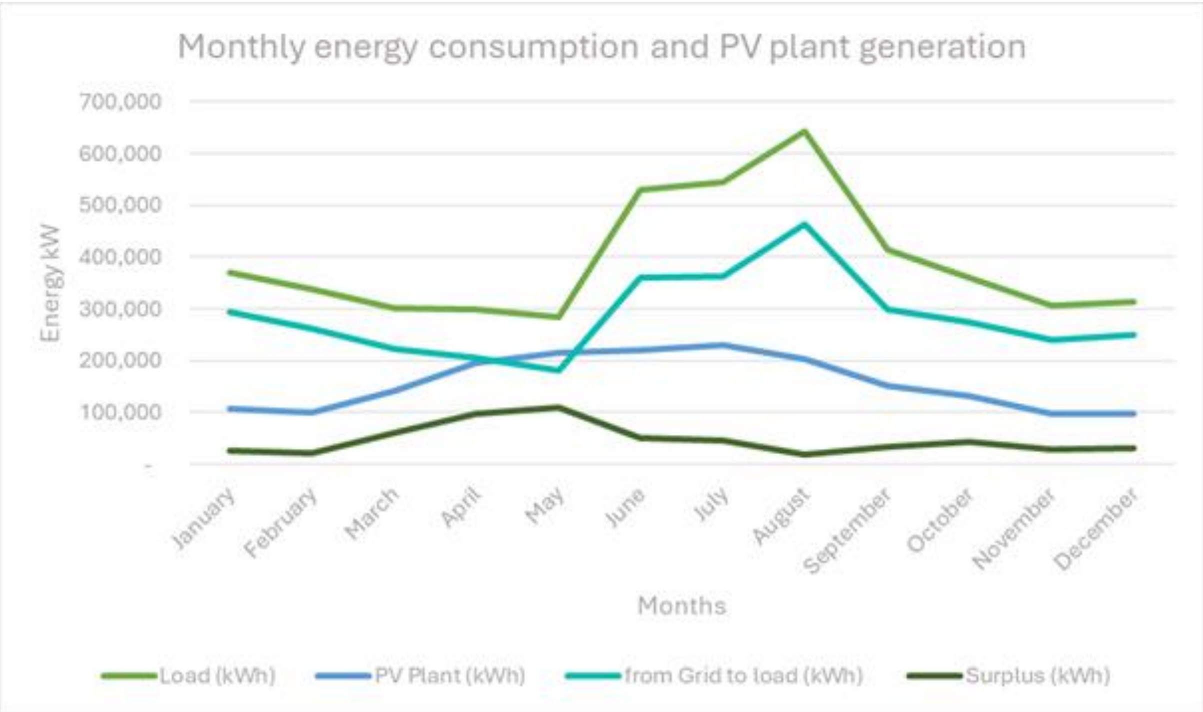

Figure 6.1 Monthly energy consumption and PV plant generation

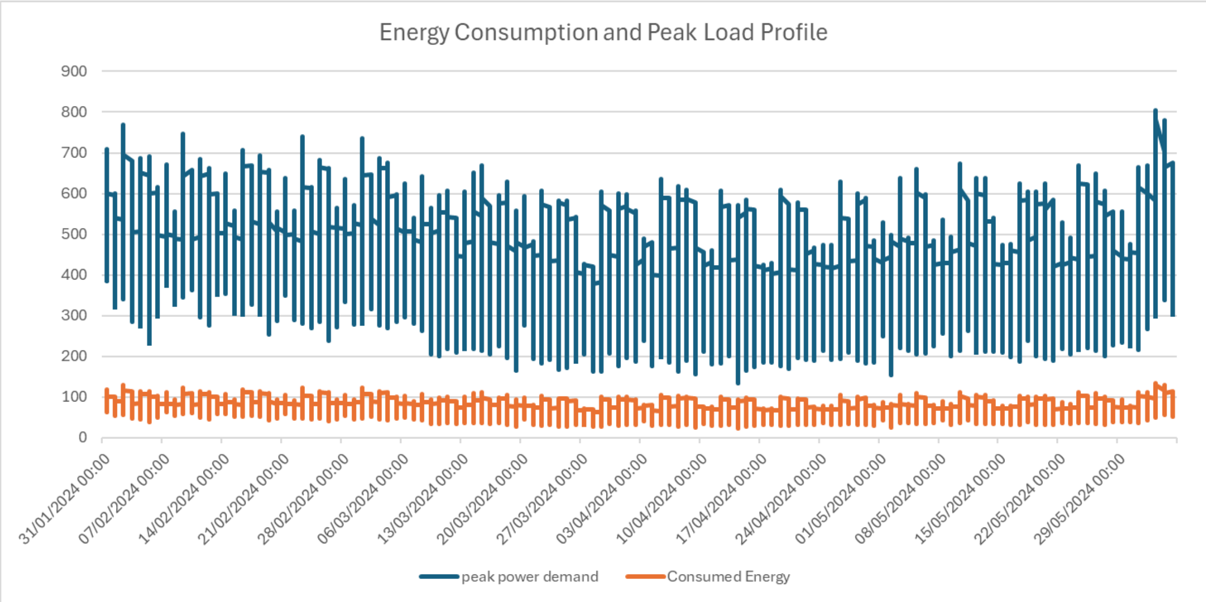

Figure 6.2 Energy consumption and peak load profile

Figure 6.2 presents the peak power demand, and the energy consumption recorded at 10-minute intervals. It highlights that peak loads are significantly high, even when overall energy consumption remains relatively moderate.

During summer, this is from June to August for the purpose of this regime, the day is divided into a four-shift regime, with the cost of importing energy from the grid fluctuating based on the time of day. The most expensive period for energy import during the day is between 13:30 and 19:00 as shown in Table 6-1. During Winter, this is from September to May for the purpose of this regime, the day is divided into a three-shift regime. The most expensive period for energy import during the day is between 7hr to 18hr as displayed in Table 6-1. In contrast, the cost of injecting energy into the grid remains constant throughout the day and the year.

Table 6-1 Four-shift regime, cost of energy purchase and selling

Shift	Summer Schedule	Winter Schedule	Energy Purchase Price (€/kWh)	Energy Selling Price (€/kWh)
Night	22hr – 8hr	21hr-7hr	0.088	0.024
Morning peak	8hr – 13:30hr	-	0.066	0.024
Day	13:30hr – 19hr	7hr to 18hr	0.122	0.024
Evening peak	19hr – 22hr	18hr to 21hr	0.11	0.024

Figure 6.3 and Figure 6.4 illustrate the total energy consumption, PV generation, grid imports, and surplus energy exported to the grid during summer and winter, respectively, across various times of the day, for both the four-shift and three-shift regimes outlined in Table 6-1. The figures show that the highest energy consumption at the demo site occurs during night hours, when the PV plant is inactive, requiring full reliance on grid imports. In the evening peak,

energy consumption is at its lowest, and again, the site depends entirely on the grid due to the absence of solar generation. In contrast, during summer mornings, the PV plant produces more energy than the site consumes, resulting in reduced grid imports and excess energy being fed back into the grid. This trend continues into the midday hours, when electricity prices are highest, where PV generation surpasses grid imports and contributes to further surplus injections. Conversely, in winter, the site's energy consumption is lower than the energy produced by the PV Plant during 'day hours' hours. This results in reduced grid imports and a surplus of energy being fed back into the grid.

Annual electricity costs include both imported energy and revenue from surplus energy fed into the grid. Throughout the year, a total of €331,244 was spent on importing electricity, while €13,594 was earned from selling surplus energy back to the grid. These values reflect seasonal and time-of-day variations between summer and winter.

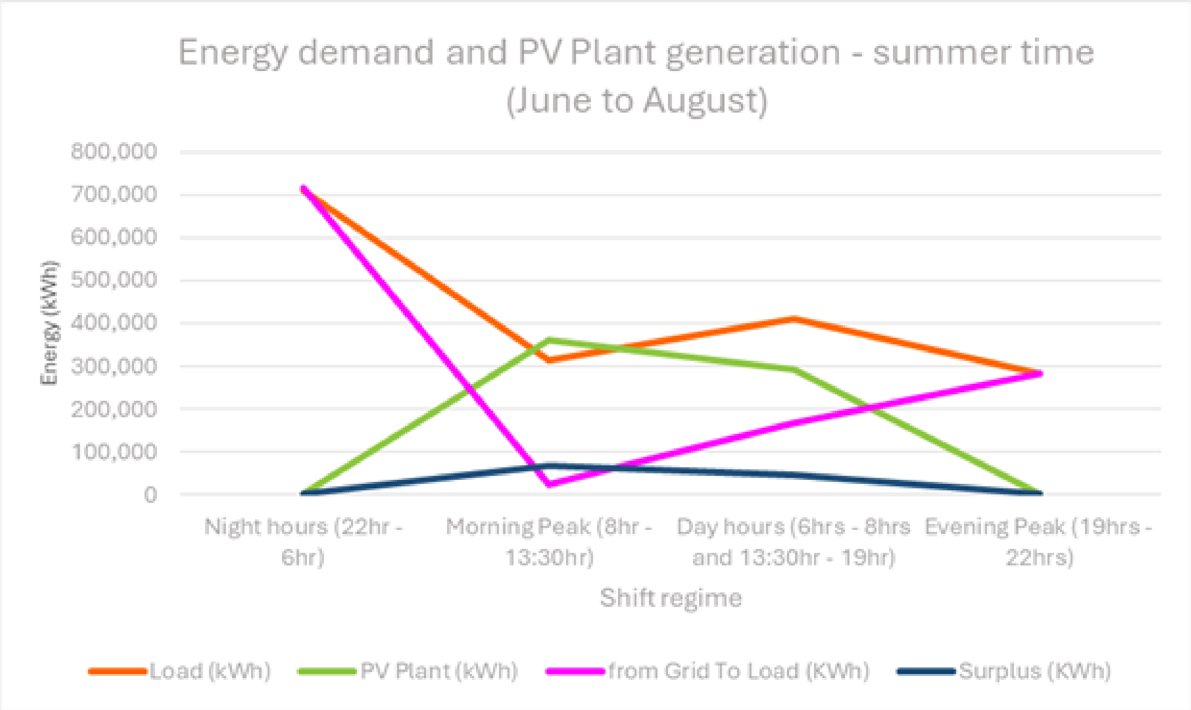

Figure 6.3 Energy demand and PV plant generation during summer-time

During the evening peak, the site's energy consumption is at its lowest for the day, and it relies entirely on the grid as the PV Plant does not generate any energy during this period. On the other hand, overall, during the three months of summer, in the morning peak hours, the Client's energy consumption is lower than the energy produced by the PV Plant, resulting in reduced grid imports during this period, leading to a surplus of energy being injected back into the grid. Overall, during the 'day hours, when the energy from the grid is the most costly of the day, the PV Plant generates more energy than is imported from the grid. Additionally, there is a surplus of energy during this period.

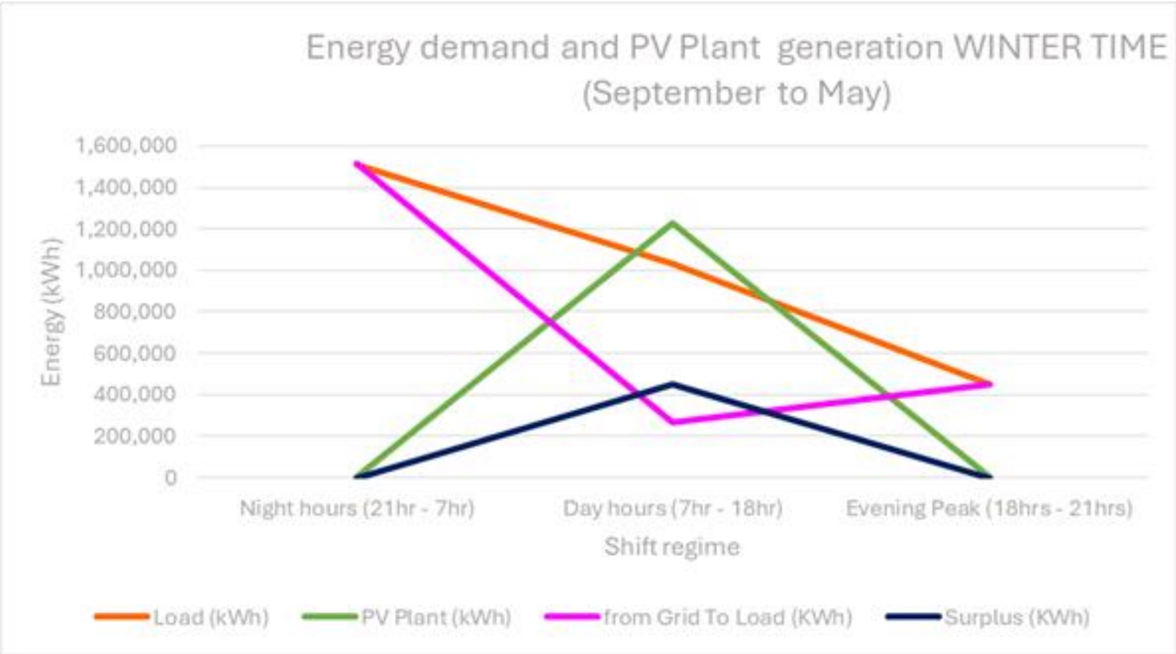

Figure 6.4 Energy demand and PV plant generation during winter-time

6.4. METHODOLOGY

6.4.1. Data Collection and Scenario Definition

To model this hybrid energy system, the software HOMER was employed. Several key inputs were provided to ensure an accurate and comprehensive simulation:

- High-resolution solar resource data (GHI) with a 1-minute time step
- Detailed electricity pricing structure for grid-supplied energy
- Site-specific electricity consumption profiles
- System configuration, including component capacities and interconnections
- Modeling parameters for the supercapacitor within the HOMER environment
- Modeling of the Vanadium Redox Flow Battery (VRFB) in HOMER
- Complete financial data for each system component (CAPEX, OPEX, lifetime, etc.)

The general system layout is illustrated in Figure 6.5.

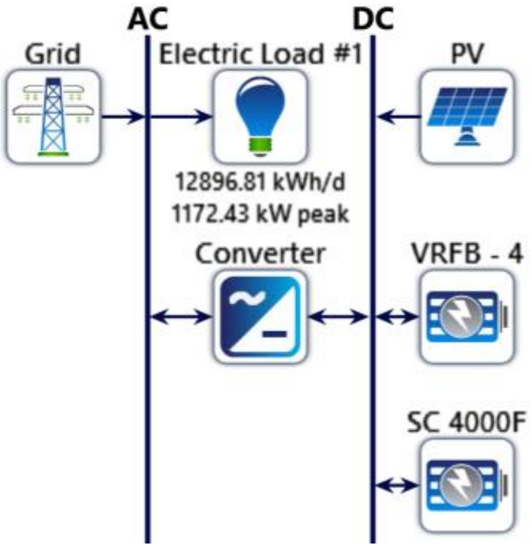

Figure 6.5 General system layout.

6.4.2. HESS components models

The modeling of the two selected storage technologies was based on the idealized models available in HOMER, which were then adapted to align with the technical specifications provided in the datasheets for both storage systems. The specifications for the RFB have already been summarized in Table 4-1 of Section 4.3.2; and the specifications for the SC are summarized in Table 3- in Section 3.4.2. For both storage technologies, Homer requested to input the parameters summarized in Table 6-2.

Table 6-2 Calculated Technical Parameters for SC submodule and VRFB Input into HOMER

Parameter	SC Values	VRFB Values
Nominal Voltage (V)	27	1000
Round Trip Efficiency (%)	80	67
Nominal Capacity (Ah)	0.60	1
Max charge current (A)	370	0.25
Max discharge current (A)	370	0.25

6.4.3. Operational constraints

The electricity price in Tunisia for systems connected to the grid via MV is given in Table 6-3. Since the price of electricity sold back to the grid is fixed and very low, discharging the battery to the grid was prohibited. Additionally, charging from the grid was only permitted during periods of lowest electricity cost, typically at night

Table 6-3 Time-of-Use Electricity Tariffs and Sellback Prices for MV Grid-Connected Systems in Tunisia

<table>
<tr><th>Period</th><th colspan="2">Time of use</th><th>Electricity Price (€/ kWh)</th><th>Sellback Price (€/ kWh)</th></tr>
<tr><td rowspan="4">Festival period
June to august</td><td>Day</td><td>06:30 AM→ 08:30 AM
&
01:30 PM → 07: 00 PM</td><td>0.088</td><td rowspan="7">0.024</td></tr>
<tr><td>Morning Peak</td><td>08:30 AM → 01:30 PM</td><td>0.122</td></tr>
<tr><td>Peak night</td><td>07:00 PM → 10:00 PM</td><td>0.110</td></tr>
<tr><td>Night</td><td>10:00 PM → 06:30 AM</td><td>0.066</td></tr>
<tr><td rowspan="3">Winter period:
September to May</td><td>Day</td><td>07:00 PM → 09:00 PM</td><td>0.088</td></tr>
<tr><td>Peak night</td><td>06:00 PM → 09:00 PM</td><td>0.110</td></tr>
<tr><td>Night</td><td>09:00 PM→ 07:00 PM</td><td>0.066</td></tr>
</table>

6.4.4. Objective Function

To identify the most cost-effective system architecture, HOMER performs an extensive sensitivity analysis by evaluating all potential system configurations—with and without the integration of the two storage technologies (VRFB and SC). The analysis focuses on minimizing the LCOE under varying economic conditions. Specifically, the model accounts for changes in grid electricity prices and investment costs in VRFB systems by applying a capital cost multiplier ranging from 0.1 to 1. Table 6-4 summarizes the sensitivity values considered in the modeling process, showing combinations of electricity prices (in €/kWh) and VRFB capital cost multipliers. This approach provides a robust comparison of how different cost scenarios affect the economic viability of HESS configurations in the Tunisian context.

Table 6-4 Sensitivity considered for modeling

Power price (€/kWh)	VRFB capital cost multiplier
0.088	0.5
0.1	0.75
0.15	1
0.2	0.1

6.4.5. Two-Tier Optimization Approach

HOMER conducts a comprehensive optimization to determine the most technically robust and cost-efficient energy system by simulating thousands of potential configurations. In this study, the tool is employed to assess various combinations that include PV systems, VRFB storage, SC units, and grid connectivity. The platform systematically examines a broad spectrum of component capacities and control approaches, evaluating each scenario in terms of energy distribution, operational cost, and system dependability. Every configuration is simulated over a full year using a high-resolution load profile with one-minute intervals, ensuring precise modeling of the interactions between energy generation, consumption, and storage.

The primary objective of the modeling is to maximize the utilization of on-site solar production, thereby improving self-consumption, while simultaneously reducing the LCOE. The optimization process considers a range of variables, including investment and maintenance costs, electricity tariffs, system inefficiencies, and the performance characteristics of storage technologies. The simulation ultimately identifies the system layout that offers the most favorable compromise between economic return and operational efficiency across the system's lifecycle.

6.4.6. Techno-Economic Modeling

The modeling approach with HOMER allowed for a detailed analysis of different energy generation, storage, and load configurations. The goal was to find the most cost-effective system setup while ensuring strong technical performance. For this case, the simulation was based on the following key inputs:

- A high-resolution load profile with a one-minute time step.
- Technical and financial data related to the SC and VRFB.
- The applicable grid electricity pricing structure.

The primary objective of the optimization process is to identify the most cost-effective and technically efficient system configuration that maximizes self-consumption of locally generated solar energy while minimizing the LCOE by

- Minimize the **levelized cost of energy (LCOE)**: This is a key financial metric that represents the cost per unit of electricity over the lifespan of the system. The goal is to find a system configuration that provides the lowest LCOE while meeting energy demand.
- Optimize the **self-consumption**: Maximize the amount of solar energy used on-site (i.e., without importing from the grid), which can reduce reliance on the grid and lower energy costs.
- Minimize **curtailment**: Ensure that excess solar energy is stored in the VRFB rather than wasted, which is particularly important in systems with high renewable generation potential.

To run the optimization effectively, several key parameters were defined:

- **Capital costs:** These include the upfront investment required for the installation of the PV system, the VRFB, and the grid connection infrastructure, along with their associated long-term maintenance costs.
- **Operating costs:** This covers regular maintenance and operational expenses for both the PV system and the VRFB, as well as any costs linked to system control and energy management.
- **Energy pricing:** The model incorporates the cost of purchasing electricity from the grid and, where applicable, potential revenues from exporting surplus energy back to the grid.
- **Discount rate:** This financial parameter is used to calculate the present value of future costs and revenues, allowing for a more accurate assessment of the project's long-term economic viability.

The simulation provided several important outputs that offer insights into both the technical performance and economic viability of the system:

- **Cost Optimization:** The model identifies the most cost-effective system configuration over the project's lifetime by accounting for CAPEX, OPEX, and applicable energy tariffs.
- **ROI:** HOMER calculates key financial indicators such as the payback period and ROI, based on reduced grid consumption, energy cost savings, and potential revenues from grid exports (if applicable).

6.5. RESULTS

Three simulations were conducted:

- Two separate simulations were run, each focusing on one of the technologies independently.
- A global simulation was performed, integrating all available technologies to assess their combined performance.

6.5.1. Battery Only Results

This section presents the results of two distinct system simulations, each modeling the performance of a different energy storage technology in conjunction with PV generation and grid integration. Two configurations are considered as shown in Figure 6.6

Left Configuration: This setup includes a VRFB, PV panels, and a grid connection. The VRFB is modeled as the primary storage component, aimed at providing long-duration energy storage and enhancing self-consumption of solar energy. The system also includes a converter for managing the energy flow between AC (grid/load) and DC (PV/VRFB) components.

Right Configuration: This simulation features a SC instead of a battery, along with PV and grid elements. The SC (specifically SC 4000F) is used to handle short bursts of high-power demand and to provide fast-response storage capability. Like the VRFB configuration, this system includes a converter to manage the AC/DC energy conversion.

Both simulations are based on the same electric load profile of 12,896.81 kWh/day with a peak demand of 1,172.43 kW, ensuring comparability between configurations. The goal is to understand how each type of storage technology performs under identical energy demand and solar generation conditions.

VRFB, PV, and grid integration	SC, PV, and grid integration
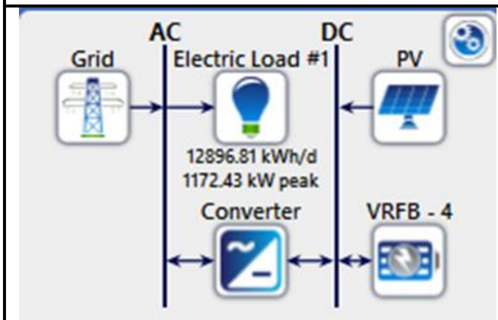	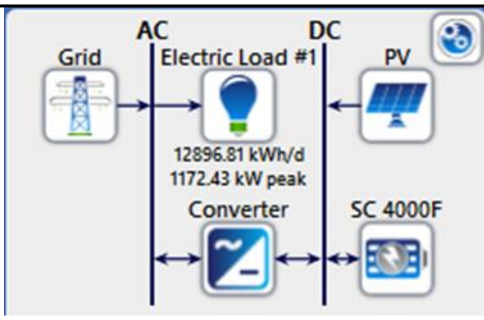

Figure 6.6 VRFB and SC system configurations with PV and grid.

Figure 6.7 compares two system configurations, PV/Grid and PV/VRFB/Grid, by evaluating their Net Present Cost (NPC) across a range of electricity prices and VRFB capital cost multipliers. The orange-shaded areas represent conditions under which a PV/Grid setup (without storage) is more cost-effective, while the grey-shaded areas indicate conditions were adding a VRFB becomes economically preferable. At low electricity prices or when VRFB costs are high, PV/Grid remains the optimal choice due to its simplicity and lower upfront cost. However, as either electricity prices increase or VRFB capital costs decrease (i.e., the capital cost multiplier drops), the model shifts in favor of PV/VRFB/Grid systems. In the scenario highlighted at €0.09/kWh and a VRFB cost multiplier of 1.00, the NPC of the PV/Grid system is slightly lower (€7,588,426) than that of the PV/VRFB/Grid system (€7,596,992), suggesting that storage is close to economic viability. This narrowing cost gap indicates that VRFB-based storage may become competitive with minor shifts in market or technology costs.

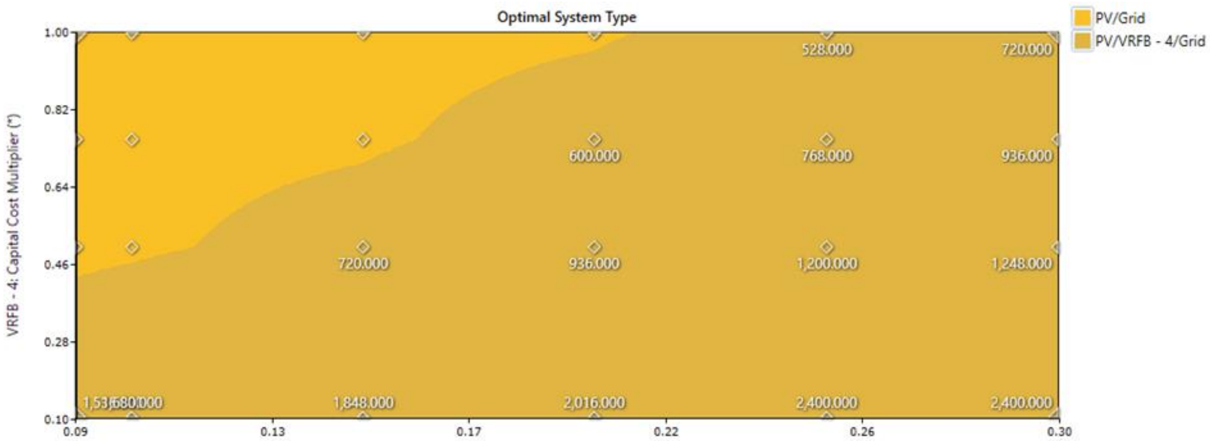

Figure 6.7 Optimal system type by electricity price and VRFB cost multiplier.

Figure 6.8 presents a cumulative discounted cash flow comparison over a 25-year period for two energy system configurations: a base case consisting of PV and grid connection, and a winner case that integrates a VRFB storage system alongside PV and grid. While the base case benefits from a lower initial capital investment (€600,953), it incurs higher operational and maintenance costs annually (€285,499), resulting in slower long-term savings. In contrast, the system with VRFB storage, despite its higher upfront cost (€670,109), achieves greater economic efficiency over time due to lower O&M expenses (€278,578 per year). This leads to a convergence and eventual overtaking of the base case in terms of total cash flow around year 15. Although the base case shows a slightly lower LCOE (€0.0577/kWh compared to €0.0607/kWh for the storage system), the figure demonstrates that LCOE alone does not fully capture the economic benefits of storage. The storage-enhanced system proves to be the more financially viable option over the project's lifetime, validating its selection as the lowest-cost system under the modeled assumptions.

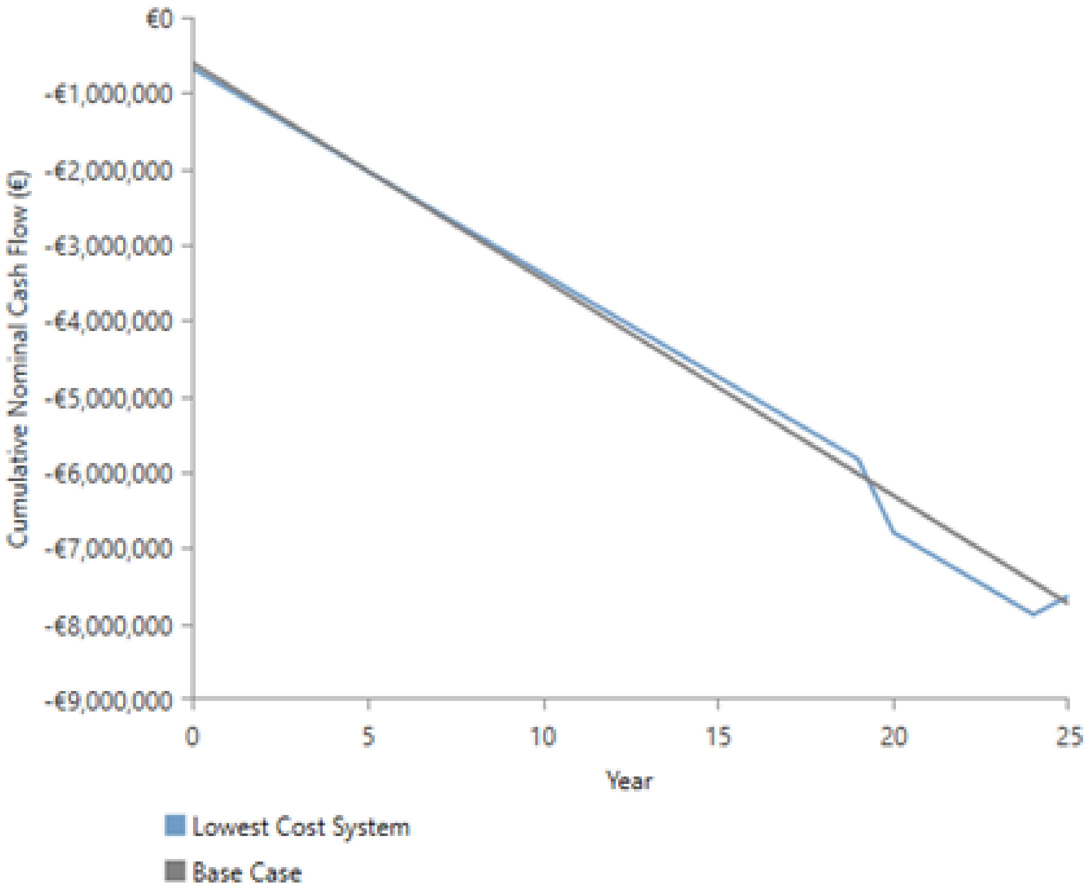

Figure 6.8 Cumulative cash flow comparison of base case and VRFB storage system over 25 years.

Table 6-5 (the summary table below) provides a simplified comparison between the Base Case Architecture (with SC) and the Winning System Architecture (without SC).

Table 6-5 Identified optimized results

Base case Architecture	Winning system Architecture

Unlimited Grid PV Plant: 1200 kWp Supercapacitor: 288 string each string contain one module in series Converter: 971 kW	Unlimited Grid PV Plant: 1200 kWp No SC, NO VRFB Converter: 953 kW

Table 6-6 presents the detailed results of the optimization simulations, comparing two system configurations: one incorporating a supercapacitor (SC 4000F) and one without any storage. Both systems include a 1,200 kWp PV plant and an unlimited grid connection. The SC-based system uses 288 supercapacitor strings and a 971-kW converter, while the system without storage relies on a slightly smaller 953 kW converter. The financial performance is similar in both cases, with the SC configuration showing a NPC of €7.75 million and a LCOE of €0.0589/kWh, while the storage-free setup achieves a slightly better NPC of €7.74 million and an LCOE of €0.0588/kWh. It confirms that the system without SC is selected as the optimal configuration, due to its lower capital and operational costs and marginally better financial performance.

Table 6-6 Identified optimized results

Architecture				Cost		
PV (kW)	**SC 4000F**	**Grid (kW)**	**Converter (kW)**	**NPC (€)**	**LCOE (€/kWh)**	**Operating cost (€/yr)**
1,200		999,999	953	€7.74M	€0.0588	€285,499
1,200	288	999,999	971	€7.75M	€0.0589	€285,440

Figure 6.9 illustrates the cumulative discounted cash flow over a 25-year project period for both configurations. The graph shows that although both systems follow a similar financial trajectory, the non-storage system achieves slightly better long-term economic performance, confirming its status as the lowest-cost solution. This analysis confirms that, under current electricity prices and cost assumptions, integrating SC does not offer a financial advantage. Due to the high initial investment and lack of performance benefits, no SC-based configuration demonstrated improved profitability in the simulation results.

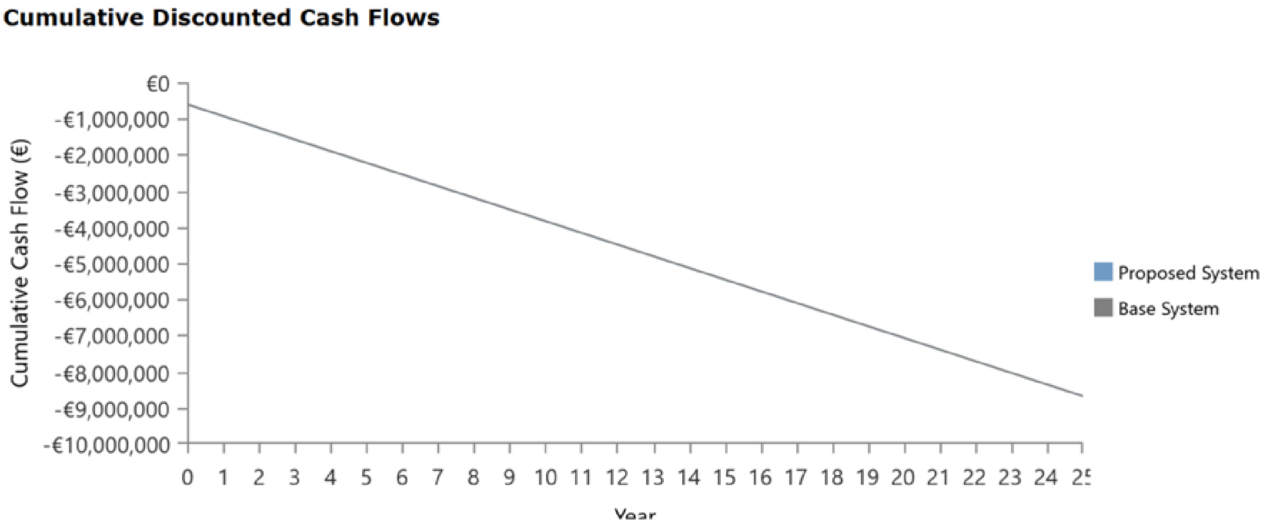

Figure 6.9 Cashflow over time – Base Case and winner case

6.5.2. HESS Results

Simulation Overview and Feasibility Results

A thousand simulations were run to determine the optimal configuration of a HESS and a PV plant connected to the grid. The results of the calculation report are summarized as follows: A total of 6,392 solutions were simulated, of which 5,407 were feasible and 985 were infeasible due to not meeting the minimum renewable fraction requirement. Additionally, 1,112 simulations were excluded: 656 due to the absence of a converter, and 312 due to the presence of an unnecessary converter

VRFB Sensitivity Analysis

Using HOMER, the study examined the impact of varying the VRFB storage capacity from 522 kWh to 2,568 kWh. The simulations showed a strong correlation between increased storage and energy throughput:

- Annual throughput increased from 116,893 kWh/year to 386,152 kWh/year.
- Meanwhile, the LCOE rose only slightly, from €0.060 to €0.0639/kWh, demonstrating cost stability even with increased storage capacity.

At the low end (522 kWh VRFB), the system required a converter size of 1,393 kW, which is substantially higher than the 1,039 kW used in other configurations. This implies that even small-capacity storage systems may require oversized converters to handle power fluctuations and match dynamic load profiles. On the other hand, increasing the VRFB to 2,400 kWh with a corresponding converter of 1,759 kW enabled greater energy capture and efficient dispatch, enhancing overall system flexibility and performance.

Table 6-7 presents selected simulation results across various combinations of electricity prices and VRFB capital cost multipliers. Each row highlights a different system architecture and the resulting LCOE and energy sold to the grid. These results show that while VRFB capacity and converter size vary, LCOE remains relatively stable and decreases as storage becomes more cost-effective, or grid prices rise.

Table 6-7 Sensitivity Results for Grid + PV + VRFB Systems

Sensitivity/ Power Price ($/kWh)	Sensitivity/ VRFB - 4 Capital Cost Multiplier (*)	Architecture /PV (kW)	Architecture /VRFB - 4 (#)	Architecture /Converter (kW)	LCOE	Grid/Energy Sold (kWh)
0.088	0.1	1200	1536	989	0.06190012	226140.9
0.088	0.5	1200	288	989	0.05985005	479447.2
0.088	0.75	1200	144	1008	0.05947229	516019.6
0.088	1	1200	24	1264	0.05897392	547069.1
0.1	0.1	1200	1680	909	0.06342722	204605.8
0.1	0.5	1200	288	989	0.06118968	479447.2
0.1	0.75	1200	144	1209	0.06083556	516026
0.1	1	1200	144	1008	0.06095817	516019.6
0.15	0.1	1200	1848	1080	0.0689514	181742.7
0.15	0.5	1200	720	1026	0.0680134	376007.8
0.15	0.75	1200	288	989	0.06702133	479447.2
0.15	1	1200	144	1209	0.0666339	516026
0.2	0.1	1200	2016	1027	0.07450044	159486.7
0.2	0.5	1200	936	934	0.07397981	330561.1
0.2	0.75	1200	600	953	0.07360144	403530.4
0.2	1	1200	288	989	0.07285299	479447.2
0.25	0.1	1200	2400	586	0.08106713	79416.36
0.25	0.5	1200	1200	1002	0.08001869	281184.7
0.25	0.75	1200	768	1707	0.0795461	365460.2
0.25	1	1200	528	1099	0.07927597	420702.3
0.3	0.1	1200	2400	586	0.086156	79416.36
0.3	0.5	1200	1248	1099	0.08540571	272777.8
0.3	0.75	1200	936	934	0.08542337	330561.1
0.3	1	1200	720	956	0.08539153	376007.8

SC Storage Sensitivity Analysis

Additional simulations were carried out using a SC-based storage system. SC capacities ranged from 4.67 kWh to 149 kWh, with corresponding autonomy values below 0.25 hours. This short duration reflects SC's specific application: peak shaving rather than long-duration storage. Despite variations in size and throughput:

- Annual throughput ranged from 1,111 to 32,960 kWh,
- LCOE remained stable, hovering around €0.060/kWh across configurations.

However, the SC systems required large converter capacities (up to 1,612 kW) and high capital investment, especially for larger units. The NPC remained around €7.99M, with minimal performance gains, rendering SC-based architectures economically unattractive under the given electricity price conditions. Table 6-8 summarizes the results for systems integrating SC 4000F modules. Despite increases in SC capacity, the economic performance remained nearly flat, with no configuration surpassing the performance of VRFB-based or non-storage systems.

Table 6-8 Impact of SC Storage on LCOE and Throughput

Architecture			Cost					SC 4000F			
PV (kW)	SC 4000F (kW)	Converter (kW)	NPC (€)	LCOE (€/kWh)	Operating Cost (€/yr)	CAPEX (€)	OPEX (€/yr)	Autonomy (hr)	Annual Throughput (kWh/hr)	Nominal Capacity (kWh)	Accessibility (kW)
1 200	288	971	7.75M	0,0589	285 440	610 187	285 440	0,00781	1 111	4,67	4,2
1 200	1 152	1 264	7.77M	0,0591	285 277	638 128	285 277	0,0313	4 259	18,7	16,8
1 200	4 223	902	7.86M	0,0599	284 760	736 038	284 760	0,115	15 293	68,4	61,6
1 200	6 323	916	7.91M	0,0604	284 336	803 252	284 336	0,172	22 746	102	92,2
1 200	8 998	938	7.99M	0,0611	283 822	888 875	283 822	0,244	32 198	146	131
1 200	9 214	989	7.99M	0,0612	283 781	895 837	283 781	0,25	32 960	149	134
1 200	9 214	1 008	7.99M	0,0612	283 781	895 856	283 781	0,25	32 960	149	134
1 200	9 214	1 044	7.99M	0,0612	283 781	895 892	283 781	0,25	32 960	149	134
1 200	9 214	1 081	7.99M	0,0612	283 781	895 829	283 781	0,25	32 960	149	134
1 200	9 214	1 118	7.99M	0,0612	283 781	895 966	283 781	0,25	32 960	149	134
1 200	9 214	1 154	7.99M	0,0612	283 781	896 002	283 781	0,25	32 960	149	134
1 200	9 214	1 209	7.99M	0,0612	283 781	896 057	283 781	0,25	32 960	149	134
1 200	9 214	1 301	7.99M	0,0612	283 781	896 149	283 781	0,25	32 960	149	134
1 200	9 214	1 319	7.99M	0,0612	283 781	896 167	283 781	0,25	32 960	149	134
1 200	9 214	1 338	7.99M	0,0612	283 781	896 186	283 781	0,25	32 960	149	134

Architecture			Cost					SC 4000F			
PV (kW)	SC 4000F (kW)	Converter (kW)	NPC (€)	LCOE (€/kWh)	Operating Cost (€/yr)	CAPEX (€)	OPEX (€/yr)	Autonomy (hr)	Annual Throughput (kWh/hr)	Nominal Capacity (kWh)	Accessibility (kW)
1 200	9 214	1 374	7.99M	0,0612	283 781	896 222	283 781	0,25	32 960	149	134
1 200	9 214	1 393	7.99M	0,0612	283 781	896 241	283 781	0,25	32 960	149	134
1 200	9 214	1 411	7.99M	0,0612	283 781	896 259	283 781	0,25	32 960	149	134
1 200	9 214	1 448	7.99M	0,0612	283 781	896 296	283 781	0,25	32 960	149	134
1 200	9 214	1 484	7.99M	0,0612	283 781	896 332	283 781	0,25	32 960	149	134
1 200	9 214	1 521	7.99M	0,0612	283 781	896 369	283 781	0,25	32 960	149	134
1 200	9 214	1 539	7.99M	0,0612	283 781	896 387	283 781	0,25	32 960	149	134
1 200	9 214	1 557	7.99M	0,0612	283 781	896 405	283 781	0,25	32 960	149	134
1 200	9 214	1 594	7.99M	0,0612	283 781	896 442	283 781	0,25	32 960	149	134
1 200	9 214	1 612	7.99M	0,0612	283 781	896 460	283 781	0,25	32 960	149	134
1 200	9 214	1 631	7.99M	0,0612	283 781	896 479	283 781	0,25	32 960	149	134
1 200	9 214	1 667	7.99M	0,0612	283 781	896 515	283 781	0,25	32 960	149	134
1 200	9 214	1 704	7.99M	0,0612	283 781	896 552	283 781	0,25	32 960	149	134
1 200	9 214	1 741	7.99M	0,0612	283 781	896 589	283 781	0,25	32 960	149	134

Comparison Between Base Case and Winning System Architecture

The comparison between two energy system architectures shows the Winning System Architecture integrates a grid connection, a 1,200 kW photovoltaic system, a 1,536 kWh VRFB, and a 989 kW converter. The Base Case, in contrast, includes a similar grid and PV system but lacks the battery, relying on a smaller 953 kW converter. Table 6-9 shows the both architectures.

Table 6-9 Comparison of Base Case and Winning System Architecture

Base case Architecture	Winning System
Unlimited Grid PV Plant: 1200 kWp No storage Converter: 953 kW	Unlimited Grid PV Plant: 1200 kWp Storage: VRFB 1536 kWh Converter: 989 kW

Economically, the Winning System demonstrates an IRR of 11%, a ROI of 6%, and a payback period of 5 years, making it financially attractive over the project lifetime. Although its initial capital cost (€670,109) is higher than the Base Case (€600,953), the Winning System benefits from slightly reduced annual operations and maintenance costs (€272,578 compared to €279,499) and a lower NPC of €7.48M versus €7.59M for the Base Case. However, its LCOE is slightly higher at €0.0607/kWh compared to the Base Case's €0.0577/kWh.

The cumulative cash flow graph (see in Figure 6.10) reveals that the Winning System slightly outperforms the Base Case over 25 years. This demonstrates that the investment in battery storage enhances the system's overall efficiency and long-term financial viability, making it an appealing option for stakeholders seeking sustainable and profitable energy solutions

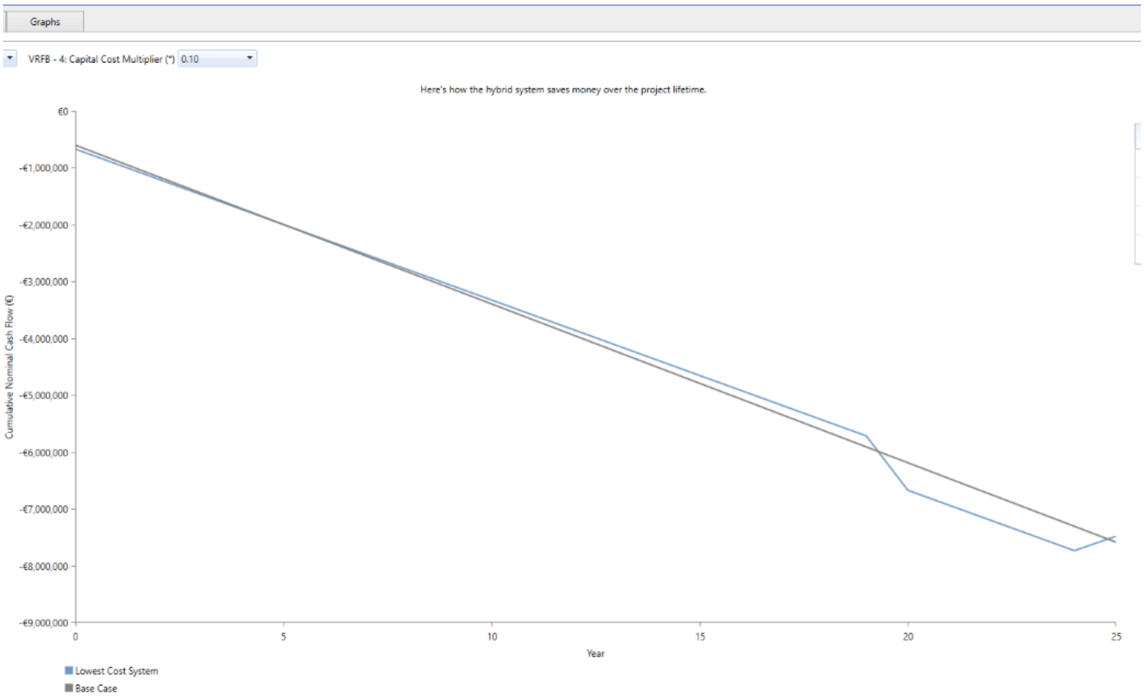

Figure 6.10 Cumulative Cash Flow Comparison: Base Case vs. Winning System (lowest cost system)

Economic Evaluation of the Base Case vs. Winning System

The techno-economic comparison between the Base Case and the Winning System, which includes VRFB storage, shows that although storage integration increases upfront CAPEX, it can enhance long-term financial performance. Table 6-10 summarizes the KPIs for both configurations:

Table 6-10 KPIs, Base Case vs. Lowest Cost System

KPI	**Base Case**	**Winning System**
NPC	€7.59 M	€ 7.48 M
Initial capital	€600,953	€ 670,109
Operation and Maintenance	€279,499	€272,578
LCOE	€0.0577	€ 0.0607

While the HESS configuration incorporating VRFB storage offers operational savings and a lower NPC, it still incurs a slightly higher LCOE. Given the current electricity prices in Tunisia and the present cost of storage technologies, a full HESS does not yet represent the most cost-effective solution. Nevertheless, the integration of VRFB alone may become financially viable if its capital and replacement costs are significantly reduced in the future.

Table 6-11 details the component-wise cost distribution for the Winning System, including capital investments, replacement costs, salvage value, and total lifecycle expenditure.

Table 6-11 Component Cost Summary of the Winning System

Name	Capital	Replacement	Salvage	Resource	Total
Generic flat plate PV	€600,000	€0.00	€0.00	€0.00	€900,000
Grid	€0.00	€0.00	€0.00	€0.00	€6.62M
System Converter	€909.09	€0.00	€0.00	€0.00	€909.09
VRFB custom - 4hours	€75,600	€756,000	-€566,995	€0.00	€265,595
System total	€676,509	€756,000	-€566,995	€0.00	€7.79M

6.5.3. Conclusion and Discussion

This case study demonstrates the technical feasibility and conditional economic viability of integrating a HESS, comprising a VRFB and a SC, within an industrial PV system under Tunisia's current grid and regulatory framework. The simulations, conducted through HOMER Pro, explored over 6,000 configurations, evaluating both standalone and combined storage technologies across varying electricity price and capital cost scenarios. The results revealed that while SC integration offered limited improvements in short-term peak shaving, it did not translate into significant economic gains. In contrast, VRFB-based systems showed greater promise, particularly when capital cost multipliers were reduced, indicating a pathway toward financial viability with future cost declines.

The Winning System, which includes a 1,536 kWh VRFB, a 1,200 kWp PV plant, and a 989 kW converter, outperformed the Base Case configuration (PV + Grid only) over a 25-year lifetime in terms of NPC, ROI, and IRR. Despite a higher upfront cost (€670,109 vs. €600,953), the Winning System achieved a lower NPC (€7.48M vs. €7.59M) and a favorable IRR of 11% with a 5-year payback period. However, its LCOE is slightly higher (€0.0607/kWh compared to €0.0577/kWh), emphasizing that storage benefits accrue primarily over the long term.

SC-based architectures, while technically effective in mitigating short bursts in load demand, is found to be economically uncompetitive. SCs high capital costs, low energy throughput, and minimal impact on overall system performance led to flat financial results, with NPC values consistently near €7.99M and LCOEs clustering around €0.060/kWh.

From a policy perspective, the case study highlights the limitations of Tunisia's current net billing scheme, which allows only 30% of PV generation to be exported at a low tariff. These conditions suppress the economic incentive to oversize PV systems and instead underscore the need for behind-the-meter storage. The integration of VRFB storage, particularly under optimized cost conditions, demonstrates a viable strategy to increase self-consumption, reduce grid reliance, and improve overall energy cost savings. A full HESS (VRFB + SC) is not yet a cost-effective solution under current conditions, VRFB-only systems show strong potential for future deployment, especially as storage prices fall and grid tariffs evolve. The insights derived from this analysis can support evidence-based regulatory reform, enabling storage technologies to play a pivotal role in Tunisia's energy transition and industrial decarbonization goals.

7. CONCLUSION AND FUTURE WORK

This deliverable conducted a comprehensive techno-economic investigation into Hybrid Energy Storage Systems (HESS), focusing on how different technology combinations, such as redox flow batteries, salt-based batteries, plus supercapacitors, can be optimally sized and deployed across varying energy contexts. The analysis is applied to four representative case studies: an isolated island grid in Portugal, a research and industrial setting in Germany, a utility-scale solar-plus-storage system in Italy, and a hybrid off-grid system in Tunisia. Each site presented unique boundary conditions shaped by its regulatory environment, market structure, load characteristics, and renewable integration challenges. To model these scenarios, different optimization approaches are adopted. In Portugal and Germany, a data-driven multi-period optimization framework is employed to account for both operational constraints and temporal energy variability. For the Italian case, a Mixed-Integer Linear Programming model is developed to explore how HESS could maximize revenues by interacting with several energy markets simultaneously. In Tunisia, simulations using the HOMER tool evaluated a wide range of technical configurations to identify the most cost-effective setups for remote areas.

These models incorporated critical system parameters such as battery degradation, thermal and power limits, and real-world load and generation data. The resulting analysis produced valuable insights into how HESS design choices affect key outcomes like diesel offset, renewable curtailment, lifecycle economics, and investment returns, expressed through metrics such as NPV, LCOE, and performance under energy arbitrage scenarios.

The main conclusions from the case studies are as follows:

- In Graciosa Island (Portugal), integrating a HESS helped reduce diesel reliance and better utilize curtailed renewable energy, making a strong case for hybrid storage in islanded systems.
- In Germany, HESS contributed to grid flexibility through load shifting and price-responsive storage strategies, supporting improved economic performance under variable pricing conditions.
- The Italian use case showed that when carefully sized, HESS could engage in multiple markets simultaneously, justifying the investment through stacked revenues.
- For Tunisia, the simulation-based approach demonstrated how hybrid storage can be a viable and resilient energy solution for off-grid communities with fluctuating renewable supply.

While this study included an exploratory assessment of SC, their deployment was not consistent across all case studies. Rather, their role is examined under selected conditions to provide insight into their potential contribution to overall system performance. Specifically, SCs are analyzed as complementary components to the primary battery technologies, particularly to mitigate performance limitations such as power de-rating and thermal constraints, issues identified in both redox flow and salt-based battery systems. In the Portugal case study, SC used to absorb rapid power fluctuations and to compensate for salt-based battery limitations arising from temperature-induced power derating, thereby improving system stability and protecting battery lifetime. Furthermore, their role in frequency regulation is assessed through high-resolution simulations, where SC demonstrate effective power smoothing and fluctuation reduction. In the Italian case study, their potential to participate in fast reserve services is also considered, highlighting a possible role for SCs in ancillary markets. Although the viability of these applications depends on favorable regulatory frameworks and advanced control strategies, the deliverable offers preliminary evidence that SCs can enhance power quality, support battery performance, and enable access to new service-based revenue streams when appropriately integrated.

Overall, the results confirm the technical promise and economic potential of HESS, particularly if capital costs for these systems decline significantly in the future. However, successful deployment remains highly dependent on local conditions, including system-specific energy needs, fuel pricing, market design, and regulatory incentives. These findings will inform future demonstration activities and policy development within the SMHYLES project, contributing to the broader conversation on how hybrid storage systems can support resilient, flexible, and low-carbon energy infrastructures.

Building upon the findings of this deliverable, future work will focus on advancing smart control strategies and adaptive dispatch mechanisms to optimize HESS performance under varying operational conditions. These include scenarios of fluctuating demand, intermittent renewable generation, market-based dispatch, and provision of grid services. This will be achieved through the development of real-time energy management strategies supported by data-driven algorithms and the integration of digital twin technologies, enabling predictive monitoring, control optimization, and pre-deployment validation in virtual environments. These analyses will help tailor HESS operation strategies under diverse regulatory and technical contexts. Lifecycle considerations, including HESS ageing, system reliability, and smart scheduling, will also be embedded in model-based evaluations to guide future deployment and replication strategies

Collaboration with regulatory bodies will be critical to support the market recognition of fast-response technologies like supercapacitors and to align incentive structures with evolving grid needs. Ultimately, future planning will aim to integrate HESS solutions into broader decarbonization pathways, coordinating with distributed generation assets, electric mobility infrastructure, and flexible demand-side resources.

8. APPENDIX1

Methodology for HESS Sizing Analysis used for Portugal and Germany use cases

The HESS sizing analysis seeks to determine the most effective combination of a Battery Energy Storage System (BESS) and a Supercapacitor (SC) to maximize technical and economic performance under various operating scenarios. By pairing the BESS's capacity for long-duration energy shifting with the SC's rapid-response power buffering, the system can reliably manage renewable intermittency, reduce curtailment, perform peak shaving, and potentially provide market-based services such as ancillary services or arbitrage[79]. To account for realistic operating conditions and financial opportunities, hourly or more granular price signals from day-ahead, intraday, or ancillary service markets are integrated into the scheduling algorithm. Year-long load and renewable generation profiles (e.g., from PV and/or wind), preferably at hourly and/or sub-hourly resolution, capture typical daily and seasonal variations as well as high-frequency fluctuations. Figure 8.1 illustrates the general workflow of the approach used in T2.3 to determine the optimal size of HESS based on various configurations between BESS and SC.

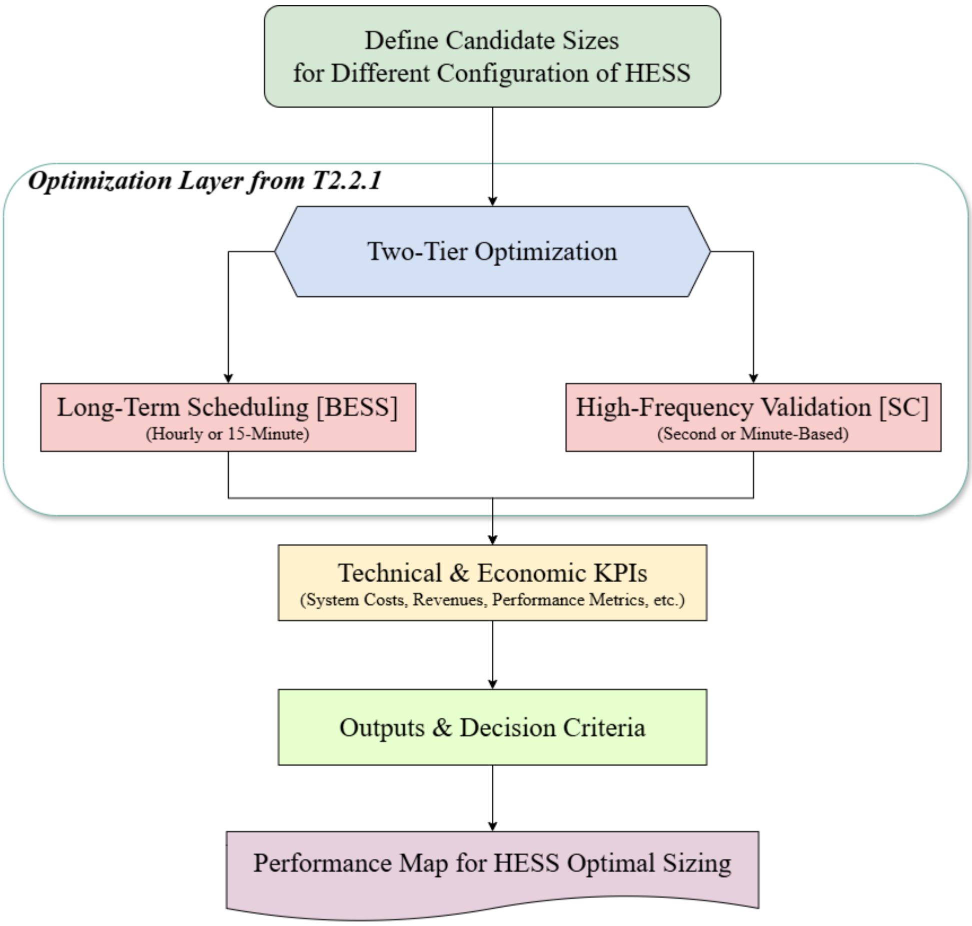

Figure 8.1 General workflow of procedure of optimal sizing of HESS

Defining Candidate Sizes

A range of potential system sizes is identified by varying the BESS's energy and power ratings (for example, 50 kWh to 500 kWh in 50 kWh increments, and 25 kW to 250 kW in 25 kW increments) and the SC's power capacity (such as 50 kW to 300 kW, or other relevant increments)[80]. Each of these candidate HESS configurations undergoes a two-tier optimization and evaluation process.

Two-Tier Optimization [81]

Long-Term Scheduling (Hourly or 15-Minute Resolution)

Using a techno-economic optimization algorithm (detailed in Section 2.2), a full-year simulation is performed to generate an "ideal" dispatch schedule for each candidate system size. The objective function typically maximizes net revenue (e.g., buying when prices are low and selling when prices are high) or minimizes energy costs over the entire year. This schedule is developed under constraints such as battery State of Charge (SOC) boundaries, ramp limits, day-ahead forecasts, and market-bid possibilities

High-Frequency Validation (Second or Minute-Based)

Once the long-term schedule is set, it is tested against higher-resolution data to ensure the battery can follow the planned power profile without violating temperature, SOC, or current constraints. If de-rating limits are reached, the SC compensates by delivering power when the BESS must throttle or absorbing surplus renewable generation that the BESS cannot accommodate. Where relevant, the SC also provides primary or ancillary services (e.g., frequency regulation) during these short intervals, potential increasing overall revenue or grid stability.

Technical and Economic KPIs

Upon completing the simulation for each candidate size, the framework calculates:

- System Costs (CAPEX/OPEX), accounting for BESS and SC hardware, installation, and maintenance[82].
- Revenues or Cost Savings, derived from market participation (arbitrage, ancillary services) or reduced grid imports in self-consumption scenarios [83].
- Performance Metrics, such as PV curtailment, unmet load, peak load reduction, and SOC excursions[84].

Performance Map, Outputs and Decision Criteria

All results are compiled into a multi-dimensional map reflecting cost–benefit relationships and other operational trade-offs[15]. This map helps identify optimal HESS configurations, those that yield the highest net benefit or meet other defined goals (e.g., a desired payback period or grid code constraints). By applying this methodology across all candidate BESS–SC sizes, the analysis produces:

- Optimal Schedules, indicating how much power to charge or discharge each hour (and, when necessary, second/minute-level adjustments) [85].
- KPI Rankings, summarizing annual net revenue, self-consumption improvement, avoided curtailment, and system efficiency [86].
- Recommended System Size, typically presented as a short list of configurations that maximize economic returns while satisfying technical constraints[87].

This systematic approach ensures that both long-term economic viability and short-term operational feasibility are considered in the final sizing and design of the HESS.

9. BIBLIOGRAPHY

[1] M. Buchajczyk, S. Korjani, M. Duranti, and E. G. Macchi, "SMHYLES Activity D2.2 Digital Twins for HESS Design Grant ID: 10113802," Jan. 2025.

[2] M. Gao, Z. Wang, D. G. Lek, and Q. Wang, "Towards high power density aqueous redox flow batteries," Mar. 01, 2023, Tsinghua University Press. doi: 10.26599/NRE.2023.9120045.

[3] S. Atatreh, B. A. Seddik, A. Qurashi, and Ozsoy, "Innovation in Battery Energy Storage Systems via Redox Flow Batteries Technology," in ADIPEC, Abu Dhabi,Dubai, Nov. 2024.

[4] M. Schulz, "Battery Types – Sodium Batteries – High-Temperature Sodium Batteries | Sodium–Nickel Chloride," Encyclopedia of Electrochemical Power Sources (Second Edition). Elsevier, pp. 858–871, 2025.

[5] A. Li, P. Y. Zavalij, and F. Omenya, "Salt-in-presalt electrolyte solutions for high-potential non-aqueous sodium metal batteries.," Nat Nanotechnol, vol. 20, pp. 388–396, Mar. 2025.

[6] K. V. G. Raghavendra et al., "An intuitive review of supercapacitors with recent progress and novel device applications," Oct. 01, 2020, Elsevier Ltd. doi: 10.1016/j.est.2020.101652.

[7] R. Das and C. S. Dash, "Science and Technology of Supercapacitor and its Applications," Current Materials Science, vol. 18, 2025.

[8] Z. Dong et al., "A Survey of Battery–Supercapacitor Hybrid Energy Storage Systems: Concept, Topology, Control and Application," Jun. 01, 2022, MDPI. doi: 10.3390/sym14061085.

[9] W. Shan, M. Schwalm, and M. Shan, "A Design Tool for Battery/Supercapacitor Hybrid Energy Storage Systems Based on the Physical–Electrochemical Degradation Battery Model BaSiS," Energies (Basel), vol. 17, no. 14, Jul. 2024, doi: 10.3390/en17143481.

[10] C. Xu et al., "Economic Analysis of Li-Ion Battery–Supercapacitor Hybrid Energy Storage System Considering Multitype Frequency Response Benefits in Power Systems," Energies (Basel), vol. 16, no. 18, Sep. 2023, doi: 10.3390/en16186621.

[11] N. A. Basyarach, V. L. B. Putri, F. G. Triyanto, I. M. Y. Negara, and A. Priyadi, "A Mixed-Integer Linear Programming-Based Power Allocation of Supercapacitor-Battery Energy Storage for Off-Grid Applications," in 2023 International Conference on Technology and Policy in Energy and Electric Power (ICT-PEP), Jakarta, Indonesia, 2023, pp. 162–167.

[12] M. Buchajczyk, S. Korjani, M. Duranti, and E. G. Macchi, "Techno-Economic Analysis and Sizing of RFB and Supercapacitor-Based HESS for an EV Charging Station," in 2024 AEIT International Annual Conference (AEIT), Trento, Italy, 2024.

[13] S. Korjani, A. Facchini, M. Mureddu, A. Rubino, and A. Damiano, "Battery management for energy communities—Economic evaluation of an artificial intelligence-led system," J Clean Prod, vol. 314, Sep. 2021, doi: 10.1016/j.jclepro.2021.128017.

[14] S. Korjani, M. Mureddu, A. Facchini, and A. Damiano, "Aging cost optimization for planning and management of energy storage systems," Energies (Basel), vol. 10, no. 11, Nov. 2017, doi: 10.3390/en10111916.

[15] S. Korjani, F. Casu, A. Damiano, V. Pilloni, and A. Serpi, "An online energy management tool for sizing integrated PV-BESS systems for residential prosumers," Appl Energy, vol. 313, May 2022, doi: 10.1016/j.apenergy.2022.118765.

[16] W. Jing, C. H. Lai, W. S. H. Wong, and M. L. D. Wong, "A comprehensive study of battery-supercapacitor hybrid energy storage system for standalone PV power system in rural electrification," Appl Energy, vol. 224, pp. 340–356, Aug. 2018, doi: 10.1016/j.apenergy.2018.04.106.

[17] K. Rafał, W. Radziszewska, O. Grabowski, H. Biedka, and J. Verstraete, "Energy Cost Minimization with Hybrid Energy Storage System Using Optimization Algorithm," Applied Sciences (Switzerland), vol. 13, no. 1, Jan. 2023, doi: 10.3390/app13010518.

[18] J. Hamilton, M. Negnevitsky, and X. Wang, "Economics of renewable energy integration and energy storage via low load diesel application," Energies (Basel), vol. 11, no. 5, 2018, doi: 10.3390/en11051080.

[19] T. Nogueira, J. Jesus, and J. Magano, "Graciosa Island's Hybrid Energy System Expansion Scenarios: A Technical and Economic Analysis," Journal of Sustainability Research, 2024, doi: 10.20900/jsr20240010.

[20] A. Amer, A. Massoud, and K. Shaban, "Optimization of hybrid renewable-diesel power plants considering operational cost, battery degradation, and emissions," Heliyon, vol. 10, no. 6, Mar. 2024, doi: 10.1016/j.heliyon.2024.e27021.

[21] S. Hajiaghasi, A. Salemnia, and M. Hamzeh, "Hybrid energy storage system for microgrids applications: A review," J Energy Storage, vol. 21, pp. 543–570, Feb. 2019, doi: 10.1016/J.EST.2018.12.017.

[22] H. Shayeghi, F. Monfaredi, A. Dejamkhooy, M. Shafie-khah, and J. P. S. Catalão, "Assessing hybrid supercapacitor-battery energy storage for active power management in a wind-diesel system," International Journal of Electrical Power & Energy Systems, vol. 125, p. 106391, Feb. 2021, doi: 10.1016/J.IJEPES.2020.106391.

[23] M. Baek, J. Roh, and JB. Park, “Optimal Sizing of Battery/Supercapacitor Hybrid Energy Storage Systems for Frequency Regulation,” Journal of Electrical Engineering & Technology, vol. 17, pp. 111–120, Oct. 2021.

[24] D. Kang et al., “Optimal planning of hybrid energy storage systems using curtailed renewable energy through deep reinforcement learning,” Energy, vol. 284, p. 128623, Dec. 2023, doi: 10.1016/J.ENERGY.2023.128623.

[25] M. Richter et al., “Development and Environmental Assessment of a Phase Change Material Based Thermal Management System for Na/NiCl2 Batteries,” Batteries, vol. 8, no. 11, Nov. 2022, doi: 10.3390/batteries8110197.

[26] Fondazione Bruno Kessler, “SMHYLES Milestone N. 3 Initial HESS Sizing and Design - Delivery of Technical Specifications to Technology Providers Grant ID: 10113802,” Jul. 2024.

[27] N. Shamim, E. C. Thomsen, V. V. Viswanathan, D. M. Reed, V. L. Sprenkle, and G. Li, “Evaluating zebra battery module under the peak-shaving duty cycles,” Materials, vol. 14, no. 9, 2021, doi: 10.3390/ma14092280.

[28] O. Vasanoja and A. Volpe, “Valuation in the Energy Storage Sector: An investor perspective,” Umea University, Umea, Sweden, 2023.

[29] I. Melo, J. P. Neto Torres, C. A. Ferreira Fernandes, and R. A. Marques Lameirinhas, “Sustainability economic study of the islands of the Azores archipelago using photovoltaic panels, wind energy and storage system,” Renew Wind Water Sol, vol. 7, no. 1, Dec. 2020, doi: 10.1186/s40807-020-00061-8.

[30] G. J. B. Chambi, “Technology Road Map for Energy Storage using Zebra Batteries,” MIT, 2021.

[31] I. BloombergNEF, “2H 2024 EU ETS Market Outlook: On Tenterhooks Over Supply.” Accessed: May 23, 2025. [Online]. Available: https://about.bnef.com/blog/2h-2024-eu-ets-market-outlook-on-tenterhooks-over-supply/

[32] Bavarian Research, “The Best of Two Systems: New EU project ‘Hyflow’ to develop a smart hybrid energy storage system.”

[33] T. B. Nkwanyana, M. W. Siti, Z. Wang, I. Toudjeu, N. T. Mbungu, and W. Mulumba, “An assessment of hybrid-energy storage systems in the renewable environments,” J Energy Storage, vol. 72, p. 108307, Nov. 2023, doi: 10.1016/J.EST.2023.108307.

[34] A. J. Pimm, T. T. Cockerill, and P. G. Taylor, “The potential for peak shaving on low voltage distribution networks using electricity storage,” J Energy Storage, vol. 16, pp. 231–242, Apr. 2018, doi: 10.1016/J.EST.2018.02.002.

[35] J. Neubauer and M. Simpson, "Deployment of Behind-The-Meter Energy Storage for Demand Charge Reduction," 2015. [Online]. Available: www.nrel.gov/publications.

[36] I. Michael Robinette et al., "Study to Reduce Peak Electrical Demand Charges for the John C. Hodges Library," Knoxville, May 2016. [Online]. Available: https://trace.tennessee.edu/utk_chanhonoproj/2016

[37] China Energy Storage Alliance, "100MW Dalian Liquid Flow Battery Energy Storage and Peak shaving Power Station Connected to the Grid for Power Generation."

[38] E. Pusceddu, B. Zakeri, and G. Castagneto Gissey, "Synergies between energy arbitrage and fast frequency response for battery energy storage systems," Appl Energy, vol. 283, p. 116274, Feb. 2021, doi: 10.1016/J.APENERGY.2020.116274.

[39] F. Núñez, D. Canca, and Á. Arcos-Vargas, "An assessment of European electricity arbitrage using storage systems," Energy, vol. 242, p. 122916, Mar. 2022, doi: 10.1016/J.ENERGY.2021.122916.

[40] BMWK, "Renewable Energy Sources Act (EEG 2017)," Jul. 2017. Accessed: May 23, 2025. [Online]. Available: https://www.bmwk.de/Redaktion/EN/Downloads/renewable-energy-sources-act-2017.pdf?__blob=publicationFile&v=1

[41] BSW Solar, "EEG 2017 – feste Einspeisevergütungen im Überblick*." Accessed: May 23, 2025. [Online]. Available: https://www.solarfuxx.de/pdf/eeg-verguetungssaetze-2018.pdf

[42] J. Stute and M. Kühnbach, "Dynamic pricing and the flexible consumer – Investigating grid and financial implications: A case study for Germany," Energy Strategy Reviews, vol. 45, Jan. 2023, doi: 10.1016/j.esr.2022.100987.

[43] Trading Economics, "Germany Electricity Price." [Online]. Available: https://tradingeconomics.com/germany/electricity-price

[44] L. Tziovani, L. Hadjidemetriou, and S. Timotheou, "Energy Storage Arbitrage and Peak Shaving in Distribution Grids Under Uncertainty," in 2022 IEEE PES Innovative Smart Grid Technologies Conference Europe (ISGT-Europe), Novi Sad, Serbia, 2022.

[45] R. Sharma, S. Choudhury, B. Jena, and S. Goel, "Electrical Energy Storage: A Great Business Ahead," Advances in Intelligent Computing and Communication. Lecture Notes in Networks and Systems, vol. 109, 2020.

[46] C. Schubert et al., "Hybrid Energy Storage Systems Based on Redox-Flow Batteries: Recent Developments, Challenges, and Future Perspectives," Apr. 01, 2023, Multidisciplinary Digital Publishing Institute (MDPI). doi: 10.3390/batteries9040211.

[47] G. He, X. Chen, Y. Yang, J. Wang, and J. Song, "Hybrid Portable and Stationary Energy Storage Systems with Battery Charging and Swapping Coordination," in 2022 IEEE/IAS Industrial and Commercial Power System Asia (I&CPS Asia), Shanghai, China, 2022.

[48] T. Wu, X. Shi, L. Liao, C. Zhou, H. Zhou, and Y. Su, "A capacity configuration control strategy to alleviate power fluctuation of hybrid energy storage system based on improved particle swarm optimization," Energies (Basel), vol. 12, no. 4, Feb. 2019, doi: 10.3390/en12040642.

[49] H. Han et al., "Optimal Sizing Considering Power Uncertainty and Power Supply Reliability Based on LSTM and MOPSO for SWPBMs," IEEE Syst J, vol. 16, no. 3, pp. 4013–4023, 2022, doi: 10.1109/JSYST.2021.3137856.

[50] D. Siface, "Optimal Economical and Technical Sizing Tool for Battery Energy Storage Systems Supplying Simultaneous Services to the Power System," in 2019 16th International Conference on the European Energy Market (EEM), 2019, pp. 1–6. doi: 10.1109/EEM.2019.8916360.

[51] A. I. Ikram, M. S.-U. Islam, M. A. Bin Zafar, M. K. Rocky, Imtiaz, and A. Rahman, "Techno-Economic Optimization of Grid-Integrated Hybrid Storage System using GA," in 2023 1st International Conference on Innovations in High Speed Communication and Signal Processing (IHCSP), 2023, pp. 300–305. doi: 10.1109/IHCSP56702.2023.10127187.

[52] L. Kumar, M. U. Manoo, J. Ahmed, M. Arıcı, and M. M. Awad, "Comparative techno-economic investigation of hybrid energy systems for sustainable energy solution," Int J Hydrogen Energy, vol. 104, pp. 513–526, Feb. 2025, doi: 10.1016/J.IJHYDENE.2024.05.369.

[53] I. S. Zaslavskiy, F. S. Nepsha, and V. A. Voronin, "Application of Hybrid Energy Storage Systems in Remote Power Grids," in 2024 IEEE 3rd International Conference on Problems of Informatics, Electronics and Radio Engineering (PIERE), 2024, pp. 900–904. doi: 10.1109/PIERE62470.2024.10804983.

[54] K.-H. Ahlert and C. van Dinther, "Sensitivity analysis of the economic benefits from electricity storage at the end consumer level," in 2009 IEEE Bucharest PowerTech, 2009, pp. 1–8. doi: 10.1109/PTC.2009.5282245.

[55] T. Jirabovornwisut, S. Kheawhom, Y. S. Chen, and A. Arpornwichanop, "Optimal operational strategy for a vanadium redox flow battery," Comput Chem Eng, vol. 136, p. 106805, May 2020, doi: 10.1016/J.COMPCHEMENG.2020.106805.

[56] N. Poli, C. Bonaldo, M. Moretto, and M. Guarnieri, "Techno-economic assessment of future vanadium flow batteries based on real device/market parameters," Appl Energy, vol. 362, p. 122954, May 2024, doi: 10.1016/J.APENERGY.2024.122954.

[57] K. E. Rodby, T. J. Carney, Y. Ashraf Gandomi, J. L. Barton, R. M. Darling, and F. R. Brushett, "Assessing the levelized cost of vanadium redox flow batteries with capacity fade and rebalancing," J Power Sources, vol. 460, p. 227958, Jun. 2020, doi: 10.1016/J.JPOWSOUR.2020.227958.

[58] Terna, "Electricity Market." Accessed: May 23, 2025. [Online]. Available: https://www.terna.it/en/electric-system/electricity-market

[59] F. Nitsch, M. Deissenroth-Uhrig, C. Schimeczek, and V. Bertsch, “Economic evaluation of battery storage systems bidding on day-ahead and automatic frequency restoration reserves markets,” Appl Energy, vol. 298, p. 117267, Sep. 2021, doi: 10.1016/J.APENERGY.2021.117267.

[60] Y. Hu, M. Armada, and M. Jesús Sánchez, “Potential utilization of battery energy storage systems (BESS) in the major European electricity markets,” Appl Energy, vol. 322, p. 119512, Sep. 2022, doi: 10.1016/J.APENERGY.2022.119512.

[61] H. Jaffal, L. Guanetti, G. Rancilio, M. Spiller, F. Bovera, and M. Merlo, “Battery Energy Storage System Performance in Providing Various Electricity Market Services,” Batteries, vol. 10, no. 3, Mar. 2024, doi: 10.3390/batteries10030069.

[62] G. Rancilio, F. Bovera, and M. Merlo, “Revenue Stacking for BESS: Fast Frequency Regulation and Balancing Market Participation in Italy,” International Transactions on Electrical Energy Systems, vol. 2022, no. 1, p. 1894003, Jan. 2022, doi: https://doi.org/10.1155/2022/1894003.

[63] D. Andreotti, M. Spiller, A. Scrocca, F. Bovera, and G. Rancilio, “Modeling and Analysis of BESS Operations in Electricity Markets: Prediction and Strategies for Day-Ahead and Continuous Intra-Day Markets,” Sustainability, vol. 16, no. 18, p. 7940, Sep. 2024, doi: 10.3390/su16187940.

[64] Y. Xiao, W. Wu, X. Wang, Y. Qu, and J. Li, “Economic potentials of energy storage technologies in electricity markets with renewables,” Energy Storage and Saving, vol. 2, no. 1, pp. 370–391, Mar. 2023, doi: 10.1016/J.ENSS.2022.10.004.

[65] B. Xu et al., “Scalable Planning for Energy Storage in Energy and Reserve Markets,” IEEE Transactions on Power Systems, vol. 32, no. 6, pp. 4515–4527, 2017, doi: 10.1109/TPWRS.2017.2682790.

[66] B. Finnah, J. Gönsch, and F. Ziel, “Integrated day-ahead and intraday self-schedule bidding for energy storage systems using approximate dynamic programming,” Eur J Oper Res, vol. 301, no. 2, pp. 726–746, Sep. 2022, doi: 10.1016/J.EJOR.2021.11.010.

[67] A. R. Silva, H. M. I. Pousinho, and A. Estanqueiro, “A multistage stochastic approach for the optimal bidding of variable renewable energy in the day-ahead, intraday and balancing markets,” Energy, vol. 258, p. 124856, Nov. 2022, doi: 10.1016/J.ENERGY.2022.124856.

[68] F. J. Heredia, M. D. Cuadrado, and C. Corchero, “On optimal participation in the electricity markets of wind power plants with battery energy storage systems,” Comput Oper Res, vol. 96, pp. 316–329, Aug. 2018, doi: 10.1016/J.COR.2018.03.004.

[69] J. C. Shang, H. Bai, M. Yang, T. Wang, Q. Li, and X. Jiang, “Grid-Side Energy Storage System Day-Ahead Bidding Strategy Based on Two-Level Decision in Spot Market,” in 2020 IEEE 3rd Student Conference on Electrical Machines and Systems (SCEMS), 2020, pp. 668–673. doi: 10.1109/SCEMS48876.2020.9352269.

[70] I. Boukas et al., “A deep reinforcement learning framework for continuous intraday market bidding,” Mach Learn, vol. 110, no. 9, pp. 2335–2387, Sep. 2021, doi: 10.1007/s10994-021-06020-8.

[71] C. F. Calvillo, A. Sánchez-Miralles, J. Villar, and F. Martín, “Optimal planning and operation of aggregated distributed energy resources with market participation,” Appl Energy, vol. 182, pp. 340–357, Nov. 2016, doi: 10.1016/J.APENERGY.2016.08.117.

[72] F. Conte, S. Massucco, G.-P. Schiapparelli, and F. Silvestro, “Day-Ahead and Intra-Day Planning of Integrated BESS-PV Systems Providing Frequency Regulation,” IEEE Trans Sustain Energy, vol. 11, no. 3, pp. 1797–1806, 2020, doi: 10.1109/TSTE.2019.2941369.

[73] A. Fusco, D. Gioffré, S. Leva, G. Manzolini, E. Martelli, and L. Moretti, “Predictive Energy Management System for a PV-BESS system bidding on Day-Ahead and Intra-Day electricity markets,” in 2023 IEEE Belgrade PowerTech, 2023, pp. 1–6. doi: 10.1109/PowerTech55446.2023.10202942.

[74] A. Nespoli, M. Mussetta, E. Ogliari, S. Leva, L. Fernández-Ramírez, and P. García-Triviño, “Robust 24 hours ahead forecast in a microgrid: A real case study,” Electronics (Switzerland), vol. 8, no. 12, Dec. 2019, doi: 10.3390/electronics8121434.

[75] R. D. Filho, A. C. M. Monteiro, T. Costa, A. Vasconcelos, A. C. Rode, and M. Marinho, “Strategic Guidelines for Battery Energy Storage System Deployment: Regulatory Framework, Incentives, and Market Planning,” Energies (Basel), vol. 16, no. 21, Nov. 2023, doi: 10.3390/en16217272.

[76] K. Tian, W. Sun, W. Liu, and H. Song, “Coordinated RES and ESS Planning Framework Considering Financial Incentives Within Centralized Electricity Market,” CSEE Journal of Power and Energy Systems, vol. 9, no. 2, pp. 539–547, 2023, doi: 10.17775/CSEEJPES.2020.02400.

[77] X. Ayón, M. Á. Moreno, and J. Usaola, “Aggregators’ optimal bidding strategy in sequential day-ahead and intraday electricity spot markets,” Energies (Basel), vol. 10, no. 4, Apr. 2017, doi: 10.3390/en10040450.

[78] Gestore Mercati Energetici, “MGP Results Zonal Prices.” Accessed: May 23, 2025. [Online]. Available: https://gme.mercatoelettrico.org/en-us/Home/Results/Electricity/MGP/Results/ZonalPrices

[79] M. Khalid, “A review on the selected applications of battery-supercapacitor hybrid energy storage systems for microgrids,” 2019, MDPI AG. doi: 10.3390/en12234559.

[80] D. Mejía-Giraldo, G. Velásquez-Gomez, N. Muñoz-Galeano, J. B. Cano-Quintero, and S. Lemos-Cano, “A BESS sizing strategy for primary frequency regulation support of solar photovoltaic plants,” Energies (Basel), vol. 12, no. 2, Jan. 2019, doi: 10.3390/en12020317.

[81] J. Peihua, M. Xiangping, Z. Hong, and P. Wei, Two-Level Multi-Objective Multi-Timescale Optimal Scheduling with User Participation and Battery Banks. 2023. doi: 10.1109/ICPET59380.2023.10367620.

[82] H. Priyanka and P. Prem, "Techno-Economic Analysis of Islanded Microgrid with Integration of Res and Bess".

[83] M. H. Mostafa, S. H. E. Abdel Aleem, S. G. Ali, Z. M. Ali, and A. Y. Abdelaziz, "Techno-economic assessment of energy storage systems using annualized life cycle cost of storage (LCCOS) and levelized cost of energy (LCOE) metrics," J Energy Storage, vol. 29, p. 101345, Jun. 2020, doi: 10.1016/J.EST.2020.101345.

[84] S. Ezzat Nousir, W. Refaat Anis, M. Abouelatta, G. Samir Adly, and M. A. Abdelaal, "Developing Techno-economic GUI-based Software for On-grid, and Off-grid Photovoltaic Systems Sizing," Ain Shams Engineering Journal, vol. 15, no. 3, p. 102508, Mar. 2024, doi: 10.1016/J.ASEJ.2023.102508.

[85] D. Wu, Q. Gui, W. Zhao, J. Wang, S. Shi, and Y. Zhou, "Battery Energy Storage System (BESS) Sizing Analysis of Bess-Assisted Fast-Charge Station Based on Double-Layer optimization Method," in 2020 IEEE 3rd Student Conference on Electrical Machines and Systems (SCEMS), 2020, pp. 658–662. doi: 10.1109/SCEMS48876.2020.9352324.

[86] F. Boutros, M. Doumiati, J.-C. Olivier, I. Mougharbel, and H. Y. Kanaan, "Optimal Sizing Assessment of an Islanded Microgrid Based on Different EMS Strategies," in 2023 6th International Conference on Renewable Energy for Developing Countries (REDEC), 2023, pp. 42–47. doi: 10.1109/REDEC58286.2023.10208177.

[87] N. Blasuttigh, S. Negri, A. Massi Pavan, and E. Tironi, "Optimal Sizing and Environ-Economic Analysis of PV-BESS Systems for Jointly Acting Renewable Self-Consumers," Energies (Basel), vol. 16, no. 3, Feb. 2023, doi: 10.3390/en16031244.

Disclaimer:

Co-Funded by the European Union. Views and opinions expressed are however those of the author(s) only and do not necessarily reflect those of the European Union nor CINEA. Neither the European Union nor the granting authority can be held responsible for them.

SAFE, SUSTAINABLE AND MODULAR HYBRID SYSTEMS FOR LONG-DURATION ENERGY STORAGE AND GRID SERVICES

COORDINATION
Edoardo Gino Macchi
Head of Battery and Electrification Technologies Unit – BET
Centre for Sustainable Energy – SE
Fondazione Bruno Kessler - FBK
Phone: +39 0461 314 887
E-mail: emacchi@fbk.eu

Co-funded by the European Union